Novel Proteases That Regulate Interleukin-1 Alpha Activity During Inflammation And Senescence

Kimberley Anne Wiggins

Clare College

University of Cambridge

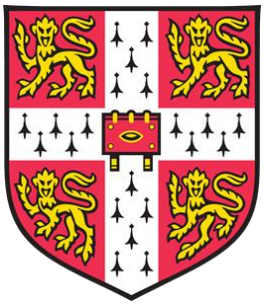

September 2017

This dissertation is submitted for the degree of Doctor of Philosophy

i. Abstract

Interleukin-1 alpha (IL-1α) is a powerful inflammatory cytokine that modulates both innate and adaptive immunity. As such, IL-1α is implicated in the development of multiple inflammatory and autoimmune diseases including atherosclerosis, arthritis and cancer. Therefore, understanding the mechanisms that regulate IL-1α activity is extremely important.

For many years, pro-IL-1α was considered to be a fully active alarmin. However, we have previously shown that the removal of the pro-domain by calpain, a protease that is activated upon necrosis, significantly increases IL-1α bioactivity. The work presented in this thesis demonstrates that multiple proteases from diverse biological systems cleave and activate IL-1α. We therefore suggest that IL-1α is an important signalling hub that integrates diverse proteolytic danger signals to alert the immune system.

In particular we have identified the inflammatory caspase, caspase-5, as a novel and potent activator of IL-1α. We show that caspase-5 directly cleaves pro-IL-1α during the activation of the non-canonical inflammasome by cytosolic LPS, which mimics intracellular bacterial infection. We also demonstrate that caspase-5-cleaved IL-1α mediates the senescence-associated secretory phenotype (SASP), which drives the deleterious effects of senescent cells in multiple age-related diseases. Therefore, therapeutically targeting caspase-5 may be of interest for pathologies mediated by the non-canonical inflammasome and/or senescent cells.

Finally we find that rs17561, a common IL1A polymorphism, reduces active IL-1α release. We find that blood from minor allele homozygotes releases significantly less IL-1α than major allele homozygotes upon LPS stimulation. Therefore, genotyping patients under consideration for anti-IL-1α therapy could predict who would be likely to respond well to the treatment.

In conclusion, the work presented in this thesis enhances our understanding of how IL-1α activity is regulated. The identification of both the caspase-5-mediated pathway of IL-1α activation and the defect conferred by the rs17561 SNP could have important clinical implications for the treatment of multiple inflammatory diseases.

ii. Declaration

This dissertation is the result of my own work and includes nothing which is the outcome of work done in collaboration except as declared in the Preface and specified in the text.

It is not substantially the same as any that I have submitted, or, is being concurrently submitted for a degree or diploma or other qualification at the University of Cambridge or any other University or similar institution except as declared in the Preface and specified in the text. I further state that no substantial part of my dissertation has already been submitted, or, is being concurrently submitted for any such degree, diploma or other qualification at the University of Cambridge or any other University or similar institution except as declared in the Preface and specified in the text.

It does not exceed the prescribed word limit for the relevant Degree Committee.

Declaration of Collaborative Work

I would like to express my sincere gratitude to all of our collaborators, who helped make the work presented in this thesis possible.

Clarke group (Dept. of Medicine, Cambridge): Mrs Melanie Humphry cloned human/mouse pro-IL-1α/β or human caspase-5 DNA into vectors for bacterial and mammalian recombinant protein expression.

Chilvers group (Dept of Medicine, Cambridge): Prof. Chilvers generously provided PBMCs.

Goodall group (Dept. of Medicine, Cambridge): Dr Steve Webster generously provided the dendritic cell and macrophage RNA for caspase gene expression analysis, and supernatants from WT, *Casp11*$^{-/-}$, *Casp1*$^{-/-}$*/Casp11*^{Tg}, or *Gsdmd*$^{-/-}$ BMDMs following intracellular LPS or *C.trachomatis* treatment.

Narita group (Cancer Research UK Cambridge Institute): Mr Aled Parry carried the out retroviral infection of J2 macrophages and provided IMR90 fibroblasts for the senescence experiments. Mr Aled Parry and Dr Liam Cassidy (with help from the CRUK biological resources unit) carried out the hydrodynamic tail vein injections for the *in vivo* senescence study under the Narita group's license and carried out the computational analysis of immunohistochemistry staining.

Albert Group (Pasteur Institute, Paris): Dr Darragh Duffy kindly provided serum samples from IL-1α secretors and non-secretors (Duffy et al., 2014).

iii. Acknowledgements

Firstly, I'd like to thank my supervisor Dr. Murray Clarke for his invaluable support and guidance throughout my PhD. Murray's passion for scientific research and his innovative thinking has been a constant source of inspiration for me. He has always been there to offer support and advice when I've needed it, but has also encouraged me to think for myself, take steps towards becoming an independent scientist, and make the most of every opportunity … including forcing me to try Guinness in Dublin (I still don't like it).

I'm also extremely grateful to everyone on Level 6 of the ACCI for creating such a warm and friendly workplace – something that every PhD student needs! In particular, thank you to Mel for teaching me so much and providing an incredible amount of support throughout my PhD, Nikki for making me feel welcome from day one, and Lakshi for the wanderlust-inspiring chats in TC that culminated in an epic hike up Trolltunga in Norway, which was the perfect mid-thesis-writing break!

A huge thanks to my family and friends, who have been so supportive during the past three years. Thanks to Mum and Dad for always encouraging me to be the best that I can be, to my sisters Ceri and Michelle for always being there for me and providing great 'big-sis' advice, and my baby nephew Harrison for the stress-busting cuddles that got me through my final year! I'd also like to thank my friends - Charis for the Friday night dinners, Laura for the regular games nights and generally being a fantastic 'work-wife', and all of the Bath girls for the many brunches and Bellini's!

Finally, thank you to my husband-to-be, Aled. Thank you for the endless love, support and pep-talks whenever I have a crisis of confidence, and for being the best adventure buddy a girl could ask for!

The work presented in this thesis was generously funded by the British Heart Foundation. In addition I would like to thank Clare College and the Charles Slater Fund for providing financial support, which has enabled me to present my work at international conferences.

iv. Abbreviations

(p/m)Ab	(Polyclonal/monoclonal) antibody
APC	Antigen presenting cell
ASC	Apoptosis-associated speck-like protein containing a CARD
ATP	Adenosine triphosphate
BMDM	Bone marrow-derived macrophage
BrDu	Bromodeoxyuridine
BSA	Bovine serum albumin
CARD	Caspase recruitment domain
CD	Cluster of differentiation
cGAS	Cyclic GMP-AMP synthase
CRP	C-reactive protein
Ct	Threshold cycle
C. trachomatis	*Chlamydia trachomatis*
DAMP	Damage-associated molecular pattern
DC	Dendritic cell
DNA	Deoxyribonucleic acid
dNTPs	Deoxyribose nucleoside triphosphate
E.coli	*Escherichia coli*
ECM	Extracellular matrix
EGF	Epidermal growth factor
ELISA	Enzyme-linked immunosorbent assay
ER	Endoplasmic reticulum
ESCRT	Endosomal sorting complexes required for transport
FPLC	Fast Protein Liquid Chromatography
GBP	Guanylate binding protein
GM-CSF	Granulocyte macrophage colony-stimulating factor
GSDMD	Gasdermin D
GST	Glutathione-S-transferase
GTP	Guanosine triphosphate
HEK	Human embryonic kidney
HIS-tag	Polyhistidine tag
HIV	Human immunodeficiency virus
hMDM	Human monocyte-derived macrophages
HRP	Horseradish peroxidase
IF	Immunofluorescence
IFN	Interferon
Ig	Immunoglobulin
IHC	Immunohistochemistry
IL	Interleukin
IL-1R	Interleukin-1 receptor
IL-1RAcP	Interleukin-1 receptor accessory protein
IRAK	Interleukin-1 receptor-associated kinase
LDH	Lactate dehydrogenase
LDL	Low density lipoprotein

(ic)LPS	(intracellular) Lipopolysaccharide
MCP-1	Monocyte chemo-attractant protein -1
MHC	Major histocompatibility complex
MMP	Matrix metalloproteinase
MyD88	Myeloid differentiation primary response 88
NET	Neutrophil extracellular trap
NF-κB	Nuclear factor kappa B
NK	Natural killer
NLRP	NACHT, LRR and PYD domain-containing protein
NLS	Nuclear localisation signal
OIS	Oncogene-induced senescence
PAGE	Polyacrylamide gel electrophoresis
PAMP	Pathogen-associated molecular pattern
PBMC	Peripheral blood mononuclear cell
PBS	Phosphate buffered saline
(q)PCR	(Quantitative) polymerase chain reaction
PE	Phycoerythrin
PRR	Pattern recognition receptor
PTM	Post translational modification
PYD	Pyrin domain
(m/si/sh) RNA	(messenger / small interfering / short hairpin) ribonucleic acid
RNS	Reactive nitrogen species
ROS	Reactive oxygen species
SAβGAL	Senescence-associated beta galactosidase
SAHF	Senescence-associated heterochromatic foci
SASP	Senescence-associated secretory phenotype
SDS	Sodium dodecyl sulphate
SEM	Standard error of the mean
(ns) SNP	(Non-synonymous) single nucleotide polymorphism
STING	Stimulator of interferon genes
T3SS	Type III secretion system
TCR	T cell receptor
TGF	Transforming growth factor
TIR	Toll-interleukin receptor
TLR	Toll-like receptor
TNF	Tumour necrosis factor
TRAF	TNF receptor associated factor
VSMC	Vascular smooth muscle cell

v. Contents

Introduction

1. INTRODUCTION

1.1 Immunity and Inflammation

1.1.1 A brief history of immunology

Throughout its existence, humankind has continuously experienced epidemics of disease. Even the most ancient civilisations, who regarded illness as a punishment from the gods, observed that those who survived a disease would not re-catch it. In 430 B.C., during the great plague of Athens, the Greek historian Thucydides wrote "*Yet it was with those who had recovered from the disease that the sick and the dying found most compassion. These knew what it was from experience, and had now no fear for themselves; for the same man was never attacked twice – never at least fatally*".

This phenomenon is now known as immunity, a term derived from the Latin word "*immunis*" meaning 'exempt'. In 925 A.D., the physician Rhazes was the first to explicitly express the theory of acquired immunity when he reported that recovering from smallpox infection led to protection against recurrence. In the 1700s, it was realised that rubbing pustular fluid from a smallpox patient into a small scratch in the skin of a healthy individual would cause the recipient to develop a considerably milder form of the disease and gain immunity. This marked the beginning of the vaccination field, which was transformed by the work of microbiologist Louis Pasteur who, with Robert Koch and others, showed that each disease is the result of infection by a specific microbe.

In 1884 Elie Metchnikoff proposed his theory of cellular immunity; that the primitive digestive functions of unicellular organisms are present in higher multicellular organisms in the form of phagocytic cells that are able to digest foreign matter. Six years later, Emil Behring and Shibasaburo Kitasato observed that animals immunised with diphtheria and tetanus toxins produced a soluble factor within their blood that could neutralise the threat and prevent disease, which became known as the antibody. (Silverstein, 2001). Over time, immunologists have gradually gained an increasingly detailed knowledge of our immune system. However immunology remains a dynamic and developing field, and there is still much left to understand.

1.1.2 An overview of the immune system

The immune system has evolved to defend against attack by invading pathogens. There are two arms of the immune system: innate and adaptive. The innate immune response is an ancient system present in all plants and animals. Innate immune cells, primarily neutrophils and macrophages, recognise molecules released by microorganisms known as pathogen-associated molecular patterns (PAMPs) through specific cell-surface receptors. For example, transmembrane toll-like receptor 4 (TLR4) has evolved to detect the Gram-negative bacterial cell wall component lipopolysaccharide (LPS) (Janssens and Beyaert, 2003). Because the innate immune system uses germline-encoded receptors to recognise common microbial ligands, it is constantly ready for immediate use and therefore represents the first line of defence. PAMP recognition promotes phagocytosis of the microbe and the release of proinflammatory mediators that initiate the process of inflammation, which is discussed in more detail below.

Although the innate response is an effective host-protection mechanism, microbes continuously adapt and change their surface molecules to evade detection. To respond to this, jawed fish and higher vertebrates have evolved an adaptive immune system. As the name suggests, adaptive immune cells tailor their response to the invader and, importantly, retain a memory of that response so that future infections by the same microbe can be dealt with more efficiently. The caveat of achieving this high level of specificity is that the activation of adaptive immunity takes between four and seven days, so the initial innate response remains indispensable for host survival. The effector cells of the adaptive immune system include CD8+ cytotoxic T cells that secrete noxious granules, CD4+ helper T cells that produce cytokines to activate other immune cells, and B cells that secrete antibodies against the target antigen (Janeway et al., 2001).

1.1.3 Inflammation

Inflammation is a process that is activated when homeostasis has been compromised, which aims to eradicate the source of the insult and remove damaged tissue to restore normality (Medzhitov, 2008). Inflammation is traditionally associated with heat, pain, redness and swelling, which are symptoms caused by pro-inflammatory cytokines that promote blood vessel dilation and permeabilisation, leading to increased blood flow and fluid leakage (Janeway et al., 2001). The inflammatory response (Figure 1.1) is initiated by molecules that can be either endogenous or exogenous. Signals from invading microorganisms include PAMPS and virulence factors, which damage host tissue and indirectly trigger inflammation by activating specific proteases or causing abnormal entry of ions into the cell. In addition, non-microbial environmental factors such as allergens and toxic compounds can trigger inflammation. For example, proteolytic allergens are similar to the enzymes released by helminths and consequently induce a similar immune response. Finally, the inflammatory response can be activated in sterile conditions by host-derived factors released from stressed or injured tissue, known as damage-associated molecular patterns (DAMPs) or alarmins. For instance, necrotic cells release the intracellular factor ATP, which binds to P2X7 receptors on macrophages to trigger a potassium ion influx that in turn activates the inflammatory cascade. It has been suggested that tissue damage and infection elicit such similar inflammatory responses because infection often follows wounding (Nathan, 2002).

These molecular danger signals activate local endothelial cells, which interact with leukocytes via selectins and integrins to allow the selective extravasation of leukocytes, but not erythrocytes, from the bloodstream into the tissue. Tissue resident macrophages are also activated, and release cytokines, chemokines and extracellular matrix (ECM) –degrading enzymes to facilitate leukocyte movement, and promote vascular permeability by secreting prostaglandins, vasoactive amines (e.g. histamine and serotonin) and vasoactive peptides (e.g. Substance P.) (Medzhitov, 2008).

Neutrophils often arrive at the site of inflammation first. They phagocytose dead microbes and release granules containing reactive oxygen and nitrogen species (ROS, RNS) and proteases that degrade the bacterial membrane. The release of ROS is energetically demanding, and this stage of inflammation is

therefore referred to as the 'respiratory burst'. Neutrophils also release proteases interweaved with chromatin fibres to form extracellular traps (NETs) that physically catch and kill microbes (Ashley et al., 2012).

The neutrophils are followed by macrophages, which phagocytose pathogens and dead cells, and T cells that mount an adaptive immune response. Resident dendritic cells capture and process antigens, which they carry to the lymph node and present to T cells via major histocompatibility complexes (MHCs). If the antigen was internalised and digested in vesicles (e.g. from an extracellular bacterium) the peptide is presented on a MHCII molecule to CD4+ T cells, whereas if the peptide was digested in the proteasome (e.g. from a virus) it is presented on an MHCI molecule to CD8+ T cells. The activated T cell then proliferates and re-enters the circulation to travel to the site of inflammation. CD4+ T cells, also known as T helper cells, are either pro-inflammatory (Th1) or anti-inflammatory (Th2). Th1 cells secrete cytokines including IFNγ, TNFα and IL-2, which promote an 'M1' phagocytic macrophage phenotype. Th2 cells secrete the cytokines IL-4 and IL-10 that induce B cell differentiation into antibody-secreting plasma cells, and promote the 'M2' remodelling macrophage phenotype. CD8+ T cells, also known as cytotoxic T cells, release granules containing the pore-forming enzyme perforin and apoptosis-inducing granzymes (Alberts et al., 2002). If the threat persists, for example when the invading organism is too large to be phagocytosed, tissue resident macrophages and dendritic cells form a physical barrier surrounding the pathogen known as a granuloma (Adams, 1976).

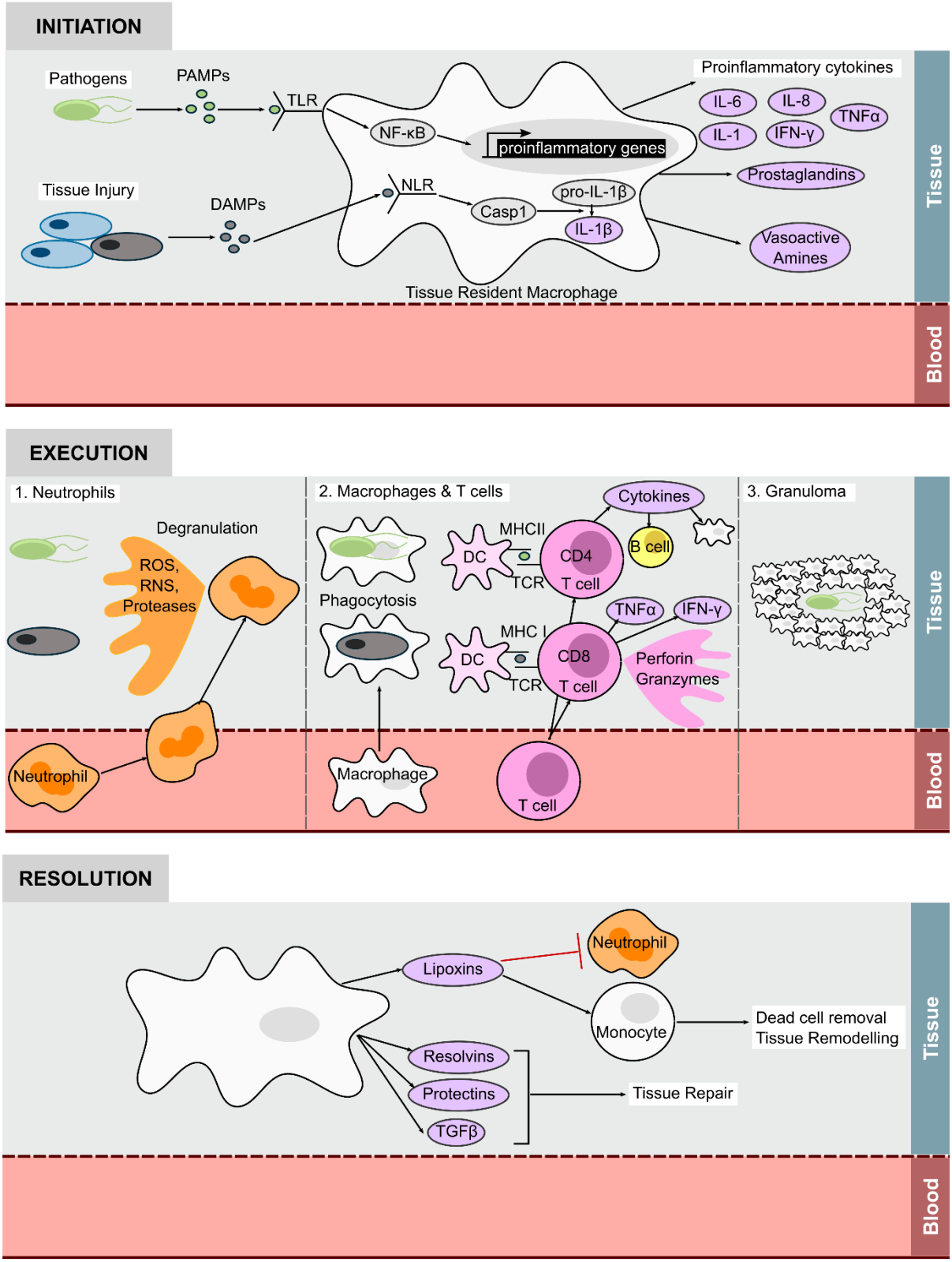

Figure 1.1: The immune response. Schematic illustrating the main stages of inflammation. PAMPs/DAMPs activate tissue macrophages and stimulate the production of proinflammatory cytokines, chemokines, hormones and vasoactive amines. Neutrophils are recruited first, and release granules containing ROS, RNS and proteolytic enzymes. Macrophages engulf the pathogen or dead cells, and T cells mount a tailored adaptive immune response. If the pathogen persists, macrophages and dendritic cells form a granuloma, physically encapsulating the invading organism. Once the threat has been neutralised, macrophages release compounds that block neutrophil recruitment and attract tissue-remodelling monocytes

1.1.4 The inflammatory caspases

The caspases are a family of cysteine-dependent proteases that cleave after an aspartic acid residue. They are produced as inactive monomeric zymogens, which are activated by oligomerisation and/or cleavage. Caspases can be categorised into two subtypes; the apoptotic caspases initiate signalling cascades and execute cleavage of key cellular substrates that culminate in programmed cell death; whereas the inflammatory caspases activate cytokines that drive inflammation. As such, the caspases are a critical group of enzymes for maintaining cellular homeostasis.

The proinflammatory caspases, also known as group I caspases, are caspase-1, -4, -5 and -12 in humans or caspase-1, -11 and -12 in mice. Their genes are clustered on human chromosome 11 and murine chromosome 9, suggesting that they arose from gene duplication events. Caspase-1 was the first inflammatory caspase to be identified through its ability to activate the proinflammatory cytokine interleukin-1 beta (IL-1β), and was originally known as IL-1β-converting enzyme (ICE) (Thornberry et al., 1992, Cerretti et al., 1992) until it was subsequently shown to also activate IL-18 (Ghayur et al., 1997).

In 1996, murine caspase-11 was identified as a relative of caspase-1, and was described to enhance caspase-1 activity (Wang et al., 1996). When the *Casp1*$^{-/-}$ and *Casp11*$^{-/-}$ mice were engineered, they were both reported to be resistant to lethal sepsis (Li et al., 1995). Although it was later uncovered that caspase-11 was solely responsible for this resistance to toxic shock, the finding was pivotal for the recognition of these caspases as immunomodulatory enzymes. It led to the search for other mammalian caspases with similar sequences to caspase-1, which revealed human caspases-4 and -5 (Kamens et al., 1995, Lin et al., 2000). Although caspase-12 is also homologous to caspase-1, it is not thought to play a key role in inflammation. The precise function of caspase-12 is poorly understood, but it is thought to mediate endoplasmic reticulum (ER) -stress-induced apoptosis (Nakagawa et al., 2000).

1.1.5 The inflammasome: a caspase-1 activation platform

The inflammasome is an intracellular protein complex that senses danger signals and recruits and activates caspase-1 in response. Active caspase-1 triggers proinflammatory cytokine release and pyroptosis, an inflammatory form of programmed cell death, thereby simultaneously alerting the immune system and destroying the infected or damaged cell. Inflammasomes are distinguished according to their sensor molecules. Each sensor detects a specific danger signal (Figure 1.2) and most recruit the adaptor protein ASC (apoptosis-associated speck-like protein containing a caspase activation and recruitment domain) that aggregates to form a highly stable 1μm structure called the "speck", which recruits the inactive precursor pro-caspase-1. The concentration of pro-caspase-1 at the speck results in proximity-induced dimerisation that triggers an activating conformational change. Caspase-1 then activates IL-1β and IL-18, and induces pyroptosis (Sharma and Kanneganti, 2016, Lu and Wu, 2015). Only one speck is formed per cell, even if multiple inflammasome sensors are engaged (Fernandes-Alnemri et al., 2007). The speck can also be released into the extracellular space upon pyroptosis where it can continue to activate extracellular IL-1β, and be phagocytosed by a neighbouring cell and cause activation of the new cell's inflammasome (Baroja-Mazo et al., 2014, Franklin et al., 2014).

The majority of protein-protein interactions in the inflammasome occur through pyrin domains (PYD) and caspase recruitment domains (CARD) that drive aggregation, also referred to as nucleation. Inflammasome sensors containing CARD domains, such as NLRP1, directly recruit pro-caspase-1 through CARD-CARD interactions. However, most sensor proteins lack a CARD domain and instead nucleate the adaptor ASC into filaments through electrostatic and hydrophobic PYD-PYD interactions. ASC then recruits caspase-1 through CARD domain associations, and the resulting speck has a multi-layered ring structure with the active caspase-1 at the core (Figure 1.3).

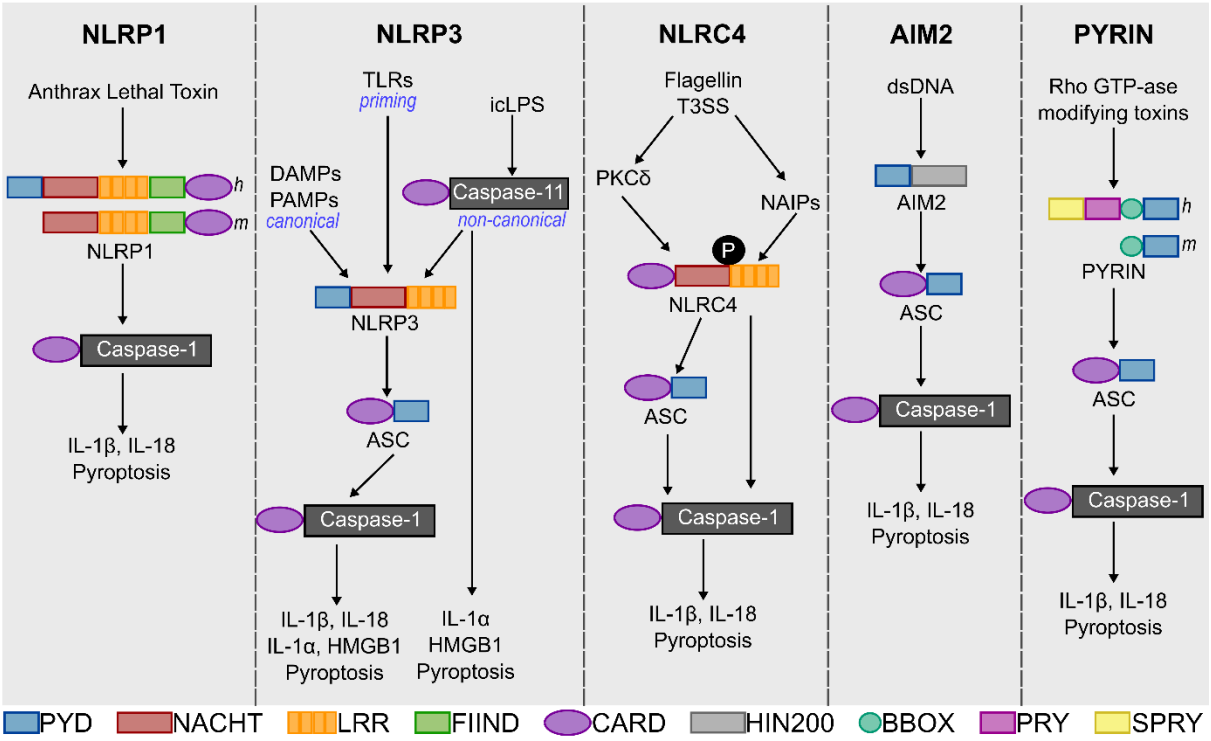

Figure 1.2: Characterised inflammasome pathways. A schematic to illustrate the known inflammasome pathways. Despite different activatory stimuli, all inflammasome pathways culminate in caspase-1 activation and subsequent cleavage and activation of IL-1β and IL-18. *Abbreviations: h* (human), *m* (mouse) NLRP (NACHT, LRR and PYD domain protein), PKC (protein kinase C), icLPS (intracellular LPS), T3SS (type 3 secretion system), NAIPS (NLR family apoptosis inhibitory proteins) , AIM2 (absent in melanoma 2), dsDNA (double stranded DNA), PYD (pyrin domain), NACHT (nucleotide-binding and oligomerisation domain), LRR (leucine-rich repeat), FIIND (domain with function to find), CARD (caspase recruitment domain), HIN200 (hematopoietic interferon-inducible nuclear protein with a 200-amino acid repeat), BBOX (B-box-type zinc finger), PRY (SPRY-associated), SPRY (*Dictyostelium discoidium* dual specificity kinase SplA and ryanodine receptor). [Adapted from (Saavedra et al., 2015)]

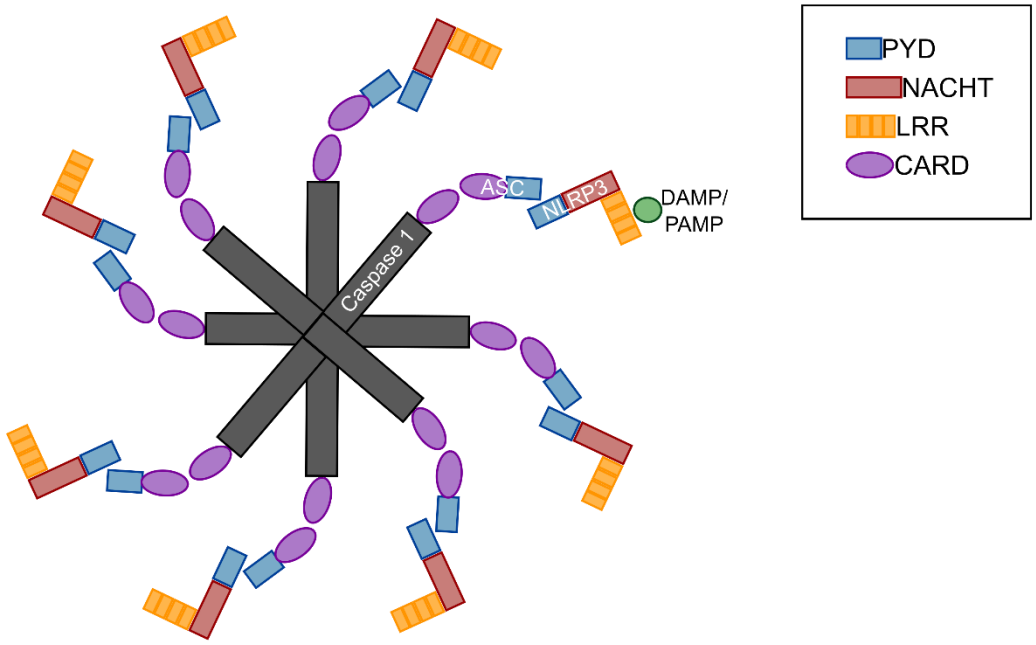

Figure 1.3: The Inflammasome ring structure. A schematic to show the ring-like structure of the inflammasome [Adapted from (Virgilio and Alexander, 2013)].

1.1.5.1 The NLRP3 inflammasome

NLRP3 is a unique inflammasome sensor because, instead of detecting a single ligand, it responds to a broad range of stimuli. These signals can be both endogenous and exogenous, ranging from LPS to asbestos. It has been suggested that NLRP3 does not sense each of these signals specifically, but rather undergoes an activating conformational change in response to secondary products of cellular stress such as ROS or potassium efflux (Sharma and Kanneganti, 2016, Man and Kanneganti, 2015). In a resting cell, NLRP3 associates with the ER whereas ASC is found in the mitochondria and cytosol (Zhou et al., 2011). Upon activation dynamic cytoskeletal rearrangements driven by the microtubule affinity regulating kinase 4 (MARK4) colocalise NLRP3 and ASC to the microtubule organising centre (MTOC) (Li et al., 2017).

Structurally, NLRP3 is composed of three domains: PYD, NACHT and LRR, which can be post-translationally modified (PTM) to modulate inflammasome activity. For example, deubiquitination of

the LRR by the enzyme BRCC3 triggers inflammasome activation (Py et al., 2013), whereas S-nitrosylation by nitric oxide restricts activity (Mao et al., 2013).

Canonical activation of the NLRP3 inflammasome is a two-step process of priming followed by activation. Priming occurs upon activation of TLRs, nucleotide-binding oligomerisation domain-containing protein 2 (NOD2), or tumour necrosis factor receptors (TNFRs), which signal via nuclear factor kappa B (NF-κB) to upregulate the expression of inflammasome components such as NLRP3 and caspase-1. Although the exact mechanism for NLRP3 activation is not fully understood and remains a rapidly progressing field, it has been reported that K^+ efflux is sufficient to induce NLRP3 inflammasome activity (Munoz-Planillo et al., 2013).

1.1.6 The non-canonical inflammasome

The NLRP3 inflammasome can also be activated through an alternative pathway involving the pro-inflammatory caspases -4, -5 and -11, known as the 'non-canonical inflammasome', which will be the focus of chapters 5 and 6 of this thesis. The most extensively studied activator of this pathway is cytosolic LPS (Figure 1.4), and as such the non-canonical inflammasome is important for combatting intracellular infections by Gram negative bacteria, such as *Salmonella typhimurium*. The lipid A component of the LPS molecule interacts with three basic residues in the CARD domain of caspase-11/-4/-5 to trigger its oligomerisation and auto-activation (Shi et al., 2014). This mechanism of proinflammatory caspase activation resembles the activation of Factor C, a serine protease in horseshoe crab blood that is also directly activated by LPS contact and triggers the coagulation cascade in response. This similarity suggests that caspases-11/-4/-5 are in fact conserved PRRs (Stowe et al., 2015).

The activated caspase-11/-4/-5 cleaves gasdermin-D (GSDMD) to generate an active 30kDa N-terminal fragment ($GSDMD^N$), which both activates the NLRP3 inflammasome, with subsequent IL-1β maturation via caspase-1, and induces pyroptosis (Kayagaki et al., 2015, Shi et al., 2015). The $GSDMD^N$ contains two regions that unwind into amphipathic β-strands that promote membrane insertion, akin to

those in the pore forming protein 'perforin' secreted by cytotoxic T cells and natural killer (NK) cells (Liu and Lieberman, 2017). $GSDMD^N$ selectively binds to inner membrane phospholipids, such as phosphoinositides and cardiolipin, to form pores of approximately 10-14nm that trigger pyroptosis. Because $GSDMD^N$ cannot interact with outer membrane lipids, it does not induce pyroptosis in neighbouring cells when it is released following cell lysis (Ding et al., 2016, Agliettia et al., 2016). It has been reported that $GSDMD^N$ can also lyse endosomes, since these are derived from the inner leaflet of the plasma membrane, and can disrupt bacterial membranes to directly kill invading microorganisms (Liu et al., 2016). However, the most widely accepted hypothesis is that pyroptosis is the principle antibacterial mechanism, destroying the pathogen's niche and exposing them to attack by neutrophils (Stowe et al., 2015).

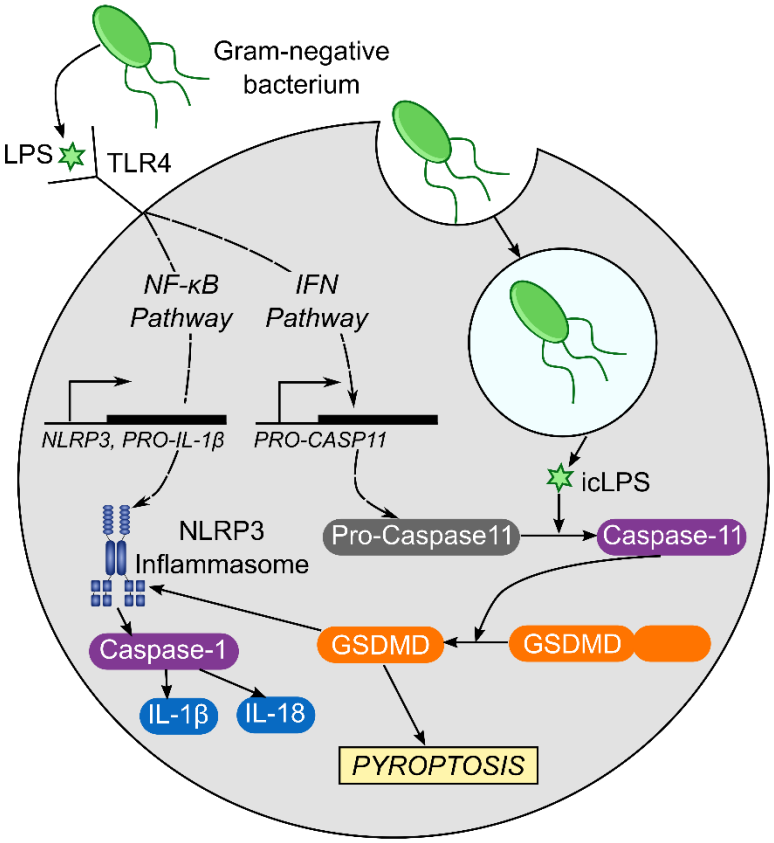

Figure 1.4: The non-canonical inflammasome. The engagement of a PRR (e.g. TLR4) by a pathogenic ligand (e.g. LPS) activates the NF-κB signalling pathway to upregulate components of the NLRP3 inflammasome, and the IFN signalling pathway to upregulate caspase-11. Bacteria that have been internalised by the phago-lysosome act as a source of intracellular LPS (icLPS), which directly binds and activates caspase-11. Caspase-11 cleaves gasdmerin D (GSDMD) to release a 30kDa N-terminal fragment that activates the NLRP3 inflammasome and triggers pyroptosis.

1.1.7 The cost of aberrant inflammation and immunity

Although inflammation is an essential defence mechanism, it comes at a cost. The unavoidable collateral damage incurred by host tissue represents a significant biological compromise. For example, the cytotoxic granules and ROS released by infiltrating leukocytes do not discriminate between host and microbial cells. Similarly, excessive granuloma formation may result in fibrosis that can culminate in organ failure. For certain organs, such as the eye and placenta, this risk of tissue damage outweighs the benefits of inflammation. As a result, these regions have evolved to become 'immune-privileged', meaning that they do not induce an inflammatory response to foreign antigens. (Ashley et al., 2012).

In addition to collateral damage, a misplaced or dysregulated activation of the inflammatory response can cause disease. Mutation of the genes encoding inflammasome components can cause autoinflammatory diseases. For instance, activating single nucleotide polymorphisms (SNPs) in the NACHT domain-encoding sequence of the *NLRP3* gene are associated with cryopyrin-associated periodic syndromes (CAPS), such as Muckle-Wells syndrome, where the patient suffers from skin rashes, joint and eye inflammation, and fever (Hoffman et al., 2001). In contrast, *NLRP3* mutations that reduce protein expression levels have been linked to increased risk of Crohn's disease and colitis. It is thought that the NLRP3 inflammasome induces IL-18 release, which facilitates the repair of the mucosal barrier in the colon thereby maintaining intestinal homeostasis and protecting against irritable bowel syndromes (Pellegrini et al., 2017). Mutations in the *CASP1* gene that alter caspase-1 expression, structure and function have been shown to increase susceptibility to inflammatory disease. Paradoxically, individuals carrying caspase-1 mutations typically display lower IL-1β levels. It has been hypothesised that a reduction in the protease function of caspase-1 may in turn favour its binding to the kinase RIPK2, which can activate inflammatory NF-κB signalling (Saavedra et al., 2015).

The inappropriate activation of the inflammatory response is also implicated in allergic and autoimmune diseases, such as eczema, asthma and psoriasis, where the body reacts to harmless allergens or host-derived factors. The 'hygiene hypothesis' suggests that allergic disease has become a problem in more developed countries due to a decreased exposure of children to infectious agents resulting from an

increase in hygiene. This insufficient stimulation of the Th1 response in early childhood leads to a Th2-dominant immunological phenotype, which is characterised by upregulated IgE production in response to allergens (Okada et al., 2010). In addition, genome-wide association studies (GWAS) have suggested that autoimmunity can result from polymorphisms in or around immunomodulatory genes, such as the human leukocyte antigen (HLA) alleles, which lead to a reduced threshold for immune cell activation. Similarly, impaired immune cell regulation can drive autoimmunity. For example, defective immature B cell deletion and receptor editing have been described to drive systemic lupus erythematosus (SLE) (Rosenblum et al., 2015).

In addition, although inflammation is initiated locally at the site of infection or injury, inflammatory mediators such as IL-1, IL-6 and TNFα can induce a systemic response. Over-production of inflammatory cytokines can lead to serious widespread endothelial damage and organ failure, commonly known as septic shock. Furthermore, a state of chronic, low-grade inflammation results in increased cell turnover and imparts a selection pressure that can result in carcinogenesis (Moss and Blaser, 2005).

1.1.7.1 Atherosclerosis: an example of a chronic inflammatory disease

Atherosclerosis is an extensively studied cardiovascular disease that results from chronic inflammation. It is a disease of the arterial wall that precedes cardiovascular events including myocardial infarction and stroke. There are a number of risk-factors associated with atherosclerosis, both genetic and environmental, which include elevated cholesterol, high blood pressure, smoking, diabetes, obesity, old age and stress (Rafieian-Kopaei et al., 2014).

The stages of atherosclerosis development (Figure 1.5) have been elucidated using animal models; in particular, mice deficient in either apolipoprotein E (ApoE) or the low-density lipoprotein receptor (LDLR) fed a high-fat diet. Atherosclerotic lesions preferentially develop at sites of disturbed flow, such as vascular bifurcations, where the endothelial cells lining the vessel wall are more permeable and allow the entry of low-density lipoprotein (LDL), cholesterol and lipoprotein(a) into the vessel intima

(Gimbrone, 1999). This accumulation of sub-endothelial lipid is referred to as an early plaque, or a fatty streak lesion.

Over time, the plaques can become more advanced and clinically relevant. LDL is oxidised (oxLDL) and activates endothelial cells that recruit leukocytes. Cholesterol crystals activate the NLRP3 inflammasome in recruited macrophages, which leads to IL-1β activation and release that in turn drives proinflammatory cytokine production (Duewell et al., 2010, Rajamaki et al., 2010). The macrophages also phagocytose the oxLDL but are unable to process it, become foam cells, and die. Vascular smooth muscle cells (VSMC) then migrate into the intima and lay down ECM to generate a fibrous cap, which contains the contents of the plaque. However, infiltrating T cells secrete interferon gamma (IFNγ) that inhibits VSMC collagen synthesis, and the increasingly necrotic core drives VSMC death. The fibrous cap becomes thinner and weaker, and eventually ruptures. The resulting contact between the plaque contents and the blood activates the coagulation cascade, leading to thrombosis and blood vessel occlusion (Lusis, 2000, Libby et al., 2002).

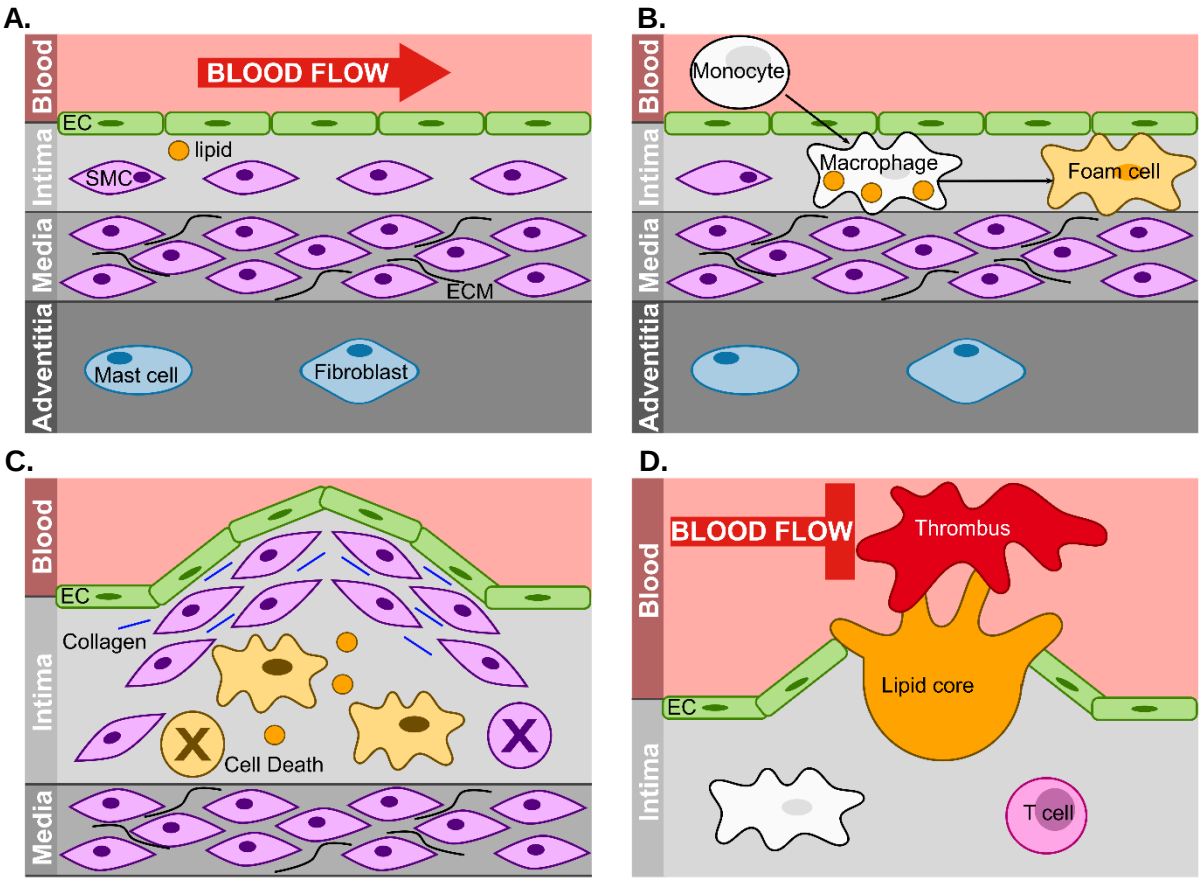

Figure 1.5: Human atherosclerotic plaque development. Adapted from (Libby et al., 2011). **(A)** The normal structure of a human artery. **(B)** The accumulation of lipid in the intima activates local endothelial cells (ECs) which recruit monocytes. The monocytes transmigrate into the vessel wall and differentiate into macrophages, which engulf the lipoproteins and become inactive foam cells. **(C)** Smooth muscle cells (SMCs) migrate from the media and secrete extracellular matrix (ECM) molecules to generate the fibrous cap. The foam cells and SMCs begin to die and release their necrotic lipid-rich contents into the plaque. **(D)** The fibrous cap gets thinner and weaker, and eventually ruptures. The necrotic core activates the coagulation cascade and platelets aggregate over the plaque to form a thrombus, which blocks the lumen of the vessel.

1.2 Interleukin-1: A master regulator of inflammation

1.2.1 The history of the IL-1 family

In the 1940's, scientists Eli Menkin and Paul Beeson described the release of a factor from leukocytes that promoted rapid onset fever when injected into rabbits. Over the next 40 years this pyrogenic factor was isolated and named IL-1. It was found to activate lymphocytes, enhance their responsiveness and stimulate the production of the acute phase response protein serum amyloid A, earning IL-1 recognition as a 'master molecule' in immunity. In 1974, it was realised that there are actually two forms of IL-1 – alpha and beta – and the individual genes were successfully cloned in 1984 (Dinarello, 2010). The IL-1 family is now known to include eleven ligands and ten receptors that either promote or inhibit inflammation (Table 1.1) (Boraschi and Tagliabue, 2013).

Table 1.1: Known Members of the IL-1 Family

Agonists (*proinflammatory*)	**Signalling Receptors**	**Decoy Receptors**	**Antagonists / Negative Regulators**
IL-1α, IL-1β	IL-1R1, IL-1RAcP, TILRR	IL-1R2	IL-1Ra, SIGIRR
IL-18	IL-18Rα, IL-18Rβ		IL-37, IL-18BP
IL-33	ST2		
IL-36α, IL-36β, IL-36γ	IL-1Rp2		IL-36Ra, IL-38

1.2.2 IL-1 signalling and function

IL-1α and IL-1β are encoded by adjacent genes on chromosome 2 and are thought to have resulted from a gene duplication that occurred over 270 million years ago. The cytokines share a similar three-dimensional structure, a β-trefoil fold composed of 12 β-strands, despite their low amino acid sequence homology (27%) (Gabay et al., 2010). A major difference between the two forms of IL-1 is their expression patterns and activation mechanisms, which is reflected by the low sequence homology between the *IL1A* and *IL1B* promoters. IL-1α is constitutively expressed in many cell types, although

its expression can be upregulated following stimulation, and it exists both within the cytosol and on the cell surface in a myristoylated form where it can mediate juxtacrine cell-cell signalling (Stevenson et al., 1993). Conversely, IL-1β is primarily produced by monocytes and macrophages and is specifically upregulated along with other inflammasome components following cell priming (Sims and Smith, 2010).

Both IL-1α and IL-1β are translated as 31kDa pro-proteins and require the removal of their pro-domains by the proteases calpain and caspase-1, respectively, for full activity (Thornberry et al., 1992, Cerretti et al., 1992, Afonina et al., 2011, Zheng et al., 2013). The mechanism of IL-1 secretion remains under investigation, since both cytokines lack a conventional signal peptide and are therefore not secreted via the ER or the Golgi apparatus (Sims and Smith, 2010). It has been suggested that IL-1α binds to IL-1β and is shuttled out of the cell following inflammasome activation (Keller et al., 2008, Fettelschoss et al., 2011).

Mature IL-1α and IL-1β signal through the same intracellular pathway (Figure 1.6). They bind to the type I receptor (IL-1R1) and trigger the recruitment of the co-receptor IL-1R accessory protein (IL-1RAcP). The receptors interact with the signalling adaptor protein myeloid differentiation primary response gene 88 (MyD88) through their intracellular Toll/interleukin-1 receptor (TIR) domains. MyD88 induces the phosphorylation of the IL-1 receptor associated kinase 4 (IRAK4), which then phosphorylates IRAK1 and IRAK2. The IRAK proteins then interact with TNF receptor-associated factor 6 (TRAF6) to activate NF-κB, p38, ERK and JNK signalling pathways that drive the expression of pro-inflammatory genes (Gabay et al., 2010).

IL-1α and IL-1β exert a plethora of diverse effects on the immune system. They stimulate the production of many pro-inflammatory cytokines, including themselves, thereby creating an auto-amplifying inflammatory loop. IL-1- signalling also upregulates adhesion molecule expression by endothelial cells to aid leukocyte recruitment, and influences adaptive immunity by driving T_H17 cell differentiation, promoting B cell and T cell expansion and survival, and upregulating MHC expression on dendritic cells to enhance their antigen presenting capacity (Sims and Smith, 2010). Furthermore, IL-1 promotes the

production of enzymes that stimulate the release of prostaglandins and nitric oxide, which contribute to systemic changes including hypotension, fever, neutrophilia and thrombocytosis (Gabay et al., 2010).

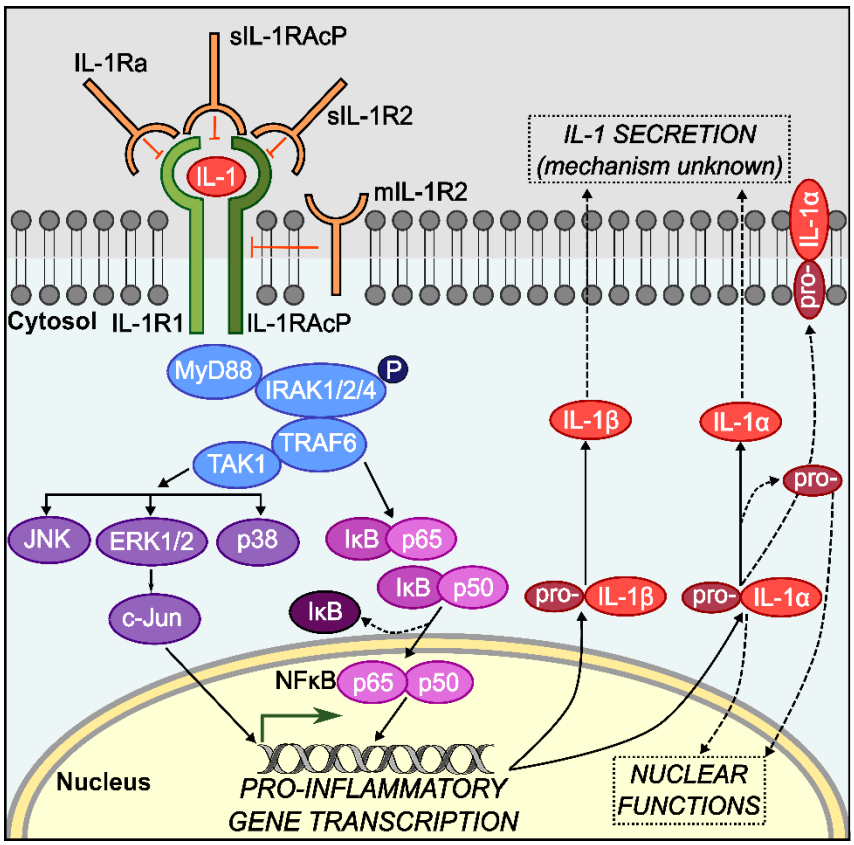

Figure 1.6: The IL-1 signalling pathway. Adapted from (Risbud and Shapiro, 2014). IL-1 forms a complex with IL-1R1 and IL-1RAcP to activate a MyD88-dependent phosphorylation cascade that activates NF-κB and MAPK signalling pathways, which drive the transcription of pro-inflammatory genes including IL-1. Both forms of IL-1 are translated as pro-proteins that are proteolytically activated. Pro-IL-1α has limited basal activity, and can exist in a membrane-bound form that signals to adjacent cells. Negative regulators of IL-1 signalling are also shown.

1.2.3 IL-1 in disease

The dysregulation of IL-1 signalling is a major causative factor in a wide range of inflammatory diseases. The disease DIRA (Deficiency of IL-1RA), caused by a loss-of-function mutation in *IL1RN* that results in unconstrained IL-1 signalling, is characterised by overwhelming inflammation in the joints, skin and bone, and results in premature death when left untreated (Dinarello et al., 2012). IL-1 is also implicated in many inflammatory diseases because of its ability to drive the differentiation of T_H17

cells, a pro-inflammatory subset of CD4+ T cells that are important for the immune response to infection. As the name suggests these cells secrete the cytokine IL-17, which induces the production of a broad range of additional proinflammatory cytokines and chemokines that recruit neutrophils and macrophages to the site of infection. Inappropriate T_H17 cell activation has been shown to occur in multiple inflammatory disorders including arthritis, psoriasis and asthma (Nakae et al., 2002, Jenson, 2011, Sims and Smith, 2010, Besnard et al., 2012).

IL-1 driven inflammation is also known to play a major role in cardiovascular disease. Expression of both IL-1 and the IL-1R1 are increased in atherosclerotic plaques, where IL-1 signalling activates endothelial cells overlying and macrophages within the lesion (Ait-Oufella et al., 2011). In addition, IL-1 is thought to drive cardiovascular events in diabetic patients, where pancreatic beta cells produce excess IL-1β that in turn contributes to beta cell death. The consequent IL-1 signalling also affects the heart by both directly supressing the contractile force of the muscle, thereby weakening the heart, and propagating an inflammatory cascade that leads to cardiomyocyte death (Dinarello et al., 2012).

IL-1 signalling also contributes to inflammatory disease in epithelial tissues where resting cells constitutively express high levels of IL-1 to facilitate their barrier function. For example IL-1 is thought to enhance the release of T cell chemoattractants by keratinocytes and contribute to the formation of psoriatic lesions (Jenson, 2011). Similarly, increased IL-1α and IL-1β levels are found in the inflamed intestinal mucosa of inflammatory bowel disease patients (Casini-Raggi et al., 1995).

Because of these well-established causative roles in inflammatory disease, IL-1 is an attractive therapeutic target (Table 1.2). Anakinra is a recombinant form of the IL-1RA that is used clinically to treat rheumatoid arthritis, recurrent gout, and CAPS, and is in clinical trials for the treatment of other inflammatory disorders including stroke (Dinarello et al., 2012). Canakinumab, a human monoclonal antibody against IL-1β that is already used to treat systemic onset juvenile idiopathic arthritis, has been shown to significantly reduce the rate of recurrent cardiovascular events in heart attack patients with elevated C-reactive protein (CRP) levels in the recent CANTOS study (Canakinumab Anti-inflammatory Thrombosis Outcomes Study). The study also showed that patients treated with

Canakinumab were at lower risk of other inflammatory pathologies including arthritis, gout and cancer (Ridker et al., 2017). Both Anakinra and Canukinumab are also currently in trials for treating type I diabetes (Dinarello et al., 2012).

Table 1.2: Anti-IL-1 Therapies *Adapted from (Dinarello et al., 2012)*

DRUG NAME	MECHANISM OF ACTION
Anakinra	Receptor antagonist for IL-1R1
Rilonacept	Soluble IL-1 decoy receptor composed of the extracellular IL-1R1 domain fused with the extracellular domain of IL-1RAcP
Canakinumab	Neutralising anti-IL-1β antibody
Gevokizumab	Neutralising anti-IL-1β antibody
LY2189102	Neutralising anti-IL-1β antibody
MABp1	Neutralising anti-IL-1α antibody
MEDI-8968	Blocking anti-IL-1R1 antibody
CYT013	Therapeutic vaccine targeting IL-1β
sIL-1R1	Soluble extracellular domain of IL-1R1
EBI-005	Chimeric IL-1Ra-IL-1β

1.3 Interleukin-1 alpha: stepping into the spotlight

1.3.1 IL-1α-specific functions

Most initial IL-1 research largely focussed on IL-1β, with our understanding of IL-1α biology developing more recently. IL-1α has a higher affinity for the signalling receptor IL-1R1, and a lower affinity for the decoy receptor IL-1R2 than IL-1β. In addition IL-1α, unlike IL-1β, is constitutively expressed in the cytosol of many cell-types and therefore serves as an inflammation-inducing DAMP when it is released during necrosis. Furthermore, unlike many other DAMP receptors, IL-1R1 is expressed on most cell types meaning that IL-1α can also activate non-immune cells. Consistent with this function, endothelial and epithelial cells, which form key immune barriers within the body, express particularly high constitutive levels of IL-1α (Di Paolo and Shayakhmetov, 2016).

Pro-IL-1α can also be expressed on the cell surface. Membrane-bound IL-1α regulates the senescence-associated secretory phenotype (SASP); the cocktail of inflammatory factors released by senescent cells that is the focus of Chapter 6 of this thesis (Orjalo et al., 2009). This is particularly important in the context of the tumour microenvironment, where the IL-1α driven SASP induces anti-tumour immune cell recruitment, but enhances cancer cell invasiveness (Coppé et al., 2010). Membrane IL-1α has also been reported to inhibit hepatocellular carcinoma development by promoting T- and NK- cell activation (Lin et al., 2016).

IL-1α has gained recognition as a 'dual function cytokine' because it elicits intracellular effects in addition to its extracellular inflammatory signalling. The intracellular activity of IL-1α is reported to be mediated by the pro-domain, which contains a nuclear localisation signal (NLS) (Wessendorf et al., 1993). Pro-IL-1α has been reported in the nucleus of many cell types (Luheshi et al., 2009) where it can act as a transcription factor by binding regulatory elements such as the histone acetyltransferase proteins p33, Gcn5 and PCAF, and colocalising with spliceosome complexes (Buryskova et al., 2004, Pollock et al., 2003). It is reported that intranuclear IL-1α regulates a number of processes including proliferation, apoptosis and migration (Luheshi et al., 2009), with oncogenic properties also reported in perivascular mesangial cells and acute T-lymphocytic leukaemia cells (Stevenson et al., 1997, Zhang et al., 2017). Nuclear IL-1α is also reported to function as a DNA damage sensor, and has been shown to localise to areas of DNA damage and shuttle in and out of the nucleus to signal chromatin damage (Cohen et al., 2015).

1.3.2 The regulation of IL-1α activity

It is perhaps not surprising, given the powerful inflammatory effects of IL-1α, that its activity is carefully regulated. Transcriptionally, *IL1A* expression is upregulated by signals of cellular insult such as LPS and TNFα (Dinarello, 2009). However, cell-specific mechanisms of transcriptional control are also in place. In monocytes, a natural antisense transcript known as AS-IL1α is induced following infection, which promotes the recruitment of RNA polymerase II to the IL-1α promoter to enhance transcription

(Chan et al., 2015). In CD4+ T cells, IL-1α expression is monoallelic and controlled by modulating the methylation status of CpG nucleotides in the promoter (Van Rietschoten et al., 2006). In pancreatic islet cells, the microRNA miR-30a binds to the 3' untranslated region (UTR) of the *IL1A* gene and inhibits transcription to prevent overt cytokine activation during inflammation (Jiang et al., 2017). Importantly, an increase in IL-1α transcription does not always correspond to an increase in translation, since N-terminal AU-rich elements (ARE) in *IL1A* regulate mRNA decay (Fenton, 1992).

IL-1α is translated as a pro-protein, the activity of which has remained a controversial subject within the IL-1α field. For many years, pro-IL-1α was considered fully active (March et al., 1985, Mosley et al., 1986, Kim et al., 2013), even after it was established as a substrate of the calcium-dependent cysteine protease calpain (Kobayashi et al., 1990). However, recent work by ourselves and others has challenged this notion and provided compelling evidence that the proteolytic removal of the pro-domain significantly increases IL-1α activity by enhancing its affinity for the IL-1R1 (Afonina et al., 2011, Zheng et al., 2013).

IL-1α activity is also regulated spatially. During apoptosis, IL-1α is rapidly shuttled into the nucleus where it associates with chromatin to limit its release and maintain the anti-inflammatory nature of programmed cell death (Cohen et al., 2010). IL-1α is also controlled in a cell-type dependent manner by the decoy receptor IL-1R2. This receptor lacks the intracellular TIR domain critical for IL-1RAcP and MyD88 recruitment and therefore cannot propagate the IL-1 signal. IL-1R2 binds to pro- and mature IL-1α, and limits interaction with calpain and IL-1R1, respectively. This interaction is abrogated by caspase-1 and -5 following cell activation and inflammasome assembly. Interestingly, vascular smooth muscle cells (VSMCs) express very low levels of IL-1R2 and consequently they are particularly inflammatory following necrosis (Zheng et al., 2013). IL-1 signalling is also negatively regulated by the receptor antagonist IL-1RA, which prevents recruitment of the IL-1RAcP into the receptor complex.

1.3.3 IL-1α in disease

The distinct expression patterns and functions of IL-1α are reflected by its unique contributions to disease. IL-1α has emerged as a key player in atherosclerosis development, where the deletion of IL-1α

in the *ApoE*$^{-/-}$ mouse model provides more protection against disease than IL-1β deletion (Kamari et al., 2011). A possible mechanism for this involves oleic acid, which accumulates within the plaque as atherosclerosis progresses. Oleic acid triggers IL-1α, not IL-1β, secretion from macrophages via the mitochondrial uncoupling protein UCP2. The uncoupling of the mitochondrial membrane leads to a calcium flux within the macrophages, allowing activation of IL-1α by calpain. Since this mechanism bypasses the inflammasome, oleic acid accumulation during plaque development shifts IL-1 release from IL-1β towards IL-1α (Freigang et al., 2013). In addition IL-1α is described to play a unique role in myocardial infarction where necrotic cardiomyocytes secrete IL-1α, not IL-1β, to drive post-ischemic inflammation (Lugrin et al., 2015). Indeed, IL-1α blockade after ischemia-reperfusion injury reduces infarct size and preserves left ventricular fractional shortening in mice (Mauro et al., 2017). Similarly, IL-1α is released before IL-1β by microglia during cerebral ischaemia, suggesting that this form of IL-1 is key to initiating sterile inflammation after stroke (Luheshi et al., 2011).

IL-1α also contributes to the pathology of other inflammatory diseases. For example, chronic inflammation that drives neuronal cell death in Alzheimer's disease is thought to be driven by IL-1α, since a SNP within the *IL1A* gene is associated with disease risk. IL-1α has also been implicated in tumour progression and is associated with multiple hallmarks of cancer. In addition to its key role in SASP production discussed previously, membrane IL-1α on tumour-infiltrating platelets activates the vascular endothelium to promote transendothelial tumour cell migration (XBiotech, 2012). Furthermore, IL-1α is a HIF-inducible factor that is upregulated during hypoxia (Rider et al., 2012) and promotes angiogenesis (Voronov et al., 2002). The secreted form of IL-1α has also been shown to enhance tumour growth and invasiveness, (Rider et al., 2013), and serves as a predictive marker of distant metastases in head and neck squamous cell carcinoma patients (León et al., 2015). Increased IL-1α levels have also been shown to contribute to a number of autoimmune diseases, including rheumatoid arthritis, psoriasis, and systemic sclerosis (Eastgate et al., 1991, Rider et al., 2013, Aden et al., 2010). The importance of IL-1α in disease is reflected by the success of mABp1 (Xbiotech), a monoclonal anti-IL-1α antibody reported to reduce inflammation in advanced stage cancers, psoriasis and acne, and prevent artery

restenosis after angioplasty (Hong et al., 2014, Coleman et al., 2015, Carrasco et al., 2015, El Sayed et al., 2016).

IL-1α is an extremely powerful pleotropic cytokine that is dysregulated in multiple inflammatory diseases, and therefore increasing our understanding of how activity is regulated could reveal novel therapeutic opportunities. This is the aim of the work presented in this thesis, which investigates novel genetic and proteolytic mechanisms regulating IL-1α activity.

1.4 PROJECT AIMS

This PhD thesis has two main objectives:

1. To investigate the inhibitory role of the IL-1α pro-domain and identify novel proteases that can activate IL-1α.

The biological activity of pro-IL-1α has been a controversial subject in the IL-1α field for many years. Recent evidence from ourselves and others has demonstrated that the removal of the pro-domain increases IL-1α activity. This project aims to determine how much of the pro-domain is required to limit IL-1α activity, identify novel proteases that activate IL-1α, and investigate physiological and pathological processes in which these newly-identified enzyme/substrate interactions might occur.

2. To investigate the effect of the common *IL1A* SNP, rs17561, on IL-1α activation. A relatively common missense polymorphism exists in the *IL1A* gene, which leads to an amino acid change in the IL-1α protein at a location important for cytokine activation. This project aims to determine whether the rs17561 SNP affects IL-1α activation.

Materials and Methods

2. Materials and Methods

2.1 Molecular cloning

2.1.1 Site-directed mutagenesis

Human/mouse pro-IL-1α/β or human caspase-5 DNA was amplified by PCR and inserted into pGEX-4T-3 (GE Healthcare, 28-9545-52) and pcDNA3.1 (Invitrogen, V79020) vectors by Melanie Humphry. Individual cleavage site mutants and the rs17561 SNP were introduced by site-directed mutagenesis using the primers listed in Table 2.1. The PCR mix included 30ng DNA, 5µl 10x buffer with magnesium (Promega, M776A), 1µl dNTPs (10mM each), 1.35µl each primer, 7µl Pfu DNA Polymerase (Promega, M774A) and water to a final volume of 50µl. The PCR programme comprised 12 cycles of 30 seconds at 95ºC, 1 minute at 55ºC and 7 minutes at 68ºC. The parental DNA strand was digested with 1µl Dpn1 endonuclease (Promega, R6231) for 1 hour at 37ºC.

2.1.2 Bacterial transformation and plasmid purification

100µl of competent XL10 Gold *Escherichia coli (E.coli)* (Stratagene) were transformed with 5µl plasmid for 30 minutes on ice, 45 seconds at 42ºC and 90 seconds on ice. Bacteria were plated on Luria Broth (LB) Agar containing 100µg/ml Ampicillin (Sigma Aldrich, A9518) (LBAmp) overnight at 37ºC. 3ml LBAmp broth was inoculated with a single colony of transformed bacteria and incubated overnight at 37ºC with shaking. Plasmid DNA was purified using a Miniprep Kit (Qiagen, 27106) as per the manufacturer's instructions and sequenced (Source Bioscience).

Box 2.1: Bacterial Culture Recipes

Luria broth (LB)	***LB agar***
10g Tryptone (BD Bacto, 211705) 5g Yeast Extract (BD Bacto, 212750) 10g NaCl (Sigma Aldrich, 433209) 1L ddH_2O pH7.5	15g of Agarose (Fischer, BP1356-500) 1L LB 100µg/ml Ampicillin was added after autoclaving

2.1.3 Truncation mutant and His-tag mutagenesis

Insert DNA was amplified by PCR; mixing 30ng DNA, 5µl 5x GoTaq buffer (Promega, M7911), 1.25µl $MgCl_2$ (Promega, A3511), 0.5µl dNTPs (10mM each), 1µl each primer (Table 2.1), 0.5µl GoTaq polymerase (Promega, M3002), 0.5µl Pfu polymerase (Promega, M7741) and water up to 25µl. The PCR programme comprised an initial denaturing step of 95º for 5 minutes, followed by 25 cycles of 30 seconds at 95ºC, 30 seconds at 55ºC and 90 seconds at 72ºC. dNTPs and template plasmid DNA were removed by an ethidium bromide (EtBr) gel clean-up (1% agarose/ 1xTBE), and plasmid DNA was extracted using a QiaQuick Gel Extraction kit (Qiagen, 28704). The insert was ligated into a pre-cut pGEMTEasy vector (Promega, A1360) by mixing 30ng insert, 0.5µl vector, 1.5µl 10x ligation buffer (Promega, C126), 1µl T4 DNA ligase (Promega, M1801) and water up to 15µl. XL10 Gold *E.coli* were transformed with 10µl ligation mix as described previously and a colony PCR was used to identify insert-positive bacteria. The colony PCR mix included 2.5µl 5xGoTaq buffer, 0.75µl $MgCl_2$, 0.25µl dNTPs, 0.5µl each primer (Table 2.1), 0.25µl Taq polymerase and 8.25µl water, and was amplified using the same programme as before. The PCR mixes were run on an EtBr gel and 3ml overnight cultures were inoculated with ligation-positive colonies. Plasmid DNA was purified using a Miniprep Kit and sequenced. The insert was removed from the pGEM-T vector by restriction digest. 1.3µg plasmid DNA, 3µl 10 Buffer C (Promega, R003A), 1.5µl 20x Bovine Serum Albumin (BSA) (Invitrogen, AM2616), 1µl BamH1 (Promega, R302A), 1µl XhoI (Promega, R616A) and water up to 30µl were mixed and incubated for 1 hour at 37ºC. The insert was cleaned up by EtBr gel, extracted, and quantified as before. The insert was ligated into a pre-cut pGEX-4T-3 vector as described previously. XL10 Gold bacteria were transformed and ligation-positive colonies were identified by colony PCR as before, and used to generate plasmid stocks.

Box 2.2: TBE recipe
5x TBE 54g Tris Base 27.5g Boric acid 20ml 0.5 M EDTA, pH 8.0 Made up to 1L with ddH_2O

Table 2.1: Molecular Cloning Primers

GENE	MUTATION	PRIMER SEQUENCES (5'-3')
Human IL-1α	Δ37 Truncation Mutant	F: ATA*GGATCC*GTAAGCTATGGCCCACTCCA R: ATACTCGAGTAAAGCCTGGTTTTCCAGTAT
	Δ56 Truncation Mutant	F: ATA*GGATCC*TCTGAAACCTCTAAAACATC R: ATACTCGAGTAAAGCCTGGTTTTCCAGTAT
	Δ77 Truncation Mutant	F: ATA*GGATCC*GGGAAGGTTCTGAAGAAGAG R: ATACTCGAGTAAAGCCTGGTTTTCCAGTAT
	Colony PCR Primers	F: CAGGAAACAGCTATGACC R: TGTAAAACGACGGCCAGT
	P111A Site Mutant	F: GAAGAAATCATCAAGGCTAGGTCAGCACCTT R: AAGGTGCTGACCTAGCCTTGATGATTTCTTC
	P115A Site Mutant	F: AAGCCTAGGTCAGCAGCTTTTAGCTTCCTGA R: TCAGGAAGCTAAAAGCTGCTGACCTAGGCTT
	D103A Site Mutant	F: GAGGCCATCGCCAATGCCTCAGAGGAAGAAATC R: GATTTCTTCCTCTGAGGCATTGGCGATGGCCTC
	A114S Site Mutant	F: ATCAAGCCTAGGTCATCACCTTTTAGCTTCCTG R: CAGGAAGCTAAAAGGTGATGACCTAGGCTTGAT
	Addition of C-terminal His Tag	F: ATAGGATCCATGGCCAAAGTTCCAGACATG R: ATA*CTCGAG*GTGGTGGTGGTGGTGGTGTAAAGCCTGGTTTTC CAGTAT
Human IL-1β	D116A Site Mutant	F: GAGGCTTATGTGCACGCTGCACCTGTACGATCA R: TGATCGTACAGGTGCAGCGTGCACATAAGCCTC
Mouse IL-1α	D106A Site Mutant	F: CAGTCCATAACCCATGCTCTGGAAGAGACCATC R: GATGGTCTCTTCCAGAGCATGGGTTATGGACTG
	D26A Site Mutant	F: TACAGTTCTGCCATTGCCCATCTCTCTCTGAAT R: ATTCAGAGAGAGATGGGCAATGGCAGAACTGTA
	D37A Site Mutant	F: CAGAAATCCTTCTATGCTGCAAGCTATGGCTCA R: TGAGCCATAGCTTGCAGCATAGAAGGATTTCTG
	D49A Site Mutant	F: CATGAGACTTGCACAGCTCAGTTTGTATCTCTG R:CAGAGATACAAACTGAGCTGTGCAAGTCTCATG
Mouse IL-1β	D116A Site Mutant	F: AACCTGCTGGTGTGTGCCGTTCCCATTAGACAA R: TTGTCTAATGGGAACGGCACACACCAGCAGGTT
	D88A Site Mutant	F: ACCTTCCAGGATGAGGCCATGAGCACCTTCTTT R: AAAGAAGGTGCTCATGGCCTCATCCTGGAAGGT
	D105A Site Mutant	F: GAGCCCATCCTCTGTGCCTCATGGGATGATGAT R: ATCATCATCCCATGAGGCACAGAGGATGGGCTC
Mouse *CASP 11*	shRNA 140	F:*TCGAGAAGGTATAT*TGCTGTTGACAGTGAGCGCAAGCAATGTACTG AAATTAAATAGTGAAGCCACAGATGTATTTAATTTCAGTACATTGCT TTTGCCTACTGCCTCGG R:*AATT*CCGAGGCAGTAGGCAAAAGCAATGTACTGAAATTAAATACA TCTGTGGCTTCACTATTTAATTTCAGTACATTGCTTGCGCTCACTGTC AACAGCA*ATATACCTTC*
	shRNA 710	F:*TCGAGAAGGTATAT*TGCTGTTGACAGTGAGCGATCCAGATGTGCTAC AGTATGATAGTGAAGCCACAGATGTATCATACTGTAGCACATCTGGA GTGCCTACTGCCTCGG R:*AATT*CCGAGGCAGTAGGCACTCCAGATGTGCTACAGTATGATACAT CTGTGGCTTCACTATCATACTGTAGCACATCTGGATCGCTCACTGTCA ACAGCA*ATATACCTTC*

	shRNA 731	F:*TCGAGAAGGTATAT*TGCTGTTGACAGTGAGCGCTACCATCTATCAGA TATTCAATAGTGAAGCCACAGATGTATTGAATATCTGATAGATGGTA TTGCCTACTGCCTCGG R:*AATT*CCGAGGCAGTAGGCAATACCATCTATCAGATATTCAATACAT CTGTGGCTTCACTATTGAATATCTGATAGATGGTAGCGCTCACTGTC AACAGCA*ATATACCTTC*
	shRNA 1124	F:*TCGAGAAGGTATAT*TGCTGTTGACAGTGAGCGCTCGGGCAACCTTGA CGAGATATAGTGAAGCCACAGATGTATATCTCGTCAAGGTTGCCCGA TTGCCTACTGCCTCGG R:*AATT*CCGAGGCAGTAGGCAATCGGGCAACCTTGACGAGATATACA TCTGTGGCTTCACTATATCTCGTCAAGGTTGCCCGAGCGCTCACTGTC AACAGCA*ATATACCTTC*
	shRNA 1160	F:*TCGAGAAGGTATAT*TGCTGTTGACAGTGAGCGATGGCAACTGAGAA CAAAGCAATAGTGAAGCCACAGATGTATTGCTTTGTTCTCAGTTGCC AGTGCCTACTGCCTCGG R:*AATT*CCGAGGCAGTAGGCACTGGCAACTGAGAACAAAGCAATACA TCTGTGGCTTCACTATTGCTTTGTTCTCAGTTGCCATCGCTCACTGTC AACAGCA*ATATACCTTC*
shRNA sub-cloning	miR30_5_XhoI	GAAGG*CTCGAG*AAGGTATATTGCTG
	Mir30_3_XmaI	CGG*CCCGGG*GTGATTTAATTTATACCATTTTAATTCAGCT

Mutated residues are underlined. Restriction enzyme sites are in *italic*.

2.1.4 shRNA Vectors

2.1.4.1 Lentiviral knockdown

Plasmids were purchased in the form of frozen glycerol stocks (Table 2.2). The glycerol stocks were streaked onto LB Agar containing 100µg/ml carbenicillin (LBCarb100) and incubated overnight at 37ºC. 3 colonies per plate were used to inoculate 6ml overnight cultures in 2X LB and incubated overnight at 37ºC with vigorous shaking. The plasmids were isolated from 5ml overnight culture by miniprep.

Box 2.3: 2X LB Broth
10g tryptone 10g yeast extract 5g NaCl 10g peptone (BD, 211677)

Table 2.2: shRNA plasmid clones

TARGET	The RNA Consortium (TRC) Code	Shorthand Code
Human Caspase 1	TRCN0000003502	2
	TRCN0000003503	3
	TRCN0000003504	4
	TRCN0000010796	6
Human Caspase 4	TRCN0000003511	84
	TRCN0000003513	86
Human Caspase 5	TRCN0000003553	89
	TRCN0000003555	90

2.1.4.2 Retroviral knockdown

The *Casp11*-targetting shRNA constructs were cloned by Aled Parry. Briefly:

J2 cells

The primers in table 2.1 containing the guide sequences were cloned into the MSCV miR30 backbone by Aled Parry. Briefly, equimolar amounts of forward and reverse primer were annealed in annealing buffer by incubation in a thermal cycler at 95ºC for 5 minutes, before gradually reducing the temperature (0.5ºC/2.5min) to 4ºC. MSCV miR30 was digested using *XhoI* and *EcoR1* before ligating with the annealed oligonucleotides using T4 DNA ligase (New England Biolabs, M0202).

Box 2.4: Annealing buffer
100mM potassium acetate 30mM HEPES-KOH pH7.4 2mM Mg-acetate

2.1.4.3 Hydrodynamic Tail Vein Injection

The selected construct was sub-cloned into pCaNIG miR30 (gifted by Lars Zender) by PCR cloning the 3' portion of miR30-shCASP11 using the primers in Table 2.1. The vector and PCR products were digested using XhoI and XmaI, and ligated with T4 DNA ligase.

2.2 Bacterial protein expression

100µl BL21 Rosetta *E.coli* were transformed with 100ng plasmid DNA, plated on LBAmp and incubated at 37ºC overnight. 50ml cultures were inoculated with a single colony and incubated at 37ºC overnight with vigorous shaking. 500ml cultures were inoculated with 5ml overnight culture and grown to OD_{600}=0.8 at 37ºC with vigorous shaking. Protein expression was induced with 1mM Isopropyl-β-D-1-thiogalactopyranoside (IPTG) (Generon, S-02122) for 4 hours at room temperature. Bacteria were centrifuged at 5100rpm for 15 minutes at 4ºC and pellets were stored at -80ºC.

2.3 Purification of GST-tagged protein

250ml bacterial pellets were lysed by rolling in 25ml lysis buffer for 30 minutes. Lysed bacteria were sonicated at 35% amplitude for 1 minute followed by 1 minute on ice, 3 times. The lysate was centrifuged for 1 hour at 4ºC at 5100rpm, and the supernatant was filtered (0.45µm). The supernatant was loaded onto a GSTrap FF 1ml glutathione column (GE Healthcare, 17513001), washed, and eluted using an ÅKTA Pure Fast Protein Liquid Chromatography (FPLC) System (GE Healthcare). The eluted protein was dialysed overnight in 10mM Tris pH8 50mM NaCl. Proteins were stored in 10% Glycerol at -80ºC.

Box 2.5: GST purification buffer recipes

Lysis buffer	***Wash buffer***	***Elution buffer***
In PBS [1 PBS Tablet (Oxoid) per 100ml ddH2O]: 150mM NaCl 1mM dithiothreitaol (DTT) (Sigma Aldrich, D9779) 1mM EDTA (Sigma Aldrich, E5134) 10µM phenylmethylsulfonyl fluoride (PMSF) (Sigma Aldrich, P1626) Protease inhibitor cocktail (Sigma Aldrich, P8849) (1:100) 100U/ml Benzonase (Sigma Aldrich, E1014) 100U/ml Lysozyme (Novagen, 71110-3)	In PBS: 1mM DTT 1mM EDTA	50mM Tris (Sigma Aldrich, T6006) pH8 100mM NaCl (Fischer, S/3160/60) 1mM DTT 50mM L-Glutathione reduced (Sigma Aldrich, G4251)

2.4 Purification of His-tagged protein

Cell pellets were resuspended in 10 packed-cell volumes of ice cold lysis buffer and incubated at room temperature for 5 minutes. Cells were centrifuged at 8000g for 20 minutes at 10°C. The supernatant was taken for purification.

50% HisPur Cobalt Resin (Fisher, 89964) was prepared by washing once with water and then resuspending in wash buffer 1. Resin was mixed with cell supernatant at a ratio of 1:6 and rolled for 1 hour at 4°C. Samples were centrifuged at 700g for 2 minutes and resuspended in wash buffer 1. Samples were centrifuged at 700g for 2 minutes and resuspended in wash buffer 2. Samples were centrifuged at 700g for 2 minutes and resuspended in elution buffer. Samples were centrifuged at 700g for 2 minutes and protein-containing supernatents were collected for further experiments.

Box 2.6: His purification buffer recipes

Lysis Buffer 25mM Tris pH7.4 0.5% NP-40 (AppliChem Panreac, A16940250) 150mM NaCl 120µM Calpeptin (Enzo, BML-P1101-0010) Protease inhibitor cocktail (Sigma Aldrich P8849) (1:100) 1µl/ml benzonase (Sigma Aldrich, E1014)	***Wash buffers*** 50mM Sodium Phosphate pH7.4 300mM NaCl 20mM (Wash 1) or 40mM (Wash 2) Imidazole
Elution buffer 50mM Sodium Phosphate pH7.4 300mM NaCl 250mM Imidazole	

2.5 Protein concentration normalisation

2.5.1 Bradford assay

BSA standards (0-2mg/ml) and protein dilutions were prepared in 10mM Tris pH8 50mM NaCl. 10µl sample/standard and 200µl dye (Sigma, B6916) were added per well of a 96-well plate. Samples were incubated at room temperature for 15 minutes and absorbance at 595nm was read.

2.5.2 SDS PAGE and Coomassie staining

Protein were diluted in 3x lamelli buffer. Concentrations were estimated and normalised to each other by SDS PAGE and Coomassie staining. Proteins were resolved on an SDS PAGE gel consisting of a stacking gel and 15% separation gel. The gel was then rinsed with water and incubated in IRDye® Blue Protein Stain (LiCor, 928-40002) for 30 minutes and destained with water. The Odyssey imager (Li-Cor) was used to measure the intensity of the infra-red coomassie pro-IL-1α/β bands and concentrations were adjusted accordingly and compared to known concentrations of BSA.

Box 2.7: SDS-PAGE buffer recipes

1x Laemmli 0.8ml Tris 1M pH 6.8 1ml 20% SDS (Sigma Aldrich, 75746) 1ml glycerol 0.53ml β-mercaptoethanol (Sigma Aldrich, M6250) 5mg bromophenol blue (Sigma Aldrich, 114391) Made to 10ml with ddH_2O	***3x Laemmli*** 2.4ml Tris 1M pH 6.8 3ml 20% SDS 3ml glycerol 1.6ml β-mercaptoethanol 5mg bromophenol blue Made to 10ml with ddH2O
Stacking gel 3.9ml ddH_2O 300µl 1M Tris pH6.8 50µl 10% sodium dodecyl sulphate (SDS) 700µl 30% Bis/Acrylamide (Biorad, 161-0158) 25µl 100mg/ml ammonium persulphate (APS) (Thermofisher, 17874) 10µl TEMED (Biorad, 1610801)	***15% separating gel*** 3ml water 2ml 2M Tris pH8.8 100µl 10% SDS 5ml 30% Bis/Acrylamide 50µl 100mg/ml APS 25µl TEMED
Anode Buffer 30g Tris 5g SDS 5L H2O pH 8.6	***Cathode buffer*** 144g glycine 30g Tris 5g SDS 5L H2O pH 8.6

2.6 Cell culture

2.6.1 HeLa, HEK-293T, human aortic vascular smooth muscle (VSMC) and mouse fibroblast cells

Cells were cultured in Dulbecco's Modified Eagle Medium (DMEM) (Sigma Aldrich, D5671) with 10% foetal calf serum (FCS), 10U/ml penicillin, 10mg/ml streptomycin and 5mg/ml L-glutamine. Cells were passaged at 80% confluence using trypsin (Sigma Aldrich, T4049)

2.6.2 THP-1, U937 and J2 cells

Cells were cultured in Roswell Park Memorial Institute (RPMI) 1640 Medium (Gibco, 31870-025) with 10% FCS, 10U/ml penicillin, 10mg/ml streptomycin and 5mg/ml L-glutamine. Cells were passaged to maintain a cell density of $2x10^5$ cells/ml.

2.6.3 Primary human macrophages

Peripheral blood mononuclear cells (PBMCs) and serum were generously provided by members of Edwin Chilvers' group (Department of Medicine, University of Cambridge) following blood separation by ficoll density gradient centrifugation. Cells were washed with Iscoves Modified Eagle Medium (IMEM) (Gibco, 21980) and centrifuged at 220g for 5 minutes. Cells were resuspended to $4x10^6$ cells/ml and plated at 4ml/6-well or 500µl/48-well. Cells were incubated at 37°C for 1 hour, and non-adherent lymphocytes were washed away by pipetting. Cells were maintained in IMEM with 10% autologous serum, 10U/ml penicillin, 10mg/ml streptomycin and 5mg/ml L-glutamine for 6-7 days until macrophage-like.

2.6.4 IMR90 fibroblasts

IMR90 cells were cultured in phenol red free DMEM (Invitrogen, 31053) supplemented with 10% L-Glutamine (Invitrogen, 25030-024), pyruvate (Invitrogen, 11360-070), penicillin, streptomycin and FCS.

2.6.5 Murine bone marrow-derived macrophages

Bone marrow-derived macrophages (BMDM) from wild-type, *Casp11*$^{-/-}$ or *Casp1*$^{-/-}$*Casp11*^{Tg} mice (C57BL6/J background, 8-12 weeks old) were differentiated in RPMI 1640 with penicillin, streptomycin, L-glutamine and 10% FCS and 15% L929 conditioned media.

2.7 Cell transfection

2.7.1 Overexpression

HEK-293T or HeLa cells were plated at 300,000 cells/well in a 6-well plate and incubated overnight at 37°C. Plasmids and Fugene-HD (Promega, E2311) were mixed at a ratio of 1µg:3µl in a 200µl solution of Optimem medium (Gibco, 31985062), vortexed briefly, and incubated at room temperature for 20 minutes. 100µl of plasmid/fugene was added per well, dropwise. Transfected cells were incubated for 2 days at 37°C before further treatment.

THP-1 and U937 cells were nucleofected with the Amaxa (Lonza) using the Cell Line Kits V (Lonza, VCA-1003) and C (VCA-1004) respectively. $1x10^6$ cells were resuspended in 100µl supplemented nucleofector solution. 2µg plasmid DNA was added to the cells, which were transferred to a cuvette and nucleofected using the programme U-001 for THP-1s or W-001 for U937s. 500µl warm media was added directly to the cuvette, and the cells were then transferred to 1ml pre-warmed media containing 100ng/ml PMA (Sigma, 16561-29-8) in a 12-well plate and incubated at 37°C overnight before treatment.

2.7.2 siRNA delivery

Knockdown in primary macrophages was performed with 10pmol of non-targeting or *CASP5*-targeted siGENOME siRNA pool (Dharmacon), whilst knockdown in IMR90s was performed with 10pmol of individual siGENOME siRNAs (Table 2.3), using Lipofectamine RNAiMAX (Invitrogen, 13778030) as per the manufacturer's instructions.

Table 2.3: siRNAs (siGENOME, GE Dharmacon)

GENE	PROBE TYPE	CATALOGUE NUMBER
CASP5	*SMARTPool*	M-004405-02-0005
	Individual	D-004405-19-0002 (si1)
	Individual	D-004405-20-0002 (si2)
CASP4	*Individual*	D-004404-01-0002 (si1)
	Individual	D-004404-02-0002 (si2)
GSDMD	*Individual*	D-016207-01-002 (si1)
	Individual	D-016207-19-002 (si2)
cGAS	*Individual*	D-015607-01-0002 (si1)
	Individual	D-015607-02-0002 (si2)

2.8 Lentiviral caspase knockdown

2.8.1 Producing lentivirus

HEK293T cells were grown to 50-70% confluency. For each tube, 1.6ml optimem and 42µl TransIT 2020 (Mirus, MIR5400) were mixed and incubated for 5 minutes at room temperature. 4µg BYE (gifted by Jane Goodall), 4µg VSVg (gifted by Jane Goodall) and 6µg shRNA plasmid were added to each tube, vortexed and incubated at room temperature for 15 minutes. The mix was transferred to 12ml warm RPMI media supplemented with 10% FCS, 10U/ml penicillin, 10mg/ml streptomycin and 5mg/ml L-glutamine. The plasmid-containing media was applied onto a T75 flask of HEK-293T cells. The media was replaced after 24 hours, and the 24 and 48 hour supernatants were pooled. The virus particles were pelleted by ultracentrifugation using a superspin 360 rotor at 30,000g for 90 minutes at 4°C. Media was tipped into virkon, and the virus was resuspended in the residual medium and stored at -80°C.

2.8.2 THP-1 infection

$1x10^5$ THP-1 cells in 100µl media were seeded per well in a 96-well U-bottomed plate. 20µl virus was added per well and the plate was centrifuged at 2000rpm for 45 minutes at 37°C. Cells were transferred to 4ml warm media in a 6 well plate and incubated at 37°C for 72 hours. Transformed cells were selected using 1µg/ml puromycin for 72 hours.

2.9 Retroviral caspase knockdown

The retroviral infection of J2 cells was carried out by Aled Parry. Briefly, to produce retrovirus, amphotrophic phoenix packaging cells were transiently transfected using the calcium phosphate method. Cells were plated to achieve approximately 50-60% confluence the day before transfection. A DNA/$CaCl_2$ solution for each plate was prepared by mixing 250mM $CaCl_2$ with 15µg DNA vector in a total volume of 500µl before adding drop-wise to 500µl of BES buffered saline with continuous and vigorous mixing. The solution was added drop-wise to the phoenix packaging cells before overnight incubation. The media was changed and virus was allowed to accumulate for 24 hours.

Conditioned media from the phoenix packaging cells was filtered (0.45µm) and transferred to the target cells with 5µg/ml polybrene three times in a single day, 4 hours apart, replacing the phoenix cell media each time. Target cells were incubated for 12-18 hours before changing the media. Cells were incubated for 24 hours to allow transgene expression, and selected using 6µg/ml puromycin for 3 days.

Box 2.8: Retroviral infection buffer recipes
BES buffered saline 280mM NaCl 1.5mM $Na_2HO_4.2H_2O$ 50mM BES (NN-bis(2-hydroxyethyl)-2aminoethanesulphonic acid) pH6.95

2.10 Generation of necrotic cell lysates

500,000 VSMCs were washed twice with 500µl PBS and resuspended in 50µl serum-free DMEM with or without 3mM calpeptin (Enzo, BML-PI101-0010) as indicated. Cells were incubated for 20 minutes at 37°C. Cells were then resuspended in 50µl of enzyme-specific cleavage buffer (as indicated in Table 2.4) and freeze/thawed three times in liquid nitrogen. Cells were then centrifuged at maximum rpm to pellet debris, and the supernatant was taken for cleavage assays.

2.11 Protease cleavage assays

All cleavage assays were carried out using recombinant GST-p33 IL-1α / p33 IL-1β / pro-caspase-5 at 4µg/ml. Enzymes were used at the concentrations / units per reaction stated. Table 2.4 below lists buffer, temperature and incubation time for each enzyme unless otherwise stated in Figure legends. Inhibitors were prepared as described in Table 2.5 and used at concentrations stated in Figure legends.

Table 2.4: Enzyme cleavage assay conditions

ENZYME	SOURCE & CATALOGUE NUMBER	ASSAY BUFFER	ASSAY TEMPERATURE	ASSAY DURATION
Calpain	Merck, Calbiochem, Z08713	100mM NaCl 2mM $CaCl_2$ 1mM DTT	Room Temperature	1 hour
Thrombin	Merck, 69671-3	10X Buffer provided in kit	Room Temperature	2 hours
Chymase	Sigma Aldrich, C8118	27mM Tris pH7.7 150mM NaCl	Room Temperature	2 hours
Elastase	Enzo, BML-SE284-0100	50mM Tris pH8.8	Room temperature	2 hours
Granzyme B	Biovision, 7233-10	PBS	Room temperature	1 hour
Staphylococcus GluC	Peprotech, 450-46	10mM Tris pH8	Room temperature	2 hours
Cathepsin B	Enzo, BML-SE 198-0025	10mM Sodium Phosphate pH6 1.3mM EDTA 1mM DTT	40ºC	1 hour
Proteinase 3	Enzo, BML-SE498-0025	100mM MOPS pH 7.5 500mM NaCl 10% DMSO	Room temperature	1 hour
Proteinase K	Roche, 03115828011	PBS	Room temperature / on ICE	30 minutes
HIV Protease	Abcam, ab84117	50mM Tris pH 4.7	Room temperature	1 hour
FAPα	R&D, 3715-SE-010	50mM Tris pH 7.5, 1M NaCl, 1mg/ml BSA	Room temperature	1 hour
MMP2	Peprotech, 420-02	50mM Tris pH7.6 5mM $CaCl_2$ 1µM $ZnCl_2$	Room temperature	30 mins
MMP8	R&D, 908-MP-010	50mM Tris pH7.6 5mM $CaCl_2$ 1µM $ZnCl_2$	Room temperature	30 mins
MMP9	R&D, 911-MP-010	50mM Tris pH7.6 5mM $CaCl_2$ 1µM $ZnCl_2$	Room temperature	30 mins
C1s	R&D, 2060-SE-010	50mM Tris pH 8 250mM NaCl	Room temperature	1 hour
KLK5	R&D, 1108-SE-010	0.1M Sodium Phosphate pH 8	Room temperature	1.5hours
Caspase 14	Enzo, BML-SE417-5000	1.1M Sodium Citrate	Room temperature	2 hours
Human Caspases 1-10	Enzo, BML-AK010-0001	50mM HEPES pH7.4, 100mM NaCl, 0.1% CHAPS, 1mM EDTA, 10% glycerol, 10mM DTT	37ºC	1 hour
Murine Caspase 11	Enzo, BML-SE155-5000	100mM MES pH6.5, 0.1% CHAPS, 10% PEG (MW8KDa), 10mM DTT	Room Temperature	1 hour
Murine Caspase 1	Novus Biologicals, NBP1-99607	50mM HEPES pH7.2, 50mM NaCl, 0.1% CHAPS, 10mM EDTA, 5% Glycerol, 10mM DTT	Room temperature	1 hour

Table 2.5: Enzyme Inhibitors

INHIBITOR	SOURCE	COMMENTS
Calpeptin	Enzo, BML-P1101-0010	Used at 120µM unless otherwise stated
PPACK	Enzo, BML-PI117	Used at 100µM unless otherwise stated.
Thrombomodulin	R&D, 3947-PA	Reconstituted at 0.1mg/ml in sterile water. Used at 10:1 thrombomodulin:thrombin.
Fibrinogen	ThermoFisher, RP-43142	Reconstituted by layering on top of 37ºC PBS at 9mg/ml and gently agitating. Sterile filtered through a 0.2µm filter.
Z-LEVD-fmk	Enzo, ALX-260-142-R100	Used 600µM in recombinant protein assays and 20µM in cell-based assays
Z-YVAD-fmk	Enzo, ALX-260-154-R100	Used 600µM in recombinant protein assays and 20µM in cell-based assays
Z-VAD-fmk	Enzo, ALX-260-138-R100	Used 600µM in recombinant protein assays and 20µM in cell-based assays

2.12 Activating complement in human serum

10ml blood was drawn using a 21G needle into 1ml 3.8% pH7 sodium citrate and centrifuged at 280g for 20 minutes at room temperature. The platelet-rich-plasma (PRP) layer was removed and transferred into a 15ml falcon tube. 22µl/ml 1M $CaCl_2$ was added and the plasma was incubated at 37ºC until clotted. The tube was centrifuged at maximum speed for 1 minute and the serum was removed and stored at -20ºC. The serum was activated with 350µg/ml Zymosan in PBS pH7.5 0.15mM $CaCl_2$ 0.5mM $MgCl_2$ for 2 hours at 37ºC with/without 1mM PPACK.

2.13 Calpain plasma IL-1α reveal assay

20µl of plasma was incubated with either 5µl PBS or 4µl calpain + 1µl 60mM $CaCl_2$ for one hour at room temperature.

2.14 IL-1 activity assay

10,000 HeLa cells or mouse fibroblasts in 200µl full media were plated in a 48-well tissue culture plate and incubated at 37ºC overnight. Media was replaced, and treatments were added as indicated, with 2µg/ml of human IL-1α (Peprotech, 500-P21A), human IL-1β (Peprotech 200-01B), murine IL-1α (Peprotech, 211-11A) or murine IL-1β (Peprotech, 211-11B) antibody to demonstrate IL-1 dependent activity. IL-1R2 (R&D, 263-2F/CF) and/or IL-1RAcp (Sino Biologics, 10121-H08H) were pre-incubated for 20 minutes and added at the doses indicated. For each experiment, a negative control of media alone and a positive control of 10ng/ml recombinant human IL-1α (Peprotech, 200-010A) human IL-1β (R&D, AF-201-NA), murine IL-1α (R&D, AF-400-NA) or murine IL-1β (Peprotech, 500-P51) were included. Data were normalised to the positive control.

2.15 Inflammasome activation

Cells were primed in full media for 4 hours with 1µg/ml LPS-Ultrapure (Sigma) or 2µg/ml PAM3CSK4 (Invivogen, tlrl-pms) as indicated. For canonical inflammasome activation cells were treated with 5mM ATP (Invivogen, tlrl-atp) in Opti-MEM (Gibco, 31985062) for 16-18 hours. For non-canonical inflammasome activation, a 2x LPS fugene mix was prepared. Per 1ml optimem, 10µl 1mg/ml LPS ultrapure and 5µl Fugene-HD (Promega, E2311) were added. The mix was vortexed briefly and incubated at room temperature for 20 minutes. Cells were treated with an equal volume of optimem and LPS/fugene mix for 16-18 hours. Supernatants were taken for future analysis and cells were lysed in

either 0.5% NP-40 (Sigma, 7435) or lamelli buffer. Supernatants from murine BMDMs infected with C*hlamydia trachomatis* were generously provided by the Goodall group.

2.16 Senescent cell assays

2.16.1 IMR90s

Senescence was induced in ER:HRAS^{G12V} IMR90 cells by treatment with 100nM 4-hydroxytamoxifen (Sigma Aldrich, H7904) for 7 days. Cells were seeded in a 6-well plate (300,000 cells/ml). siRNA-mediated knockdown was performed on day 3 for surface IL-1α analysis, or day 5 for cytokine measurements. Cells were harvested for flow cytometry and cytokine measurement on days 5 and 7 respectively. IMR90s were treated from day 0 with 5μM punicalagin (Sigma ,P0023) or 100μM ascorbic acid (Sigma, A4403) where indicated.

2.16.2 Primary murine fibroblasts

Senescence was induced with 50μg/ml bleomycin sulphate (Sigma, B1141000) for 3 hours, followed by 7-14 days of incubation at 37ºC.

2.17 Hydrodynamic tail vein injection

This animal work was carried out by the Narita group at the Cancer Research UK Cambridge Institute. Mice were handled and kept under pathogen-free conditions in accordance with UK law and institutional guidelines at the University of Cambridge. Transposon-mediated gene transfer by hydrodynamic tail vein injection was as previously described (Kang et al., 2011). Briefly, female C57BL/6 mice (Charles River) were injected via the lateral tail vein with MLP CaNIGmir30 (20μg) and SB13 transposase vector (5μg) in PBS at a volume equivalent to 10% of body weight in less than 10 seconds, and livers were harvested at the times indicated.

2.18 Human SNP study design

Study participants were recruited by the Cambridge Bioresource (CBR) based on pre-defined criteria. Subjects were males aged 18-40 with a BMI between 18.5 and 32 and no known inflammatory conditions or infections. Subjects were not included if they had been vaccinated within the last three months, taken painkillers (e.g. paracetamol, asprin, ibuprophen) on the day of blood donation, or steroids on the week of blood donation. Individuals were also excluded if they were taking medication for allergies or high blood pressure. Blood was drawn by nurses at the CBR and passed directly to the researcher waiting outside so that participants remained anonymous. The initial pilot study included 20 participants: 10 homozygous for the major allele and 10 homozygous for the minor allele. Power calculations based on the results from the pilot study led to the recruitment of a further 15 individuals per group (50 total participants). Both the pilot and subsequent studies were carried out blinded, and genotypes were revealed after all data had been collected.

2.19 Whole blood LPS stimulation

Blood was drawn into either EDTA for full blood counts or lithium heparin for IL-1α assays, which were carried out in triplicate. Blood was diluted as indicated in a 6-well plate into IMEM with 10U/ml penicillin, 10mg/ml streptomycin and 5mg/ml L-glutamine with or without 1μg/ml LPS (Sigma, L2630). The blood was incubated at 37^{o}C for 22 hours and centrifuged at 400g for 5 minutes. Plasma from individual triplicates was taken and stored at -80^{o}C for later analysis, and the remaining red blood cell pellets were pooled and stored at -80^{o}C. Adherent monocytes were washed with PBS and harvested into trizol, pooling triplicate wells, and stored at -80^{o}C for later analysis.

2.20 RNA extraction

RNA from most samples was extracted using the RNeasy Mini Kit (Qiagen, 74104) according to kit instructions. For liver-derived RNA, the tissue was collected into RNAlater, stored overnight at 4ºC, and transferred to -80ºC until purification, and homogenised in RLT using a TissueLyser-LT (Qiagen). RNA from the whole blood LPS-stimulation experiments were extracted using trizol. Adherent monocytes were directly collected into 200µl trizol and incubated at room temperature for 5 minutes. 40µl chloroform was added and each sample was shaken vigorously for 15 seconds and incubated at room temperature for 2-3minutes. The samples were centrifuged at 12000g for 15 minutes at 4ºC. The upper aqueous phase was taken for RNA extraction. 100µl 100% isopropanol was added to each sample and incubated for 10 minutes at room temperature. Samples were centrifuged at 12000g for 10 minutes at 4ºC to pellet the RNA. The supernatant was discarded and the RNA pellet was washed with 200µl 75% ethanol. The samples were vortexed briefly and centrifuged at 7500g for 5 minutes at 4ºC. The supernatants were discarded and the pellets were air dried and resuspended in 20µl RNAase/DNAase free water. RNA was incubated at 55-60ºC for 10 minutes. All RNA was quantified using a Nanodrop and stored at -80ºC.

2.21 cDNA Synthesis

cDNA was synthesised using the Reverse Transcription System (Promega, A3500) 1.5µg RNA was diluted to 9µl with water. 1µl oligodT, 0.5µl random primers and 2µl dNTPs per sample were added, and tubes were incubated at 70ºC for 10 minutes and then immediately transferred to ice. 4µl $MgCl_2$, 5µl 10x buffer, 0.5µl RNAsin and 1µl AMV Reverse Transcriptase were added per tube and samples were incubated for 10 minutes at 25ºC, 50 minutes at 42ºC, and 5 minutes at 95ºC. Samples were cooled to 4ºC and stored at -20ºC.

cDNA from study participants of the human recall-by-genotype study was prepared using the SuperScript™ VILO™ cDNA synthesis kit (ThermoFisher, 11754050). 8µl RNA was added to 2µl

mastermix, and incubated for 10 minutes at 25ºC, 10 minutes at 50ºC, and 5 minutes at 85ºC. 0.5µl of each sample was pooled for the standard curve, and samples were stored at -20ºC.

2.22 qPCR

Each sample contained 2µl 10X Buffer, 1.6µl 25mM $MgCl_2$, 0.1µl AmpliTaq Gold (all from Thermofisher, LifeTechnologies), 0.4µl dNTPs (10mM each), 0.5µl Taqman Probe (Table 2.6) 1µl cDNA and 14.4µl H_2O. The qPCR reaction was carried out using a Rotorgene thermocycler and analysed using the $2^{-\Delta\Delta CT}$ method. For the rs17561 human study, a standard curve was produced by pooling 1µl of each RNA sample, and creating a serial dilution.

Table 2.6: Taqman Probes (Life Technologies)

SPECIES	GENE	CATALOGUE NUMBER
HUMAN	*GUSB*	Hs00939627_m1
	CASP1	Hs00354836_m1
	CASP4	Hs01031951_m1
	CASP5	Hs00362078-m1
	cGAS	Hs00403553_m1
	GSDMD	Hs00986739_g1
MOUSE	*GUSB*	Mm00446957_m1
	CASP1	Mm00438023_m1
	CASP11	Mm00432304_m1

2.23 LDH assay

Reagents from the Pierce LDH Cytotoxicity Assay Kit (Thermoscientific, 88954) were warmed to room temperature prior to use and the assay was carried out as per the kit instructions.

2.24 IL-1R2 ELISA

Reagents from the IL-RII ELISA kit (R&D, DR1B00) were warmed to room temperature prior to use and the ELISA was carried out as per the kit instructions.

2.25 Bead ELISAs

Reagents from kits listed in Table 2.7 were used for the bead ELISAs in a 96-well MultiScreen 1.2µm filter plate (Merck Millipore, MSBVN1250). Per well, 1.25µl antibody beads, 5µl biotinylated secondary antibody and 20µl buffer (PBS 1% BSA) were added to 25µl sample and incubated for 2 hours at room temperature in the dark with agitation. Wells were washed twice with 200µl buffer. 50µl 4µg/ml streptavidin-PE (eBioscience 12-4317-87) was added per well and incubated for 1 hour at room temperature in the dark. Wells were washed twice with 200µl buffer, resuspended in a 200µl buffer, and analysed by flow cytometry. The average PE fluorescence was measured for 300 beads on the flow cytometer (BD Accuri), and concentrations were determined using a standard curve.

Table 2.7: Luminex Bead Kits (Novex Life Technologies)

SPECIES	CYTOKINE	CATALOGUE NUMBER
HUMAN	IL-1α	LHC0811
	IL-1β	LHC0011
	IL-6	LHC0061
	IL-8	LHC0081
	MCP-1	LHC1011
	CRP	LHP0031
MOUSE	IL-1α	LMC0811
	IL-1β	LMC0011
	IL-6	LMC0061

2.26 p18 IL-1α ELISA

The anti-hIL-1α/Immp18 antibody was generated by immunising rabbits with a KLH conjugated peptide, followed by affinity purification and biotinylation (Innovagen).

A 96-well flat bottom ELISA plate (CoStar, 3591) was coated with 100µl 1µg/ml anti-human IL-1α antibody in PBS (R&D, AF-200-NA) overnight. The plate was washed four times, blotted dry on paper towel, and blocked for 1 hour. The plate was washed 4 times and 100µl sample/standard (Peprotech, 200-01A) was added per well and incubated for 2 hours. The plate was washed 4 times and 100µl 400ng/ml anti-hIL1α/Immp18 antibody (Innovagen) was added per well and incubated for 2 hours. The plate was washed 4 times and 100µl of 164ng/ml biotinylated anti-rabbit antibody (Dako, E0432) was added per well and incubated for 1 hour. The plate was washed 4 times and 100µl of Streptavidin-HRP (R&D, DY998) was added per well and incubated for 1 hour. The plate was washed 4 times and 100µl of substrate solution was added per well and incubated in the dark until good standard curve colour development was achieved. 50µl 2N H_2SO_4 was added per well to stop the reaction, and the plate was read at 450nm (corrected at 540nm). All incubations were at room temperature with agitation.

Box 2.9: p18 ELISA buffers	
Wash buffer 0.05% Tween 20 PBS	***Block buffer*** 1% BSA PBS
Antibody / HRP diluent buffer 0.1% BSA 005% Tween PBS	***Substrate solution*** 0.1M Sodium citrate pH5 0.006% H_2O_2 75µg/ml TMB

2.27 Western blotting

Western blots on caspase 11 cleavage assay samples were run using pre-cast 1mm NuPAGE™ Novex™ 4-12% Bis-Tris Protein Gels (ThermoFisher, NP0322BOX) in MES Buffer. For all other blots, proteins were resolved on a 15% SDS PAGE gel. 15µl Western Blot lysates were loaded and run alongside 15µl of protein ladder (Biorad, 161-0374). The gel was run using a chamber filled with anode and cathode buffers at 100V until the dye front reached the bottom of the gel. The gel was equilibrated with transfer

buffer (2M Glycine, 250mM Tris pH 8.6) for 5 minutes before being blotted onto 0.2µm PVDF membrane (Biorad, 162-0177) at 85mA for 2 hours. The gel was stained with coomassie (Biorad, 161-0787) and vacuum dried whilst the membrane was blocked for 1 hour in PBS 5% milk (Marvel). The membrane was incubated with primary antibody diluted in block buffer overnight at 4°C, washed 4 times with PBS/Tween 0.05%, incubated in secondary antibody diluted in block buffer for 1 hour at room temperature, washed 4 times with PBS/Tween 0.05%, developed with mixed ECL reagent (GE Healthcare, RPN2106) and exposed to film (Fujifilm). All antibody combinations are listed in Table 2.8.

When used, the unstained protein ladder (Biorad,1610343) was run alongside the stained ladder. Following transfer, the membrane was cut halfway through the stained ladder. The membrane was then stained with 0.1% Coomassie R-250 in 50% MeOH (BioRad, 1610400) for 30 minutes at room temperature and destained with 50%MeOH 10%Acetic Acid and allowed to dry. The stained ladder was used to realign the membrane.

Table 2.8: Western Blot Antibodies

TARGET	PRIMARY ANTIBODY (DILUTION)	SECONDARY ANTIBODY (DILUTION)
Human IL-1α	Rabbit anti-hIL-1α ,Peprotech 500-P21A (1:250-1:500)	Donkey Anti-Rabbit HRP, GE Healthcare NA934V (1:2000)
Human IL-1β	Goat anti-hIL1β, R+D AF-201-NA (1:500)	Cow Anti-Goat HRP, Jackson 805-035-186 (1:2000)
Human Caspase 5	Rabbit anti-human caspase-5, ProteinTech 17991-1-AD (1:500)	Donkey Anti-Rabbit HRP, GE Healthcare NA934V (1:2000)
Murine IL-1α	Goat anti-mIL-1α, R&D AF-400-NA (1:500)	Cow Anti-Goat HRP, Jackson 805-035-186 (1:2000)
Murine IL-1β	Rabbit anti-mIL-1β, Peprotech 500-P51 (1:500)	Donkey Anti-Rabbit HRP, GE Healthcare NA934V (1:2000)

2.28 N-terminal sequencing

Samples containing the cleavage reaction, the enzyme alone and the substrate alone were resolved on a 15% SDS-PAGE gel and transferred onto a PVDF membrane as previously described. The membrane was rinsed with water and stained with 0.1% Coomassie R-250 in 50% MeOH for 5 minutes at room temperature, destained with 50%MeOH 10%Acetic Acid, air-dried, and sent for N-terminal sequencing (Alta Bioscience).

2.29 Immunohistochemistry (IHC) and immunoflourescence (IF)

Sectioning and IHC was kindly carried out by the histology core facility at the CRUK Cambridge Institute. After processing paraffin sections were cleared before antigen retrieval with 10mM sodium citrate pH6 and blocking for 1 hour with M.O.M. (Vectorlabs, MKB-2213) and 0.5% donkey serum (Sigma Aldrich, D9663). Sections were incubated at 4^{o}C for 16 hours with the primary antibodies (Table 2.9), washed three times with TBS-tween, and incubated with secondary antibody (Table 2.9) and DAPI (Sigma Aldrich, D8417-10MG) for 1 hour at room temperature. Autofluorescence was reduced by 10 minutes incubation with 0.1% Sudan Black (Sigma Aldrich, 199664-25G) before mounting in VECTASHIELD (Vector Laboratories, H-1400). IHC sections were counterstained with haematoxylin. Slides were imaged on a TCS SP8 microscope or scanned on an Aperio AT2 (both Leica). Images were analysed with HALO (Indica Labs) and the Cytonuclear v1.4 algorithm.

Table 2.9: IF / IHC Antibodies

TARGET	PRIMARY ANTIBODY (DILUTION)	SECONDARY ANTIBODY (DILUTION)
NRAS (IF)	Mouse anti-mouse NRAS, Santa Cruz, sc-31 (1:250)	Donkey anti-mouse 647, Life Technologies A-31571 (1:250)
Mouse Caspase-11 (IF)	Rat anti-mouse Casp11, R&D, MAB86481 (1:50)	Donkey anti-rat 488, Life technologies A-21208 (1:250)
Mouse CD355 (IF)	Rat anti-mouse CD355, Biolegend, 137602 (1:100)	Donkey anti-rat 488, Life technologies A-21208 (1:250)
Mouse Ki67 (IF)	Rabbit anti-mouse Ki67, Genetex, 16667[SP8] (1:500)	Donkey anti-rabbit 555, Life technologies A-31572 (1:250)
NRAS (IHC)	Mouse anti-mouse NRAS, Santa Cruz, sc-31 (1:250)	Envision+ Kit, K500711-2, Aligent Techologies
F4/80 (IHC)	Rat anti-mouse F4/80 Serotec, MCA497 (1:100)	Envision+ Kit, K500711-2, Aligent Techologies

2.30 BrDu and SAHF staining

Cells were incubated with 100µg/ml 5-Bromo-2'-deoxyuridine for 6 hours at 37ºC, before fixing with 4% formaldehyde for 15 mins at room temperature. Cells were permabilised with 0.2% Triton X-100/PBS and blocked with 0.5% goat serum (Sigma Aldrich, G6767). Cells were incubated with anti-BrdU (BD, 555627, 1:500) for 45 minutes at room temperature, washed three times with 0.05% Tween/PBS, and incubated for 1 hour with goat anti-mouse Alexa-488 (ThermoFisher, A-11034, 1:500) and 1µg/ml DAPI. Cells were mounted in VECTASHIELD and slides were imaged with a TCS SP8 microscope (Leica).

2.31 Senescence-associated beta galactosidase staining

Cells were fixed with 2% formaldehyde for 3 minutes at room temperature, and washed 4 times with PBS. Cells were incubated for 18 hours at 37ºC in SAβGAL staining solution.

Box 2.10: SAβGAL staining solution
40mM citric acid/sodium phosphate buffer pH6.0 5mM $K_4[Fe(CN)_6]3H_2O$ 5mM $K_3[Fe(CN)_6]$ 150mM NaCl 2mM $MgCl_2$ 1mg/ml Xgal

2.32 Cell surface IL-1α staining

Cells were detached with accutase, fixed in 2% formaldehyde for 5 minutes at room temperature, and washed with 0.5%BSA/0.05%NaN3/PBS. Cells were blocked with 1:100 human Fc block (Biolegend, 422301) for 10 minutes at room temperature, before incubation with 1:20 anti-IL-1α-PE (IC002P, R&D) or 1:20 isotype control-PE (FAB200-P, R&D; 1:20) for 30 minutes at room temperature. Cells were then washed and analysed by flow cytometry (Accuri C6).

2.33 Statistical analysis

All data are expressed as mean ± standard error of the mean (SEM), unless otherwise stated. To compare the means of two populations, an unpaired t-test was used. For experiments with more than two populations, a one-way ANOVA was used unless there were two variables (e.g. time and concentration), in which case a two-way ANOVA was used. For comparison of each mean with a control mean, a Dunnett's post-hoc test was used. To compare every mean to every other mean, a Tukey's post-hoc test was used. Linear regression analysis was applied to determine correlation. All statistical analyses were carried out using the software GraphPad Prism with a threshold for significance set at $p \leq 0.05$.

Results

3. Results: The IL-1α pro-domain inhibits cytokine activity

3.1 Introduction

IL-1α is translated as a precursor protein containing a pro-domain of approximately 100 amino acids, which can be proteolytically removed by the calcium-dependent cysteine protease calpain (Kobayashi et al., 1990). The secretion of IL-1α has been an area of ongoing interest because it lacks a conventional signal peptide, does not localise to the Golgi apparatus or ER, and is translated on ribosomes that are associated with the cytoskeleton rather than the membrane (Stevenson et al., 1992). The pro-domain does, however, contain a stretch of basic amino acids that form a nuclear localisation signal (NLS) (Wessendorf et al., 1993).

Multiple functions have been described for nuclear IL-1α, which are thought to be driven by the propiece. These functions include binding to histone acetyl transferases (HATs) to regulate chromatin remodelling, and detecting DNA damage (Zamostna et al., 2012, Buryskova et al., 2004, Cohen et al., 2015). Nuclear IL-1α has also been described to regulate senescence by decreasing endothelial cell proliferation and migration (McMahon et al., 1997). Overexpression of the IL-1α propiece in transformed HEK cells also induces apoptosis by localising to spliceosome assembly sites, where it interacts with RNA-processing enzymes to alter the splicing of apoptotic proteins such as Bcl-X (Pollock et al., 2003).

In contrast to this, the IL-1α propiece has been reported to promote tumour progression by acting as a transforming oncoprotein. Overexpression of the pro-domain in glomerular mesangial cells leads to their malignant transformation into malignant Karposi sarcoma spindle cells (Stevenson et al., 1997). Similarly, overexpression in T cell leukaemia cells promotes proliferation by binding to the SP1 promoter and upregulating NF-κB signalling, leading to the increased transcription of mitogen and growth factor genes (Zhang et al., 2017).

The role of the pro-domain in regulating intracellular IL-1α actions is reasonably well established. However, its function in regulating classical IL-1α cytokine activity has been a topic of considerable

debate. The longstanding view in the literature was that pro-IL-1α is "fully active". However, most publications that make this statement either lack an appropriate reference or cite another article that in turn does not provide a source (Garlanda et al., 2013, Dinarello, 2009, Dinarello et al., 2012). Although an early paper by March and colleagues reports that pro-IL-1α exerts biological activity, there is no direct comparison to mature IL-1α (March et al., 1985). There is a single study that investigated the biological activity of the IL-1 precursors, which reported that pro-IL-1α is active whereas pro-IL-1β is not (Kim et al., 2013). However, in this study the recombinant IL-1α used was purified by high-pressure liquid chromatography (HPLC), whereas the recombinant IL-1β was purified by ion exchange chromatography. During HPLC, the sample is passed through a column at high pressure in a denaturing solvent such as acetone, and as a result the purified proteins often lose their native conformation. Therefore, it is possible that the IL-1α generated for these experiments was partially or fully unfolded. Furthermore, the data presented in this report consistently shows that although pro-IL-1α has some cytokine activity, the mature form is significantly more potent.

Recent research, by ourselves and others, demonstrates that the biological activity of pro-IL-1α is reduced compared to the mature cytokine. Afonina and colleagues showed that IL-1α is cleaved by the cytotoxic protease Granzyme B, which significantly increases cytokine activity. They demonstrated this both *in vitro* using recombinant IL-1α in cell assays, but also *in vivo* by showing that the granzyme B-cleaved form of IL-1α exhibited significantly higher adjuvant activity in ovalubumin-immunised mice. They expanded this finding by showing that the additional enzymes elastase, chymase, and calpain could all dramatically enhance IL-1α cytokine activity (Afonina et al., 2011). Work from our group has supported this finding by demonstrating that calpain-cleaved IL-1α is significantly more active than pro-IL-1α due to a 50-fold higher affinity for the IL-1R1 (Zheng et al., 2013).

3.1.1 Chapter 3 project rationale

The fact that pro-IL-1α is markedly less active than mature IL-1α strongly suggests that the pro-domain inhibits cytokine activity. The work presented in this chapter explores this in more detail by validating our previous observations regarding the relative activities of pro- and mature IL-1α, and interrogating how much of the pro-domain is required for this inhibitory function.

3.2 Results

3.2.1 Making recombinant human pro-IL-1α

To investigate the effect of proteolytic cleavage on IL-1α activity, human recombinant GST-tagged pro-IL-1α was expressed, purified and quantified (Figure 3.1). Although a GST-tag is larger than a His-tag and potentially more sterically obstructive, the method of GST purification produces soluble protein in a native structure. We have previously observed that the basal activity of His-pro-IL-1α is higher than GST-pro-IL-1α, probably due to the denaturation and renaturation that is required to solubilise the protein from inclusion bodies during His purification. Importantly, we have previously shown that the GST tag does not affect IL-1α activity or detection (Zheng et al., 2013).

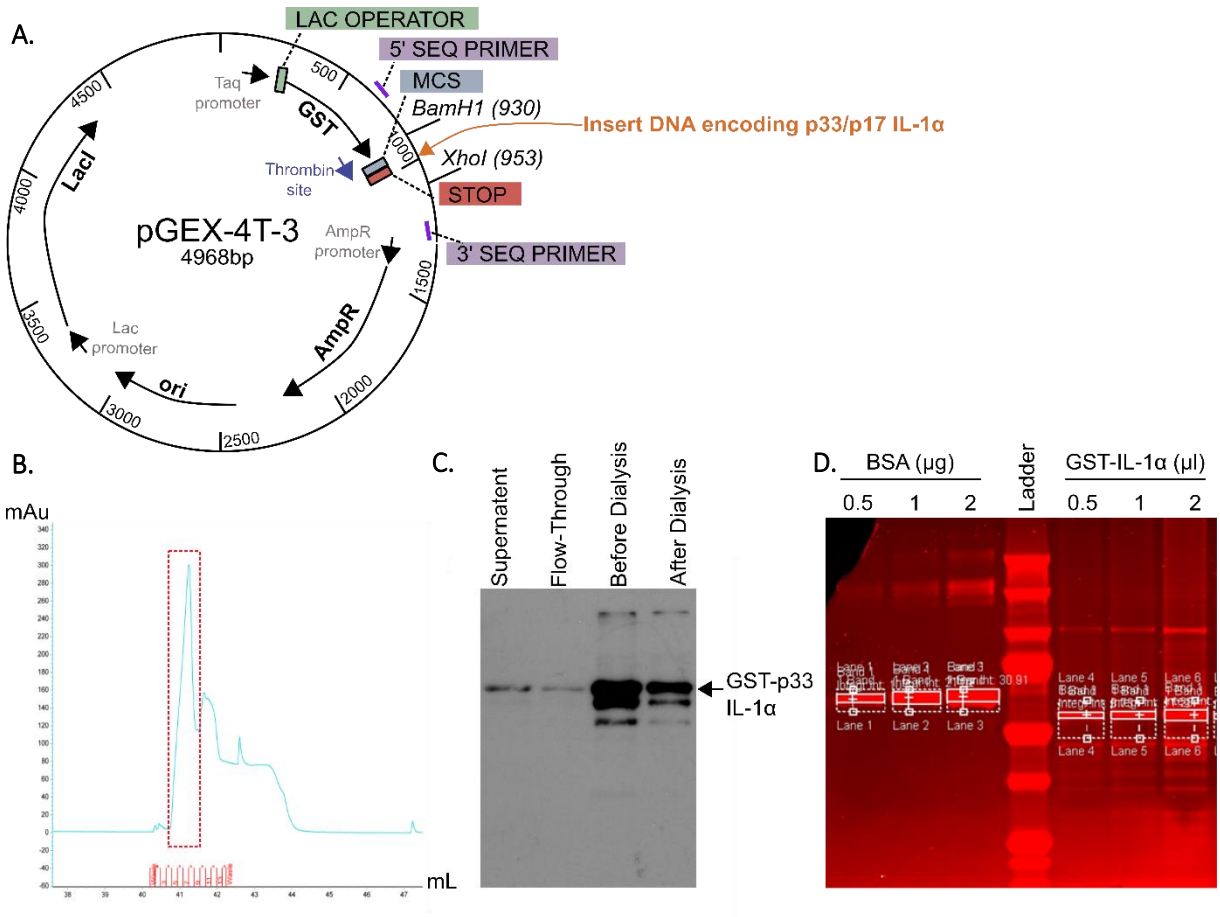

Figure 3.1: Production of human recombinant IL-1α. **(A)** pGEX-4T-3 vector map annotated with key features including the multiple cloning site (MCS). **(B)** Trace of the elution of purified recombinant IL-1α from the AKTA FPLC highlighting the fractions containing the major peak (red box). **(C)** Western blot for IL-1α at each stage of the protein purification process. **(D)** Example gel scan for concentration normalisation by coomassie staining.

3.2.2 Mature human IL-1α is significantly more active than pro-IL-1α

Two assays were used to evaluate IL-1α processing and bioactivity. All commercial IL-1α ELISA kits only detect the cleaved form of IL-1α, and not the pro-form. Figure 3.2A below exemplifies this, showing that when over 55,000pg/ml of p33 pro-IL-1α was applied to the ELISA, less than 40pg/ml was detected. To complement the IL-1α ELISA, a bioassay was used to assess IL-1α activity. In this assay HeLa cells secrete IL-6 in response to active IL-1α, which can be measured by ELISA (Figure 3.2B).

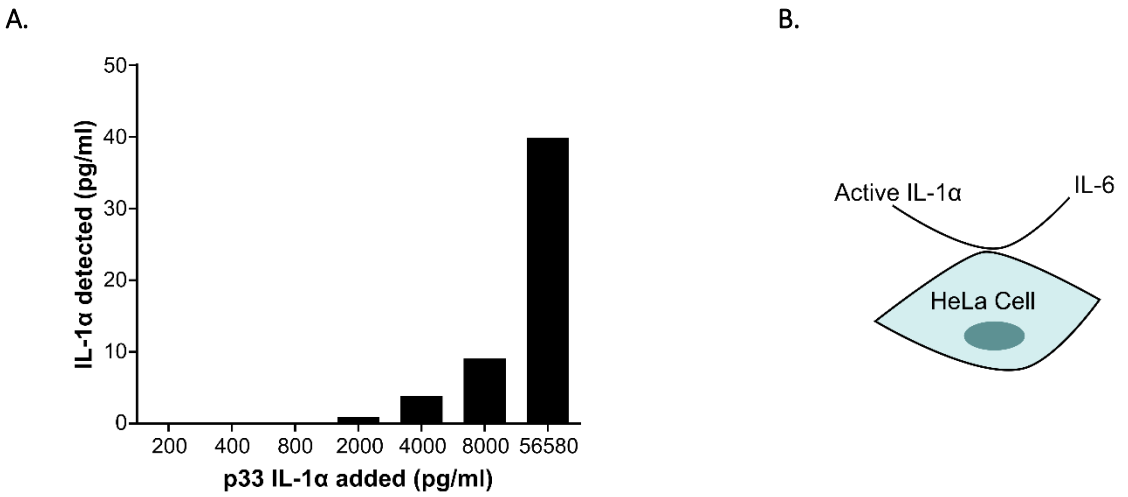

Figure 3.2: Techniques for assessing IL-1α cleavage and activity. (A) IL-1α ELISA data showing minimal detection of p33 pro-IL-1α. **(B)** Schematic of the IL-1α bioassay.

To determine which form of IL-1α is most active, two recombinant proteins were produced: p33 pro-IL-1α and p17 IL-1α (representative of the calpain-cleaved product). HeLa cells were treated with a dose response of each form of IL-1α, and IL-6 release was measured as a readout of bioactivity (Figure 3.3). The p17 mature IL-1α was significantly more active than the p33 pro-IL-1α, particularly at lower concentrations. This data shows that the absence of the pro-domain leads to increased IL-1α activity.

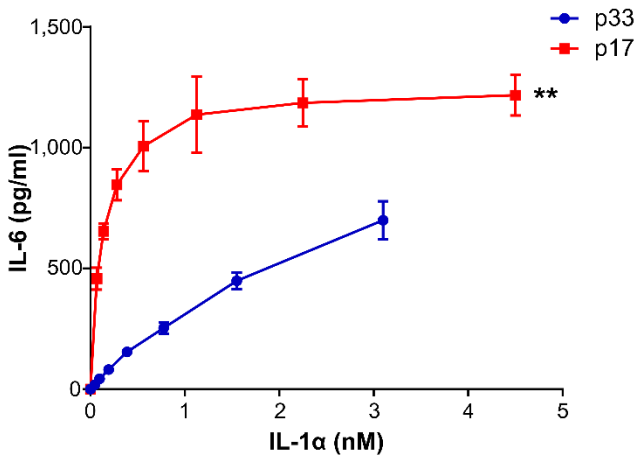

Figure 3.3: Recombinant mature IL-1α is significantly more active than pro-IL-1α. ELISA data showing IL-6 secretion by HeLa cells treated with increasing concentrations of mature IL-1α (p17) or pro-IL-1α (p33). Data represents mean ± SEM of n=3, p = **≤0.01.

To demonstrate that the proteolytic activation of IL-1α is not an artefact of using bacterial recombinant protein, human vascular smooth muscle cells (VSMCs) were used as a source of mammalian cell-derived IL-1α. Unlike most cell types, VSMCs do not express significant levels of the decoy receptor IL-1R2 that would otherwise 'protect' IL-1α from calpain processing during necrosis (Zheng et al., 2013). Freeze/thaw VSMC lysates were prepared with or without pre-incubation with the calpain inhibitor calpeptin. Calpeptin prevented IL-1α processing, as shown by both western blot (Figure 3.4A) and the cleaved IL-1α-specific ELISA (Figure 3.4B). The IL-1 bioassay indicated that the lysates prepared without calpeptin contained significantly more IL-1α-specific activity (as evidenced by a neutralising antibody) than those made with calpeptin (Figure 3.4C). Together these results support the recombinant protein data, and confirm that mature IL-1α is significantly more active than pro-IL-1α.

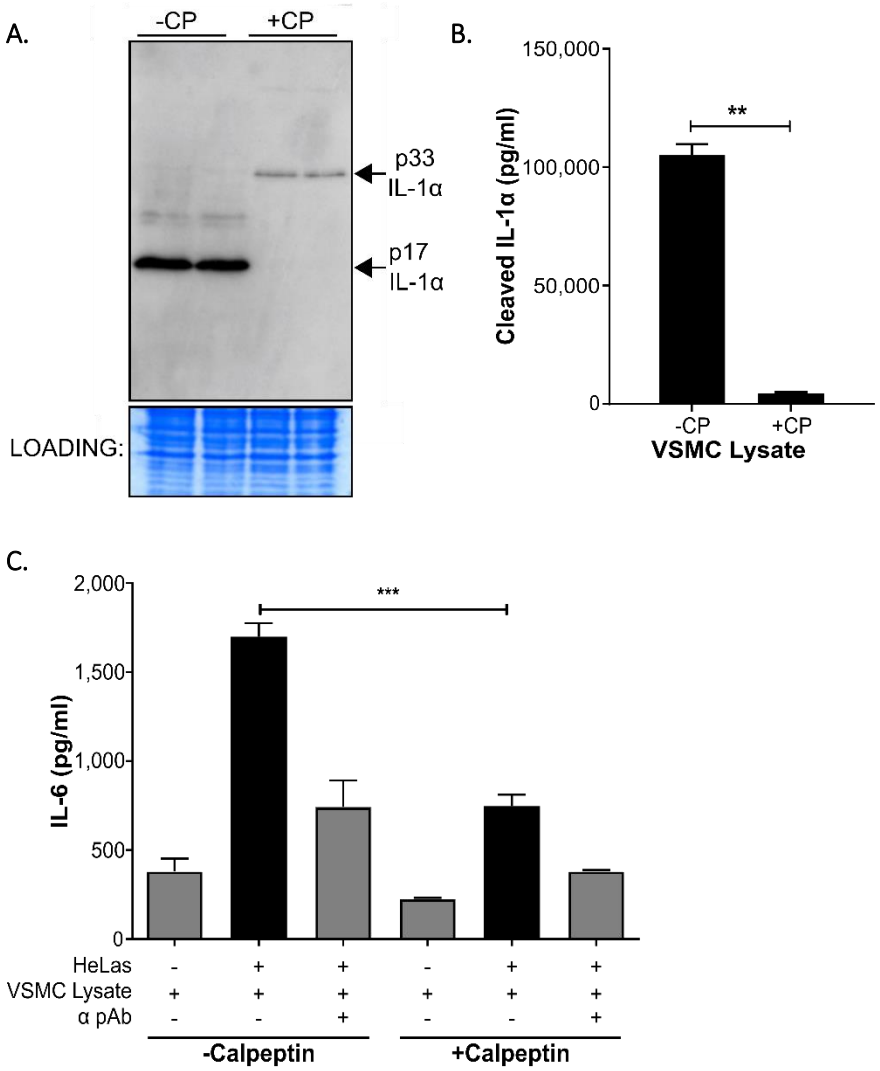

Figure 3.4: Calpain-cleaved cell-derived IL-1α is significantly more active than pro-IL-1α. (A-B) Western blot for IL-1α (**A**) and cleaved IL-1α ELISA data (**B**) showing levels of IL-1α processing in vascular smooth muscle cell (VSMC) lysates prepared ± preincubation with calpeptin (CP). **(C)** ELISA data showing baseline levels of IL-6 present in VSMC lysates and IL-1α-dependent IL-6 release by HeLa cells treated with VSMC lysates ± a neutralising IL-1α antibody (α pAb). Data represents mean ± SEM of n=3, p = **≤0.01, ***≤0.001.

3.2.3 A model of IL-1α autoinhibition

Based on the presented functional data, we propose a model of IL-1α autoinhibition (Figure 3.5) that resembles that reported for IL-1β (Mosley et al., 1987b). We suggest that the pro-domain folds over the cytokine domain and obscures key residues for receptor interaction and cytokine activity. This physical obstruction would also explain the lack of pro-IL-1α detection by the ELISA kits, because the pro-piece is 'hiding' one of the two epitopes that the ELISA antibodies bind. We also propose that the region between the pro-domain and cytokine domain protrudes from the IL-1α protein to form a 'loop' structure that is particularly accessible to proteases.

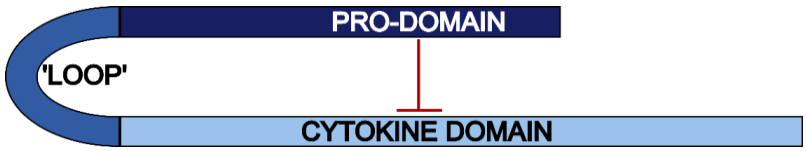

Figure 3.5 Proposed autoinhibition model. A schematic illustrating our working model of the pro-domain folding over and masking key residues in the cytokine domain for IL-1α function.

3.2.4 IL-1α autoinhibition is mediated by amino acids 56-77

To define how much of the pro-domain is required to limit IL-1α activity, a series of N-terminal truncation mutants were produced. The pro-domain of IL-1α contains blocks of highly conserved amino acids with no reported function. Since conservation is often indicative of function, the truncation mutants were designed based on these regions of conservation (Figure 3.6).

Figure 3.6 Truncation mutant design. Multiple species alignment of IL-1α protein sequence, with highly conserved areas shaded in grey. Red annotations indicate the N-terminal region of IL-1α protein removed in each truncation mutant.

To assess the effect of each truncation on activity, HeLa cells were treated with a range of matched concentrations of each mutant, pro-IL-1α (p33), and mature IL-1α (p18) (Figure 3.7). The dose response curves revealed that removing the first 56 amino acids of pro-IL-1α did not affect autoinhibition. Only the mutant lacking the first 77 amino acids (Δ77) had identical activity to mature IL-1α. This indicates that the N-terminal half of the pro-piece is not required for its autoinhibitory function, and that cytokine activity is limited by amino acids 57-77.

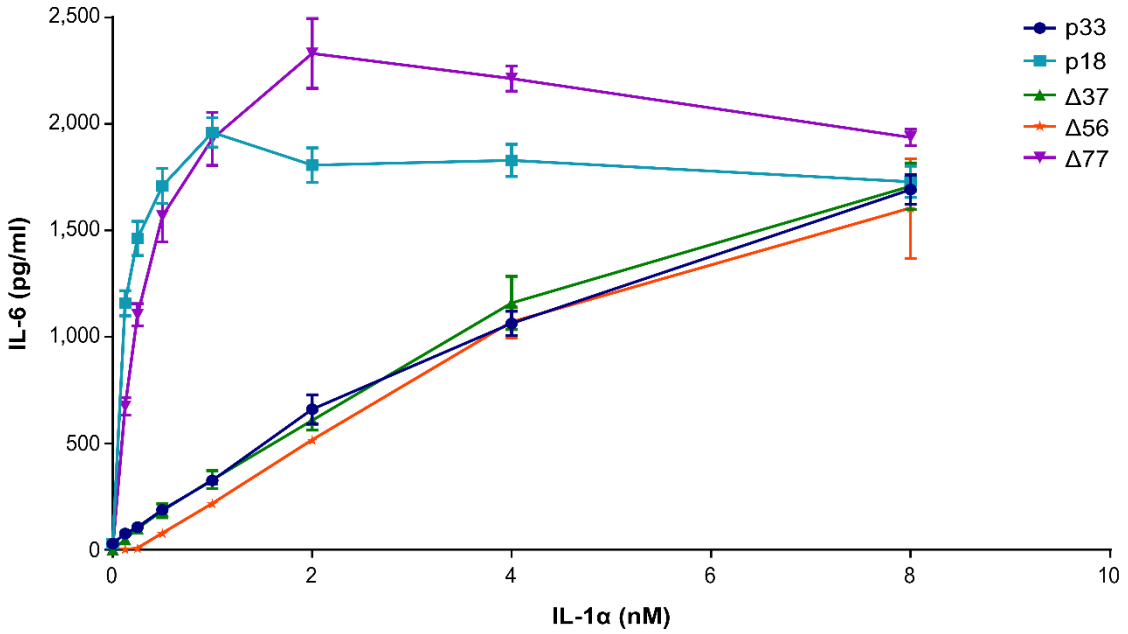

Figure 3.7 Amino acids 56-77 are critical for IL-1α autoinhibition. ELISA data showing IL-6 secretion by HeLa cells treated with increasing concentrations of mature IL-1α (p18), pro-IL-1α (p33), or truncated pro-IL-1α (Δ37, Δ56 and Δ77). Data represents mean ± SEM of n=3.

3.2.5 The PXXXP motif maintains basal pro-IL-1α activity

In our model of IL-1α autoinhibition, we propose the region between the pro-domain and cytokine domain forms a 'loop' that is targeted by proteases. The multiple species IL-1α alignment shows a conserved PXXXP motif within this 'loop' (Figure 3.8). Proline is an important determinant of protein structure due to the covalent bond between its side chain and the peptide backbone. This is disruptive to α-helix and β-strand conformations, and proline residues therefore occur in turns and direct protein folding (Deber et al., 2010).

Figure 3.8 The PXXXP Motif. Multiple species alignment of the IL-1α protein sequence, with highly conserved areas shaded in grey. Green annotation indicates location of the PXXXP motif.

To test if the PXXXP motif forms a hinge in the IL-1α protein and positions the pro-domain over the cytokine domain to facilitate autoinhibition, one (P111A) or both (P111A/P115A) prolines were mutated an alanine. These mutations were expected to restore full IL-1α activity by unfolding the hinge in the loop region. However, both proline mutations completely abrogated basal p33 IL-1α activity (Figure 3.9). This suggests that these prolines are indeed important for the structure of pro-IL-1α, but are not holding the cytokine in an inhibitory conformation as predicted.

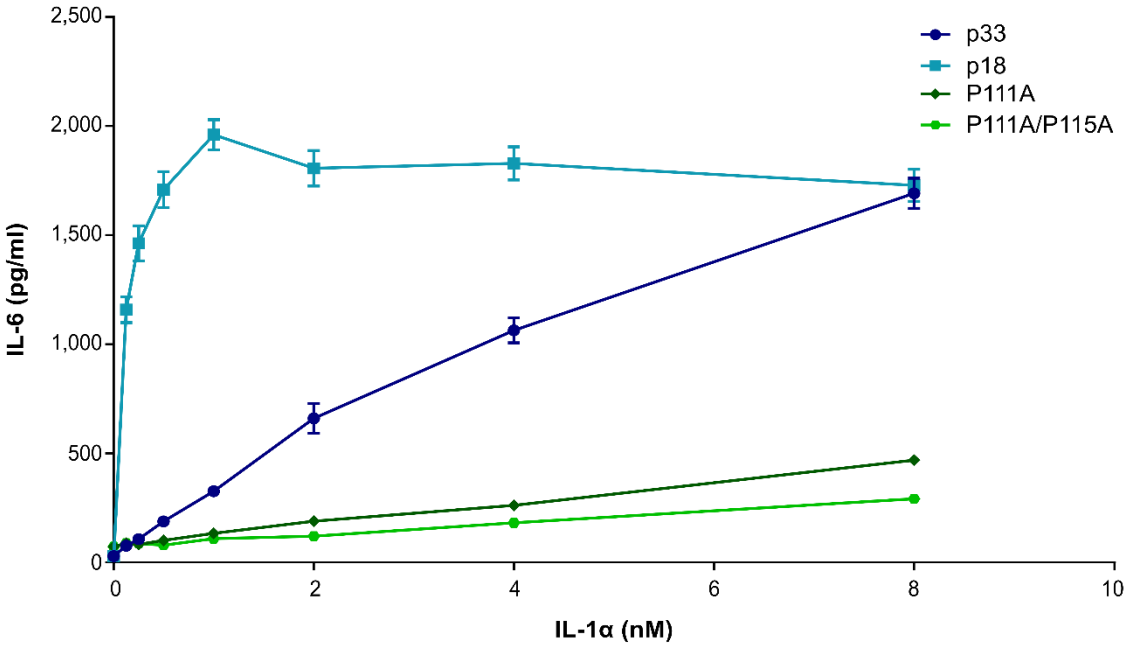

Figure 3.9 The PXXXP motif regulates basal pro-IL-1α activity. ELISA data showing IL-6 secretion by HeLa cells treated with increasing concentrations of mature IL-1α (p18), pro-IL-1α (p33), or proline-mutant pro-IL-1α (P111A and P111A/P115A). Data represents mean ± SEM of n=2.

3.3 Discussion

The biological activity of pro-IL-1α has been a matter of great controversy for a number of years. An early study suggested that pro-IL-1α is active (March et al., 1985); a statement that has become accepted over time without proper validation. More recent publications reporting that pro-IL-1α is fully active reference a single study that specifically addressed the relative bioactivities of the precursor and mature forms of IL-1α and IL-1β (Kim et al., 2013). However, the authors of this study purified recombinant IL-1α, but not IL-1β, by HPLC, which is a technique known to cause protein unfolding. Furthermore, despite the high basal activity of pro-IL-1α in this study, mature IL-1α was still significantly more active. Both ourselves, and others, have demonstrated that IL-1α activity is dramatically enhanced via cleavage by multiple proteases including calpain and granzyme B (Afonina et al., 2011, Zheng et al., 2013).

Here, we show that calpain-mediated processing dramatically enhances the bioactivity of both bacterial recombinant and human VSMC-derived IL-1α, particularly at low concentrations (Figures 3.3 and 3.4). IL-1α is constitutively expressed by most cell types, with particularly high levels found in cells with an important barrier function such as keratinocytes in the skin (Schmitt et al., 1986). As such, IL-1α is an important DAMP that is released during necrosis to signal to the surrounding tissue. When a cell undergoes necrosis, there is an influx of calcium ions that activate the canonical IL-1α protease, calpain (Brough et al., 2003). Most cells express the decoy receptor IL-1R2 in their cytosol, which binds pro-IL-1α during necrosis and 'protects' it from calpain to contain the inflammatory response. However, VSMCs do not express significant levels of IL-1R2, meaning that calpain is able to cleave IL-1α when the cell dies. As such, VSMC death is extremely inflammatory and is known to drive the development of the chronic inflammatory disease atherosclerosis (Zheng et al., 2013, Clarke et al., 2010).

The basal activity of pro-IL-1α allows it to function as an alarmin when released during the necrosis of large numbers of IL-1R2-expressing cell types. However, the fact that cleavage significantly enhances IL-1α activity means that this response can be potentiated when necrosis occurs in response to, or alongside, an inflammatory stimulus. For example, bacterial infection leads to the activation of caspases-1 and -5, which are both able to cleave IL-1R2 and liberate IL-1α (Zheng et al., 2013).

From the activity data we propose a model of IL-1α autoinhibition, in which the pro-domain folds over the cytokine domain and masks residues that mediate interaction with IL-1R1 (Figure 3.5). The IL-1 bioassay dose response curves of three IL-1α truncation mutants revealed that a surprisingly small portion of the pro-domain (amino acids 56-77) was critical for IL-1α autoinhibition (Figure 3.7). Unfortunately, the three-dimensional structure of pro-IL-1α has not yet been solved. However, it would be interesting to elucidate whether amino acids 56-77 interact with Arg128, Ile130, Ile180 and Trp225 that are reported to be the key residues for binding IL-1R1 (Labriola-Tompkins et al., 1993, Ozbabacan et al., 2014). Interestingly, the N-terminal half of the pro-domain was dispensable for IL-1α autoinhibition. Perhaps the C-terminal half of the propiece is responsible for *intra*molecular interactions, allowing the N-terminal part greater flexibility to modulate *inter*molecular interactions, for example with chromatin or splicing enzymes.

For proteases to remove the IL-1α propiece, they must be able to access the region between the pro-domain and cytokine domain. We hypothesise that this linker region forms a loop-like structure that allows the pro-domain to fold over the cytokine domain, but also protrudes from the protein to facilitate interaction with enzymes. There is a conserved PXXXP motif in the IL-1α loop, which is known to direct protein folding and hinge formation. Here, we show through site-directed mutagenesis that the prolines do not hold pro-IL1α in an inhibitory conformation as expected, but rather preserve a structure with a low level of biological activity (Figure 3.9). It is possible that the prolines hold the pro-domain slightly away from the cytokine to allow some receptor interaction, meaning that the immune system can be activated upon the necrosis of large numbers of IL-1R2-expressing cells that release pro-IL-1α as a DAMP. The effect of these proline mutations on secondary protein structure could be further investigated using circular dichroism.

In conclusion, the work presented in this chapter validates previous observations that mature IL-1α is significantly more active than the pro-form, and has provided novel insights into the mechanisms of IL-1α autoinhibition. This finding underlies the rest of the work presented in this thesis and emphasises the

important observation that IL-1α signalling can be potentiated by proteolytic cleavage to amplify the inflammatory response.

4. Results: Proteases from diverse biological systems activate IL-1α

4.1 Introduction

Proteases are enzymes that catalyse the hydrolysis of peptide bonds to break down proteins. They account for approximately two percent of the genome, with around 600 individual proteases identified to date. Over the course of evolution, proteases have adapted to withstand the varied pH and oxidation levels found in increasingly complex organisms. There are two major classes with distinct mechanisms of action: serine, cysteine and threonine proteases perform covalent catalysis using an amino acid as the nucleophile, whilst metallo and aspartic proteases carry out non-covalent catalysis by deriving their nucleophile from an activated water molecule (Turk, 2006).

Proteases were originally thought to only drive total protein degradation, for example during digestion. However, we now know that restricted and specific protease activity regulates a number of cellular processes including cell-cycle progression, proliferation, death, DNA replication, and immune cell function. Proteases are key components of numerous signalling pathways, and can form proteolytic cascades where the signal is propagated by the sequential cleavage and activation of zymogens. Protease signalling can be highly complex, for example Cathepsin C converts to a transferase at high pHs, thereby switching to catalyse the reverse reaction (Turk et al., 2001b). As such, proteases are now recognised as key regulators of both development, homeostasis and disease.

Due to their powerful signalling function, protease activity is tightly regulated at multiple levels. Transcription itself is highly controlled, with many enzymes transcribed as inactive zymogens. At the protein level, inhibitors and cofactors are important modulators of protease activity. However, as with many potent signalling molecules, dysregulated protease function is implicated in disease. Mutations in genes encoding proteases can cause insufficient activity. For instance, the lysosomal storage disorder galactosialidosis is caused by a mutation in the gene encoding cathepsin A (Ketterer et al., 2016). Conversely, over-activation of protease signalling is also deleterious. For example, inappropriate

activation of the most studied protease signalling pathway – the coagulation cascade – by ruptured atherosclerotic plaques leads to thrombus formation and blood vessel occlusion (Lusis, 2000).

Since excessive protease activity is causative in a number of diseases including cancer, atherosclerosis and neurodegenerative disorders, they hold significant therapeutic potential. They can be used as diagnostic markers, for example the serine protease kallikrien 3 (also known as prostate-specific antigen, PSA) is a biomarker for prostate cancer. Furthermore, thanks to their on/off status, proteases are attractive drug-targets. For instance, angiotensin-converting enzyme (ACE) inhibitors have been highly successful in treating hypertension and heart failure (Turk, 2006).

Proteases are important regulators of the IL-1 cytokines. Most family members are synthesised as precursor proteins that share a similar three-dimensional structure with analogous domain organisation. Due to their highly inflammatory nature, most IL-1 precursors have little or no biological activity, and proteolysis is an absolute requirement for their function. This extra level of control helps protect against aberrant inflammation (Afonina et al., 2015).

IL-1α is distinct from IL-1β because it is able to bind the IL-1R1 and induce signalling in its pro-form (Mosley et al., 1987b). This initial finding in the late 80's lead to the ongoing assumption that pro-IL-1α is fully active, despite a simultaneous paper from the same research group confirming that mature IL-1α has a significantly higher receptor affinity than pro-IL-1α (Mosley et al., 1987a). As such, the significance of IL-1α proteolysis has been underappreciated for many years. The IL-1α field, however, is gradually undergoing a paradigm shift in thinking, with increasing recognition that IL-1α cleavage increases its potential. Although IL-1α has been an established substrate of the calcium-dependent cysteine protease calpain for many years (Kobayashi et al., 1990), the activatory nature of this cleavage event has only been acknowledged recently (Afonina et al., 2011). Work by our group demonstrated that calpain cleavage increased the affinity of IL-1α for its receptor 50-fold. We also identified IL-1R2 as an important negative regulator of IL-1α processing by calpain that limits inflammation during necrosis in most cell types (Zheng et al., 2013).

4.1.1 Chapter 4 project rationale

Research by Seamus Martin's group showed that additional proteases are capable of cleaving IL-1α, identifying immune cell proteases granzyme B, elastase and chymase as potent activators of the cytokine (Afonina et al., 2011). With the exception of digestion, protease secretion or activity generally indicates loss of homeostasis and would therefore be a simple, yet elegant, way to activate the immune system in response. As such, IL-1α may act as a signalling hub that can integrate multiple proteolytic signals that homeostasis has been compromised. The work presented in this chapter aims to explore this hypothesis further by confirming previous findings and identifying additional proteases that can activate IL-1α.

4.2 Results

4.2.1 Calpain-I activates IL-1α

Calpain-I is the canonical protease widely reported to cleave IL-1α during necrotic cell death (Kobayashi et al., 1990). We confirmed this finding with our recombinant protein, showing that calpain-I cleaved pro-IL-1α in a dose dependent manner (Figure 4.1A), which resulted in a significant increase in IL-1α-specific activity (Figure 4.1B). Although, despite being the most established IL-1α-processing enzyme, the calpain-cleaved form of IL-1α was barely visible by western blot (Figure 4.1C) for reasons that remain unclear.

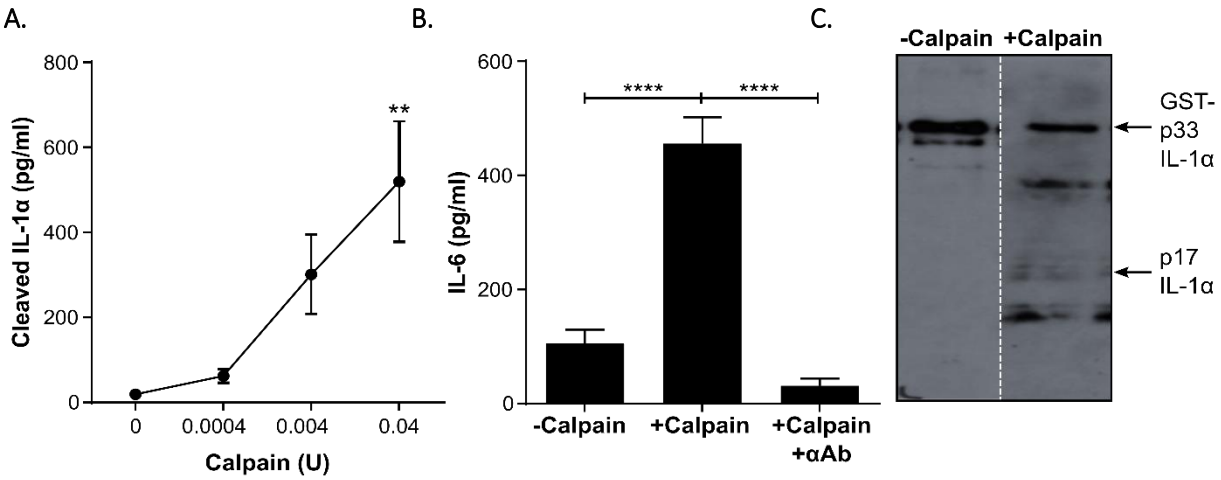

Figure 4.1: Calpain-I activates IL-1α. (A) ELISA data showing level of cleaved IL-1α following incubation of pro-IL-1α with increasing concentrations of calpain. (B) IL-1α-dependent IL-6 production by HeLa cells treated with reaction products from pro-IL-1α incubated ± calpain, ± neutralising IL-1α antibody (αAb). (C) Western blot for IL-1α after incubation of pro-IL-1α ± calpain. Data represent mean ± SEM of n=7 (A) or n=10 (B); p= **≤0.01, ****≤0.0001.

4.2.2 Thrombin activates IL-1α

The most extensively studied protease pathway is the coagulation cascade, which involves the sequential cleavage of serine proteases culminating in thrombin activation. Thrombin then cleaves fibrinogen into fibrin, which forms a blood clot. Previous work by our group has demonstrated that thrombin can cleave IL-1α with a similar efficiency to calpain (Burzynski et al, *publication in progress*). We were able to

recapitulate this finding using the recombinant pro-IL-1α, showing that thrombin cleaves in a dose-dependent manner (Figure 4.2A) and significantly increases IL-1α activity (Figure 4.2B.). Furthermore, an extremely clear 18kDa product was visible by western blot, suggesting that thrombin cleaves at a single site (Figure 4.2C). To examine this specificity further, a time-course experiment was carried out under the assumption that if the interaction was not absolutely specific, non-specific processing over time would gradually decrease IL-1α bioactivity. However, no decrease in IL-1α-specific activity was observed after 20 hours of incubation with thrombin (Figure 4.2 D,E), confirming that this interaction is highly specific. The plateau in IL-1α activity following longer incubations with thrombin is likely due to saturation of the bioassay (Figure 4.2 E).

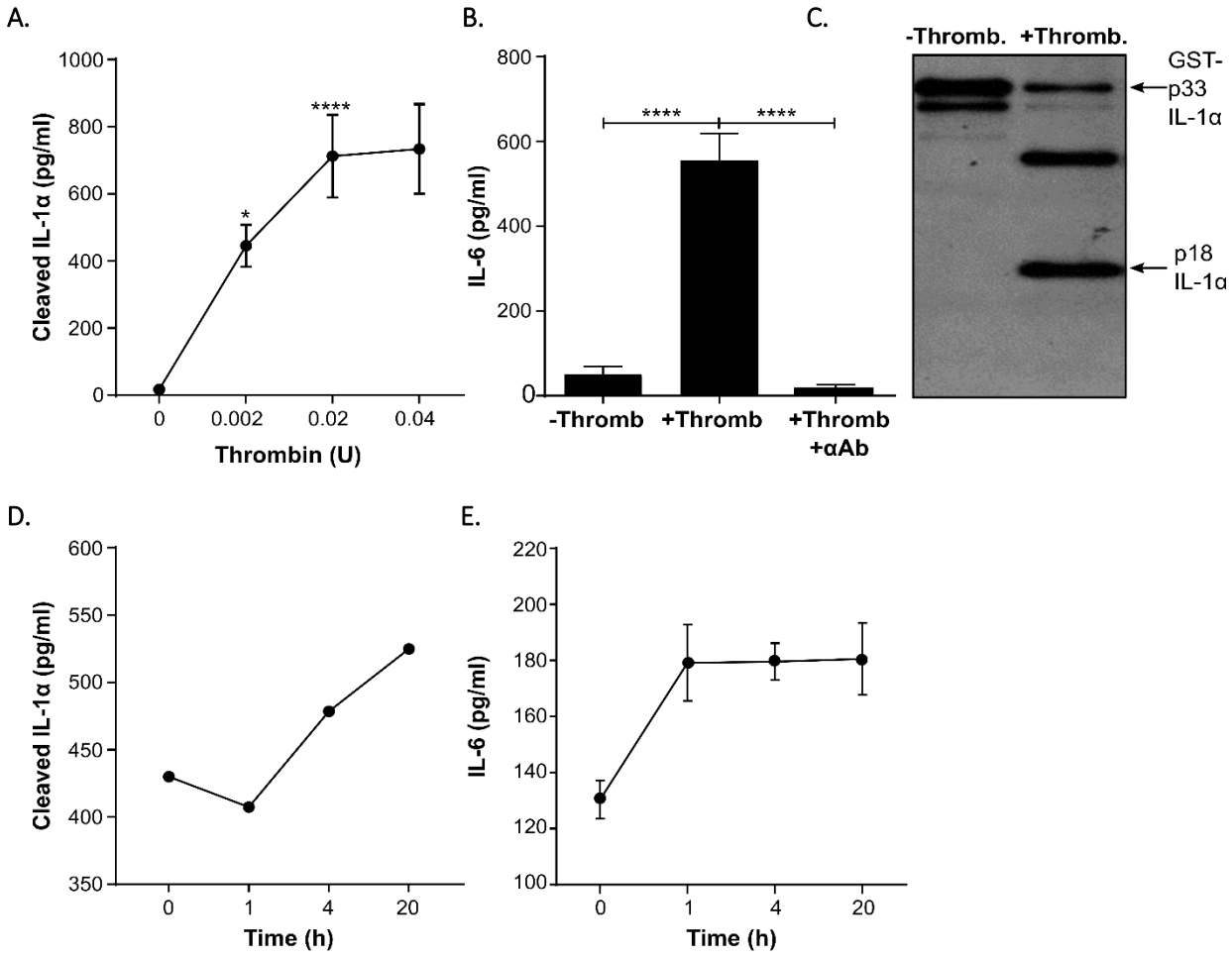

Figure 4.2: Thrombin activates IL-1α. (A) ELISA data showing level of cleaved IL-1α following incubation of pro-IL-1α with increasing concentrations of thrombin. **(B)** IL-1α-dependent IL-6 production by HeLa cells treated with reaction products from pro-IL-1α incubated ± thrombin (Thromb) ± neutralising IL-1α antibody (αAb). **(C)** Western blot for IL-1α after incubation of pro-IL-1α ± thrombin. **(D-E)** ELISA data measuring cleaved IL-1α levels in reaction products (**D**) and IL-1α-dependent IL-6 production by HeLa cells treated with reaction products (**E**) following incubation of pro-IL-1α with thrombin for a range of time points. Data represent mean ± SEM of n=7 (**A**) n=6 (**B**), or n=1 (**D,E**); p= *≤0.05, ****≤0.0001.

The time-course data (Figure 4.2D,E) and clear 18kDa western blot band (Figure 4.2C) indicated that thrombin cleaves IL-1α at a specific site that is upstream to the calpain site (amino acids 118/119), with calpain cleavage generating a 17kDa product. N-terminal sequencing of the 18kDa cleavage product by Edman degradation revealed that thrombin indeed cleaves IL-1α between amino acids 112 and 113 (Figure 4.3).

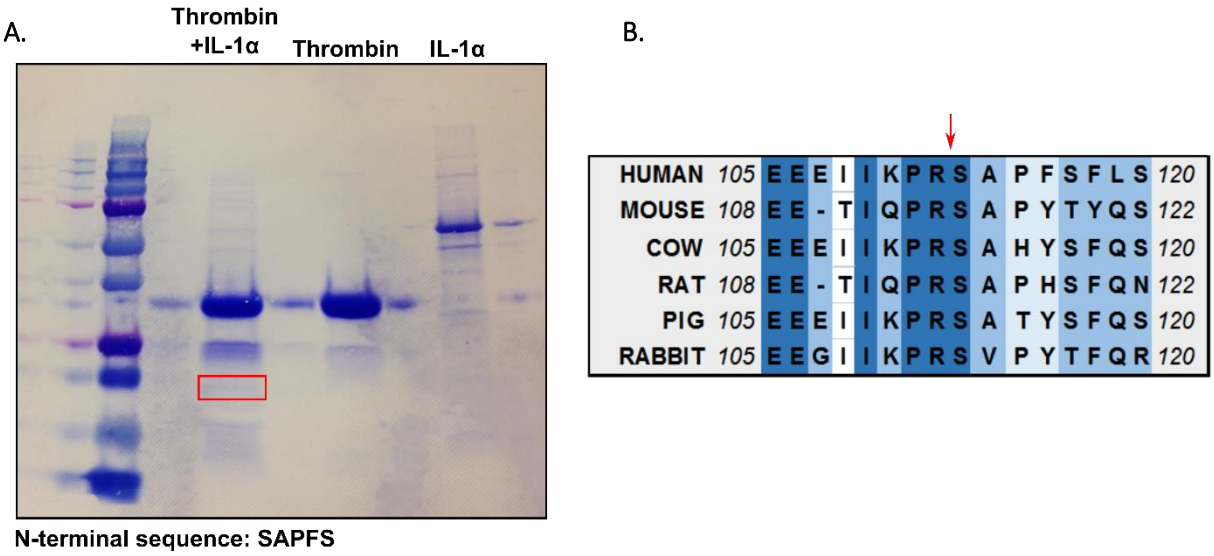

Figure 4.3: Thrombin cleaves IL-1α at R112. (A) Coomassie-stained PVDF membrane showing the thrombin-cleaved IL-1α band sent for N-terminal sequencing by Edman degradation, returned sequence shown underneath. **(B)** Multi species IL-1α protein alignment showing conserved thrombin-cleavage site (arrow).

We have shown that activated platelets express surface IL-1α, which can be removed using thrombin. However, when thrombin is added to platelet-rich-plasma (PRP) to form a clot, no IL-1α is detected (Burzynski et al, *publication in progress*). To investigate if the IL-1α that is cleaved off the platelets becomes trapped in the fibrin clot, we attempted to block the interaction between fibrinogen and thrombin in the PRP (Figure 4.4).

Fibrinogen is a large molecule that requires interaction with multiple thrombin sites. During clot resolution thrombomodulin binds to exosite 1 of thrombin to prevent fibrinogen from interacting, and could therefore be used to block fibrinogen processing. There is some suggestion that thrombomodulin also induces allosteric changes in thrombin (Lane et al., 2005). However, the addition of thrombomodulin had no effect on the thrombin-IL-1α dose-response curve (Figure 4.4A) suggesting

that exosite 1 is not used for IL-1α processing and any allosteric changes do not render thrombin completely inactive. Next, we incubated p17 IL-1α with thrombin and increasing concentrations of fibrinogen to see if the cytokine became trapped in the developing clot (Figure 4.4B). Fibrinogen had no effect on p17 detection, indicating that p17 IL-1α is not trapped or may be small enough to diffuse out of the clot. Fibrinogen did, however, competitively inhibit the cleavage of IL-1α by thrombin in a dose-dependent manner (Figure 4.4C), possibly because thrombin has a higher affinity for fibrinogen than pro-IL-1α. Thrombomodulin, again, had no influence on this inhibition, despite the fact that it is known to disrupt the interaction between thrombin and fibrinogen. Interestingly, thrombomodulin purchased from two distinct sources failed to relieve the competitive inhibition by fibrinogen (Figure 4.4D), suggesting that the interaction of thrombomodulin with thrombin may not be strong enough for use in an *in vitro* setting, or that commercially sourced thrombomodulin is non-functional. Together these findings suggest that IL-1α is not trapped by the fibrin clot in PRP. One possible explanation for the lack of cleaved IL-1α detection in clotted PRP is that fibrinogen is present in such high quantities that it saturates the thrombin.

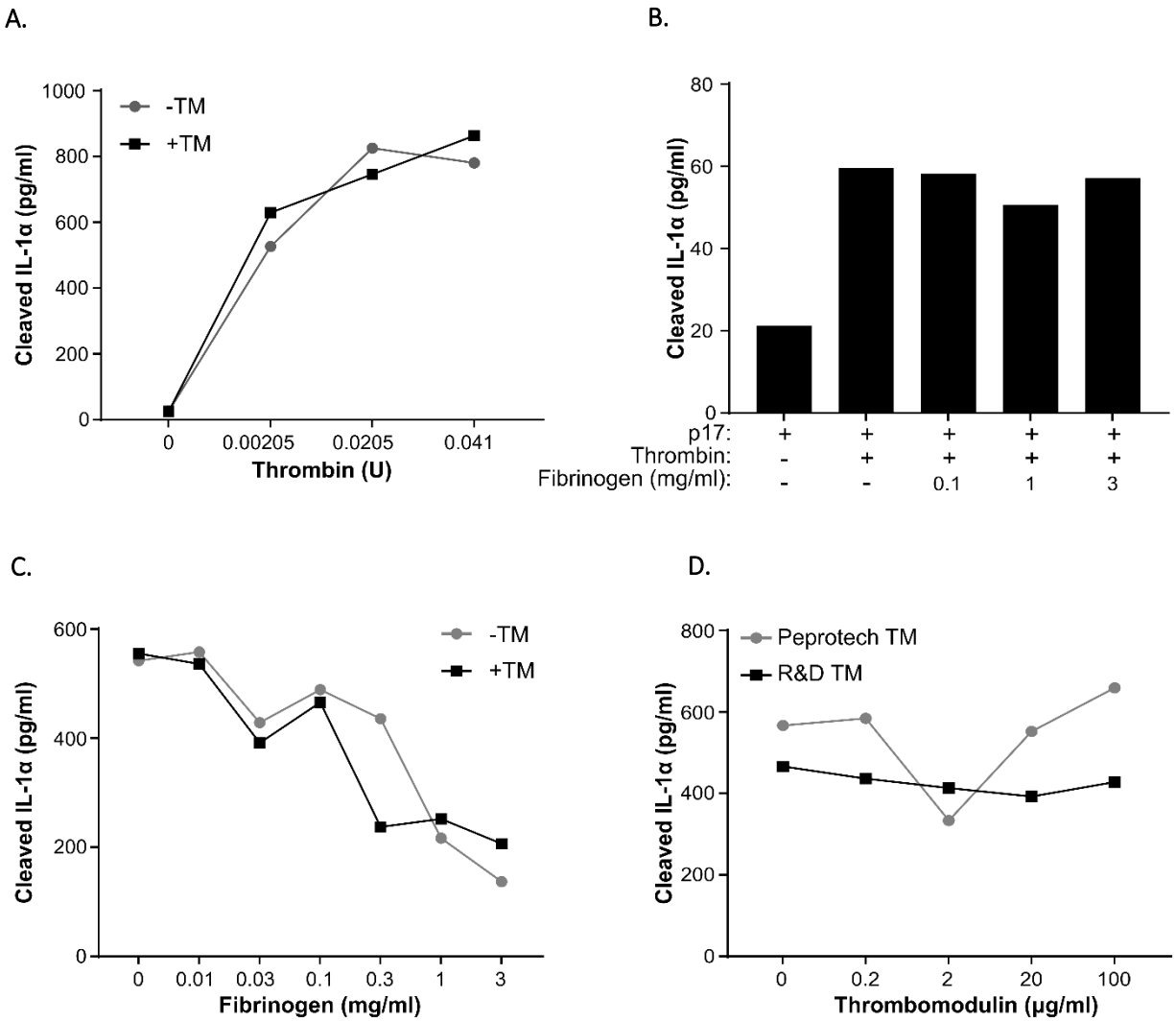

Figure 4.4: IL-1α does not get trapped within the fibrin clot. (A-D) ELISA data showing level of cleaved IL-1α following incubation of pro-IL-1α with a range of thrombin concentrations ± thrombomodulin (**A**), incubation of p17 IL-1α ± thrombin ± increasing concentrations of fibrinogen (**B**), incubation of pro-IL-1α with thrombin and increasing concentrations of fibrinogen ± thrombomodulin (**C**), or incubation of pro-IL-1α with thrombin and increasing concentrations of thrombomodulin from either Peprotech or R&D (**D**). Data is n=1.

4.2.3 Multiple host defence serine proteases cleave IL-1α

The discovery that thrombin could activate IL-1α with a similar efficiency to calpain prompted us to question what other proteases are able cleave IL-1α. The IL-1 signalling pathway is found throughout evolution and is thought to be related to the Spaetzle-Toll pathway in *Drosophila melanogaster*. Both IL-1 and Spaetzle require the proteolytic removal of their pro-domains to interact with their cell-surface receptors and activate NF-κB signalling (Hoffmann, 2003). Because of the conserved nature of IL-1, the serine proteases were a logical starting point for our studies because they are the most ancient protease systems found in both prokaryotes and eukaryotes (Di Cera, 2009).

Granzyme B is primarily released in the secretory granules of NK and CD8+ T cells, but can also be expressed by some non-cytotoxic cells including keratinocytes. The protease enters target cells, which may be tumourigenic or infected by a virus, and induces apoptosis by activating caspase-3. It is also present in advanced atherosclerotic plaques where it drives VSMC and foam cell death (Choy et al., 2003). Granzyme B activated recombinant IL-1α dose-dependently to generate a 19kDa product (Figure 4.5A-C), confirming observations reported previously (Afonina et al., 2011). A limitation of using recombinant protein expressed in bacteria is that it is not post-translationally modified. Alterations like phosphorylation or glycosylation could affect enzyme-substrate interactions, and so necrotic human vascular smooth muscle cells (VSMCs) were used as a source of mammalian IL-1α. As discussed in chapter 3, VSMCs do not express significant levels of the decoy receptor IL-1R2 and therefore release huge amounts of cleaved IL-1α during necrosis. Because of this, necrotic lysates were prepared following pre-incubation with the calpain inhibitor calpeptin. Granzyme B cleavage of VSMC-derived IL-1α was less robust (Figure 4.5D,E), however this data represents a single experiment only. The time-course experiment revealed that Granzyme B-cleavage of recombinant IL-1α is reasonably specific, with only a slight decrease in IL-1α activity after 20 hours of incubation (Figure 4.5F,G).

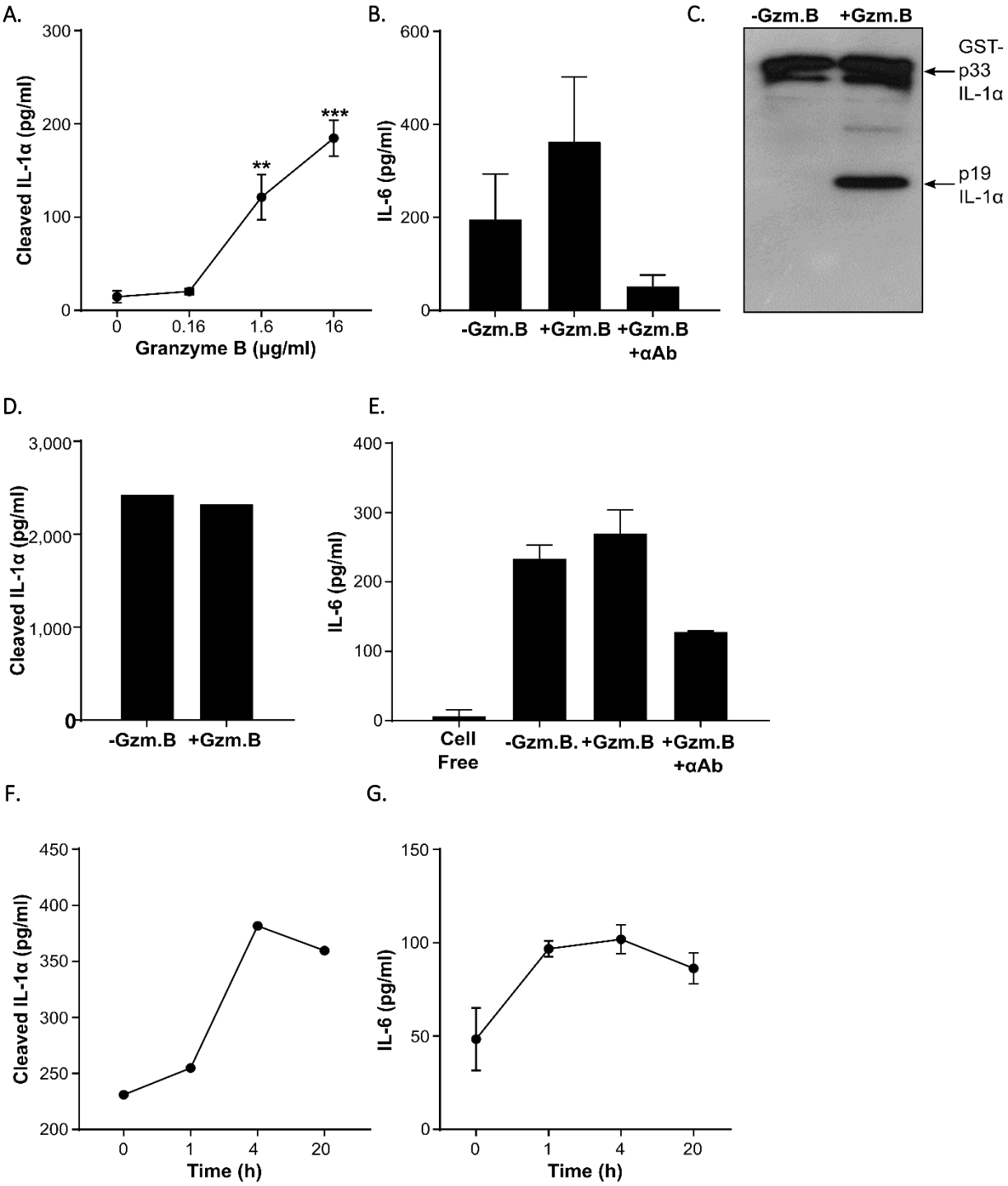

Figure 4.5: Granzyme B activates IL-1α. (A) ELISA data showing level of cleaved IL-1α following incubation of pro-IL-1α with increasing concentrations of granzyme B. **(B)** IL-1α-dependent IL-6 production by HeLa cells treated with reaction products from pro-IL-1α incubated ± granzyme B (Gzm.B) ± neutralising IL-1α antibody (αAb). **(C)** Western blot for IL-1α after incubation of pro-IL-1α ± granzyme B. **(D-E)** ELISA data showing level of cleaved IL-1α in reaction products (**D**) and IL-1-dependent IL-6 production by HeLas treated with reaction products (**E**) following incubation of calpeptin-containing VSMC lysates ± granzyme B. **(F-G)** ELISA data measuring cleaved IL-1α levels in reaction products (**F**) and IL-1α-dependent IL-6 production by HeLa cells treated with reaction products (**G**) following incubation of pro-IL-1α with granzyme B for a range of time points. Data represent mean ± SEM of n=3 (**A**) n=5 (**B**), n=2 (**E**) or n=1 (**D,F,G**); p= **≤0.01, ***≤0.001.

Elastase and proteinase-3 are produced by neutrophils, the most abundant leukocyte that arrives first at sites of inflammation. They function both intracellularly by digesting phagocytosed microorganisms, and extracellularly interweaved with chromatin fibres in neutrophil extracellular traps (NETs) that physically catch and kill invading pathogens. Neutrophil proteases are implicated in numerous diseases, such as cystic fibrosis, where they promote matrix destruction and inflammation (Korkmaz et al., 2010). Elastase is present in atherosclerotic plaques where it increases vulnerability through ECM degradation (Dollery et al., 2003). Conversely, an atheroprotective role has been described for proteinase-3 that is reported to improve endothelial barrier function (Knuckleurg and Newman, 2012). Both elastase (Figure 4.6) and proteinase-3 (Figure 4.7) activated recombinant and VSMC-derived IL-1α. Both proteases generated multiple cleavage products visible by western blot (Figures 4.6C and 4.7C), and gradually reduced IL-1α bioactivity over longer incubation times (Figure 4.6 F,G and 4.7 F,G), suggesting a lower level of specificity. This gradual degradation of IL-1α could represent a mechanism of 'switching off' the cytokine once the immune system has been alerted to avoid excess inflammation.

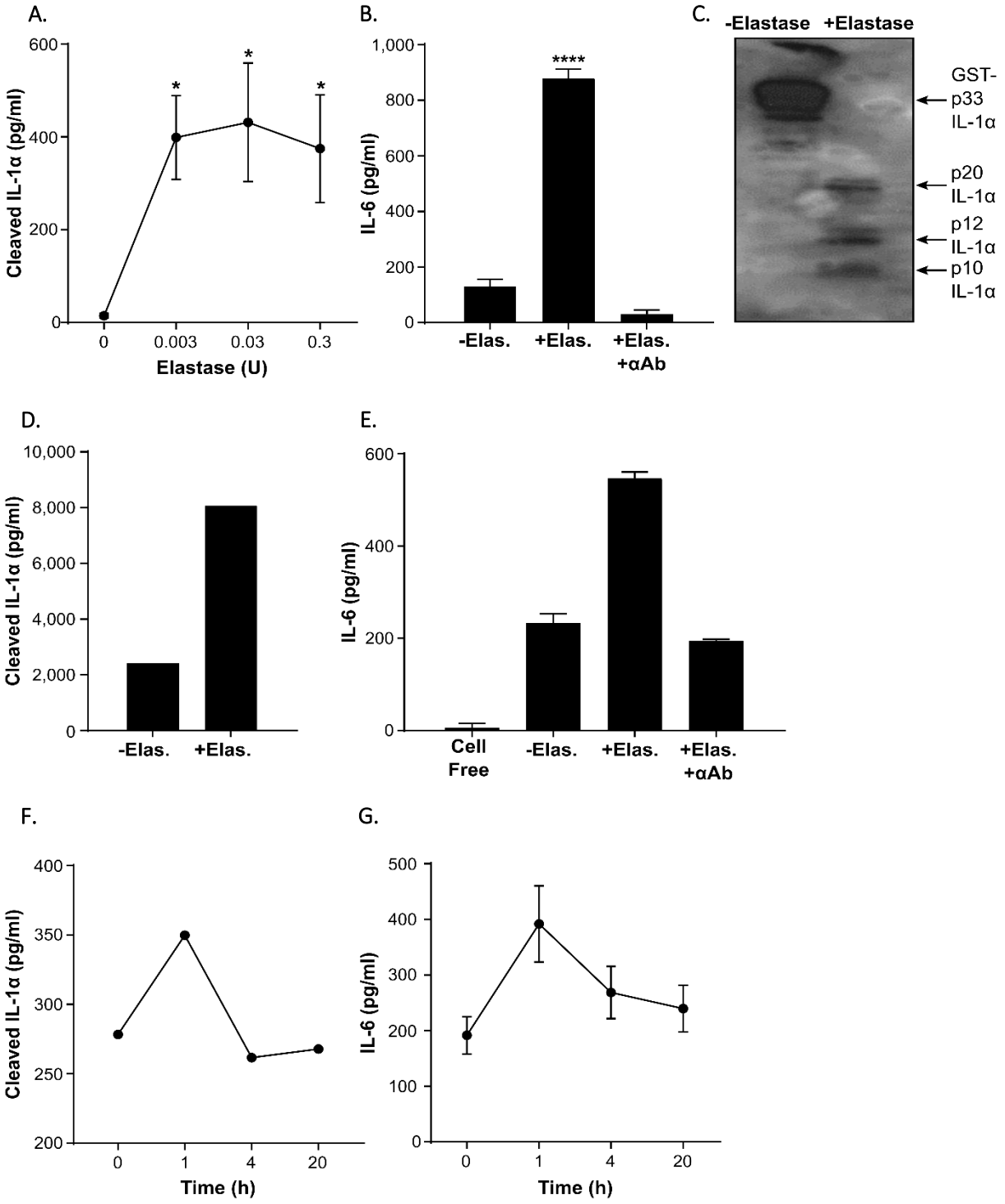

Figure 4.6: Elastase activates IL-1α. **(A)** ELISA data showing level of cleaved IL-1α following incubation of pro-IL-1α with increasing concentrations of elastase. **(B)** IL-1α-dependent IL-6 production by HeLa cells treated with reaction products from pro-IL-1α incubated ± elastase (Elas.) ± neutralising IL-1α antibody (αAb). **(C)** Western blot for IL-1α after incubation of pro-IL-1α ± elastase. **(D-E)** ELISA data showing level of cleaved IL-1α in reaction products (**D**) and IL-1-dependent IL-6 production by HeLas treated with reaction products (**E**) following incubation of calpeptin-containing VSMC lysates ± elastase. **(F-G)** ELISA data measuring cleaved IL-1α levels in reaction products (**F**) and IL-1α-dependent IL-6 production by HeLa cells treated with reaction products (**G**) following incubation of pro-IL-1α with elastase for a range of time points. Data represent mean ± SEM of n=5 (**A**) n=4 (**B**), n=2 (**E**) or n=1 (**D,F,G**); p= **≤0.01, ***≤0.001.

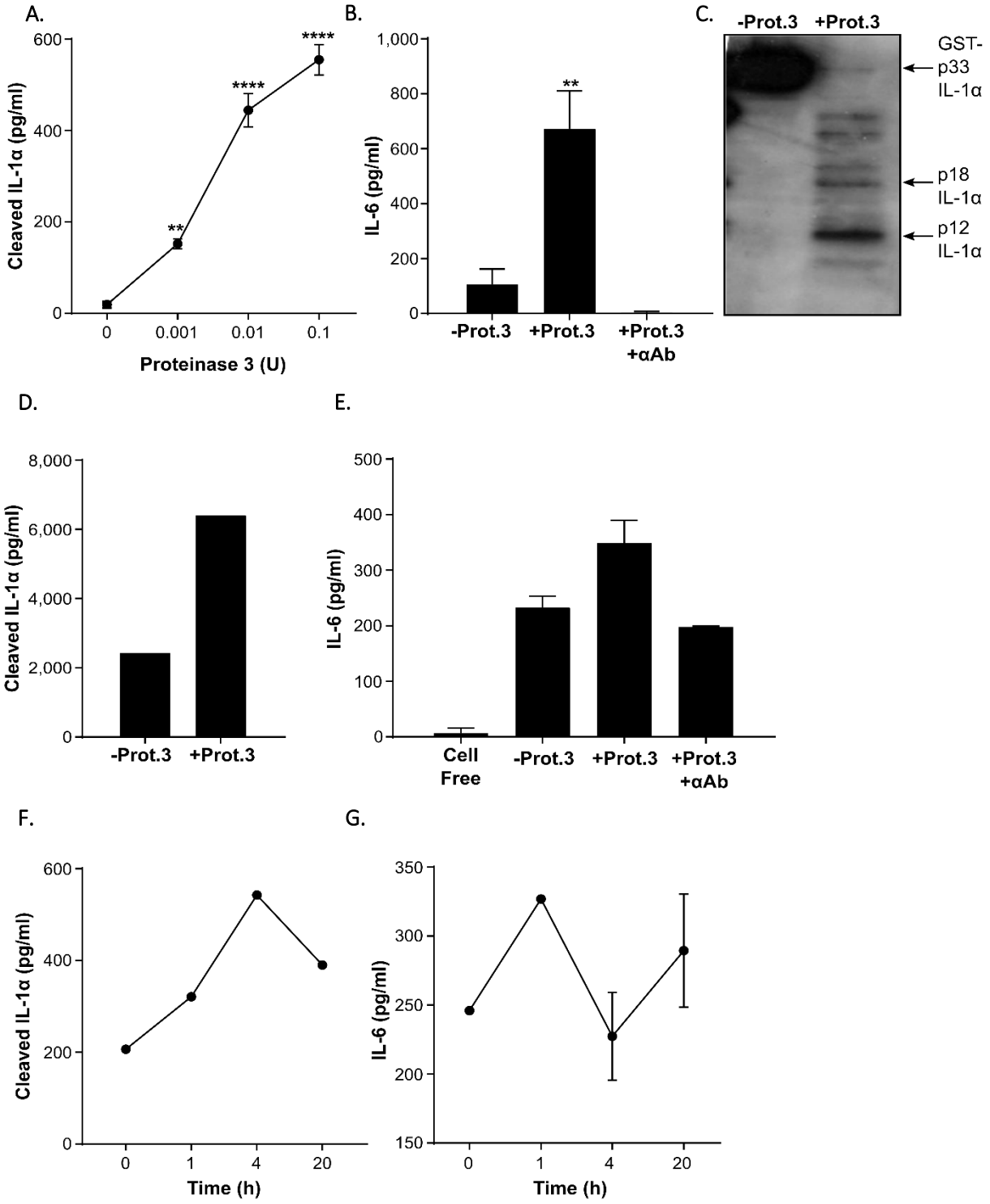

Figure 4.7: Proteinase-3 activates IL-1α. (A) ELISA data showing level of cleaved IL-1α following incubation of pro-IL-1α with increasing concentrations of proteinase-3. **(B)** IL-1α-dependent IL-6 production by HeLa cells treated with reaction products from pro-IL-1α incubated ± proteinase-3 (Prot.3) ± neutralising IL-1α antibody (αAb). **(C)** Western blot for IL-1α after incubation of pro-IL-1α ± proteinase-3. **(D-E)** ELISA data showing level of cleaved IL-1α in reaction products (**D**) and IL-1-dependent IL-6 production by HeLas treated with reaction products (**E**) following incubation of calpeptin-containing VSMC lysates ± proteinase-3. **(F-G)** ELISA data measuring cleaved IL-1α levels in reaction products (**F**) and IL-1α-dependent IL-6 production by HeLa cells treated with reaction products (**G**) following incubation of pro-IL-1α with proteinase-3 for a range of time points. Data represent mean ± SEM of n=4 (**A**) n=3 (**B**), n=2 (**E**) or n=1 (**D,F,G**); p= **≤0.01, ****≤0.0001.

Chymase is released by mast cells and has multiple functions including attracting leukocytes, inducing apoptosis, degrading ECM, and converting angiotensin I to angiotensin II to promote blood vessel narrowing. Chymase contributes to atherosclerotic plaque instability, and its inhibition has been shown to reduce disease progression *in vivo* (Bot et al., 2011). Mast cell chymase activated recombinant IL-1α, generating two major fragments of 18KDa and 12KDa (Figure 4.8). This is suggestive of two specific cleavage events potentially generating active (18kDa) and inactive (12kDa) cytokine.

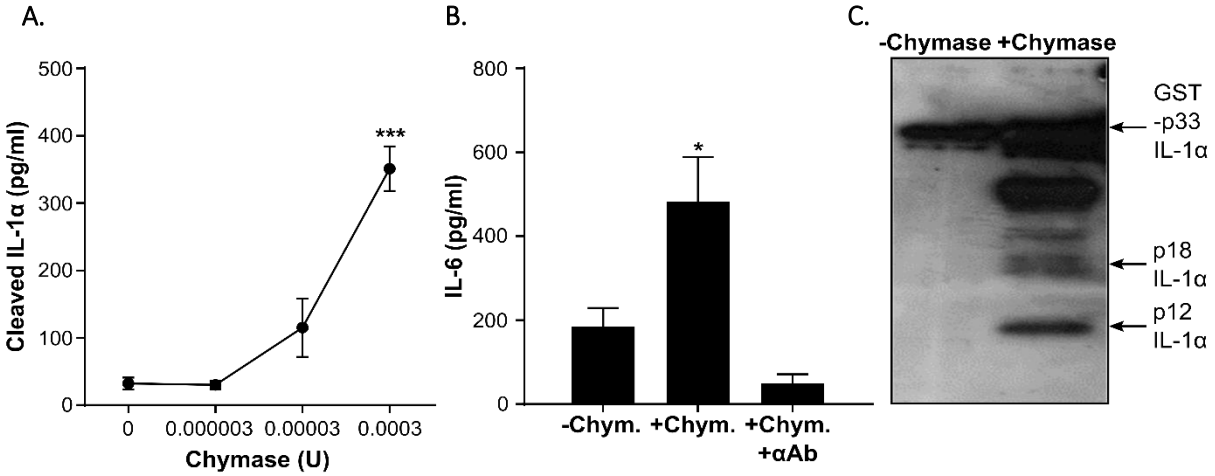

Figure 4.8: Chymase activates IL-1α. (A) ELISA data showing level of cleaved IL-1α following incubation of pro-IL-1α with increasing concentrations of chymase. **(B)** IL-1α-dependent IL-6 production by HeLa cells treated with reaction products from pro-IL-1α incubated ± chymase (Chym.) ± neutralising IL-1α antibody (αAb). **(C)** Western blot for IL-1α after incubation of pro-IL-1α ± chymase.Data represent mean ± SEM of n=3 (**A**) n=5 (**B**) p= *≤0.05, ***≤0.001.

The immune system also has a non-cellular component composed of soluble factors called the complement system. The complement system encompasses three serine protease cascades - classical, lectin and alternative - that result in the formation of a membrane attack complex, which destroys invading pathogens. The MASP proteases of the lectin pathway have been described as thrombin-like due to their similar substrate and inhibitor profiles, (Presanis et al., 2004) and were therefore obvious candidates for IL-1α activation. Due to a lack of commercial MASP sources the ability of the homologous classical pathway protease, C1s, to activate IL-1α was tested instead. C1s induced some IL-1α activity, but this effect was not as profound as those observed for other serine proteases and no

cleavage product was visible by western blot (Figure 4.9). We also tried to activate MASP2 in human serum using zymosan, a compound derived from the yeast cell wall that is known to activate the alternative complement pathway (Smith et al., 1982) (Figure 4.10). Incubation of p33 pro-IL-1α with serum lead to processing, but this was largely due to thrombin as evidenced using the thrombin inhibitor PPACK. The addition of zymosan to the reaction did slightly increase cleavage, but this was not significant and was reversed using PPACK. As such, it is difficult to conclude from this data whether the serine proteases of the complement pathway can really activate IL-1α.

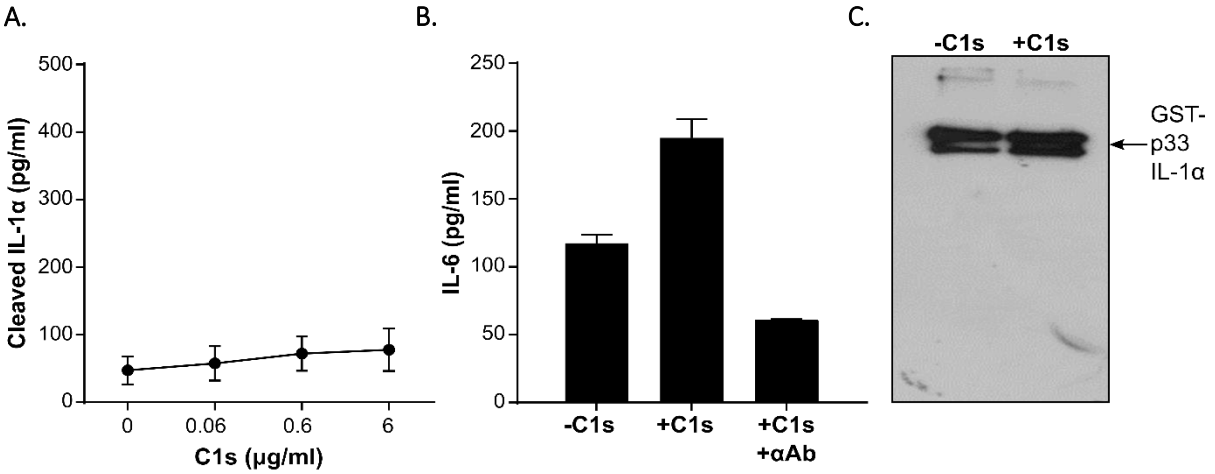

Figure 4.9: C1s may activate IL-1α. (A) ELISA data showing level of cleaved IL-1α following incubation of pro-IL-1α with increasing concentrations of C1s. **(B)** IL-1α-dependent IL-6 production by HeLa cells treated with reaction products from pro-IL-1α incubated ± C1s ± neutralising IL-1α antibody (αAb). **(C)** Western blot for IL-1α after incubation of pro-IL-1α ± C1s. Data represent mean ± SEM of n=3 (**A**) n=2 (**B**).

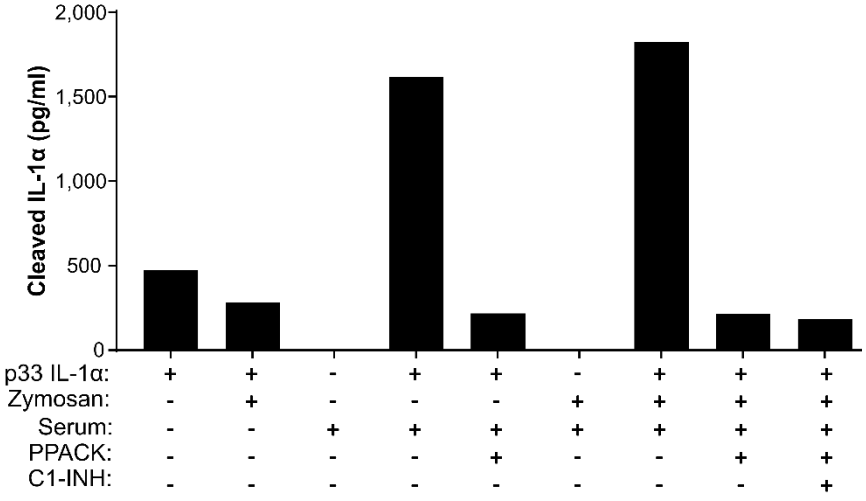

Figure 4.10: Serum complement activation by zymosan. ELISA data showing level of cleaved IL-1α in reaction products from p33 IL-1α ± Zymosan ± Serum ± thrombin inhibitor PPACK ± C1 inhibitor (C1-INH). Data is n=1.

Epidermal cells of the skin, a critical barrier tissue, express high basal levels of IL-1α. Mice overexpressing IL-1α suffer from skin inflammation, with a more severe phenotype observed when IL-1R1 is also overexpressed in keratinocytes (Groves et al., 1995, Groves et al., 1996). Despite being only a few layers of cells thick, the epidermis has an extremely complex structure. It is organised into layers of keratinocytes at different developmental stages, with each layer exhibiting a distinct protease and inhibitor profile. KLK5 forms part of a kallikrien cascade in the outer layers of the skin that regulates desquamation, and is upregulated in inflammatory skin disorders such as psoriasis (Komatsu et al., 2007). KLK5 cleaved recombinant IL-1α to a 17kDa product (Figure 4.11A,C), but unexpectedly this product was inactive (Figure 4.11B). KLK5 was unable to inactivate p17 IL-1α (Figure 4.11D), indicating that this lack of activity was not due to a second C-terminal cleavage event.

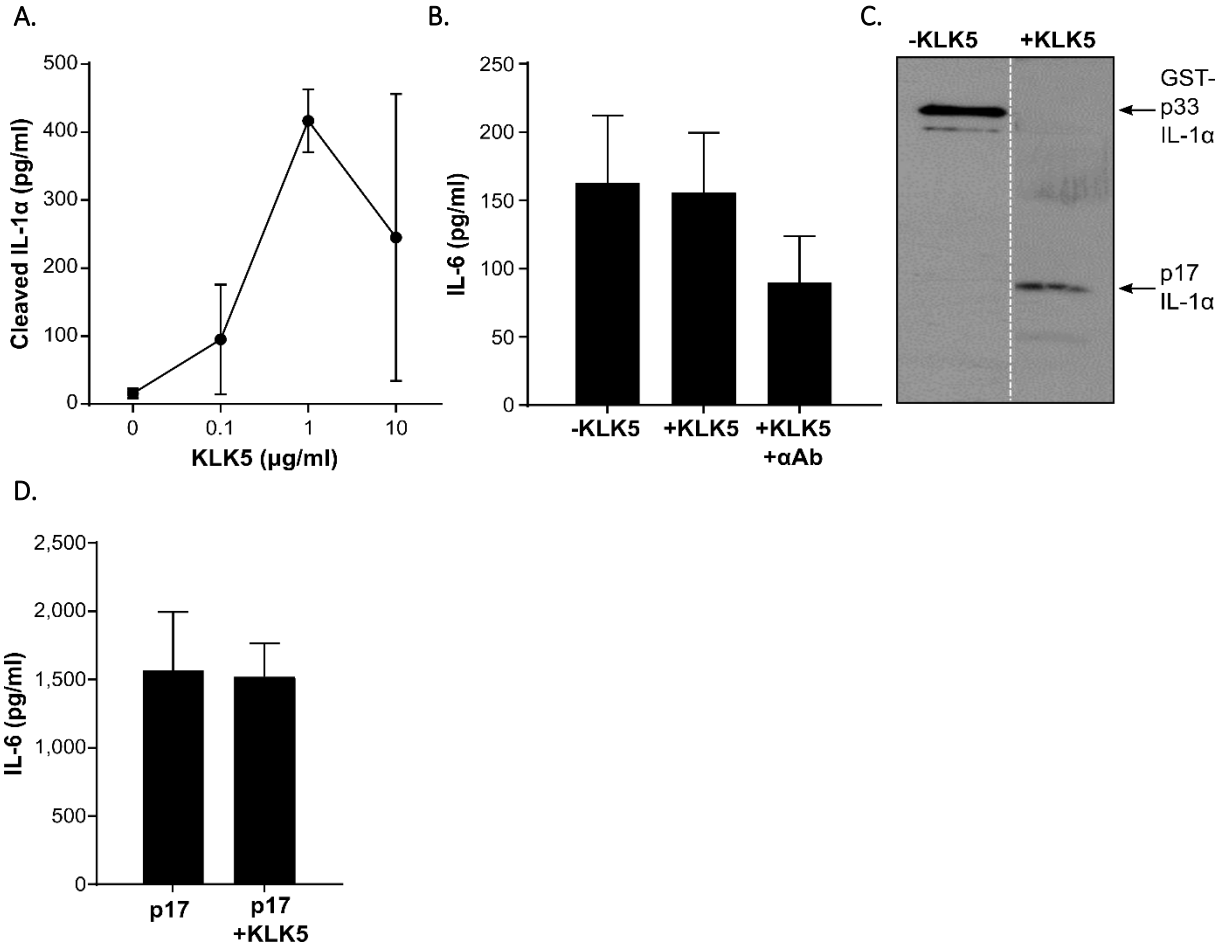

Figure 4.11: KLK5 cleaves, but does not activate IL-1α. (A) ELISA data showing level of cleaved IL-1α following incubation of pro-IL-1α with increasing concentrations of KLK5. **(B)** IL-1α-dependent IL-6 production by HeLa cells treated with reaction products from pro-IL-1α incubated ±KLK5 ± neutralising IL-1α antibody (αAb). **(C)** Western blot for IL-1α after incubation of pro-IL-1α ± KLK5. **(D)** ELISA data showing level of cleaved IL-1α following the incubation of p17 IL-1α ± KLK5. Data represent mean ± SEM of n=2 or n=3 (**B**).

4.2.4 Multiple matrix metalloproteinases activate IL-1α

Matrix metalloproteinases (MMPs) are calcium and zinc-dependent proteases that degrade the extracellular matrix. MMPs have important roles in tissue remodelling and cellular processes including apoptosis and differentiation, and their dysregulation is implicated in a number of diseases including cancer metastasis. The gelatinases MMP2 and MMP9 and the collagenase MMP8 are upregulated in atherosclerosis (Vacek et al., 2015). MMP2 cleaved recombinant and VSMC-derived IL-1α with high specificity (Figure 4.12), indicated by a clear western blot band of approximately 17kDa (Figure 4.12C) and sustained IL-1α activity over longer incubation times (Figure 4.12F,G). MMP8 was also able to activate IL-1α (Figure 4.13), whereas cleavage by MMP9 was less pronounced (Figure 4.14).

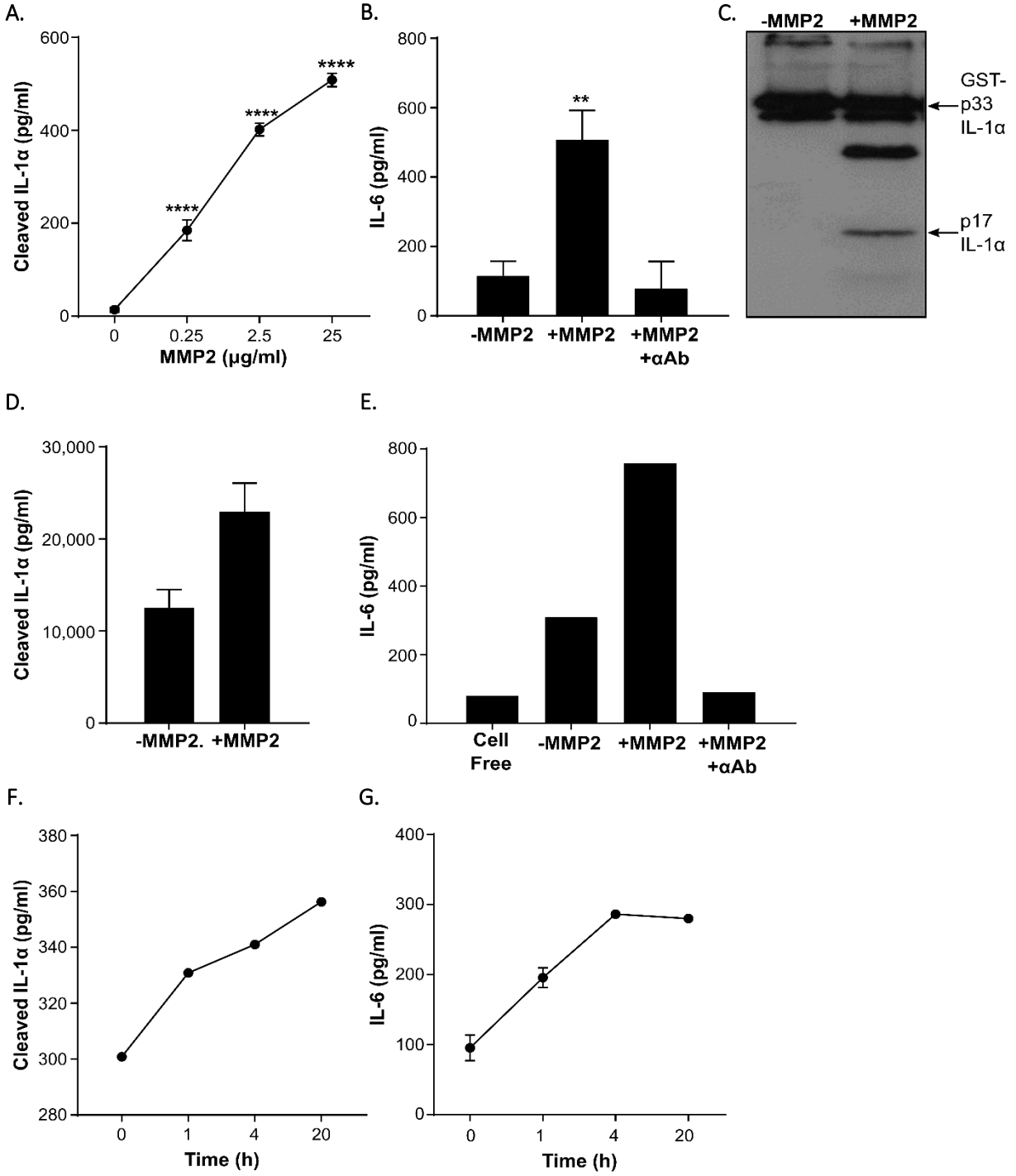

Figure 4.12: MMP2 activates IL-1α. **(A)** ELISA data showing level of cleaved IL-1α following incubation of pro-IL-1α with increasing concentrations of MMP2. **(B)** IL-1α-dependent IL-6 production by HeLa cells treated with reaction products from pro-IL-1α incubated ± MMP2 ± neutralising IL-1α antibody (αAb). **(C)** Western blot for IL-1α after incubation of pro-IL-1α ± MMP2. **(D-E)** ELISA data showing level of cleaved IL-1α in reaction products (**D**) and IL-1-dependent IL-6 production by HeLas treated with reaction products (**E**) following incubation of calpeptin-containing VSMC lysates ± MMP2. **(F-G)** ELISA data measuring cleaved IL-1α levels in reaction products (**F**) and IL-1α-dependent IL-6 production by HeLa cells treated with reaction products (**G**) following incubation of pro-IL-1α with MMP2 for a range of time points. Data represent mean ± SEM of n=5 (**A**) n=4 (**B**), n=2 (**E**) or n=1 (**D,F,G**); p= **≤0.01, ****≤0.0001.

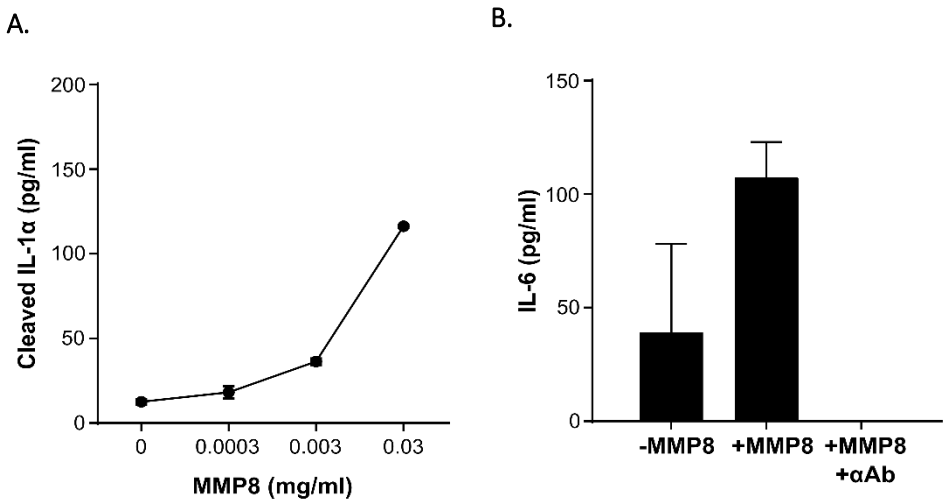

Figure 4.13: MMP8 activates IL-1α. (A) ELISA data showing level of cleaved IL-1α following incubation of pro-IL-1α with increasing concentrations of MMP8. **(B)** IL-1α-dependent IL-6 production by HeLa cells treated with reaction products from pro-IL-1α incubated ± MMP8 ± neutralising IL-1α antibody (αAb). Data represent mean ± SEM of n=2.

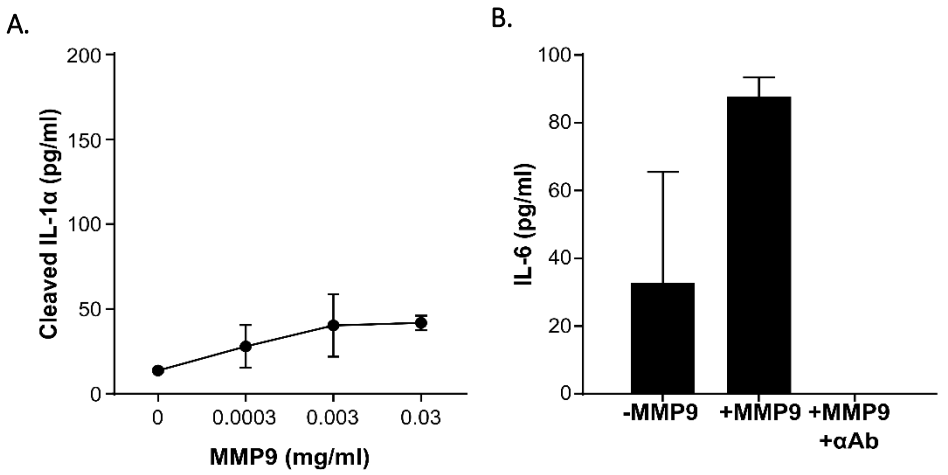

Figure 4.14: MMP9 activates IL-1α. (A) ELISA data showing level of cleaved IL-1α following incubation of pro-IL-1α with increasing concentrations of MMP9. **(B)** IL-1α-dependent IL-6 production by HeLa cells treated with reaction products from pro-IL-1α incubated ± MMP9 ± neutralising IL-1α antibody (αAb). Data represent mean ± SEM of n=2.

4.2.5 Proteases released by pathogens activate IL-1α

Whilst it is important to understand the proteolytic activation of IL-1α during sterile inflammation in the context of atherosclerosis and other chronic inflammatory diseases, it is also of interest under non-sterile conditions because many pathogens use proteases during host invasion. The bacterial protease Staphyloccocus GluC, also known as the V8 protease, has been reported to disrupt epidermal barrier function (Hirasawa et al., 2010). Staphylococcus GluC was capable of modest IL-1α activation, although this was not statistically significant or visible by western blot (Figure 4.15). The HIV protease cleaves viral polyproteins into mature proteins, a process that is essential for the viral replication cycle (Kohl et al., 1988). HIV protease activated recombinant and VSMC-derived IL-1α (Figure 4.16) by producing a single 17kDa product (Figure 4.16C). There was only a modest reduction in IL-1α bioactivity after 20 hours of incubation suggesting that this interaction is reasonably specific (Figure 4.16G).

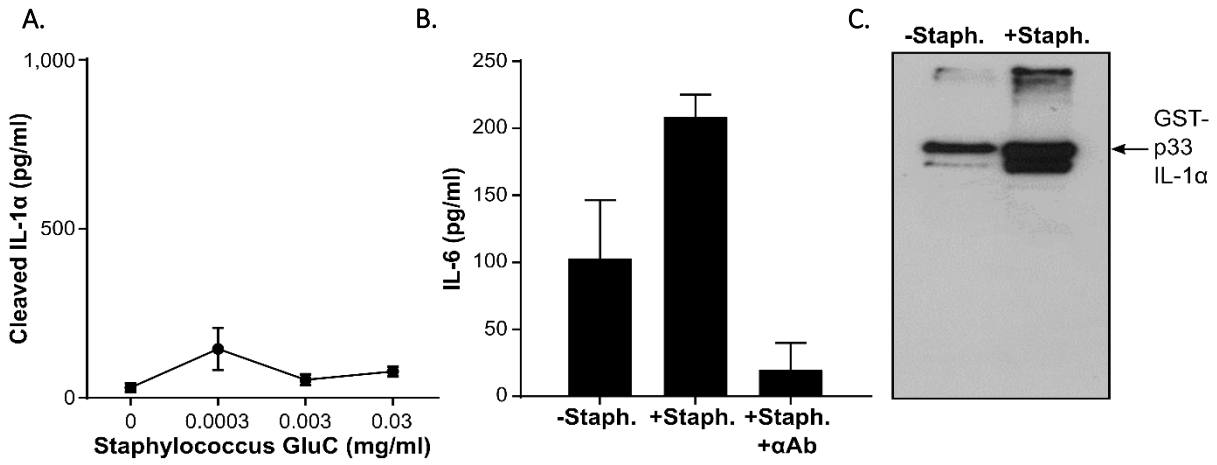

Figure 4.15: Staphylococcus GluC may activate IL-1α. (A) ELISA data showing level of cleaved IL-1α following incubation of pro-IL-1α with increasing concentrations of Staphylococcus GluC. (B) IL-1α-dependent IL-6 production by HeLa cells treated with reaction products from pro-IL-1α incubated ± Staphylococcus GluC (Staph.) ± neutralising IL-1α antibody (αAb). (C) Western blot for IL-1α after incubation of pro-IL-1α ± Staphylococcus GluC. Data represent mean ± SEM of n=3 (A) n=5 (B) p= *≤0.05, ***≤0.001.

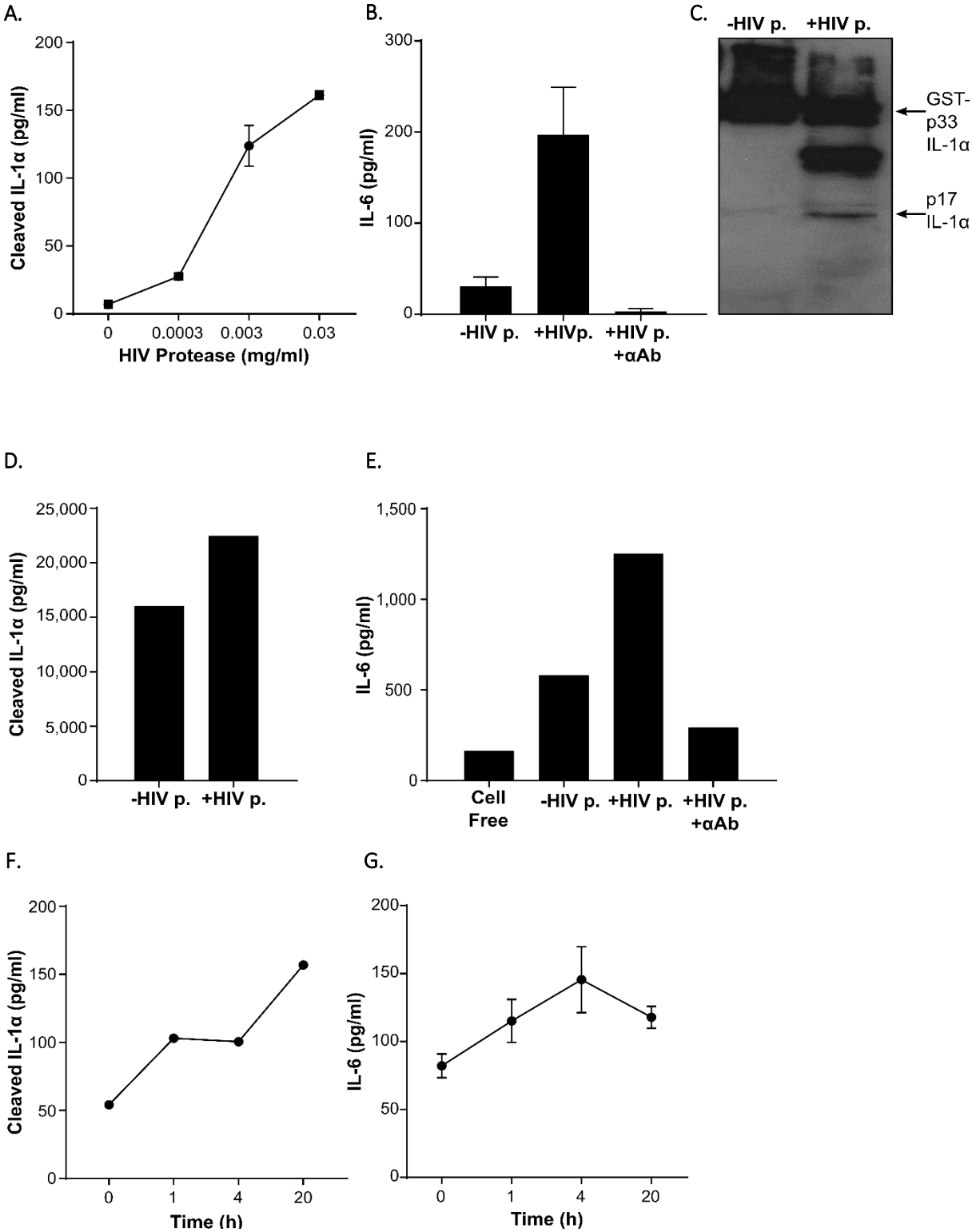

Figure 4.16: HIV protease activates IL-1α. (A) ELISA data showing level of cleaved IL-1α following incubation of pro-IL-1α with increasing concentrations of HIV protease. **(B)** IL-1α-dependent IL-6 production by HeLa cells treated with reaction products from pro-IL-1α incubated ± HIV protease (HIV p.) ± neutralising IL-1α antibody (αAb). **(C)** Western blot for IL-1α after incubation of pro-IL-1α ± MMP2. **(D-E)** ELISA data showing level of cleaved IL-1α in reaction products (**D**) and IL-1-dependent IL-6 production by HeLas treated with reaction products (**E**) following incubation of calpeptin-containing VSMC lysates ± HIV protease. **(F-G)** ELISA data measuring cleaved IL-1α levels in reaction products (**F**) and IL-1α-dependent IL-6 production by HeLa cells treated with reaction products (**G**) following incubation of pro-IL-1α with HIV protease for a range of time points. Data represent mean ± SEM of n=2 (**A,B**) n=1 (**D-G**).

4.2.6 Proteases involved in protein degradation activate IL-1α

In the autoinhibition model presented in Chapter 3 of this dissertation, we suggest that the region connecting the pro- and cytokine-domains of IL-1α protrudes from the protein to form a loop that is particularly accessible to proteases. Based on this theory, it would be reasonable to suggest that non-specific proteases with roles in protein degradation would temporarily activate IL-1α due to preferential cleavage in the loop region. Indeed, incubation with proteinase-K, which is known to have an extremely broad substrate specificity, increased IL-1α activity (Figure 4.17).

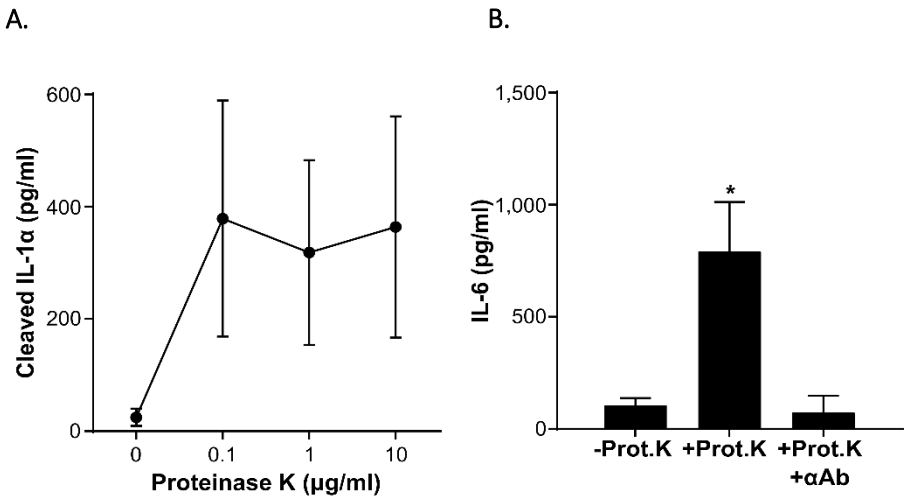

Figure 4.17: Proteinase-K activates IL-1α. (A) ELISA data showing level of cleaved IL-1α following incubation of pro-IL-1α with increasing concentrations of proteinase K. **(B)** IL-1α-dependent IL-6 production by HeLa cells treated with reaction products from pro-IL-1α incubated ± proteinase K (Prot.K) ± neutralising IL-1α antibody (αAb). Data represent mean ± SEM of n=3; p= *≤0.05.

Cathepsin B is a lysosomal cysteine protease involved in the digestion of organelles, removal of invading pathogens and cell autolysis. Its expression has been shown to be upregulated in both early and advanced atherosclerotic plaques (Chen et al., 2002, Jaffer et al., 2011). Cathepsin B activated both recombinant and VMSC-derived IL-1α to generate two products of 21kDa and 17kDa (Figure 4.18A-F). Cathepsin B-mediated IL-1α was, in fact, highly specific since there was no loss of activity at longer time points (Figure 4.18G,H).

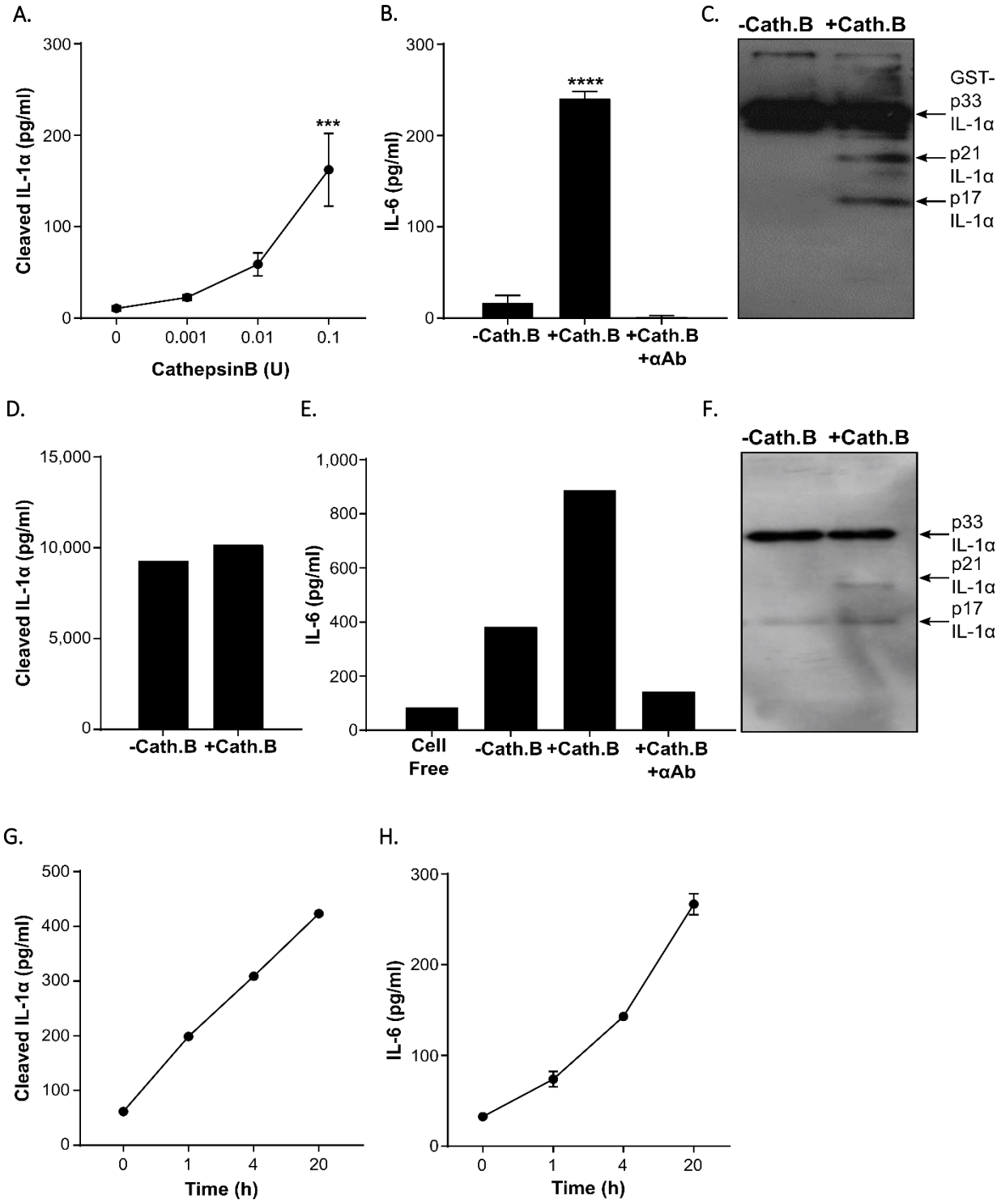

Figure 4.18: Cathepsin B activates IL-1α. **(A)** ELISA data showing level of cleaved IL-1α following incubation of pro-IL-1α with increasing concentrations of cathepsin B. **(B)** IL-1α-dependent IL-6 production by HeLa cells treated with reaction products from pro-IL-1α incubated ± cathepsin B (Cath.B) ± neutralising IL-1α antibody (αAb). **(C)** Western blot for IL-1α after incubation of pro-IL-1α ± cathepsin B. **(D-E)** ELISA data showing level of cleaved IL-1α in reaction products (**D**) and IL-1-dependent IL-6 production by HeLas treated with reaction products (**E**) following incubation of calpaptin-containing VSMC lysates ± cathepsin B. **(F)** Western blot for IL-1α after incubation of calpeptin-containing VSMC lysates ± cathepsin B **(G-H)** ELISA data measuring cleaved IL-1α levels in reaction products (**G**) and IL-1α-dependent IL-6 production by HeLa cells treated with reaction products (**H**) following incubation of pro-IL-1α with cathepsin B for a range of time points. Data represent mean ± SEM of n=4 (**A**), n=3 (**B**) or n=1 (**D-H**); p=***≤0.001, ****≤0.0001.

4.2.7 Caspases-5 and -14 cleave IL-1α

The caspases are cysteine-dependent proteases that can be categorised into two subgroups according to their function; apoptotic or inflammatory. Caspase-14 is expressed in the skin where it regulates the final stage of keratinocyte differentiation, known as cornification, which leads to the formation of hair or nails. Psoriatic lesions are characterised by impaired cornification, and display reduced caspase-14 expression (Denecker et al., 2008). Caspase-14 cleaved IL-1α at high concentrations, but this processing did not increase activity (Figure 4.19). We also tested the ability of caspases 1-10 to cleave IL-1α, and western blot analysis revealed that caspase-5 produced a 19kDa cleavage product (Figure 4.20), which will be explored in depth in Chapters 5 and 6 of this dissertation.

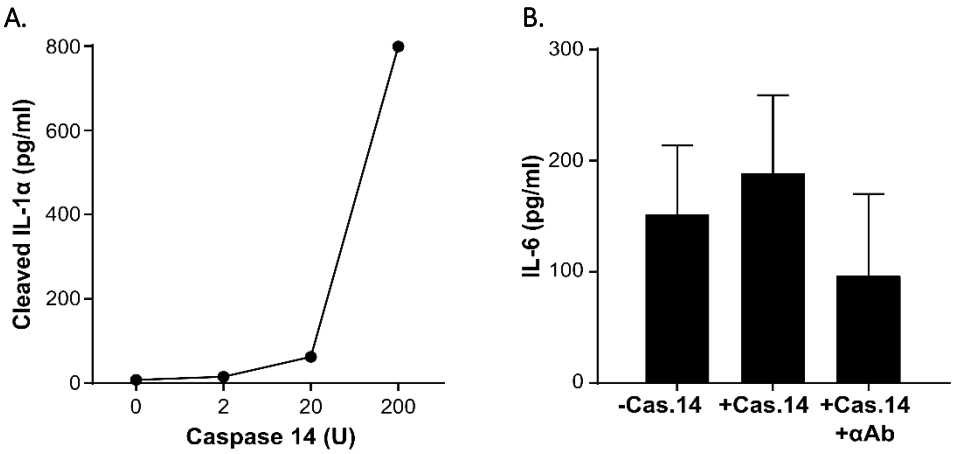

Figure 4.19: Caspase-14 cleaves, but does not activate IL-1α. (A) ELISA data showing level of cleaved IL-1α following incubation of pro-IL-1α with increasing concentrations of caspase-14. **(B)** IL-1α-dependent IL-6 production by HeLa cells treated with reaction products from pro-IL-1α incubated ± caspase-14 (Cas.14) ± neutralising IL-1α antibody (αAb). Data is n=1.

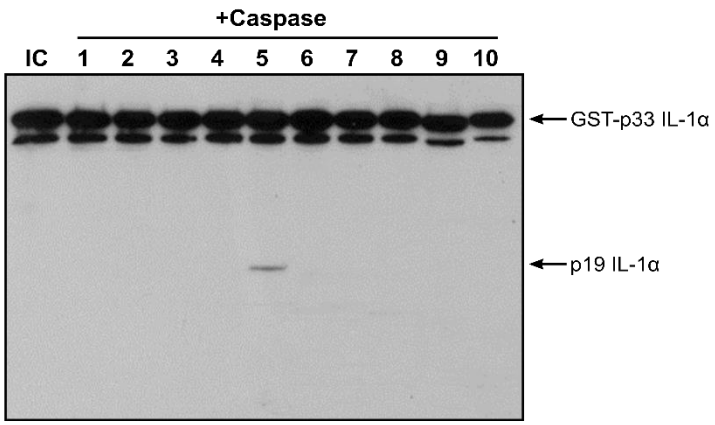

Figure 4.20: Caspase-5 cleaves IL-1α. Western blot for IL-1α after incubation of pro-IL-1α ± caspases 1-10. (IC=incubation control).

4.2.8 Not all proteases can cleave IL-1α

Fibroblast activating protein alpha (FAPα) is a serine protease that is upregulated in a number of cancers. It functions as a collagenase and has been implicated in atherosclerosis where it contributes to fibrous cap thinning to promote plaque instability (Brokopp et al., 2011). FAPα was unable to activate recombinant IL-1α in our assays (Figure 4.21). The fact that FAPα and the caspases (except 5 and 14) could not cleave IL-1α was somewhat promising, as it gave us confidence that the cleavage detected by other proteases was not an artefact of incubating recombinant substrate with recombinant enzyme at non-physiological concentrations.

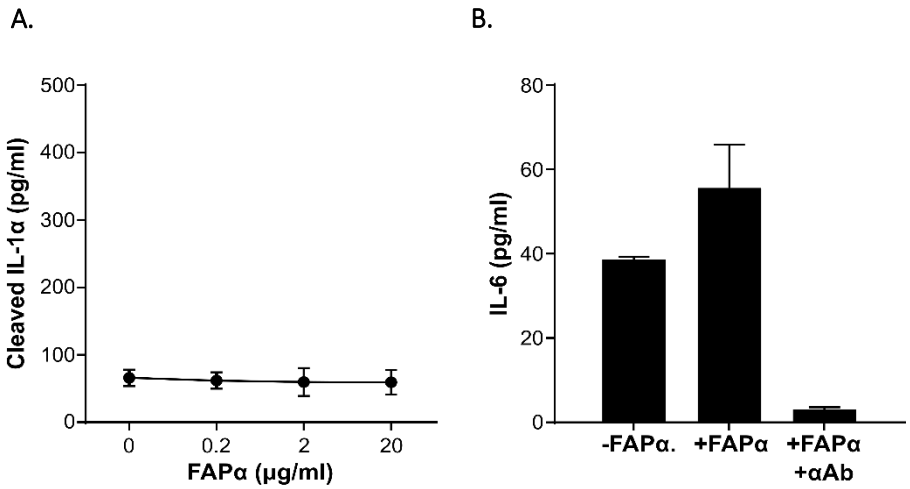

Figure 4.21: FAPα does not activate IL-1α. (A) ELISA data showing level of cleaved IL-1α following incubation of pro-IL-1α with increasing concentrations of FAPα. **(B)** IL-1α-dependent IL-6 production by HeLa cells treated with reaction products from pro-IL-1α incubated ± FAPα ± neutralising IL-1α antibody (αAb). Data represent mean ± S.E.M. of n=3 (**A**) or n=4 (**B**).

4.3 Discussion

The activity of most IL-1 family members is modulated by proteolytic cleavage. For many years, IL-1α was believed to be the exception to this rule and was described as fully active in its pro-form. However, recent work by ourselves and others has shown that the removal of the IL-1α pro-domain by the canonical protease calpain significantly enhances its activity by increasing its affinity for the IL-1R1 (Afonina et al., 2011, Zheng et al., 2013). Furthermore, there is emerging evidence that additional proteases, such as Granzyme B and thrombin, can also activate IL-1α (Afonina et al., 2011) (Burzynski et al, *publication in progress*).

Here, we show that IL-1α can, in fact, be activated by a range of proteases from diverse biological systems that are summarised in Table 4.1. The most robust, and specific, of these proteases were MMP-2, HIV protease and Cathepsin B (Figures 4.12, 4.16 and 4.18). MMP-2-mediated ECM remodelling is heavily involved in metastasis. For instance, it drives the initiation of an invasive phenotype in ovarian cancer cells by promoting their attachment to the peritoneum by cleaving fibronectin and vibronectin (Kenny et al., 2008). IL-1 has also been implicated in tumour invasiveness (Voronov et al., 2002), and is known to enhance the expression of multiple cancer-associated genes through the NF-κB pathway (Charbonneau et al., 2014). The processing of IL-1α by MMP2 may therefore be important for triggering the immune-mediated killing of malignant cells, or may contribute to disease progression by establishing an inflammatory environment. The robust activation of IL-1α by HIV protease was particularly unexpected because the natural role of this enzyme is to cleave viral polyproteins, which would suggest restricted substrate specificity. This interaction could represent a host defence mechanism for alerting the immune system to the HIV infection. However, IL-1α activation may actually be beneficial for the virus because it drives NF-κB signalling, a pathway harnessed by HIV to drive its own gene transcription (Hiscott et al., 2001). In fact, *IL1A* overexpression has been shown to increase the production of HIV in infected cells by up to seven-fold (McLaren et al., 2015). The seemingly specific activation of IL-1α by Cathepsin B was also unanticipated, since the two proteins are spatially segregated in healthy cells. Lysosomal membrane permeabilisation occurs during cell death; complete permeabilisation causes

necrosis whereas partial permabilisation causes activation of the apoptotic caspases and proteins Bid and Bax. The potent activation of cytosolic IL-1α by cathepsin B may represent a mechanism to alert the immune system to loss of intracellular homeostasis and recruit immune cells to clear away the dead cell. Furthermore, cathepsin B has been reported to translocate to the nucleus and induce rapid DNA damage and chromatin condensation. Cathepsin B could therefore also cleave nuclear IL-1α and potentially disrupt its apoptotic association with chromatin mediating a switch towards inflammatory necrotic death (Boya and Kroemer, 2008).

We demonstrate that although some proteases such as granzyme B (Figure 4.5) cleaved IL-1α at a single site to impart sustained bioactivity, other proteases such as elastase, chymase and proteinase-3 (Figures 4.5-4.7) were less specific and gradually inactivated IL-1α over time. Granzyme B activity is tightly regulated; it is released from cytotoxic lymphocytes inside endocytic vesicles, only exits the vesicles following perforin activity and specifically activates caspase 3 in target cells to initiate the cell death programme (Lord et al., 2003). This protease would therefore come into contact with IL-1α under specific conditions, with regulation of enzyme-substrate interaction at the level of enzyme availability. In contrast, chymase, elastase and proteinase 3 have broader substrate specificities and are released into the extracellular milieu (Caughey, 2007, Korkmaz et al., 2010). These proteases generated both active IL-1α fragments of 18-20kDa and shorter fragments of 10-12kDa that are likely to be inactive. The fact that broad-specificity proteases can generate activity supports our working hypothesis that the loop region between the pro and the cytokine domains of IL-1α is particularly susceptible to cleavage. The subsequent generation of smaller fragments may represent an internal ‘off-switch’ within IL-1α, where it is transiently activated by these promiscuous proteases and subsequently degraded to stop aberrant inflammation amplification.

Not all proteases tested were able to activate IL-1α. Some proteases, such as KLK5 (Figure 4.11), were able to cleave IL-1α but did not induce activity, which highlights the importance of complementing the cleaved IL-1α ELISA with the IL-1 bioassay. Other proteases were completely unable to cleave IL-1α. For instance all of the apoptotic caspases (caspases-2, -3, -6, -7, -8, -9, and -10) (Figure 4.20) were

unable to process IL-1α. Since pro-IL-1α is constitutively expressed by most cell types, this lack of interaction is extremely important to maintain the anti-inflammatory nature of programmed cell death. The fact that some proteases were incapable of IL-1α processing and activation also imparts confidence that the proteases that do activate IL-1α are not simply an artefact of the *in vitro* system.

To enhance our understanding of IL-1α activation further, the cleavage sites of the highly specific proteases could be defined by sequencing the N-terminal residues of the cleavage products by Edman degradation and/or mutating predicted sites based on known protease specificity. For example, cathepsin B has a strong preference for a glycine residue at position P3' (Biniossek et al., 2011), which is highly conserved between species at amino acid 78 in IL-1α. For proteases that exhibited high specificity but where western blot analysis revealed only a small proportion of the total IL-1α protein was processed (e.g MMP-2 and HIV protease), the cleavage product could be enriched by cloning a C-terminal His-tag onto the pro-IL-1α protein and purifying the product over a column containing cobalt resin. Finally, although the VSMC lysates are a useful source of mammalian, post-translationally modified IL-1α, they must be prepared in the presence of calpeptin to prevent calpain activation upon necrosis. Calpeptin is known to inhibit other proteases, such as caspase-3 (Peng et al., 2011). An alternative approach could be to prepare post-translationally modified recombinant pro-IL-1α by overexpression in HEK or HeLa cells or using a baculovirus expression system in insect cells. This would allow further validation of enzyme-substrate interactions without the interference of calpain or calpeptin.

To conclude, the work presented in this chapter has demonstrated that multiple proteases from diverse biological systems are able to activate IL-1α, some transiently, others permanently. Unlike IL-1β, pro-IL-1α is constitutively expressed by most cell types and is therefore always available for activation. As such, IL-1α may represent a crucial signalling molecule that integrates diverse proteolytic signals of compromised homeostasis.

ENZYME	MAIN FUNCTION	PREFERRED P1 AMINO ACID (IF KNOWN)	CLEAVES IL-1α?	ACTIVATES IL-1α?	SPECIFICITY OF IL-1α INTERACTION	IL-1α CLEAVAGE SITE IF KNOWN OR PREDICTED*
Calpain	Apoptosis and necrosis	Unknown	✓	✓	Highly specific	118/119
Thrombin	Fibrinogen cleavage during coagulation	Arg	✓	✓	Highly specific	112/113 (Chpt4)
Granzyme B	Apoptosis induction	Asp	✓	✓	Highly specific	103/104 (Afonina et al., 2011)
Neutrophil Elastase	Bacterial membrane breakdown	Val or Ala	✓	✓	Specific, but degrades over time	101/102* (Afonina et al., 2011)
Neutrophil Proteinase-3	Antimicrobial peptide generation	Unknown	✓	✓	Specific, but degrades over time	Unknown
Chymase	Leukocyte attraction, ECM degradation, apoptosis	Tyr or Phe (Andersson et al., 2009)	✓	✓	Unknown	116/117* (Afonina et al., 2011)
C1s	Classical complement pathway activation	Arg (Kerr et al., 2005)	?	?	Unknown	Unknown
KLK5	Keratinocyte desquamation	Arg (Debela et al., 2008)	✓	X	Unknown	Unknown
MMP2	ECM remodelling	Ser, Gly, Ala, or Glu (Turk et al., 2001a)	✓	✓	Highly specific	Unknown
MMP8	ECM remodelling	Unknown	✓	✓	Unknown	Unknown
MMP9	ECM remodelling	Ser (Turk et al., 2001a)	?	?	Unknown	Unknown
Staph. GluC	Bacterial growth & survival	Glu	?	?	Unknown	Unknown
HIV protease	Viral polyprotein processing	Unknown	✓	✓	Highly specific	Unknown
Proteinase K	Protein digestion (in lab)	Non-specific	✓	✓	Non-specific	Unknown
Cathepsin B	Lysosomal protein degradation	Arg, Lys (Choe et al., 2006)	✓	✓	Highly specific	Unknown
Caspase-1	Inflammation activation	Asp	X	X	N/A	N/A
Caspase-2	Apoptosis initiation	Asp	X	X	N/A	N/A

Caspase-3	Apoptosis execution	Asp	X	X	N/A	N/A
Caspase-4	Inflammation activation	Asp	X	X	N/A	N/A
Caspase-5	Inflammation activation	Asp	✓	✓	Highly specific	103/104 (Chpt5)
Caspase-6	Apoptosis execution	Asp	X	X	N/A	N/A
Caspase-7	Apoptosis execution	Asp	X	X	N/A	N/A
Caspase-8	Apoptosis initiation	Asp	X	X	N/A	N/A
Caspase-9	Apoptosis initiation	Asp	X	X	N/A	N/A
Caspase-10	Apoptosis initiation	Asp	X	X	N/A	N/A
Caspase-14	Keratinocyte cornification	Asp	✓	X	N/A	Unknown

Table 4.1: Summary of proteases tested for IL-1α activation. A table listing each protease tested in this chapter, it's function, its known preferred substrate consensus sequence, whether it cleaves and activates IL-1α, how specific it's interaction with IL-1α is, and the IL-1α cleavage site if known or predicted. All target sequences from ExPASy Peptide cutter, unless cited specifically. References or thesis locations are provided for solved/suggested IL-1α cleavage sites.

5. Results: IL-1 is activated by caspase-5/-11 of the non-canonical inflammasome

5.1 Introduction

The inflammatory caspases are an extensively studied group of proteases due to their important role in host defence. The inflammasome serves as a platform for caspase-1 activation, and provides a mechanism for a cell to sense danger and respond by alerting the immune system whilst engaging a self-destruct programme. Over the last six years a significant effort has been placed on understanding an alternative pathway of inflammasome activation mediated by the additional inflammatory caspases-4 and -5 in humans, or -11 in mice, known as the non-canonical inflammasome.

The *Casp11*$^{-/-}$ and *Casp1*$^{-/-}$ mice engineered in the 1990s were both found to be resistant to septic shock (Li et al., 1995, Wang et al., 1998), and as a result the two caspases were assumed to phenocopy each other. However, in 2011 Vivsha Dixit's group realised that the original knockout mice were derived from embryonic stem (ES) cells of the 129 mouse strain, which harbour an endogenous caspase-11 mutation. This mutation, a 5 base pair deletion in exon 7, leads to the splicing of exons 6 and 8 that results in a frameshift and a premature stop codon. The extremely close proximity of the *Casp1* and *Casp11* genes excluded the possibility for segregation by recombination, which meant that the *Casp-1*$^{-/-}$ mice were in fact a double knockout for both caspases-1 and -11. Transgenically reintroducing caspase-11 using a bacterial artificial chromosome (BAC) showed that caspase-1 deficiency did not protect the animals from sepsis - only caspase-11 deficiency did, thus revealing that caspase-11 was the sole driver of LPS-induced lethality (Kayagaki et al., 2011). The *Casp11* passenger mutation in 129 mice was a critical discovery that influenced multiple scientific fields, since injecting targeted 129 ES cells into C57BL/6 blastocysts was a common strategy for making early genetic knockouts. Importantly, the mutation was not only carried forward when genes adjacent to *Casp11* were targeted, but also in knockout animals, such as *Casp3*$^{-/-}$, where the target gene was located on a different chromosome.

Therefore, the re-characterisation of mice engineered using this method is essential because their described phenotypes may actually be driven by caspase-11 (Stowe et al., 2015).

Following the discovery that caspase-11 mediates septic shock, four groups independently demonstrated that intracellular LPS from the Gram negative bacterial cell wall directly activates caspases-11, -4 and-5 (Kayagaki et al., 2013, Hagar et al., 2013, Shi et al., 2014, Baker et al., 2015). The lipid A moiety of the LPS molecule must be hexa-acylated for caspase activation to occur; which is a feature exploited by some pathogens, such as *Helicobacter pylori*, that interfere with this interaction by decreasing their number of acyl chains to evade immune detection (Raetz et al., 2007).

In most cell types, non-canonical inflammasome activation is a two-step process: priming followed by activation (Figure 5.1). Priming requires PRR engagement by a PAMP, which activates two intracellular signalling pathways. NF-κB signalling upregulates the canonical inflammasome components NLRP3, ASC, caspase-1 and IL-1, whilst the TRIF-IRF-IFN pathway promotes the expression of non-canonical inflammasome factors. Although human caspases-4 and -5 are both referred to as caspase-11 orthologues based on sequence similarity (Lin et al., 2000), caspases-11 and -5 are highly inducible through type I IFN signalling, whereas caspase-4 is constitutively expressed at a high levels in many cell types. The IFN pathway is essential for caspase-11 activation during bacterial infection, but dispensable for the response to directly transfected LPS. A plausible explanation for this is that the IFN pathway also upregulates the guanylate-binding protein (GBP) GTPases that promote the lysis of bacteria-containing vacuoles (Yang et al., 2015, Meunier et al., 2014). The GBPs also liberate LPS from the outer membrane vesicles of external bacteria that have been endocytosed, facilitating activation of the non-canonical inflammasome by extracellular pathogens (Vanaja et al., 2016).

Our understanding of the non-canonical inflammasome pathway was further advanced in 2015, when Vivsha Dixit and Feng Shao's research groups independently identified Gasdermin D (GSDMD) as the effector protein of the non-canonical inflammasome. Caspases-11/-4/-5 cleave GSDMD to liberate a 30kDa N-terminal fragment ($GSDMD^N$) that both activates the NLRP3 inflammasome and caspase-1, and also drives pyroptosis (Kayagaki et al., 2015, Shi et al., 2015). $GSDMD^N$ causes cell death by

translocating to the plasma membrane and binding to inner membrane phospholipids to form pores (Aglietta et al., 2016, Ding et al., 2016, Liu et al., 2016). Over time, the accumulation of these pores leads to the loss of plasma membrane integrity, and the cell ruptures. However, recent studies indicate that there is a delay between caspase-11 activation and pyroptosis, during which the plasma membrane undergoes 'bubbling' (Petr Broz, *unpublished data*). This bubbling is mediated by the ESCRT III protein complex that causes the pore-containing regions of plasma membrane to 'pinch-off' so that cell integrity is preserved, in a similar manner to that reported for necroptosis (Gong et al., 2017). This delay is thought to give the cell time to secrete cytokines to communicate its state of damage and recruit immune cells before it dies.

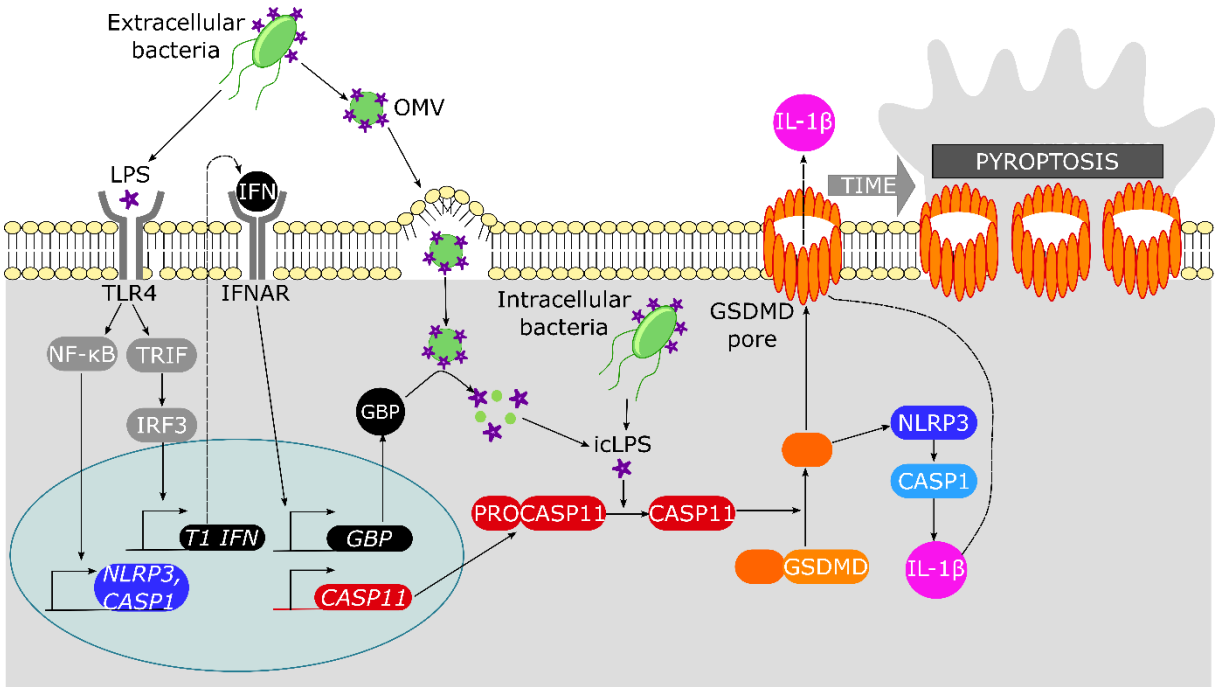

Figure 5.1: The non-canonical inflammasome. TLR4 ligation by LPS serves as a priming signal to activate the NF-κB and TRIF signalling pathways to upregulate the expression of inflammasome components and type I interferons (T1 IFN), respectively. Type 1 IFN signalling induces the expression of pro-caspase-11 and guanylate binding proteins (GBPs). The GBPs liberate LPS from outer membrane vesicles (OMVs) from extracellular gram negative bacteria that have been endocytosed by the cell. Intracellular LPS (icLPS) from the OMVs or intracellular bacteria activates caspase-11 (CASP11), which cleaves gasdermin D (GSDMD). The N-terminal GSDMD fragment forms membrane pores and activates the NLRP3 inflammasome to drive IL-1β activation. The GSDMD pores allow cytokine secretion, but increased pore number over time results in loss of plasma membrane integrity and induction of pyroptosis.

5.1.1 Emerging roles of the non-canonical inflammasome

Although the non-canonical inflammasome pathway has predominantly been described as a specialised response to bacterial infection, it may also drive sterile inflammation. In dendritic cells, the oxidised phospholipid oxPAPC has been reported to activate caspase-11 by eliciting the formation of a caspase-11 heterocomplex, which potentiates T cell activation (Zanoni et al., 2016). Furthermore palmitate, a saturated fatty acid involved in atherosclerosis progression, has been described to activate caspases-4 and -5 in human monocytes (Pillon et al., 2016). Caspase-5 is also activated by extracellular heme, which is associated with a number of conditions including malaria, sickle cell disease and sepsis (Boucher-Hayes, 2017). In addition, a common mutation of a polyA repeat within the *CASP5* gene that leads to a frameshift and premature stop codon has been associated with lung, colon and gastric cancers (Offman et al., 2005, Yamaguchi et al., 2006, Bian et al., 2011). The mutation of this polyA motif is particularly common in microsatellite instability cancers, suggesting that caspase-5 could play a protective role against these types of malignancies in particular. Interestingly, caspase-1 and caspase-4 mutations are rarely associated with these types of carcinoma, suggesting this protective function is truly caspase-5 specific (Soung et al., 2008). The missense *CASP5* polymorphism rs5074879 has also been associated with increased risk of renal, bladder, and lung cancer, and ageing (Dong et al., 2009, Ulybina et al., 2010, Mittal et al., 2011, Zhang et al., 2013).

The non-canonical inflammasome may also be important in maintaining normal barrier function in non-myeloid cells. Intestinal epithelial cells (IECs) express particularly high levels of caspase-11, in contrast to the low basal level expressed by most cell types. Although this is most likely due to LPS from the commensal Gram-negative gut bacteria, it allows these cells to respond rapidly to enteric infection and inflammation. The activation of caspase-11 in IECs causes infected cells to undergo pyroptosis and removal from the barrier. It also leads to the activation of IL-18, which is an important cytokine for sustaining barrier integrity by stimulating proliferation and repair. In line with this function, *Casp11*$^{-/-}$ mice are more susceptible to dextran sodium sulphate-induced colitis, exhibiting higher levels of tissue damage and leukocyte infiltration than their wildtype counterparts (Williams et al., 2015). Human IECs

also express high levels of caspase-4, which activates IL-18 that in turn promotes proliferation and neutrophil recruitment (Knodler et al., 2014).

5.1.2 Cell-type specific properties of the non-canonical inflammasome

Different cell types display distinct non-canonical inflammasome properties. Monocytes proliferate rapidly following bacterial infection, and have been described to activate their inflammasome in response to LPS alone through a 'one-step' mechanism. They express high levels of the LPS co-receptor CD14, which induces Syk activation and promotes LPS endocytosis and calcium mobilisation. This in turn triggers caspase and subsequent inflammasome activation (Vigano et al., 2015). LPS has also been proposed to activate an 'alternative inflammasome' pathway in human monocytes, but not murine monocytes, that signals through caspase-8 to indirectly promote NLPR3 activation and IL-1β secretion without pyroptosis (Gaidt et al., 2016). In addition, monocytes secrete mature IL-1β more rapidly than macrophages due to their distinct redox status. Monocytes produce low levels of ROS at a resting state that increases with LPS, whereas macrophages contain an antioxidant system that buffers the TLR-induced ROS surge (Carta et al., 2011).

Neutrophils also exhibit unique inflammasome characteristics. Although most studies have focussed on canonical inflammasome activation, neutrophils seem to be particularly resistant to pyroptosis and their cytokine secretion typically precedes cell death. Kate Schroder and colleagues reported that *Salmonella* infection leads to NLRC4 inflammasome activation within neutrophils, which secrete huge amounts of IL-1β without dying (Chen et al., 2014). This finding was supported by the Pearlman group, who demonstrated IL-1β secretion occurs before pyroptosis during ATP-induced NLRP3 inflammasome activation (Karmakar et al., 2016). Recent work by the Schroder lab has revealed that neutrophils engage two distinct response pathways. When the bacteria are extracellular or vacuolar, an NLRC4-caspase-1-IL-1β pathway promotes IL-1 release without cell death. However, when bacteria enter the cytosol, signifying that the neutrophil has become compromised, the cell activates caspase-11-mediated pyroptosis. In addition to initiating cell death caspase-11 drives neutrophil extracellular trap (NET)

formation, so that as the neutrophil pyroptoses it releases NETs as a last attempt to kill the invading microbes (Schroder, 2017).

5.1.3 Chapter 5 project rationale

It is commonly reported in the literature that, in addition to IL-1β, mature IL-1α is released following non-canonical inflammasome activation (Kayagaki et al., 2011, Gross et al., 2012, Casson et al., 2015, Vigano et al., 2015). However, the mechanisms of IL-1α activation are unknown, and it is often assumed that IL-1α release is a passive by-product of pyroptosis. However, we hypothesised that the pro-inflammatory caspases might directly activate IL-1α prior to cell death. Indeed, our western blot for IL-1α following incubation with caspases 1-10 revealed a distinct 19kDa product in the caspase-5 lane (Figure 4.20). The work presented in this chapter aims to characterise the interaction between caspase-5/-11 and IL-1 further.

5.2 Results

5.2.1 Caspase-5 activates recombinant human IL-1α

Mature IL-1α is released during non-canonical inflammasome activation, but the proteases that activate it are unknown. It is generally assumed that IL-1α is passively activated by calpain during pyroptosis, but the 19kDa IL-1α fragment produced after incubation with caspase-5 (Figure 4.20) alluded to a more direct interaction. Incubation of pro-IL-1α with each of the pro-inflammatory caspases revealed that only caspase-5 was capable of processing IL-1α (Figure 5.2A). Caspase-5 induced IL-1α activation (Figure 5.2B), which was dependent on the proteolytic action of caspase-5 since incubation with the caspase-5 inhibitor Z-LEVD-fmk significantly reduced both cleavage (Figure 5.3A) and activity (Figure 5.3B).

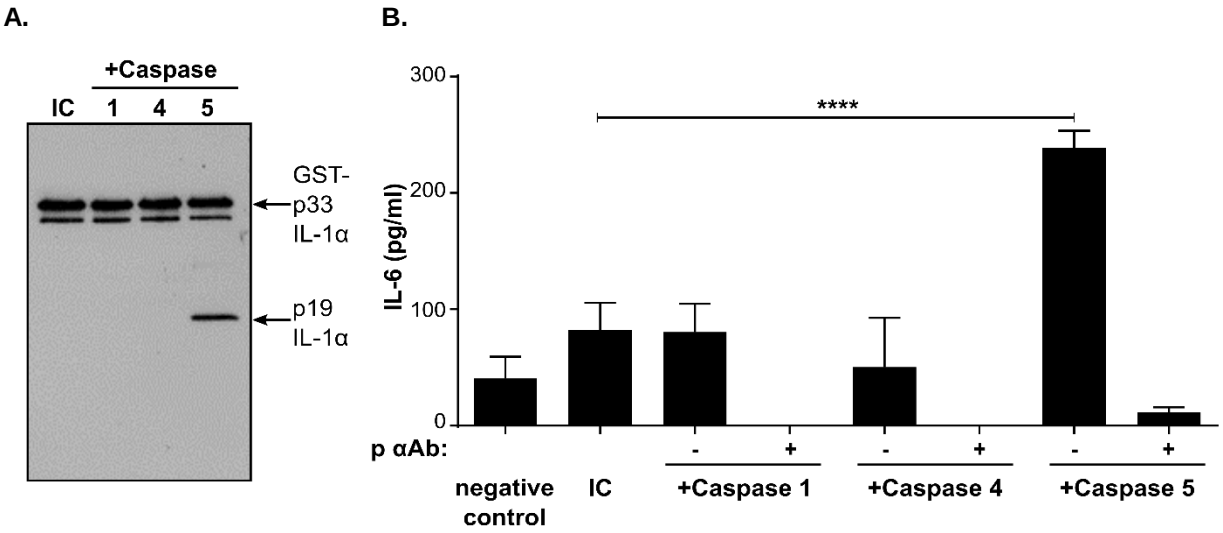

Figure 5.2: Caspase-5 cleaves and activates IL-1α. (A) Western blot for IL-1α after the incubation of pro-IL-1α with active caspase-1, -4 or-5, or alone (incubation control, IC). (B) IL-1-dependent IL-6 production by HeLa cells treated with reaction products from pro-IL-1α incubation ± active caspases, ± a neutralising IL-1α antibody (p αAb). Data represent mean +SEM of n=4. p = ****≤0.0001.

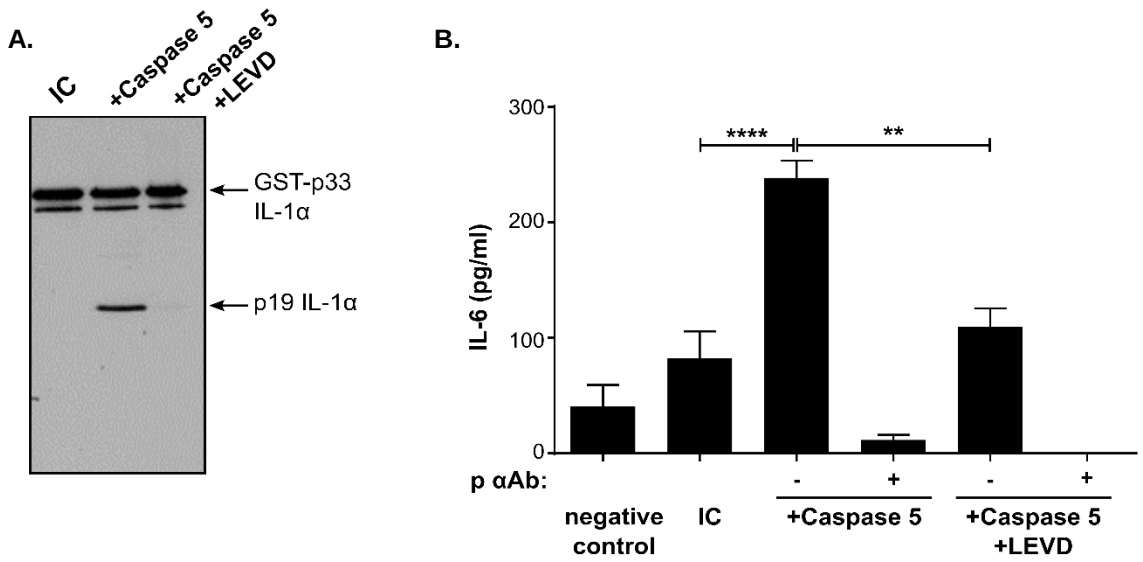

Figure 5.3: Z-LEVD-FMK inhibits the activation of IL-1α by caspase-5. (A) Western blot for IL-1α after the incubation of pro-IL-1α alone (incubation control, IC) or with active caspase-5 ± Z-LEVD-FMK. **(B)** IL-1-dependent IL-6 production by HeLa cells treated with reaction products from pro-IL-1α incubation ± active caspase-5, ± Z-LEVD-FMK, ± a neutralising IL-1α antibody (p αAb). Data represent mean +SEM of n=4, p = **≤0.01, ****≤0.0001.

5.2.2 Caspase-5 cleaves human IL-1α at aspartic acid 103

Caspases exhibit a strong preference for cleaving after aspartic acid residues (Howard et al., 1991). As such, important caspase substrates often exhibit conservation of a consensus sequence between species. Analysis of aligned IL-1α protein sequences revealed a conserved IAND tetrapeptide motif in the region corresponding to a 19kDa product size (Figure 5.4A). Mutation of the Asp^{103} to an alanine (D103A) in pro-IL-1α completely abolished cleavage (Figure 5.4B) and activation (Figure 5.4C) by caspase-5, confirming the location of the cleavage site.

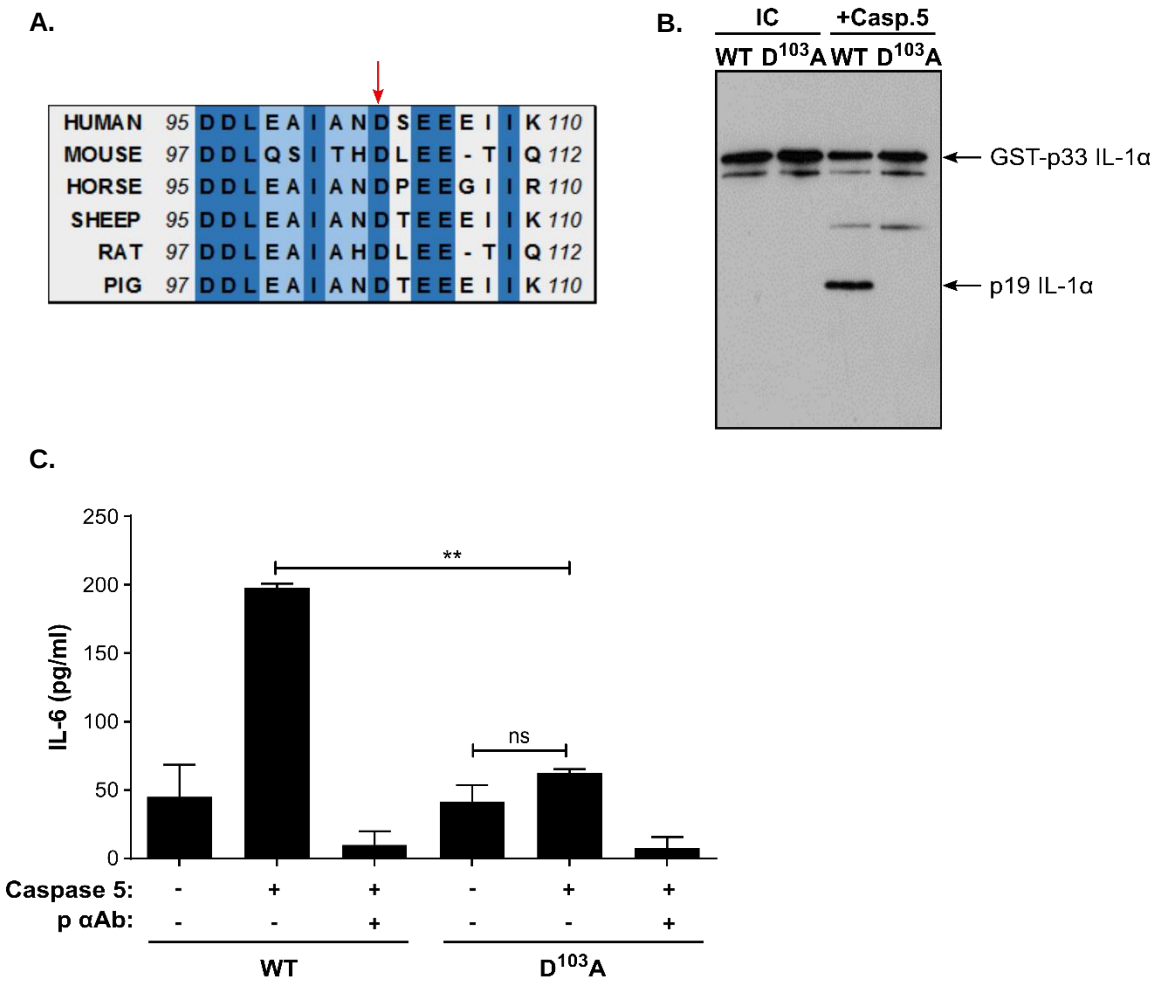

Figure 5.4: Caspase-5 cleaves IL-1α at aspartic acid 103. (A) Multiple species alignment of IL-1α sequence in region corresponding to 19kDa cleavage product size. Red arrow indicates candidate aspartic acid 103. **(B)** Western blot for IL-1α after the incubation of WT or $D^{103}A$ mutant pro-IL-1α alone (incubation control, IC) or with active caspase-5. **(C)** IL-1-dependent IL-6 production by HeLa cells treated with reaction products from WT or $D^{103}A$ pro-IL-1α incubation ± active caspase-5, ± a neutralising IL-1α antibody (p αAb). Data represent mean +SEM of n=4, p = **≤0.01.

5.2.3 Caspase-5 activates recombinant human IL-1β

The specific cleavage and activation of IL-1α by caspase-5 then prompted us to question whether additional caspases were also capable of IL-1β activation. The incubation of recombinant pro-IL-1β with caspases 1-10 revealed that caspases-1 ,-5 and -7 were able to cleave IL-1β (Figure 5.5). Focussing on the inflammatory caspases in more detail, both caspases-1 and -5 cleaved IL-1β to produce a 17kDa (Figure 5.6A) active (Figure 5.6B) product. Again, Z-LEVD-FMK prevented the cleavage (Figure 5.7A)

and activation (Figure 5.7B) of IL-1β by caspase-5, demonstrating that this interaction was dependent on proteolysis.

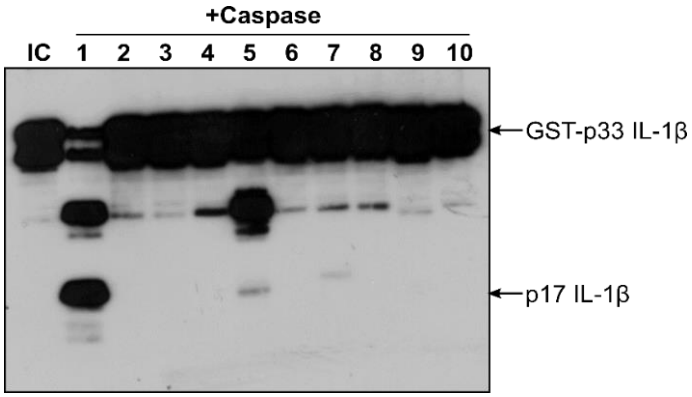

Figure 5.5: Caspases-1, -5 and -7 cleave human IL-1β. Western blot for IL-1β after the incubation of pro-IL-1β with active caspases-1-10, or alone (incubation control, IC).

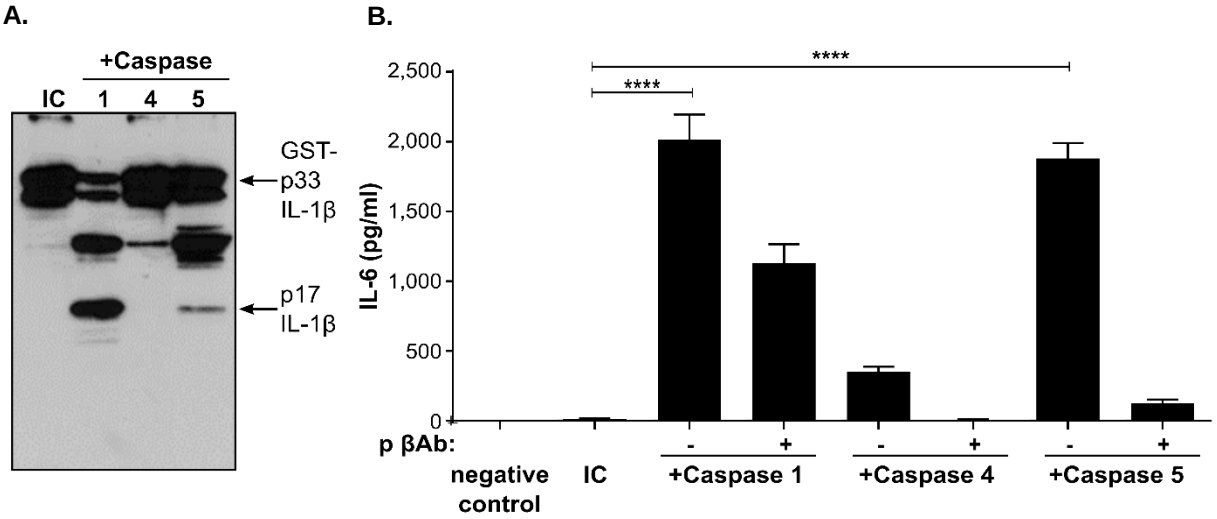

Figure 5.6: Caspases-1 and -5 activate IL-1β. (A) Western blot for IL-1β after the incubation of pro-IL-1β with active caspase-1, -4 or-5, or alone (incubation control, IC). **(B)** IL-1-dependent IL-6 production by HeLa cells treated with reaction products from pro-IL-1β incubation ± active caspases, ± a neutralising IL-1β antibody (p βAb). Data represent mean +SEM of n=4, p = ****≤0.0001.

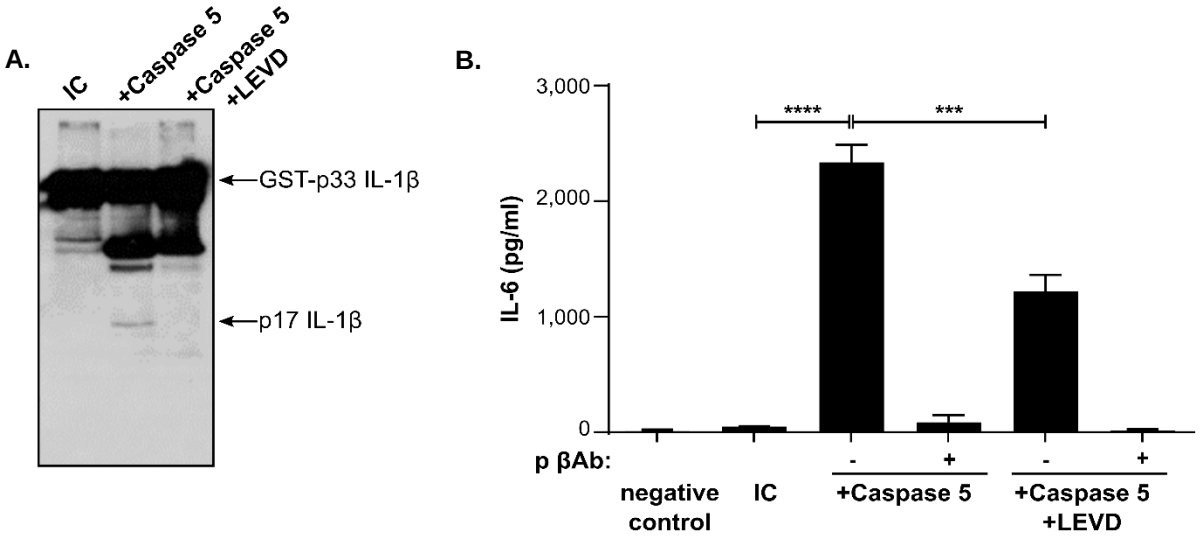

Figure 5.7: Z-LEVD-FMK inhibits the activation of IL-1β by caspase-5. (A) Western blot for IL-1β after the incubation of pro-IL-1β alone (incubation control, IC) or with active caspase-5 ± Z-LEVD-FMK. **(B)** IL-1-dependent IL-6 production by HeLa cells treated with reaction products from pro-IL-1β incubation ± active caspase-5, ± Z-LEVD-FMK, ± a neutralising IL-1β antibody (p βAb). Data represent mean +SEM of n=4, p = ***≤0.001, ****≤0.0001.

5.2.4 Caspase-5 cleaves human IL-1β at aspartic acid 116

Since caspase-5 generated a similar 17kDa IL-1β product to caspase-1, the highly conserved Asp^{116} was the primary candidate for the cleavage site (Figure 5.8A). Indeed, mutation of this aspartic acid to an alanine (D116A) completely prevented the cleavage (Figure 5.8B) and activation (Figure 5.8C) of IL-1β by caspase-5, demonstrating that caspase-5 cleaves IL-1β at the same site as caspase-1.

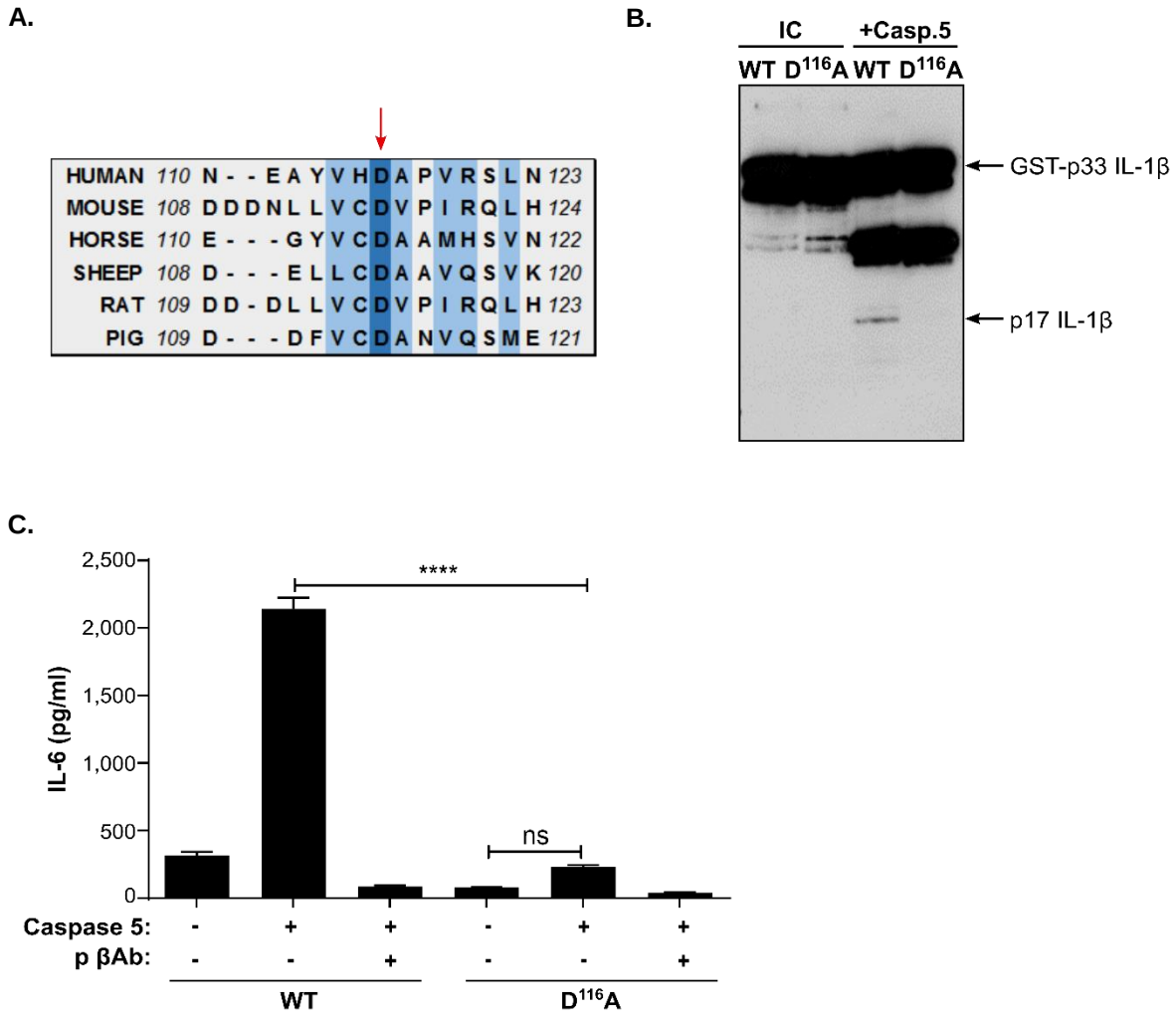

Figure 5.8: Caspase-5 cleaves IL-1β at aspartic acid 116. (A) Multiple species alignment of IL-1β sequence in region corresponding to 17kDa cleavage product size. Red arrow indicates candidate aspartic acid 116. **(B)** Western blot for IL-1β after the incubation of WT or $D^{116}A$ mutant pro-IL-1β alone (incubation control, IC) or with active caspase-5. **(C)** IL-1-dependent IL-6 production by HeLa cells treated with reaction products from WT or $D^{116}A$ pro-IL-1β incubation ± active caspase-5, ± a neutralising IL-1β antibody (p βAb). Data represent mean +SEM of n=4, p = ****≤0.0001

5.2.5 THP-1 as a cell line model of non-canonical inflammasome activation

The human cell lines THP-1 and U937 are commonly used to study the non-canonical inflammasome (Carta et al., 2011, Shi et al., 2014, Baker et al., 2015, Kayagaki et al., 2015, Vigano et al., 2015). Although THP-1 cells are monocytes of blood origin and U937s are lymphoblasts of tissue origin, both are considered to be macrophage-like when differentiated using phorbol-12-myristate-13-acetate (PMA) (Chanput et al., 2015).

To characterise non-canonical inflammasome activation in THP-1 cells, a model of cell differentiation and activation was established (Figure 5.9A). THP-1 cells were differentiated for 24 hours with PMA, primed for 4 hours with the TLR4 agonist LPS, and LPS transfected into the cytosol before incubation for 18 hours. Upregulation of *CASP5* expression was observed following priming, and a further increase was detectable following activation with intracellular LPS (Figure 5.9B). A similar pattern was observed for IL-1α and IL-1β secretion (Figure 5.9C,D).

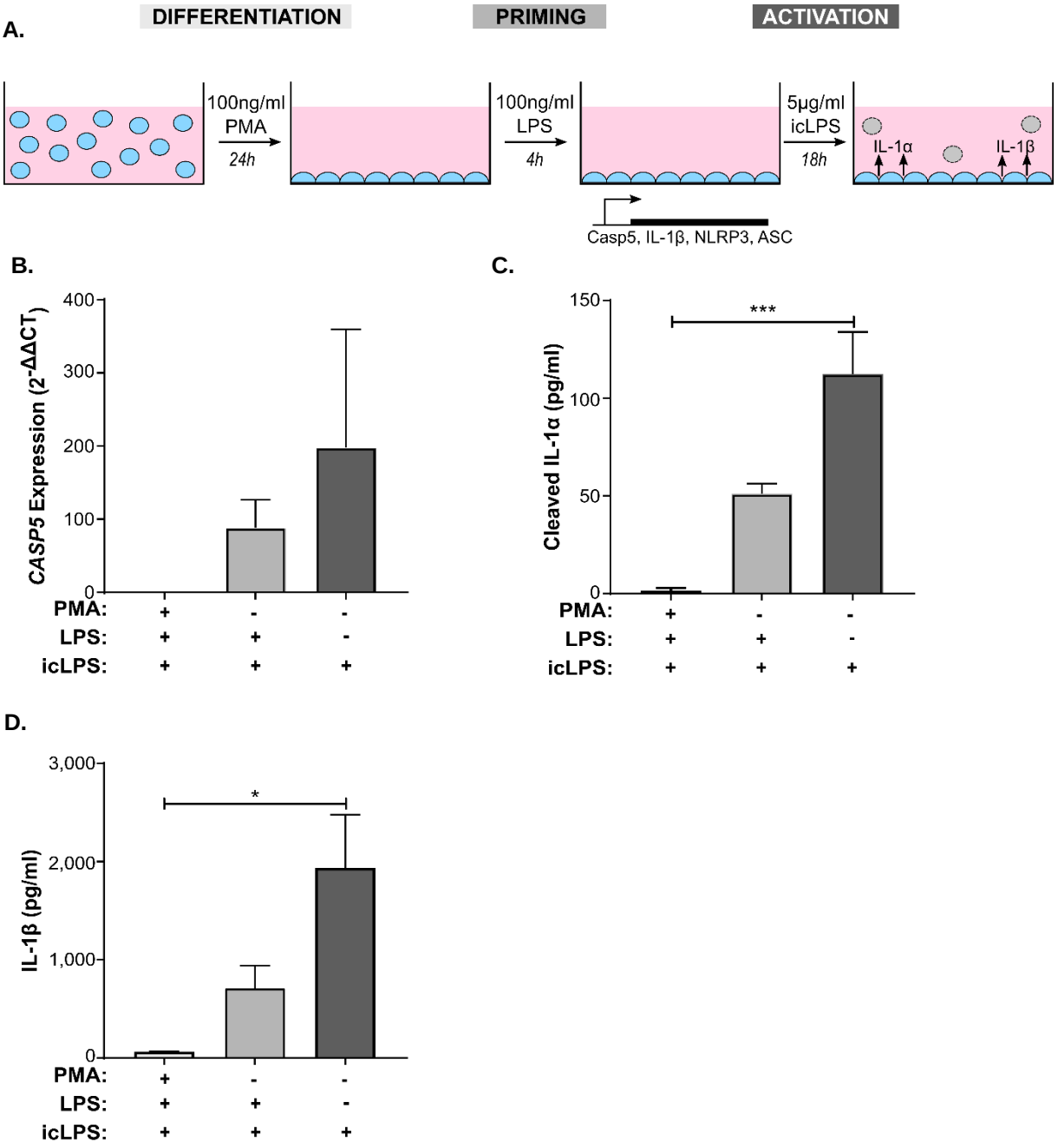

Figure 5.9: Activation of the non-canonical inflammasome in THP-1 cells. (A) Schematic showing the protocol for the differentiation of THP-1 cells and the subsequent activation of the non-canonical inflammasome with intracellular LPS (icLPS). **(B-D)** Characterisation of differentiated, primed and non-canonically activated THP-1 cells. **(B)** RT-PCR data showing *CASP5* gene expression. **(C)** IL-1α release measured by ELISA. **(D)** IL-1β release measured by ELISA. Data represent mean +SEM of n=3 (**B**) or 7 (**C,D,**), p = *≤0.05, ***≤0.001.

To interrogate the individual roles played by the inflammatory caspases, each gene was knocked down. Since THP-1 cells are in suspension and difficult to transiently transfect with siRNA, knockdown was performed using shRNA delivered by lentivirus, which is less toxic to cells than adenovirus delivery. The second generation lentiviral system (Figure 5.10) used three plasmids; a VSVg plasmid encoding the envelope containing a g-protein that binds to most mammalian cells, a BYE plasmid containing the lentiviral packaging factors gag, polymerase and reverse transcriptase, and a third plasmid encoding the shRNA against the target gene, LTRs to allow integration into the THP-1 genome, the ϕ packaging signal and the puromycin resistance gene used for selection. Separating the lentiviral components into three vectors reduces the potential of generating a replication competent virus and therefore increases biosafety. The three vectors were transfected into HEK-293T cells, which produced pseudovirus particles that were used to infect THP-1 cells.

Multiple shRNAs were used per gene to increase confidence that any effects observed in response to the knockdowns were specific (Figure 5.11). Four new caspase-1 shRNAs were tested, with two caspase-4 and -5 shRNAs that had previously been validated (Goodall group, *unpublished*). In addition, a non-targeting shRNA was used to control for effects of lentiviral infection and integration of an exogenous DNA sequence. Two infections were carried out per shRNA, denoted A and B.

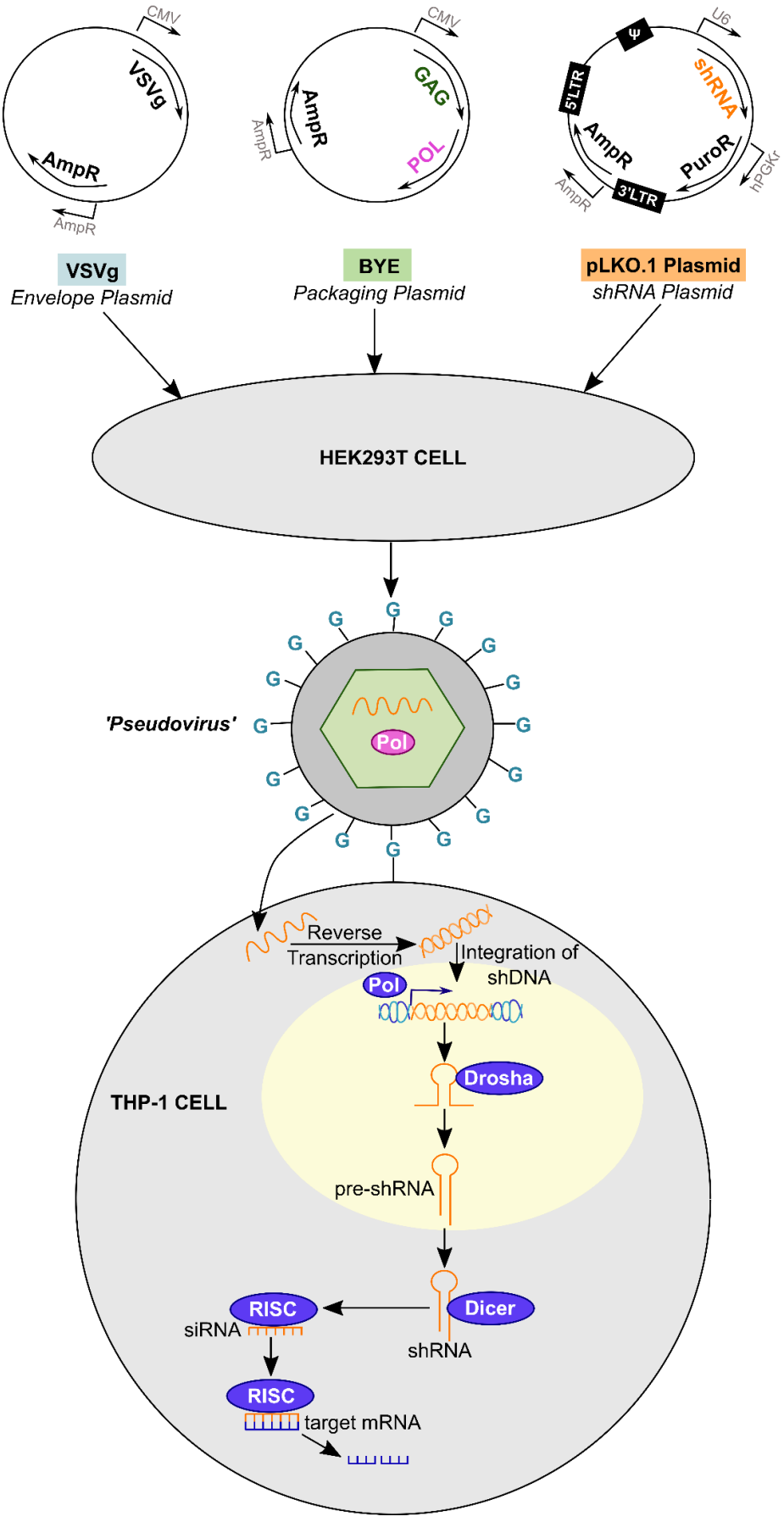

Figure 5.10: Lentiviral shRNA delivery. Schematic illustrating the mechanism of shRNA-mediated gene knockdown.

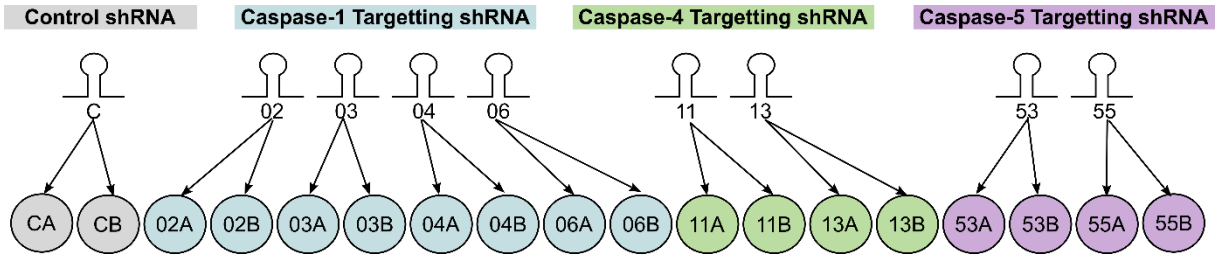

Figure 5.11: shRNA strategy. Schematic illustrating the 18 THP-1 lines produced by using multiple shRNAs per caspase gene and carrying out duplicate infections for each shRNA.

To determine which control THP-1 line resembled the uninfected cells more closely, *CASP1*, *CASP4* and *CASP5* expression was measured (Figure 5.12). Although both lines infected with control virus showed an upregulation of caspase-1 expression, line CA expressed similar levels of *CASP4* and *CASP5* to uninfected cells, whereas CB showed a slight reduction. Because of this, the control line CA was used for all further experiments. To evaluate which THP-1 lines exhibited the highest level of knockdown, the expression of their target gene was compared to expression in the CA cells (Figure 5.13). This analysis revealed that the shRNA02 was considerably less effective at *CASP1* knockdown than the other caspase-1-targeted shRNAs, whilst all shRNAs used to knockdown *CASP4* and *CASP5* reduced gene expression by 50-80%. The *CASP5* gene expression analysis in THP-1 cells infected with shRNA55 illustrate the importance of carrying out duplicate infections since a stronger knockdown was observed in line 55B compared to 55A, even though these cells were infected with identical virus.

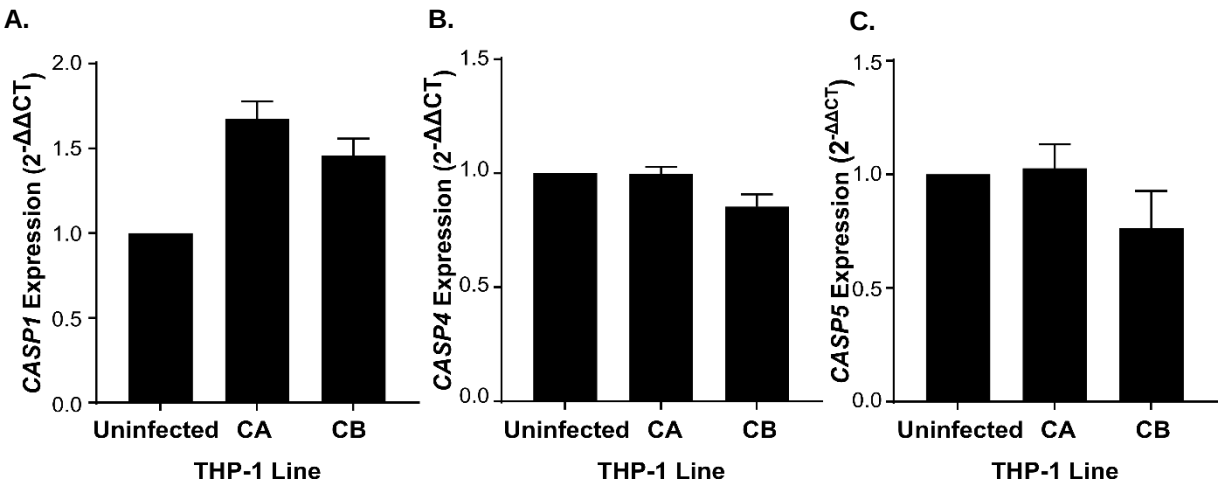

Figure 5.12: The caspase expression profile of control line CA resembles uninfected THP-1 cells. (A-C) qPCR analysis showing levels of *CASP1* (**A**), *CASP4* (**B**) and *CASP5* (**C**) gene expression in uninfected and control-virus infected THP-1s measured by RT-PCR. Data is mean +SEM of n=2.

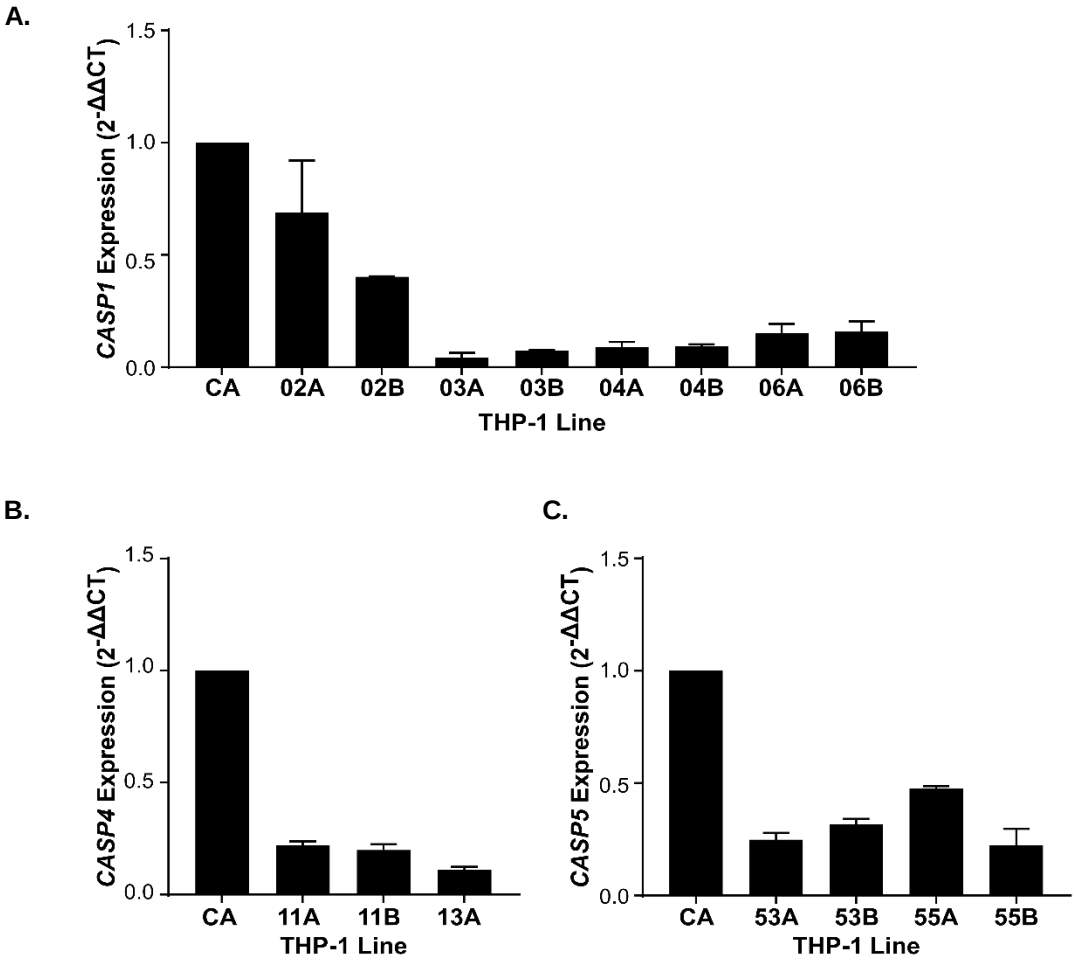

Figure 5.13: The knockdown efficiency for each THP-1 line generated. (A-C) qPCR analysis showing level of knockdown achieved by shRNAs targeting *CASP1* (**A**), *CASP4* (**B**) and *CASP5* (**C**) compared to cells infected with a control shRNA measured by RT-PCR. Data is mean +SEM of n=2.

Although the shRNA knockdown seemed very effective when measuring the expression of the target genes, analysis of the expression of the other pro-inflammatory caspases revealed that in most cases knockdown was not specific (Figure 5.14). *CASP1*-targeted shRNAs 03 and 06 also slightly reduced *CASP5* expression, every shRNA targeting *CASP4* also repressed *CASP1* expression, and most of the *CASP5*-targeted lines also exhibited lower *CASP1* expression. Off-target effects are a recognised disadvantage of using shRNA for gene knockdown. However, the loss of *CASP1* observed in all lines expressing *CASP4*-targeted shRNAs suggests that caspase-4 may really influence *CASP1* expression.

In addition, although lentiviral delivery is reported to stably integrate the shRNA into the host genome, a second gene expression analysis two weeks after infection revealed that the knockdowns were not stable (Figure 5.15). In particular, the expression of *CASP1* seemed to dramatically increase during the two weeks after transfection. A possible explanation for this lack of stability could be that a subpopulation of the transduced cells suppressed the shRNA production but kept the antibiotic resistance and therefore outcompeted their neighbours.

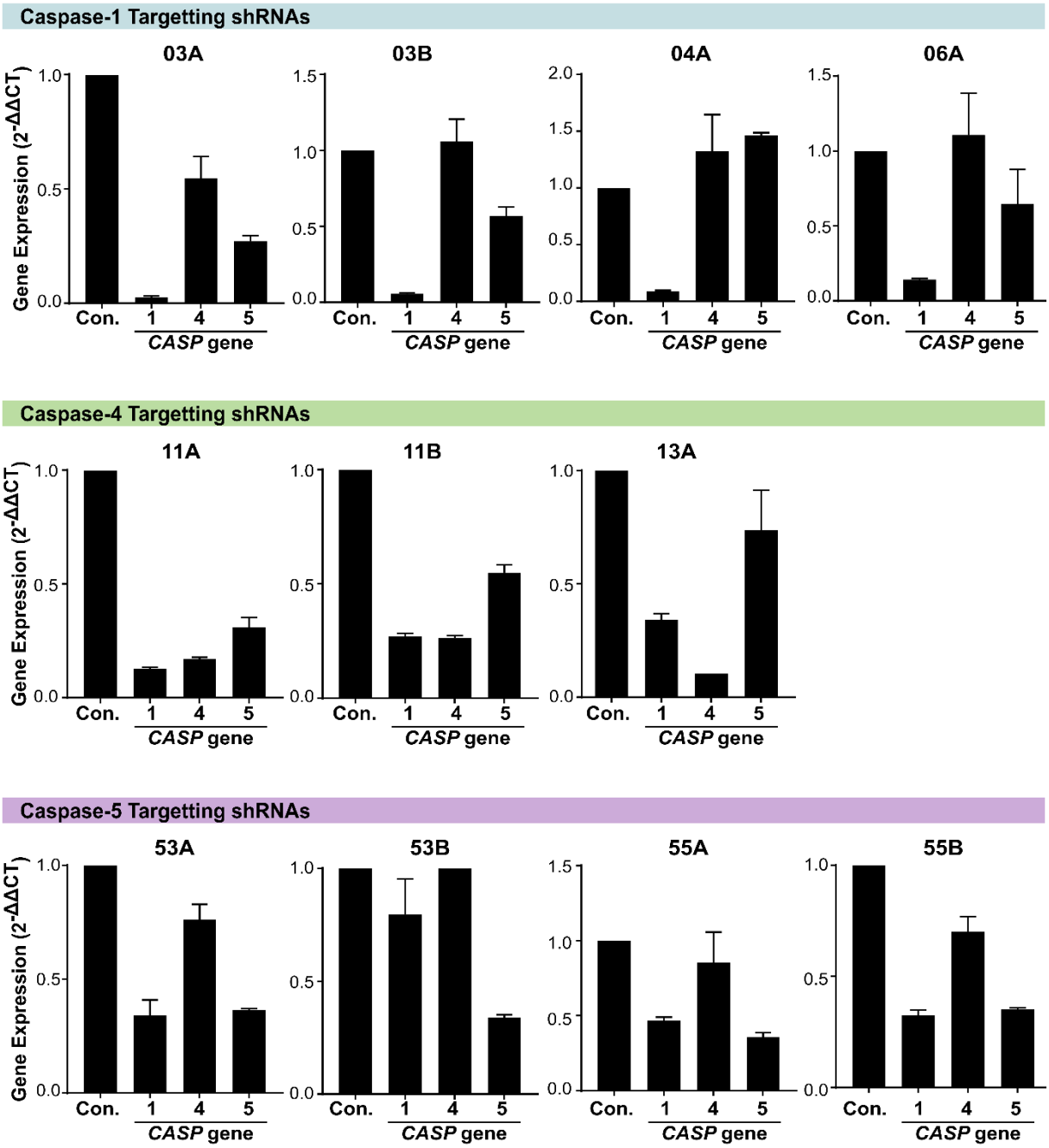

Figure 5.14: The shRNA knockdown was not specific. qPCR data showing the level of *CASP1, CASP4* and *CASP5* expression following infection with *CASP1*, *CASP4*, and *CASP5* targeted shRNAs. Data is mean +SEM of n=2.

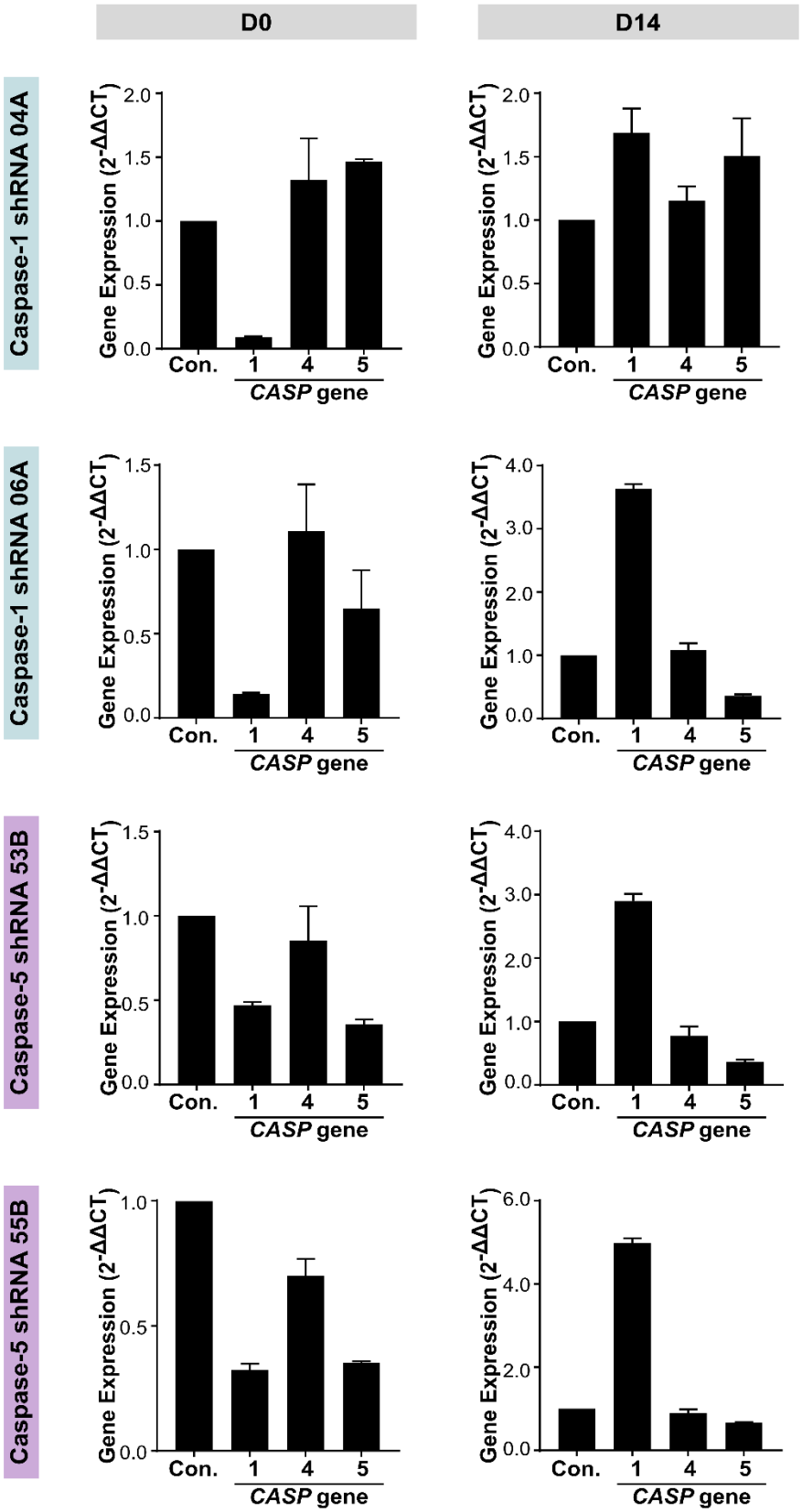

Figure 5.15: The shRNA knockdown was not stable. A comparison of the gene expression profiles of two *CASP1*- and two *CASP5*- targetted THP-1 lines at the time of (d0), and two weeks after (d14), transfection. Gene expression measured by RT-PCR. Data is mean +SEM of n=2.

Despite the lack of specificity and stability with the shRNA system, the effect of caspase-1 or caspase-5 knockdown on IL-1α and IL-1β secretion in response to intracellular LPS was investigated using the best THP-1 lines (Figure 5.16). IL-1 levels were measured in both the supernatants and the lysates, in case interfering with caspase expression affected IL-1 secretion. *CASP1* knockdown appeared to increase IL-1α levels in both the supernatant and cell lysate, which is in line with our suggestion that IL-1α activation and release bypasses the caspase-1 inflammasome. The effect of *CASP1* knockdown on IL-1β release was variable; shRNA 04A significantly reduced IL-1β release as expected, whereas shRNA 06A increased IL-1β release. *CASP5* knockdown using the shRNA53B significantly reduced both IL-1α and IL-1β secretion, whereas shRNA55B had little effect on IL-1 levels. Although this data exhibits some promising trends, the lack of specificity and consistency with the lentiviral system in THP-1 cells made it difficult to draw definitive conclusions.

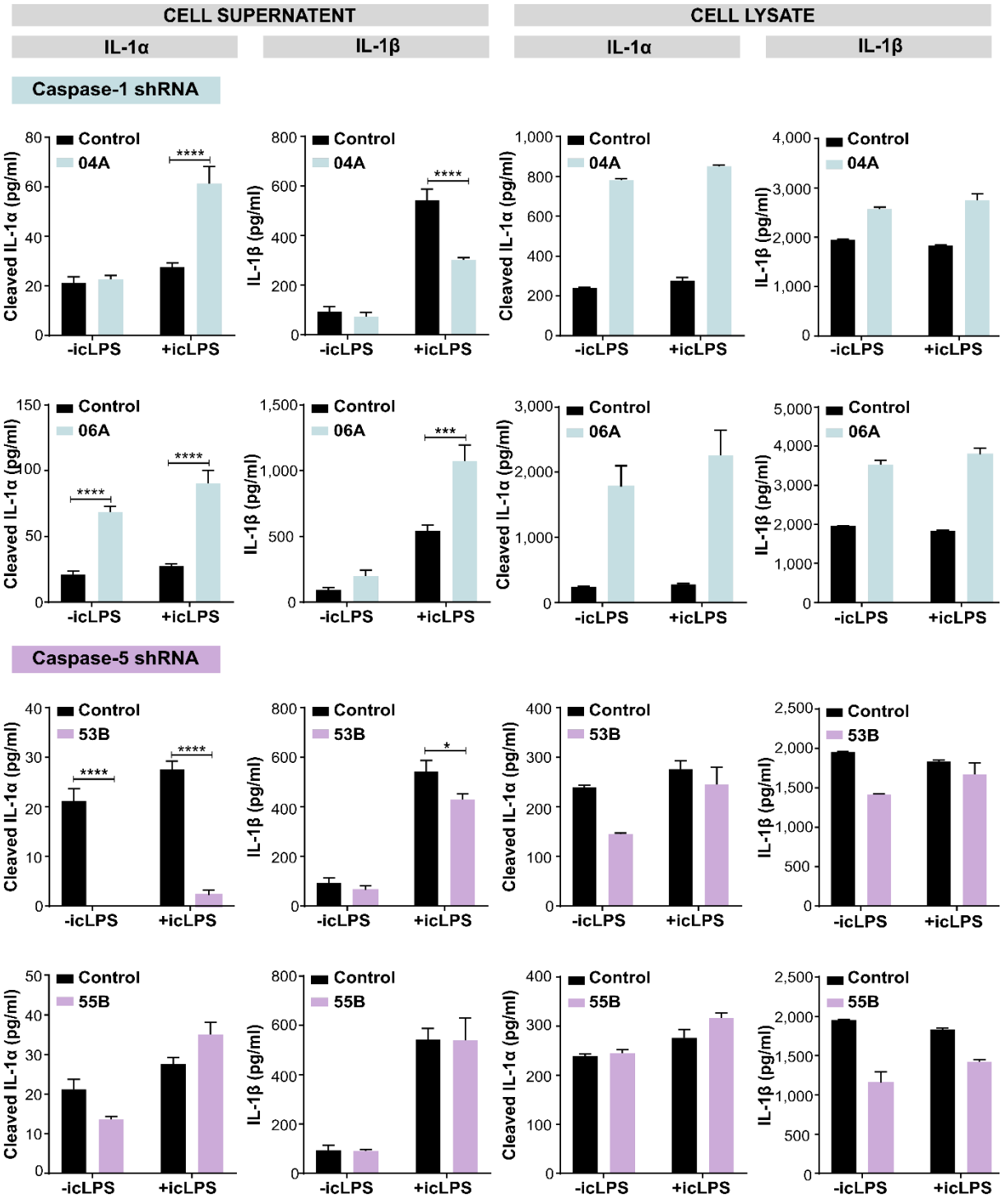

Figure 5.16: The effect of caspase-1 or -5 knockdown on the IL-1 response to icLPS ELISA data showing levels of IL-1α and IL-1β in the supernatants or lysates of LPS-primed THP-1 cells treated ± intracellular LPS (icLPS). Data is mean +SEM of n=5 for supernatant samples or n=2 for lysate samples.

Due to the consistency problems with the lentiviral knockdown system in THP-1 cells, we attempted an alternative model of overexpression. We overexpressed either WT or the caspase-5 site mutant D105A form of pro-IL-1α in THP-1 cells in the hope that the site mutant might act as a dominant negative and mute the IL-1α response to intracellular LPS. However, as with the shRNA, the results were highly variable and inconclusive (Figure 5.17).

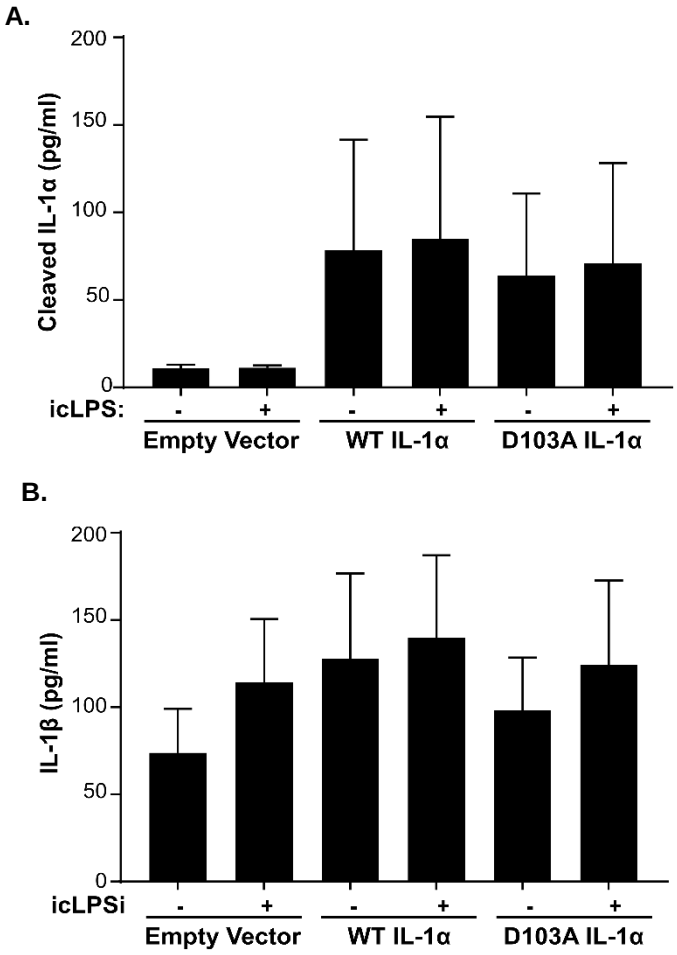

Figure 5.17: The effect of overexpressing WT or D103A IL-1α in THP-1 cells (A-B) ELISA data showing the levels of IL-1α (**A**) and IL-1β (**B**) in the conditioned media of THP-1 cells nucleofected with an empty vector or a vector inducing WT or D103A IL-1α overexpression. Data represent mean +SEM of n=3.

Since genetically manipulating THP-1 cells was extremely challenging, we attempted to visualise the endogenous p19 IL-1α cleavage product following non-canonical inflammasome activation by western blot (Figure 5.18). Directly lysing the THP-1 cells into Laemelli buffer revealed an extremely faint 19kDa band in the cells treated with intracellular LPS, which may be an artefact. We also prepared freeze-thaw lysates with and without the calcium chelator BAPTA (to prevent overt calpain activation

during necrosis). However, the lysates did not reveal any IL-1α processing. All lysates showed that intracellular IL-1α was predominantly in its pro-form, implying that IL-1α is cleaved immediately prior to secretion, or that the GSDMD pore is not large enough to mediate pro-IL-1α secretion. Unexpectedly, a second slightly lower molecular weight form of pro-IL-1α was induced upon TLR2 ligation with PAM3CSK4. It would be interesting to determine if this priming-induced form of IL-1α is differentially modified to render it more susceptible to proteolytic cleavage than the higher molecular weight form present in resting cells.

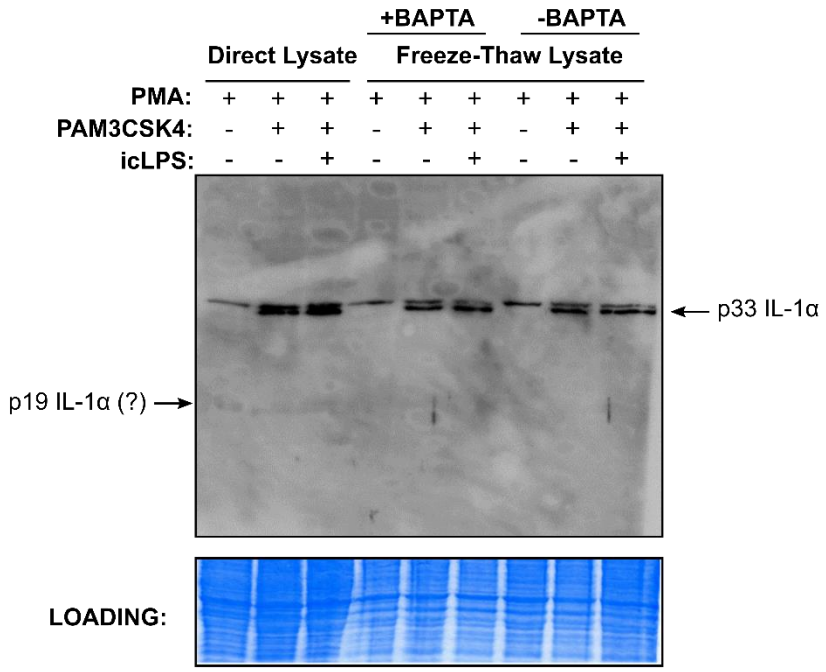

Figure 5.18: Intracellulular IL-1α is predominantly pro-IL-1α. Western blot for IL-1α in the lysates of THP-1 cells differentiated with PMA ± PAM4CSK4 priming ± intracellular LPS activation (icLPS). Lysates were either made directly into Laemelli buffer, or by freeze-thawing in liquid nitrogen ± BAPTA.

5.2.6 Developing a tool to detect caspase-5 cleaved IL-1α

After experiencing significant difficulty establishing a model of non-canonical inflammasome activation in THP-1 cells, we developed a tool to detect the endogenous caspase-5 cleaved IL-1α released by primary cells. We produced a peptide antibody reactive to the region between the caspase-5 and calpain cleavage sites (Figure 5.19A) and developed this into a sandwich ELISA that recognised the longer caspase-5 cleaved form of IL-1α, but not pro- or calpain cleaved- IL-1α (Figure 5.19B, C), compared to the commercial IL-1α ELISA that recognised both forms of cleaved IL-1α (Figure 5.19D)

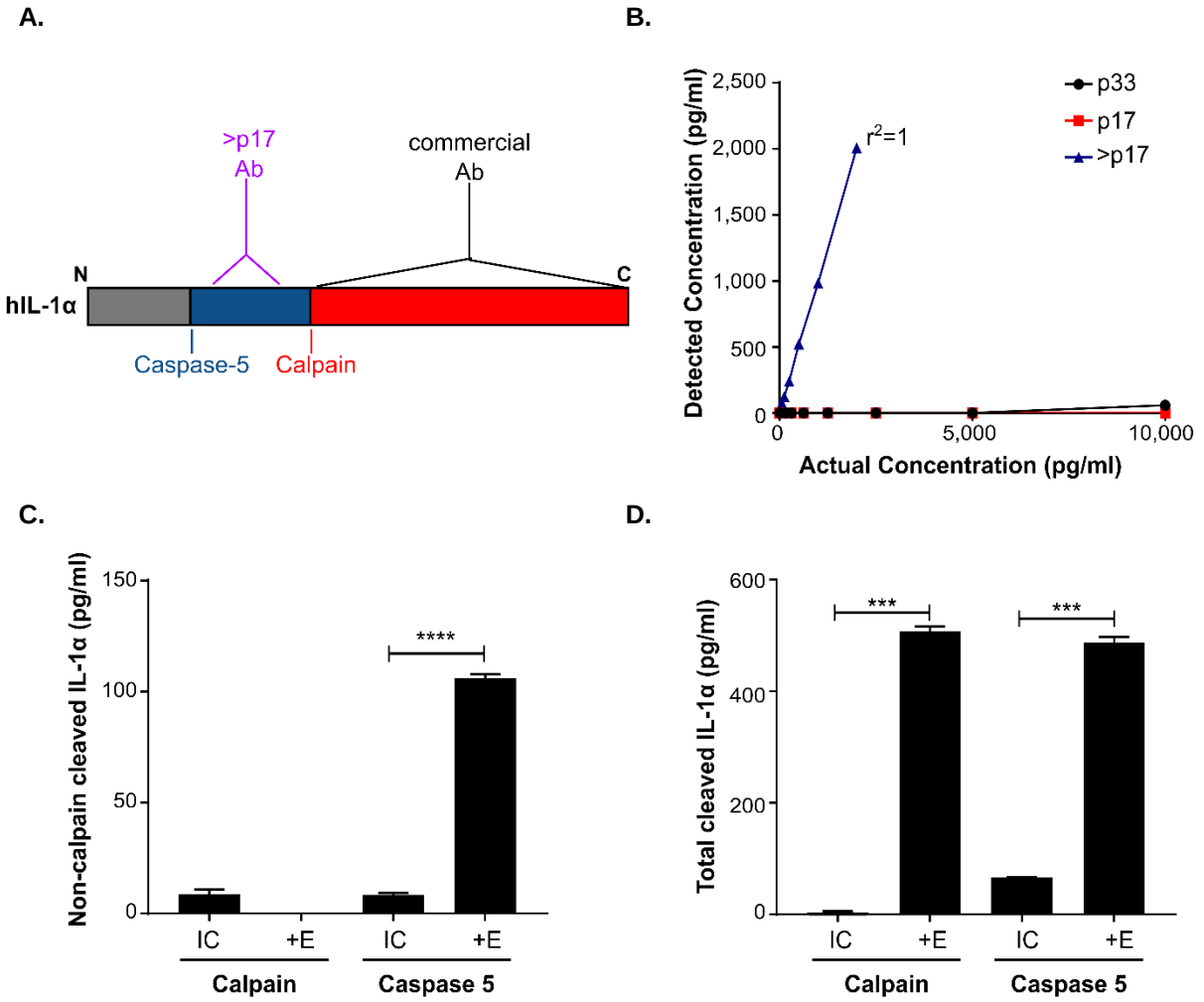

Figure 5.19: Development of an ELISA to detect non-calpain-cleaved IL-1α. (A) Schematic showing the location of the custom peptide antibody relative to the calpain and caspase-5 cleavage sites in pro-IL-1α. **(B)** ELISA data showing detection of recombinant pro (p33), calpain cleaved (17) or non-calpain cleaved (>p17) IL-1α. **(C-D)** ELISA data showing specificity of our custom non-calpain cleaved IL-1α ELISA (**C**) or a total cleaved IL-1α ELISA (**D**) for detecting either calpain or caspase-5 cleaved pro-IL-1α. Data represent mean +SEM of n=3, p = ***≤0.001, ****≤0.0001.

5.2.7 Cleavage and release of IL-1α from primary human macrophages depends on caspase-5

To see if caspase-5-cleaved IL-1α is released from cells, we activated the non-canonical inflammasome in primary human monocyte derived macrophages (hMDMs) by priming followed by intracellular LPS delivery (Figure 5.20A). The conditioned media of cells from three individual donors contained detectable levels of caspase-5-cleaved IL-1α (Figure 5.20B). Due to the limited cells and serum available, a siRNA SMARTpool was used to knockdown *CASP5* in the hMDMs. Although a mixture of 4 different siRNAS could increase likelihood of off-target effects, these should theoretically be avoided because each siRNA is used at a lower (¼X) concentration. Importantly, *CASP5* knockdown had no effect on *CASP1* expression, meaning that canonical inflammasome signalling was unaffected (Figure 5.20C). *CASP5* knockdown lead to a significant reduction in total IL-1α (Figure 5.20D), non-calpain cleaved IL-1α (Figure 5.20E) and IL-1β (Figure 5.20F) release following intracellular LPS treatment. Together, this data suggests that caspase-5 processing of IL-1 is not an artefact of using recombinant proteins, but occurs physiologically within cells.

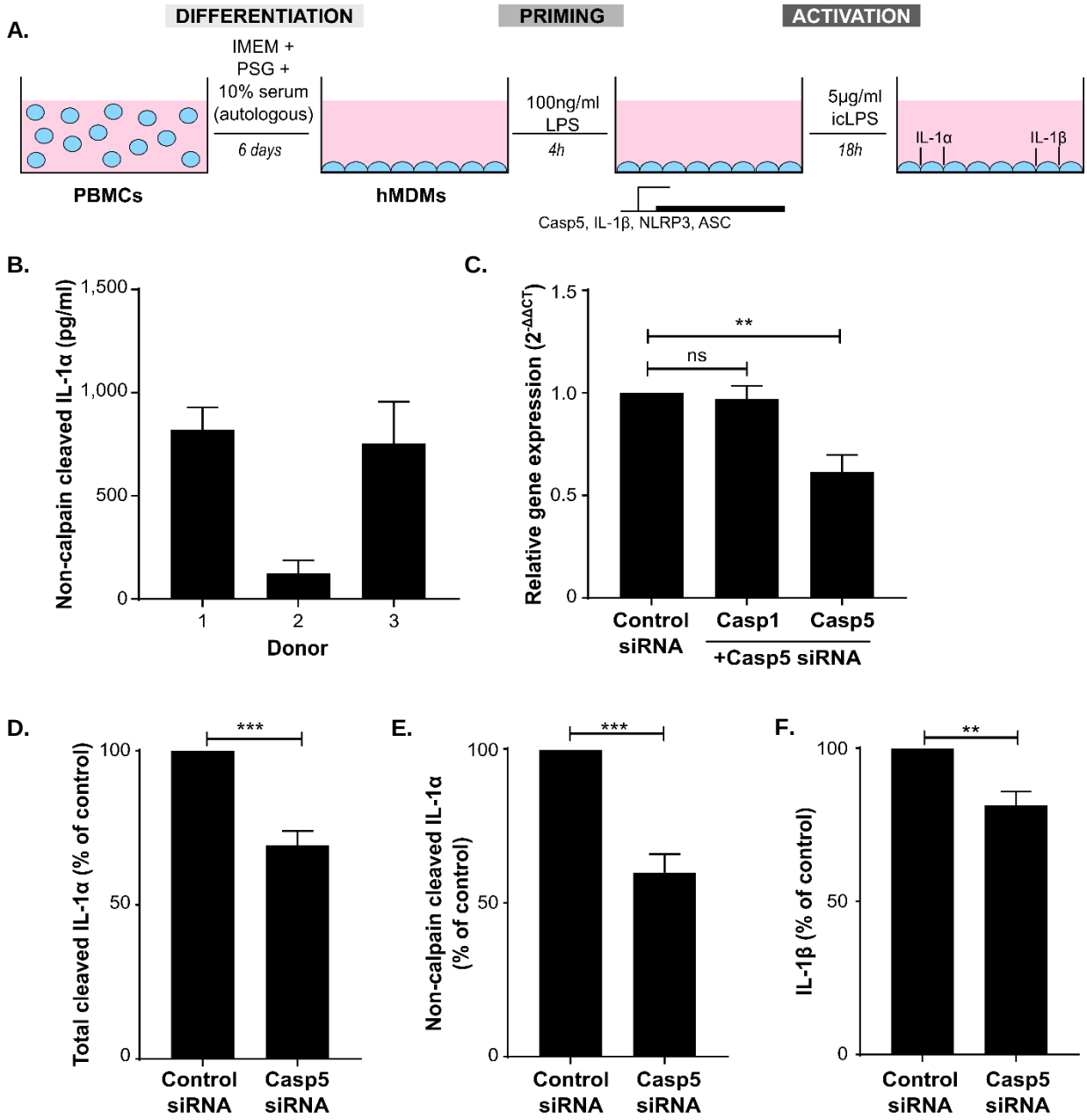

Figure 5.20: Cleavage and release of IL-1α during non-canonical inflammasome activation in hMDMs depends on caspase-5. **(A)** Schematic showing the differentiation and treatment of human monocyte derived macrophages (hMDMs) from peripheral blood mononuclear cells (PBMCs). **(B)** ELISA data showing detection of non-calpain cleaved IL-1α in the conditioned media from hMDMS treated with intracellular LPS from three donors. **(C)** qPCR data showing *CASP1* and *CASP5* expression in hMDMs after control and *CASP5*-targeted siRNA delivery. **(D-F)** ELISA data showing level of total cleaved IL-1α (**D**), non-calpain cleaved IL-1α (**E**) and IL-1β (**F**) after *CASP5* knockdown. Data represent mean +SEM of n=3, p = **≤0.01, ***≤0.001.

To investigate a potential role for caspase-5 in canonical inflammasome pathways, hMDMs were also primed and treated with ATP. Surprisingly, LPS/ATP activation also induced secretion of non-calpain cleaved IL-1α (Figure 5.21). This suggests crosstalk between human inflammasome pathways, similar to the reported activation of caspase-11 by caspase-1 in the murine system (Kayagaki et al., 2011).

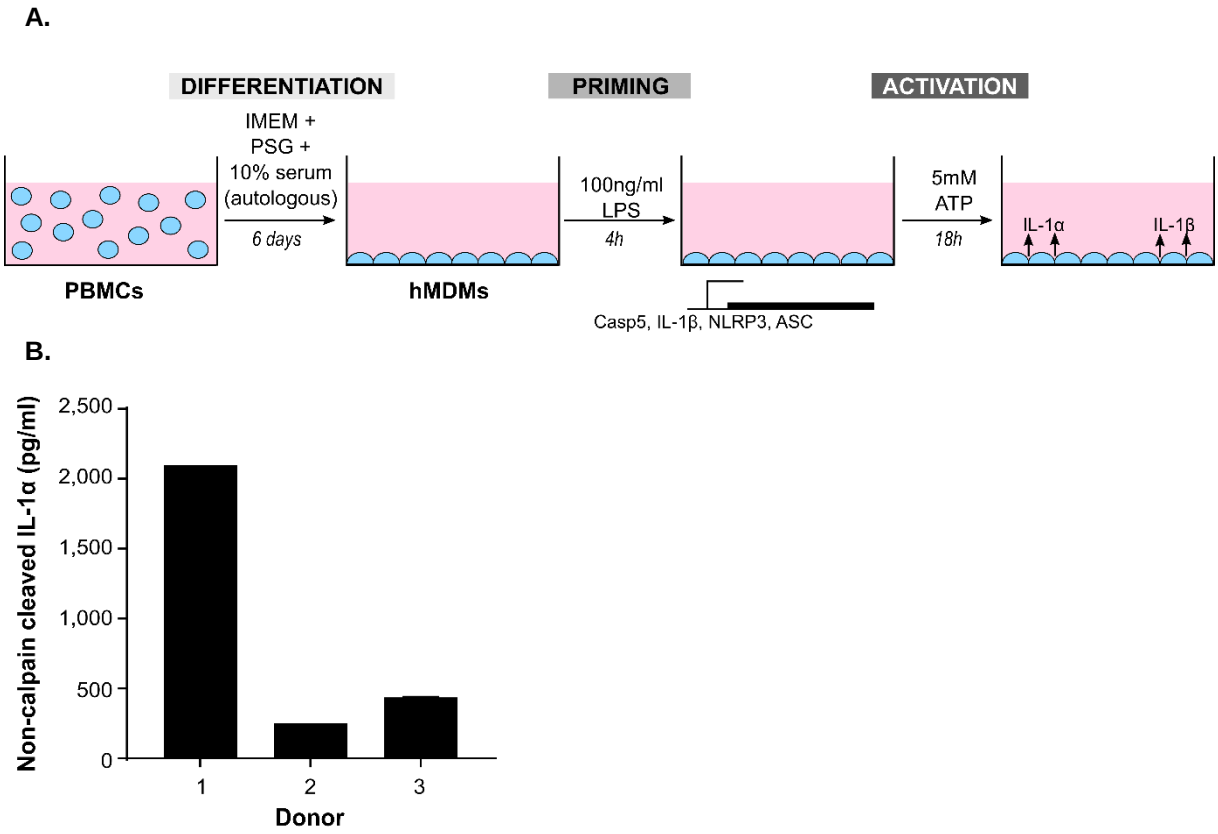

Figure 5.21: Caspase-5 cleaved IL-1α is released during canonical inflammasome activation in hMDMs. (A) Schematic showing the differentiation and canonical treatment of human monocyte derived macrophages (hMDMs) from peripheral blood mononuclear cells (PBMCs). **(B)** ELISA data showing detection of non-calpain cleaved IL-1α in the conditioned media from hMDMS treated with ATP from three donors.

5.2.8 Caspase-5 cleaves IL-1α in HeLa cells

To support our primary macrophage data using another cell type we reconstituted the non-canonical inflammasome system in HeLa cells, which are very easy to transfect. We overexpressed either WT or D103A pro-IL-1α with pro-caspase5 in the cells, and treated them with intracellular LPS. This system required the cytosolic LPS to activate the pro-caspase-5, which could in turn cleave IL-1α. Significantly less total cleaved and non-calpain cleaved IL-1α was secreted by the D103A IL-1α-expressing cells (Figure 5.22A,B) suggesting that the site mutant acts as a dominant negative in this system. Notably, calpain could cleave D103A pro-IL-1α equivalently to WT (Figure 5.22C) implying that this mutation only affects non-canonical processing. Furthermore, treatment with intracellular LPS produced a 19kDa IL-1α fragment in cells overexpressing WT IL-1α, which was absent in the D103A site mutant cells (Figure 5.22D). Unfortunately, we could not take a similar approach for investigating IL-1β cleavage within a cell system, since caspase-5 cleaves at the same site as caspase-1.

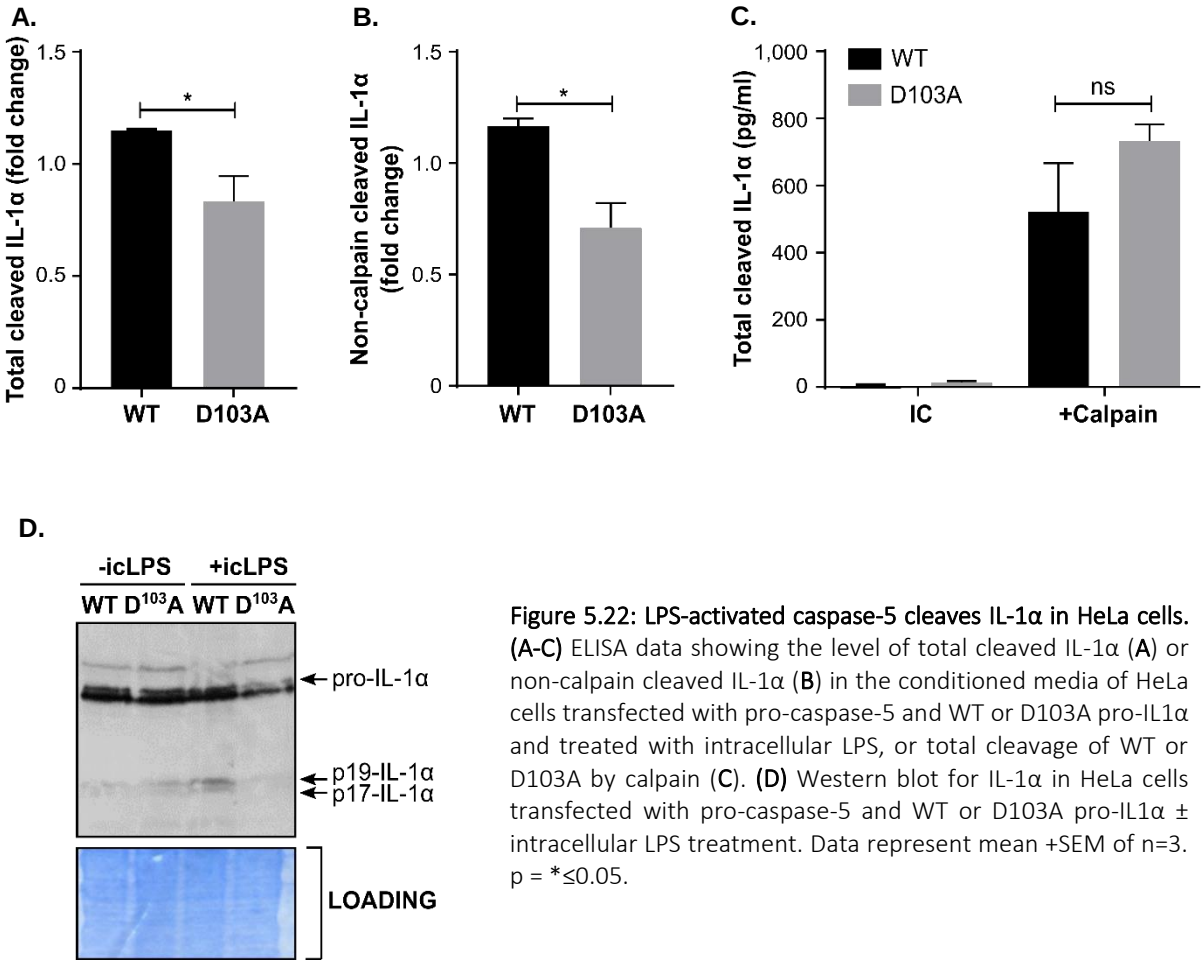

Figure 5.22: LPS-activated caspase-5 cleaves IL-1α in HeLa cells. **(A-C)** ELISA data showing the level of total cleaved IL-1α (**A**) or non-calpain cleaved IL-1α (**B**) in the conditioned media of HeLa cells transfected with pro-caspase-5 and WT or D103A pro-IL1α and treated with intracellular LPS, or total cleavage of WT or D103A by calpain (**C**). **(D)** Western blot for IL-1α in HeLa cells transfected with pro-caspase-5 and WT or D103A pro-IL1α ± intracellular LPS treatment. Data represent mean +SEM of n=3. p = *≤0.05.

5.2.9 Investigating the role of caspase-4 in caspase-5 activation

Although caspases-4 and -5 are often both referred to as the human orthologues of murine caspase-11, our data shows that only caspase-5 can activate IL-1. Research by Alessandra Mortellaro's group has shown that in human monocytes *CASP4* knockdown reduces the IL-1α, IL-1β and IL-6 responses to LPS, whereas *CASP5* knockdown only affects the release of IL-1 (Vigano et al., 2015). This suggests that caspase-4 could be upstream of caspase-5, and prompted us to question if caspase-4 activates caspase-5. Interrogating pro-caspase-5 processing by western blot was challenging due to a lack of specific anti-caspase-5 antibodies (Figure 5.23A). Recombinant protein assays showed caspase-4 was unable to activate pro-caspase-5 to induce subsequent IL-1α activation (Figure 5.23B,C). This suggests that either caspase-4 does not activate recombinant pro-caspase-5, or their interaction requires a post-translational protein modification that is not present in the bacterial-derived recombinant proteins used in these assays.

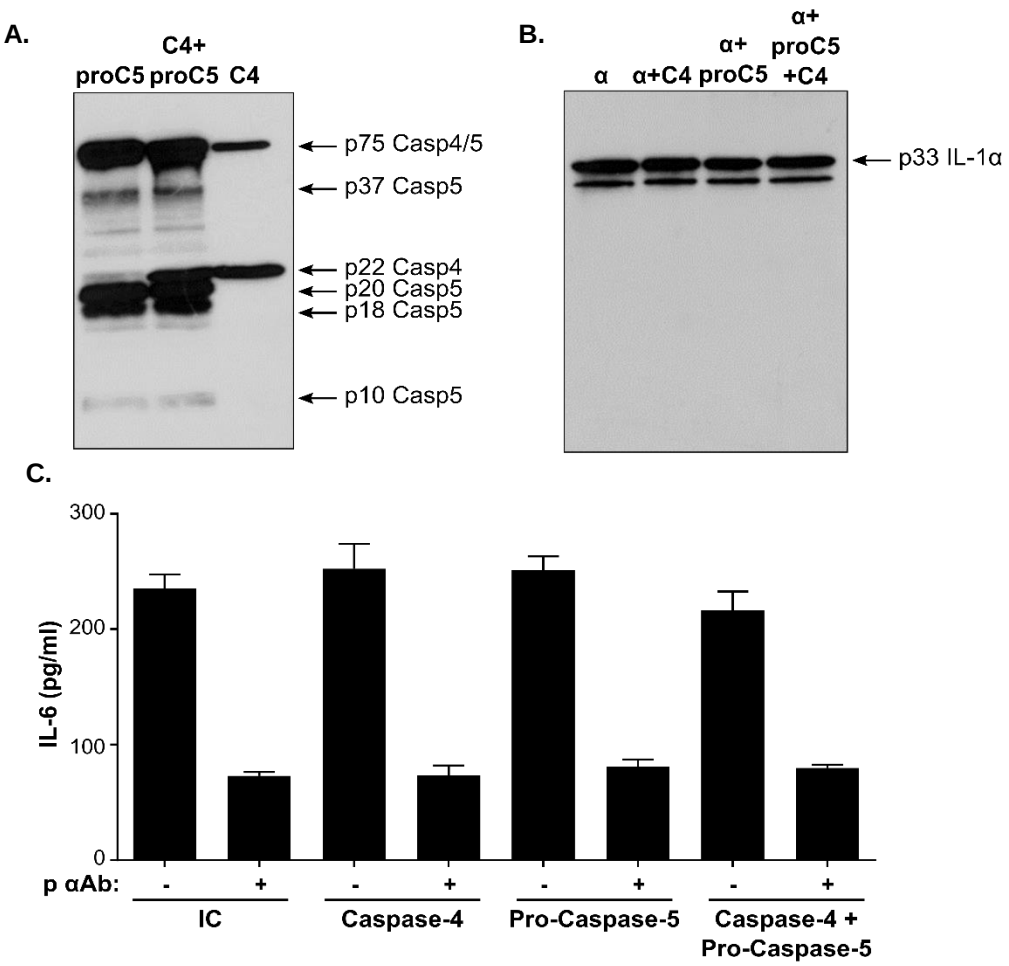

Figure 5.23: Recombinant caspase-4 cannot activate pro-caspase-5. **(A)** Western blot for caspase-5 after incubation of pro-caspase 5 (proC5) ± caspase-4 (C4). **(B)** Western blot for IL-1α after incubation of pro-IL-1α ± pro-caspase-5 ± caspase-4, or caspase-4. **(C)** ELISA data showing IL-1α-dependent IL-6 release from HeLa cells treated with the reaction products from the incubation of pro-IL-1α ± pro-caspase-5 ± caspase-4, or caspase-4. Data represent mean +SEM of n=3.

5.2.10 CASP5 and Casp11 are upregulated upon cell priming

Human *CASP4* and *CASP5* are thought to have arisen from a gene duplication of an ancestral *Casp11*-like gene. All three caspases have been found to directly bind and respond to intracellular LPS, which implies a functional conservation (Shi et al., 2014, Kayagaki et al., 2013). However, gene expression analysis revealed that *CASP4* is constitutively expressed, whereas *CASP5* and *Casp11* are significantly upregulated after TLR ligation, suggesting greater functional equivalence between these two proteases (Figure 5.24).

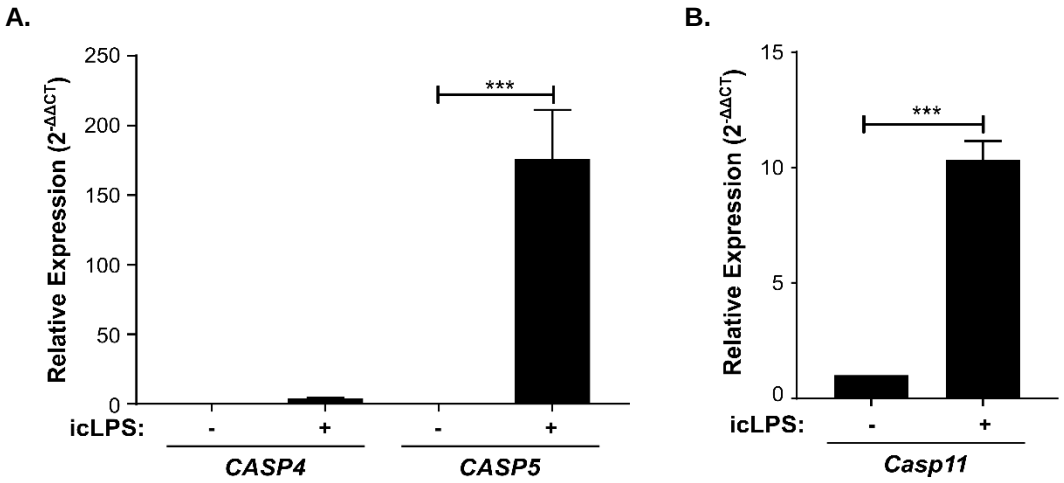

Figure 5.24: *CASP5* and *Casp11* share a similar gene expression patterns. (A-B) qPCR data showing changes in *CASP4* and *CASP5* (A) or *Casp11* (B) transcript after LPS treatment of primary dendritic cells (A) or macrophages (B). Data represent mean +SEM of n=3, p = ***≤0.001.

5.2.11 Caspase-11 activates recombinant murine IL-1α

To test if the similarities between caspases-5 and -11 extend to their substrate specificities, recombinant murine pro-IL-1α was incubated with the murine inflammatory caspases-1 and -11. Incubation with caspsase-1 did not result in IL-1α processing (Figure 5.25A) or activation (Figure 5.25B), in line with our findings in the human system and observations reported in the literature (Howard et al., 1991). In contrast, murine IL-1α was cleaved (Figure 5.25C) and activated (Figure 5.25D) by caspase-11.

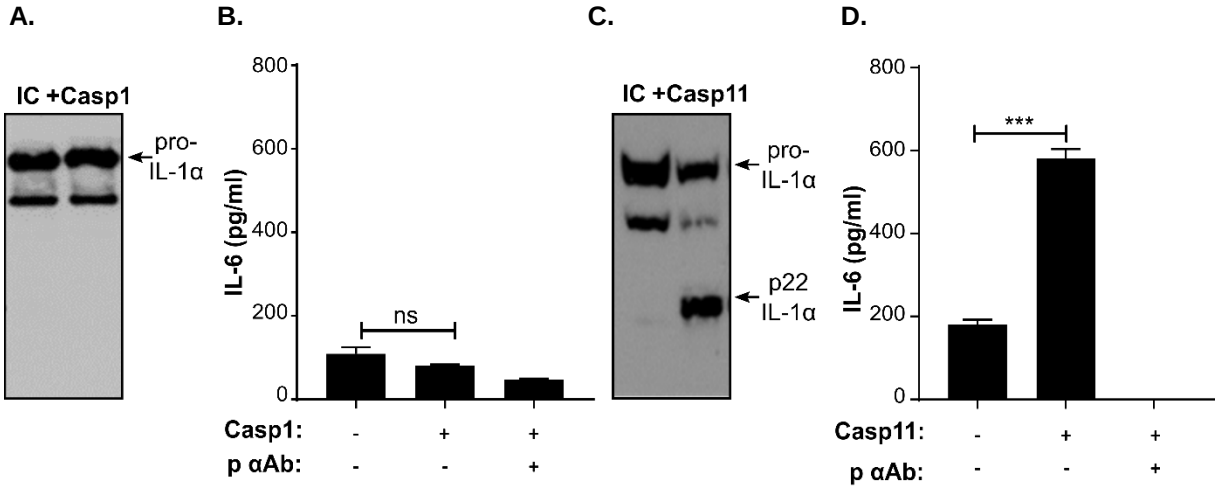

Figure 5.25: Caspase-11, not -1, activates murine IL-1α. (A-D) Western blot for IL-1α (A,C) or ELISA data showing IL-1α-dependent IL-6 production by HeLa cells treated with the reaction products (B,D) following incubation of pro-IL-1α with caspase-1 (A,B) or caspase-11 (C,D) ± a neutralising IL-1α antibody (p αAb). Data represent mean +SEM of n=3, p =***≤0.001.

5.2.12 Caspase-11 activates recombinant murine IL-1β

Next, we examined the activation of IL-1β by the murine inflammatory caspases. As expected, murine IL-1β was cleaved (Figure 5.26A) and activated (Figure 5.26B) by murine caspase-1, where the negligible effect of the IL-1β neutralising antibody is likely due to saturation of the system. Caspase-11 was also able to cleave (Figure 5.26C) and activate (Figure 5.26D) IL-1β at an equivalent efficiency *in vitro* to caspase-1.

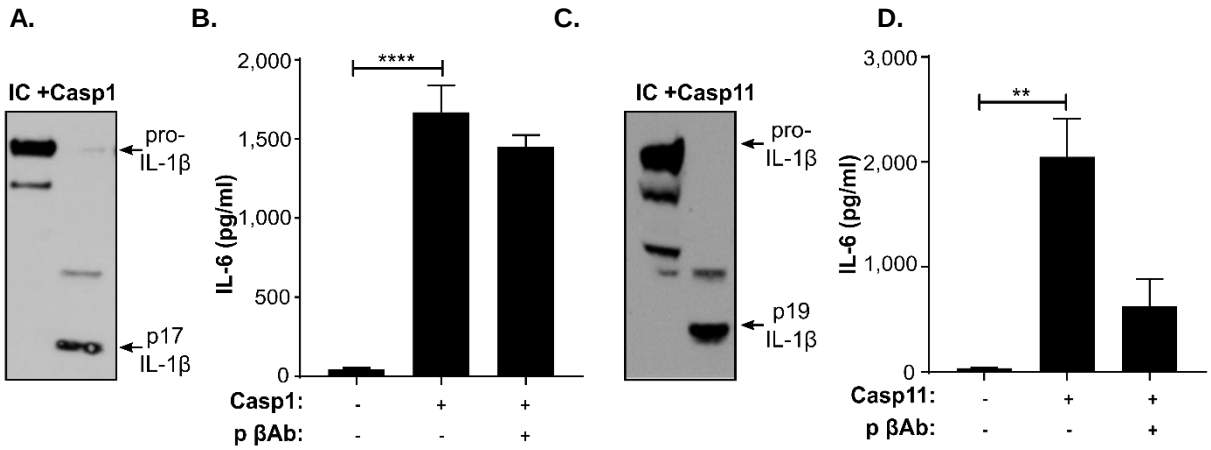

Figure 5.26: Caspase-1 and -11 activate murine IL-1β. (A-D) Western blot for IL-1β (A,C) or ELISA data showing IL-1β-dependent IL-6 production by HeLa cells treated with the reaction products (B,D) following incubation of pro-IL-1β with caspase-1 (A,B) or caspase-11 (C,D) ± a neutralising IL-1β antibody (p βAb). Data represent mean +SEM of n=3, p = **≤0.01, ****≤0.0001

5.2.13 The caspase-11 reaction buffer affects the rate of high molecular weight protein migration during electrophoresis

To elucidate whether caspase-11 cleavage of murine IL-1 was as specific as caspase-5 processing of human IL-1, we sought to locate the specific cleavage sites. The molecular weight of a cleavage product allows a rough estimation of where the enzyme cleaves. However, when we resolved the caspase-1 and caspase-11 cleavage reactions alongside each other on a western blot, it became apparent that a component of the caspase-11 reaction mix was increasing the speed of protein migration (Figure 5.27A). The caspase-11 buffer contains polyethylene glycol (PEG) which interacts with SDS under reducing

conditions (Zheng et al., 2007). When the SDS binds to the IL-1α protein, PEG increases the charge and speed of migration. Carrying out the caspase-11 cleavage reaction in the caspase-1 buffer, which does not contain PEG, revealed that the PEG was essential for caspase-11 activity (Figure 5.27B). Running a protein marker in the presence of the caspase-11 buffer revealed that PEG skews the apparent molecular weight of higher molecular weight proteins, but does not affect lower molecular weight (<20kDa) proteins (Figure 5.27C).

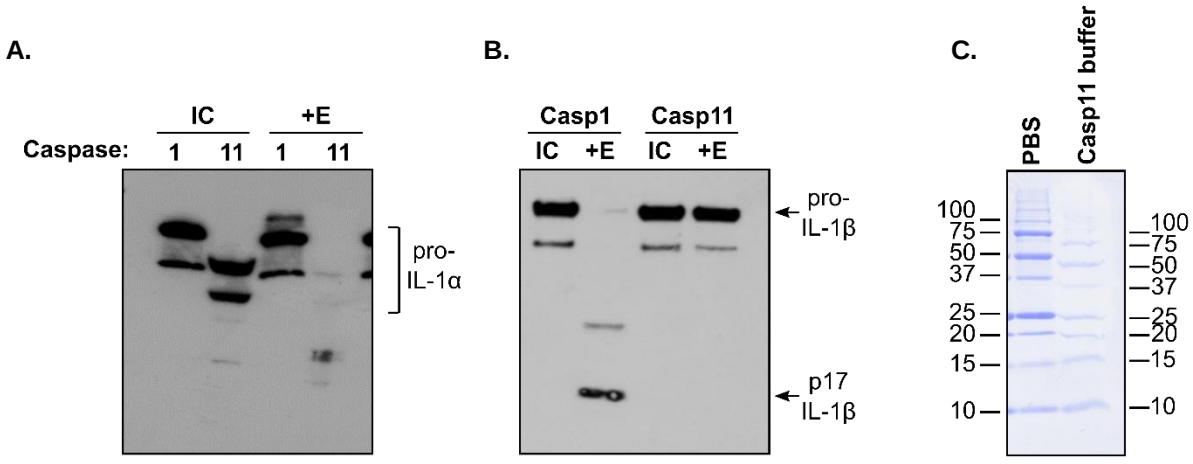

Figure 5.27: The Caspase-11 cleavage buffer makes higher Mw proteins migrate faster. (A) Western blot for IL-1α following incubation of pro-IL-1α ± caspase-1 or -11. (B) Western blot for IL-1β following incubation of pro-IL-1β ± caspase-1 or caspase-11 in caspase-1 reaction buffer. (C) Coomassie-stained PVDF membrane showing migration of unstained protein marker in PBS or caspase-11 reaction buffer.

5.2.14 Caspase-11 can cleave IL-1α at multiple sites, including D106A

Our initial experiments suggested that caspase-11 cleaved murine IL-1α to give a product of approximately 22-25kDa. However, due to the PEG in the buffer, it is difficult to be sure of the exact size of this cleavage product. As such, we mutated candidate aspartic acids to alanine based on conservation across species and location in the *IL1A* sequence (Figure 5.28A). Mutation of Asp106, the equivalent amino acid to the caspase-5 target site in human IL-1α, did not appear to affect murine IL-1α processing by caspase-11 (Figure 5.28B), suggesting a refinement of caspase-5 substrate specificity over evolution. We also mutated Asp37 and/or Asp49 in the region of the IL-1α protein that would correspond to a 22-25kDa product size, which are highly conserved across rodent species. However mutation of one, or both, of these sites had no effect on IL-1α processing suggesting that these are not the caspase-11 sites (Figure 5.28D-I).

To interrogate the cleavage of murine IL-1α by caspase-11 more thoroughly and to account for the promiscuity of the murine caspase, we conducted the cleavage assay using ten-fold less enzyme over a range of time points to identify a preferred cleavage site and/or any transient cleavage products. This lower level of cleavage revealed a 19kDa cleavage product (Figure 5.29A), which was lost in the D106A mutant (Figure 5.29B), suggesting that caspase-11 prefers to cleave at this aspartate, but will cleave elsewhere if the site is unavailable. Indeed, caspase-11-cleaved D106A murine IL-1α exhibited slightly lower activity than caspase-11-cleaved WT IL-1α (Figure 5.29C).

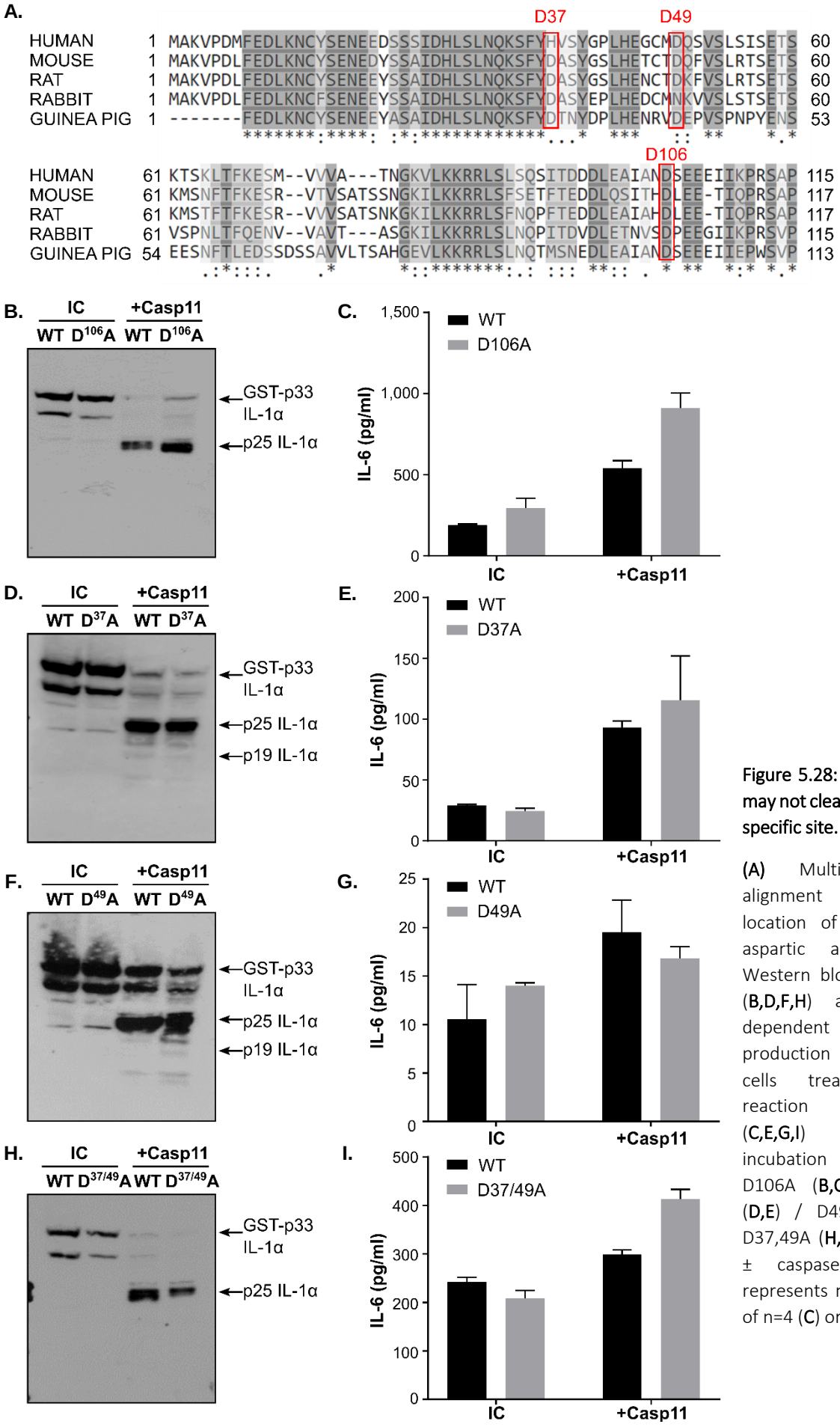

Figure 5.28: Caspase-11 may not cleave IL-1α at a specific site.

(A) Multi species alignment showing location of conserved aspartic acids. **(B-I)** Western blot for IL-1α (**B,D,F,H**) and IL-1α-dependent IL-6 production by HeLa cells treated with reaction products (**C,E,G,I**) following incubation of WT or D106A (**B,C**) / D37A (**D,E**) / D49A (**F,G**) / D37,49A (**H,I**) pro-IL-1α ± caspase-11. Data represents mean +SEM of n=4 (**C**) or n=2 (**E,G,I**).

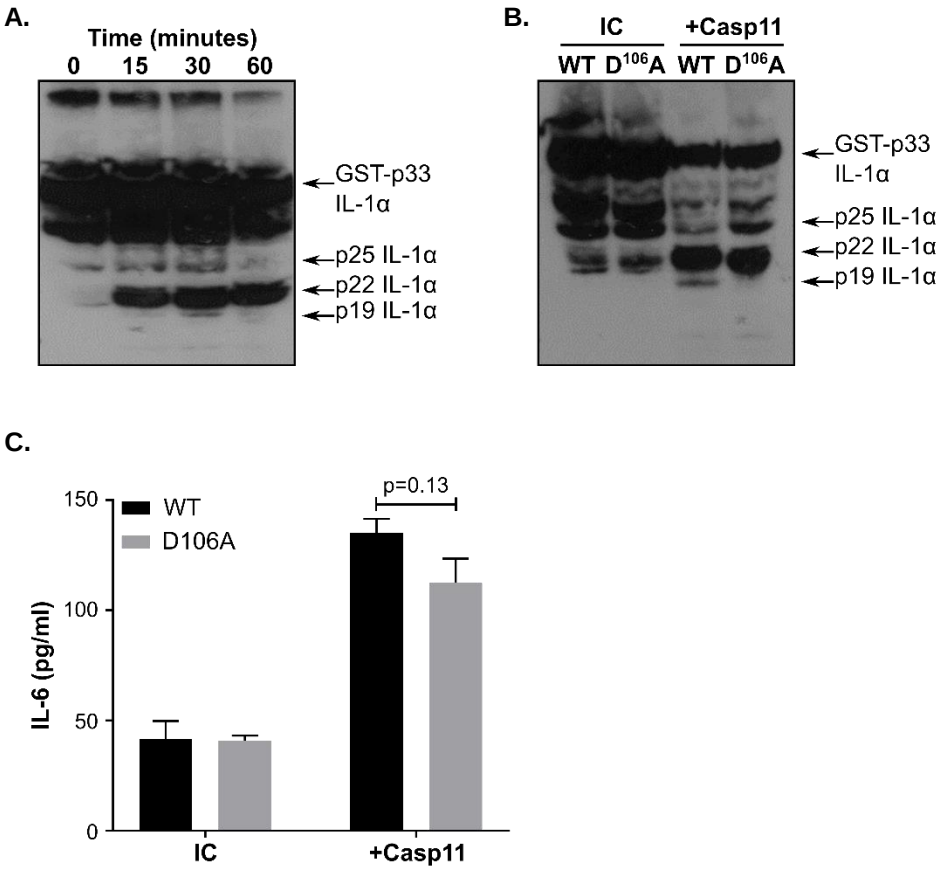

Figure 5.29: Caspase-11 cleaves murine IL-1α at D106A. (A) Western blot for IL-1α following incubation of WT pro-IL-1α with caspase-11 for a range of time points. **(B-C)** Western blot for IL-1α (**B**) or IL-1α dependent IL-6 production by HeLa cells treated with reaction products (**C**) following incubation or WT or D106A pro-IL-1α ± caspase-11. Data represents mean +SEM of n=3.

5.2.15 Caspase-11 cleaves IL-1β at Asp105

Unlike for IL-1α, caspase-11 cleaved murine IL-1β to produce a clear 19kDa fragment, for which electrophoretic migration was unaffected by PEG due to its relatively low molecular weight. Alignment of IL-1β protein sequences revealed a conserved aspartic acid, Asp105, which corresponds to the 19kDa product (Figure 5.30A). Mutation of this aspartic acid to an alanine reduced cleavage (Figure 5.30B) and activation of IL-1β (Figure 5.30C) by a lower concentration of caspase-11. However, the remaining activity of D105A IL-1β implied it was still being cleaved and activated, and repeating the cleavage

with more caspase-11 resulted in total processing of both WT and D105A IL-1β (Figure 5.30D) and no significant difference in activation (Figure 5.30E).

To confirm our hypothesis that caspase-11 has a preferred, but not exclusive, IL-1β target site we performed N-terminal sequencing on caspase-11 cleaved WT IL-1β. Although the sequence was weak, likely due to N-terminal blocking of the Ser106 residue during sample preparation, the Edman degradation confirmed that capase-11 cleaves at Asp105 (Figure 5.31A). Performing the same sequencing analysis on caspase-11-cleaved D105A IL-1β revealed a shift to alternative processing at Asp111 and Asp117 (Figure 5.31B). Therefore, caspase-11 specifically targets murine pro-IL-1β at Asp105, but when this site is blocked it can cleave at alternative aspartic acid residues towards the C-terminus of the protein (Figure 5.31C).

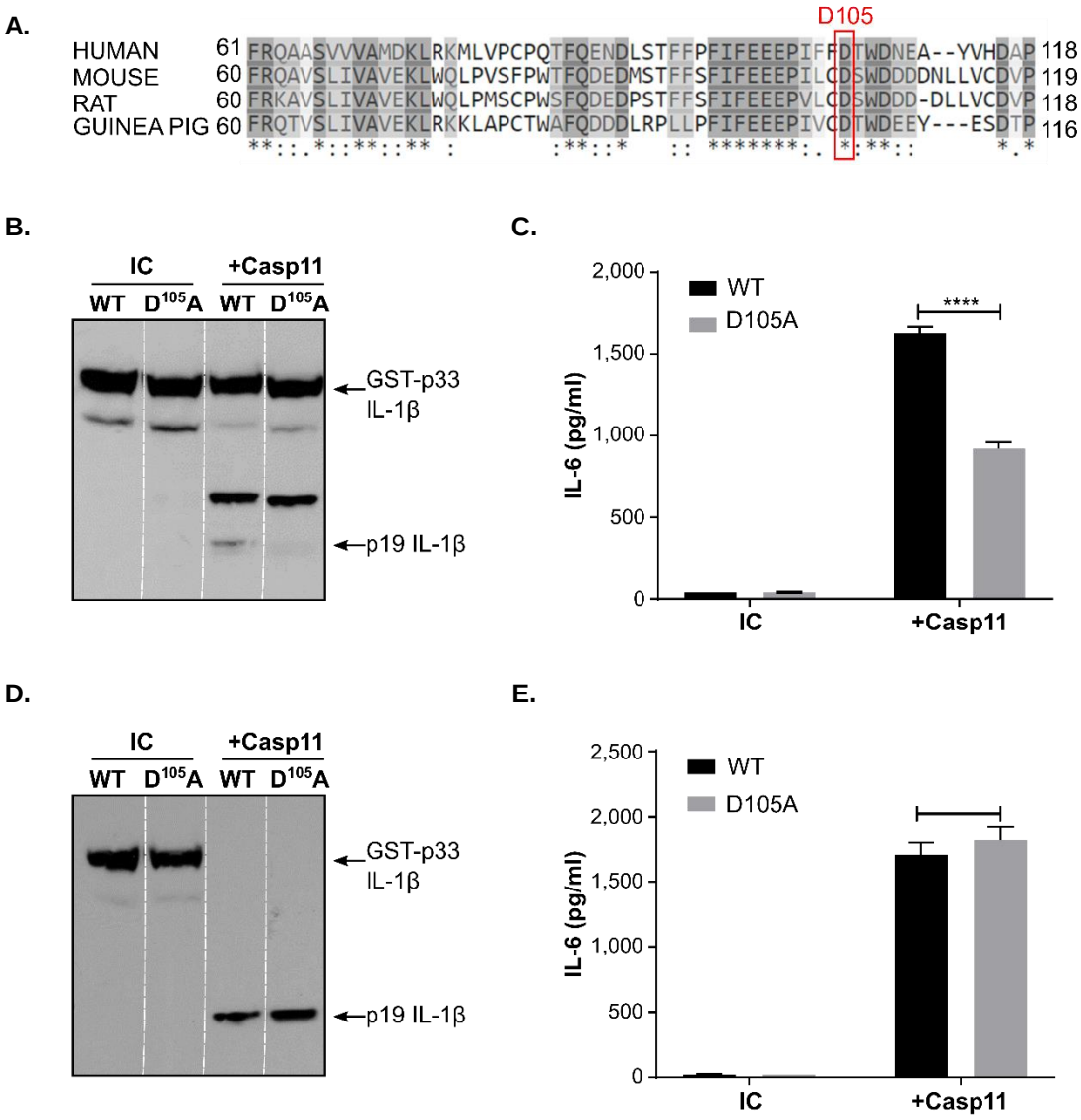

Figure 5.30: Caspase-11 cleaves murine IL-1β at Asp105. (A) Multi species alignment showing location of conserved Asp105. **(B-E)** Western blot for IL-1β (**B,D**) or IL-6 production by HeLa cells treated with the reaction products (**C,E**) following incubation of pro-IL-1β with a low (**B,C**) or high (**D,E**) concentration of caspase-11. Data represent mean +SEM of n=3, p =****≤0.0001.

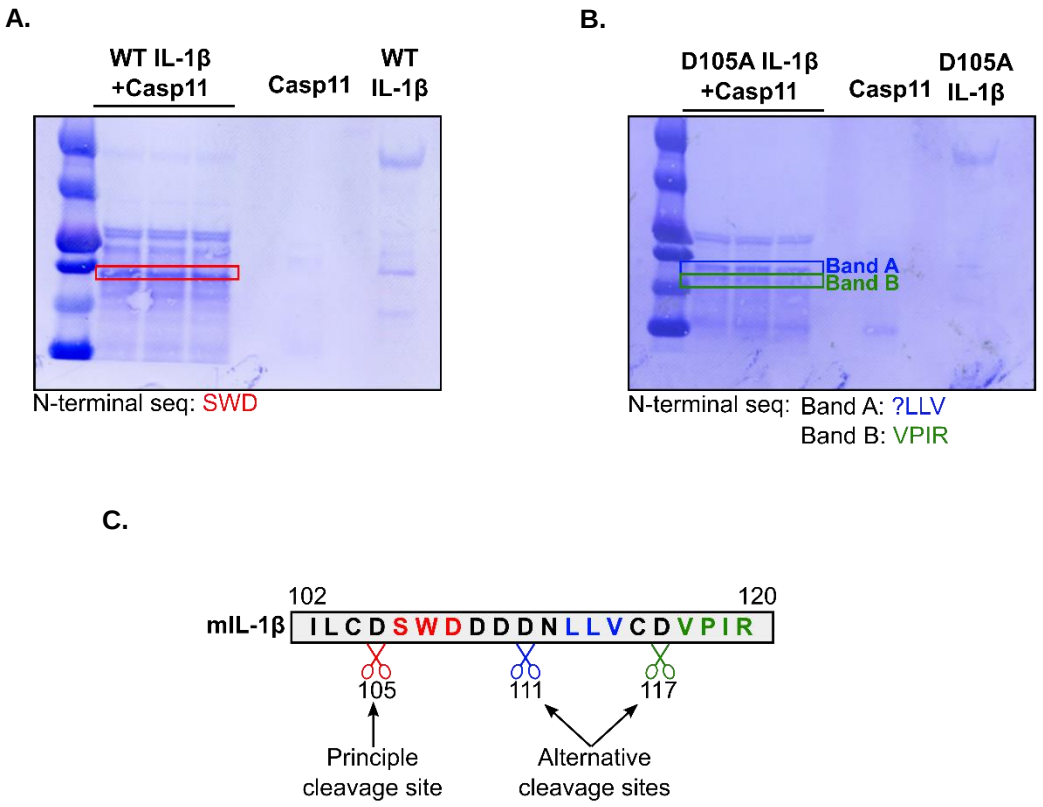

Figure 5.31: Caspase-11 cleaves murine IL-1β at Asp111 and Asp117 if Asp105 is unavailable. (A-B) Coomassie stained PVDF membrane sowing the caspase-11 cleaved bands from WT (**A**) or D105A (**B**) pro-IL-1β that were combined and sent for N-terminal sequencing by Edman degradation. Returned sequences are shown underneath. **(C)** Outline of and preference for caspase-11 cleavage sites in pro-IL-1β.

5.2.16 IL-1α release after intracellular LPS only requires caspase-11

To further examine the requirement for caspase-1 and/or caspase-11 in the secretion and processing of IL-1α and IL-1β we used bone marrow-derived macrophages (BMDMs) from WT, *Casp11*$^{-/-}$, and *Casp1*$^{-/-}$*/Casp11 Transgenic (Tg)* mice. IL-1 release in response to intracellular LPS was absolutely dependent on caspase-11, as evidenced by the complete loss of cleaved IL-1α (Figure 5.32A) and IL-1β (Figure 5.32B) secretion in the *Casp11*$^{-/-}$ BMDMs. Importantly, significant levels of cleaved IL-1α were secreted by the *Casp1*$^{-/-}$*/Casp11*^{Tg} BMDMs following intracellular LPS treatment (Figure 5.32C), suggesting that

IL-1α bypasses the caspase-1 inflammasome and only requires caspase-11 for cleavage and release. The modest reduction in IL-1α secretion in *Casp1*$^{-/-}$*/Casp11*^{Tg} BMDMs compared to WT BMDMS is likely due to incomplete complementation of the endogenous *Casp11* by the transgene, as reported previously (Kayagaki et al., 2011). Interestingly, the treated *Casp1*$^{-/-}$*/Casp11*^{Tg} BMDMs failed to release any IL-1β (Figure 5.32D), suggesting that although caspase-11 can cleave and activate IL-1β *in vitro*, cleavage and/or release *in vivo* also requires caspase-1.

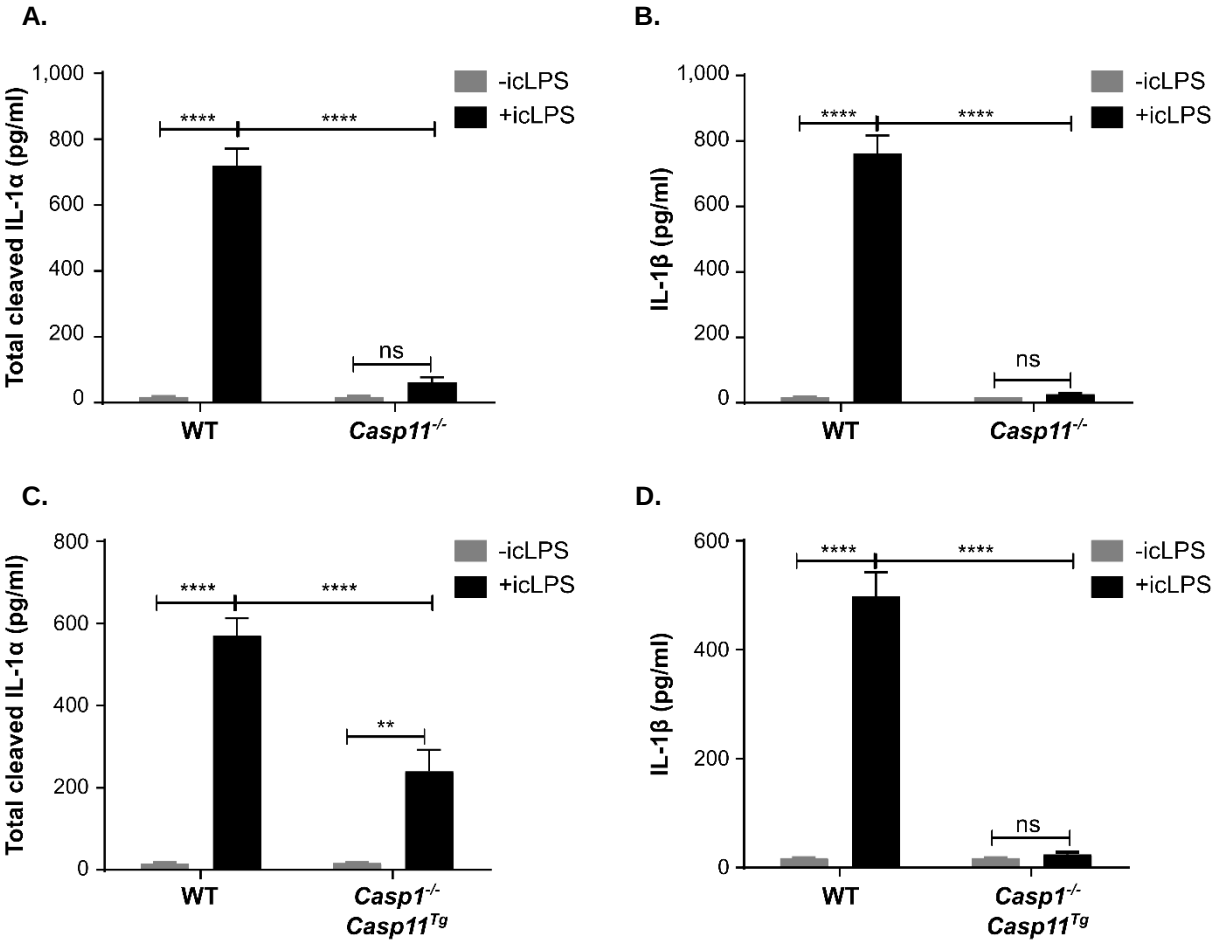

Figure 5.32: IL-1α cleavage and release in response to intracellular LPS only requires caspase-11. (A-D) ELISA data showing the level of cleaved IL-1α (**A,C**) or IL-1β (**B,D**) detected in the conditioned media of murine bone marrow-derived macrophages from *Casp11*$^{-/-}$ (**A,B**) or *Casp1*$^{-/-}$*/Casp11*^{Tg} (**C,D**) mice that had been primed with LPS and then transfected intracellular LPS (icLPS). Data represent mean +SEM of n=3, p = ****≤0.0001.

To investigate if the discordance between our *in vitro* and *in vivo* findings for murine IL-1β was due to incorrect folding or a lack of post-translational modification rendering *E.coli* recombinant murine IL-1β easier to cleave, we tested the ability of caspase-11 to process mammalian cell-derived IL-1β. Pro-IL-1β derived from LPS-treated primary BMDMs was cleaved to the p19 form by caspase-11 (Figure 5.33A) indicating that caspase-11 is capable of cleaving mammalian cell-derived pro-IL-1β. The p22 form of IL-1β also present in the BMDM lysates without caspase-11 was blocked by using a protease inhibitor cocktail, showing that this second band was due to background proteolysis (Figure 5.33B).

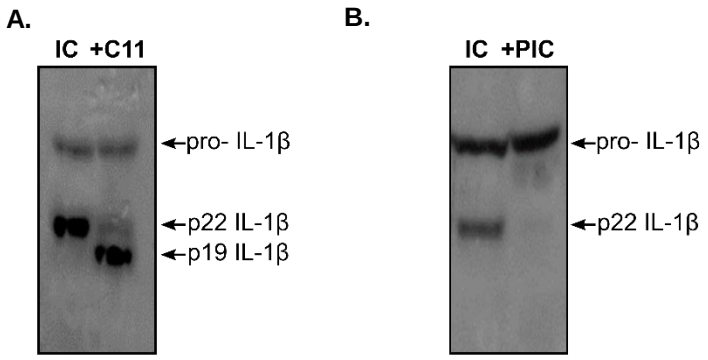

Figure 5.33: Caspase-11 cleaves primary BMDM-derived pro-IL-1β. (A-B) Western blot for IL-1β following incubation of LPS-primed BMDM lysates alone (IC) or with caspase-11 (C11) (**A**), or a protease inhibitor cocktail (PIC) (**B**).

5.2.17 IL-1α release after Chlamydia trachomatis infection only requires caspase-1

To investigate the dependency of IL-1 secretion on each caspase during live bacterial infection, primary BMDMs from WT, *Casp11*$^{-/-}$ or *Casp1*$^{-/-}$*/Casp11*^{Tg} mice were infected with the Gram negative bacteria *Chlamydia trachomatis*. Interestingly, IL-1α secretion in response to *C.trachomatis* infection was dependent on caspase-1, not caspase-11. IL-1β release was completely dependent on caspase-1, but was also partially affected by the loss of caspase-11 (Figure 5.34). *C.trachomatis* is not a straightforward activator of the non-canonical inflammasome. Many non-canonical activators, such as *E.coli*, have hexa-acylated Lipid A moieties, whereas *C.trachomatis* Lipid A is only penta-acylated. LPS from this bacterium therefore cannot induce TLR4 dimerisation and endocytosis (Tan et al., 2015), which may

explain why *C.trachomatis* appears to preferentially engage the canonical inflammasome pathway despite being an intracellular Gram negative bacterium. Indeed, recent work from Jane Goodall's group has demonstrated that although *C.trachomatis* activates both the canonical and non-canonical inflammasomes, only the canonical pathway mediates IL-1β release and pyroptosis (Webster et al., 2017).

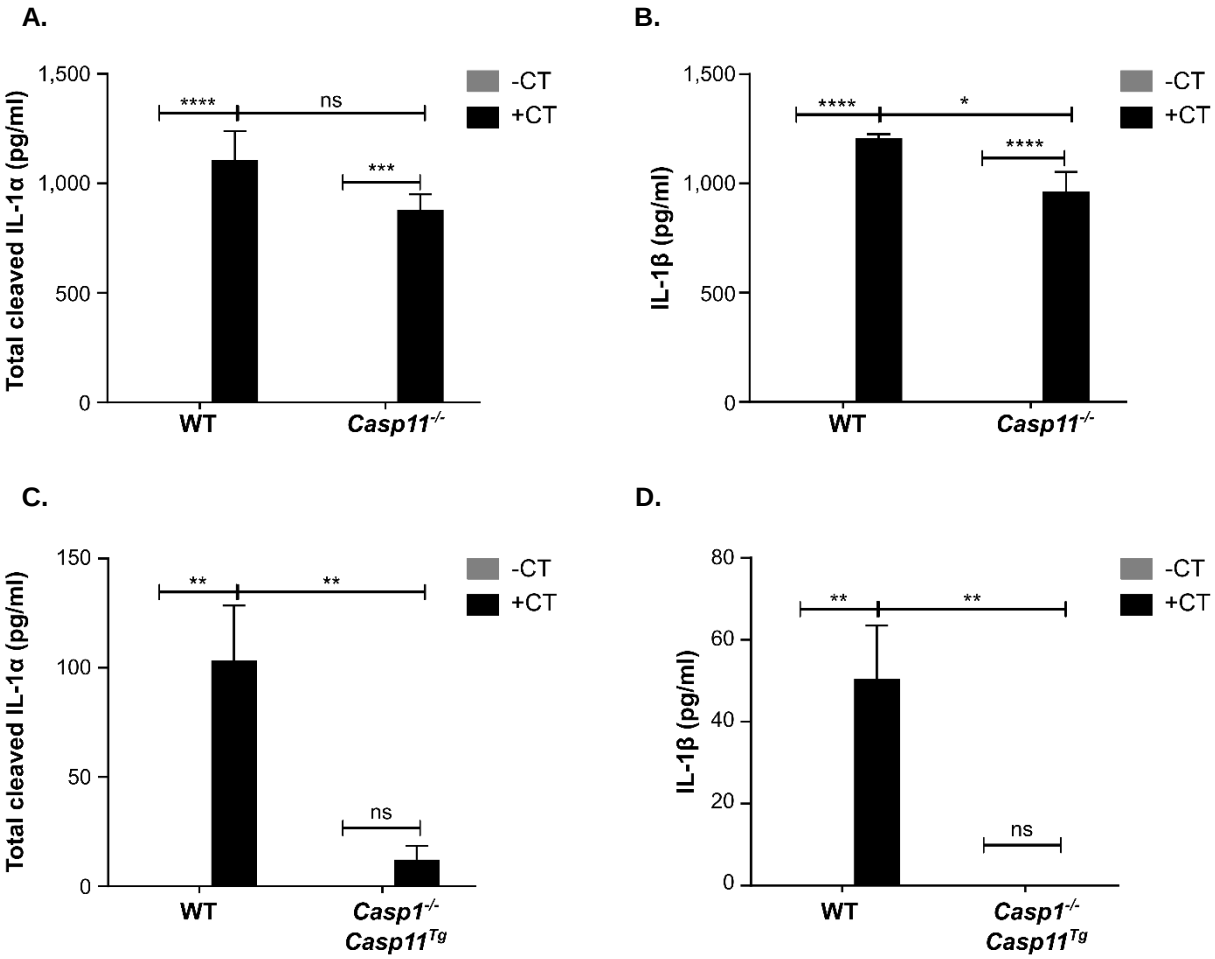

Figure 5.34: IL-1α cleavage and release in response to *C. trachomatis* is dependent on caspase-1. (A-D) ELISA data showing the level of cleaved IL-1α (**A,C**) or IL-1β (**B,D**) detected in the conditioned media of murine bone marrow-derived macrophages from *Casp11*$^{-/-}$ (**A,B**) or *Casp1*$^{-/-}$*/Casp11*^{Tg} (**C,D**) mice that had been primed with LPS and then transfected *Chlamydia trachomatis* (CT). Data represent mean +SEM of n=3, p = *≤0.05, **≤0.01, ****≤0.0001.

5.2.18 IL-1α and IL-1β release in response to intracellular LPS is dependent on gasdermin D

Both caspase-1 and caspase-11 are known to liberate the N-terminal fragment of GSDMD that binds to inner membrane phospholipids and mediates pore formation. Eventually the accumulation of the GSDMD pores drives loss of plasma membrane integrity and pyroptosis, but the cell delays this death through membrane 'bubbling'. This delay is thought to allow the cell time to communicate its situation by releasing cytokines through the GSDMD pores, which recruit immune cells. To examine whether GSDMD pores are required for IL-1α and IL-1β secretion in response intracellular LPS, primary BMDMs from WT or *GsdmD*$^{-/-}$ mice were primed and transfected with LPS. Both the IL-1α and IL-1β responses were lost in the *GsdmD*$^{-/-}$ cells (Figure 5.35), suggesting that these cytokines exit the cell through the GSDMD pores during LPS-mediated non-canonical inflammasome activation.

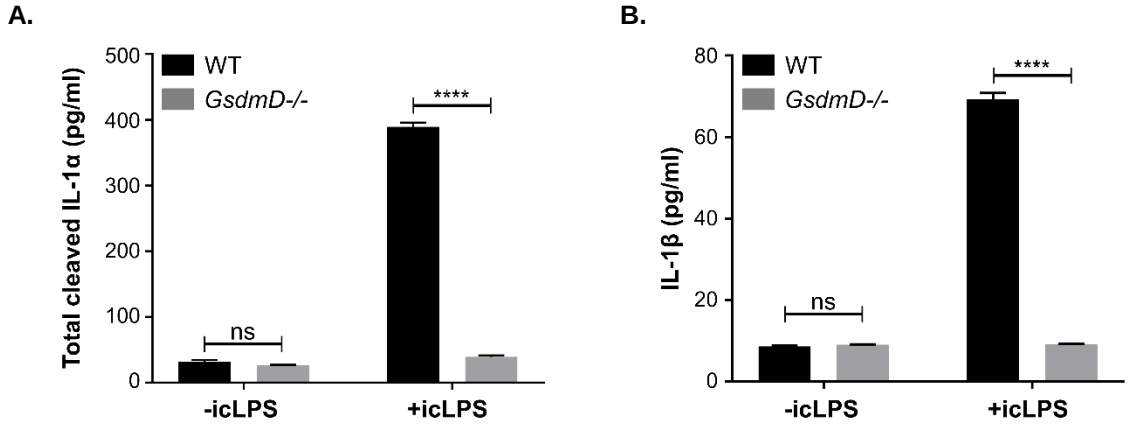

Figure 5.35: IL-1α and IL-1β release in response to intracellular LPS are dependent on GSDMD. (A-D) ELISA data showing the level of cleaved IL-1α (**A**) or IL-1β (**B**) detected in the conditioned media of murine bone marrow-derived macrophages from WT and *GsdmD*$^{-/-}$ mice that had been primed with LPS and then transfected intracellular LPS (icLPS). Data represent mean +SEM of n=3, p = ****≤0.0001,

5.3 Discussion

Successful host defence requires an immune response that effectively resolves an insult without causing overt tissue damage. IL-1 is an extremely powerful inflammatory cytokine that is subject to multiple levels of regulation. The inflammasome represents an important platform for IL-1 activation, and multiple inflammasome sensors have evolved to detect and distinguish a wide range of endogenous and exogenous danger signals. Over the last 6 years, the non-canonical inflammasome has emerged as an important mechanism for sensing intracellular bacterial infection via LPS-mediated inflammatory caspase activation. However, it is not fully understood how IL-1, particularly IL-1α, is activated by the non-canonical inflammasome, and very few studies have investigated the human system.

We find that IL-1α and IL-1β are directly cleaved by human caspase-5, but not caspase-4, and murine caspase-11 at highly conserved sites, and this processing leads to enhanced cytokine activity (Figures 5.2, 5.6, 5.25 and 5.26). In humans, *CASP4* and *CASP5* arose due to the duplication of an ancestral *Casp11*-like gene. Most literature focusses on caspase-4, which is often described to be the closer orthologue of caspase-11 (Shi et al., 2014). Although all three caspases have been shown to bind LPS, only *CASP5* and *Casp11* are upregulated by TLR ligation, whereas *CASP4* is constitutively expressed (Figure 5.24). Furthermore, we show that both caspase-5 and -11 can directly activate IL-1, which suggests a closer functional connection between these two proteases. Our data does, however, suggest that caspase-11 is more promiscuous than caspase-5. For both murine IL-1α and IL-1β, if the preferred cleavage site is blocked, caspase-11 simply cleaves elsewhere (Figures 5.29 and 5.30), in contrast to the complete blockage of human IL-1 activation by caspase-5 following mutation of the target sites (Figures 5.4 and 5.8). We therefore suggest that caspases-4 and 5 have undergone both substrate specificity refinement, and sub-functionalisation, with the functionality of the ancestral caspase-11-like gene now distributed between both enzymes.

We show that caspase-5-cleaved IL-1α is released by primary human macrophages following both canonical and non-canonical inflammasome activation (Figures 5.20 and 5.21), which suggests there may be crosstalk between the two pathways. Indeed, caspase-11 has been previously shown to activate

caspase-1 (Kang et al., 2000). Using our in-house ELISA to detect the release of this longer cleaved form of IL-1α from cells demonstrates that IL-1α is not released passively during pyroptosis, but is actively processed during non-canonical inflammasome activation before calpain is activated.

Intriguingly, our murine BMDM data showed that IL-1α secretion following intracellular LPS treatment requires caspase-11 only, whereas IL-1β release requires both caspases-1 and -11 (Figure 5.32). This finding was somewhat surprising, since our recombinant protein data suggested that caspase-11 cleaved murine pro-IL-1β very efficiently. We confirmed that this difference was not an artefact of using recombinant protein, because caspase-11 could efficiently process BMDM-derived pro-IL-1β (Figure 5.33). One possible explanation for this is that active caspase-11 could be compartmentalised away from pro-IL-1β inside cells. Indeed, IL-1β is upregulated and translated alongside other components of the canonical inflammasome that are known to aggregate at a single point within the cell known as the 'speck', and so it is possible that IL-1β is also targeted to this specific intracellular location. Unfortunately, due to a lack of commercially available IL-1β immunofluorescence antibodies, it is difficult to interrogate this hypothesis further. Another simple explanation could be that recombinant caspase-11 is promiscuous and cuts IL-1β non-specifically *in vitro*. However, caspase-11 preferentially cuts IL-1β at a conserved tetrapeptide sequence 13 residues upstream of the caspase-1 site, which strongly suggests cleavage and activation of IL-1β by caspase-11 is a specific action.

The original *Casp1*$^{-/-}$ mice showed complete loss of IL-1β release from macrophages during endotoxemia. Unexpectedly, reduced levels of IL-1α release were also reported, which has been an ongoing puzzle in the caspase field given that IL-1α is not a substrate for caspase-1 (Kuida et al., 1995, Li et al., 1995). However, because the *Casp1*$^{-/-}$ mice were made using stem cells from a mouse of a 129/Sv background, they also contained an inactivating mutation in their *Casp11* gene. Our data suggests that the defective IL-1α cleavage and release observed in the original *Casp1*$^{-/-}$ mice is likely because IL-1α cannot be processed by caspase-11 in these animals. Indeed, serum levels of cleaved IL-1α are undetectable during endotoxemia in *Casp11*$^{-/-}$ and *Casp1*$^{-/-}$/*Casp11*$^{-/-}$ but are restored in the *Casp1*$^{-/-}$*Casp11*^{Tg} mice (Kayagaki et al., 2011).

The direct activation of IL-1α by caspase-5 may represent an extremely important immune defence pathway. A number of pathogens release proteins that target the canonical inflammasome as part of their immune evasion strategy. For example, the viral serpin CrmA, and Myxoma and Vaccinia proteins directly inhibit caspase-1, while the *Pseudomonas aeruginosa* T3SS effector Exoenzyme U and *Mycobacterium tuberculosis* zinc metalloproteinase *zmp1* interfere with inflammasomes (Lamkanfi and Dixit, 2011, Taxman et al., 2010). The caspase-5 IL-1α activation pathway completely bypasses the canonical caspase-1 inflammasome, and could therefore represent a way of reinstating the immune response after caspase-1 inflammasome blockade. Furthermore, pro-IL-1α is constitutively expressed by most cell types, although held in an inactive state by the decoy receptor IL-1R2, whereas IL-1β must be upregulated following priming. We have previously demonstrated that caspases-1 and -5, but not caspase-4, are able to cleave IL-1R2 (Zheng et al., 2013). Caspase-5 is therefore an extremely powerful protease that can both liberate and activate IL-1α rapidly following intracellular infection.

In conclusion, the work presented in this chapter has identified caspase-5 as a novel activator of IL-1α during non-canonical inflammasome activation by intracellular LPS. Therefore, therapeutically targeting caspase-5 may be of great interest in diseases driven by the non-canonical inflammasome, such as septic shock.

6. Results: Caspase-5/-11 cleavage of IL-1α drives the senescence-associated secretory phenotype

6.1 Introduction

Senescence is a permanent state of stable cell cycle arrest that occurs in response to cellular stress. It was first described in the 1960's, when Hayflick and Moorhead showed that primary human fibroblasts undergo permanent proliferative arrest following extended *in vitro* culture (Hayflick and Moorhead, 1961). This form of cell cycle arrest is now known as replicative senescence, which naturally occurs due to the progressive shortening of telomeres with each cell division and subsequent DNA damage. Senescence is an important and protective cellular process with roles in embryonic development, normal tissue homeostasis, and wound healing (Storer et al., 2013, Munoz-Espin et al., 2013, Jun and Lau, 2010). However, senescence is also induced by a number of pathophysiological stimuli, including high ROS levels, oncogene hyperactivation (oncogene-induced senescence, OIS), cytotoxic drugs, and ageing (Chen et al., 1995, Serrano et al., 1997, Ogryzko et al., 1996, Parry and Narita, 2016). As such, senescent cells are implicated in multiple diseases including cancer, arthritis, and atherosclerosis (Pérez-Mancera et al., 2014, Price et al., 2002, Childs et al., 2016).

Senescent cells have a number of characteristic features that distinguish them from other non-dividing cells, such as those that are terminally differentiated or quiescent. For example, senescent cells develop a large and flat morphology *in vitro*, do not proliferate (e.g. Ki67-negative), upregulate tumour suppressors and cell cycle inhibitors (e.g. p16 and p21), and rearrange their genetic material into distinct heterochromatic foci to reduce cell cycle gene accessibility (Collado and Serrano, 2006, Narita et al., 2003). However, perhaps the most widely used marker of senescent cells is senescence-associated beta-galactosidase (SAβGAL) (Dimri et al., 1995). Importantly, SAβGAL itself is not an enzyme; rather it describes the overexpression and accumulation of lysosomal beta-galactosidase that drives the production of a blue precipitate when incubated with the substrate X-gal at pH 6.0. Although senescent cells exhibit high levels of lysosomal beta-galactosidase activity, there is evidence suggesting that other

cell types including macrophages can also upregulate this enzyme (Bursuker et al., 1982). As such, although SAβGAL remains an appropriate marker for cellular senescence *in vitro*, it may not be suitable for use *in vivo* where multiple cell populations are present.

In addition to these distinct intracellular changes, senescent cells secrete a cocktail of inflammatory mediators including cytokines, chemokines, growth factors and proteases, collectively known as the senescence-associated secretory phenotype (SASP) (Figure 6.1). The SASP reinforces senescence in both an autocrine and paracrine manner, and is reported to be driven by IL-1α (Orjalo et al., 2009, Gardner et al., 2015). Whilst the SASP drives immune cell recruitment and therefore the elimination of damaged senescent cells, it also induces chronic inflammation that contributes to disease progression. For instance, the SASP of senescent vascular smooth muscle cells (VSMCs) in atherosclerotic lesions likely drives plaque instability (Gardner et al., 2015). In addition, the SASP within a tumour supports metastasis by increasing epithelial cell proliferation, driving epithelial-mesenchymal transition and promoting tumour cell invasiveness (Coppé et al., 2010).

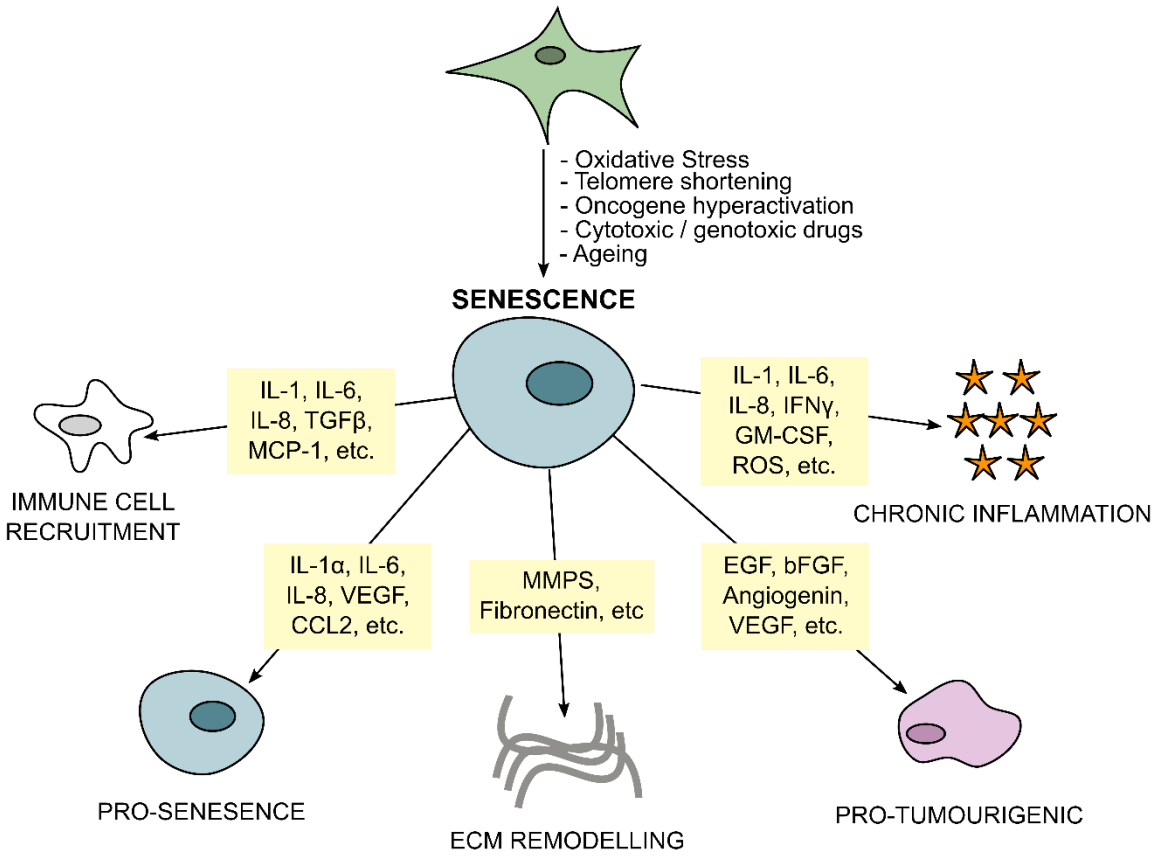

Figure 6.1: The senescence-associated secretory phenotype. Schematic showing the causes of cellular senescence, examples of SASP factors and their effects.

6.1.1 Chapter 5 project rationale

The IL-1α-dependent SASP is an important sterile inflammatory pathway that is involved in both normal tissue homeostasis and inflammatory disease. The protease that activates IL-1α in senescent cells is unknown. Previous studies have suggested that the NLRP3 inflammasome modulates the SASP (Acosta et al., 2013), even though the proteolytic component caspase-1 is unable to activate IL-1α. We have shown that caspase-5, which lies upstream of NLRP3 in the non-canonical inflammasome pathway, is a potent inducer of IL-1α activity (Chapter 5). The work presented in this chapter aims to determine if caspase-5 regulates the IL-1α-driven SASP.

6.2 Results

6.2.1 Senescence as a model of sterile inflammation

Four years ago, Jesús Gil's group reported that the canonical NLRP3 inflammasome drives the SASP (Acosta et al., 2013). They observed that mature IL-1β was released from senescent fibroblasts, and that the canonical inflammasome components caspase-1, NLRP3 and ASC were upregulated during senescence. Acosta and colleagues reported that treatment of senescent cells with the caspase-1 inhibitor Z-YVAD-fmk inhibited the SASP, and concluded that the NLRP3 inflammasome drives IL-1 secretion. However, we find that the caspase inhibitors are not specific. The caspase-1 inhibitor Z-YVAD-fmk inhibited caspase-5-mediated IL-1α activation with equal potency to the caspase-5 inhibitor Z-LEVD-fmk (Figure 6.2A). Similarly, Z-LEVD-fmk was a more potent inhibitor of caspase-1-mediated IL-1β activation than Z-YVAD-fmk (Figure 6.2B). As such, these inhibitors are not a reliable tool for teasing apart the contribution of individual caspases in a cell. Since the NLRP3 inflammasome activation occurs downstream of caspase-5 activation, we hypothesised that the non-canonical inflammasome could play a role in senescence, and that the effects of Z-YVAD-fmk on the SASP reported by Acosta *et al* were in fact due to the inhibition of caspase-5.

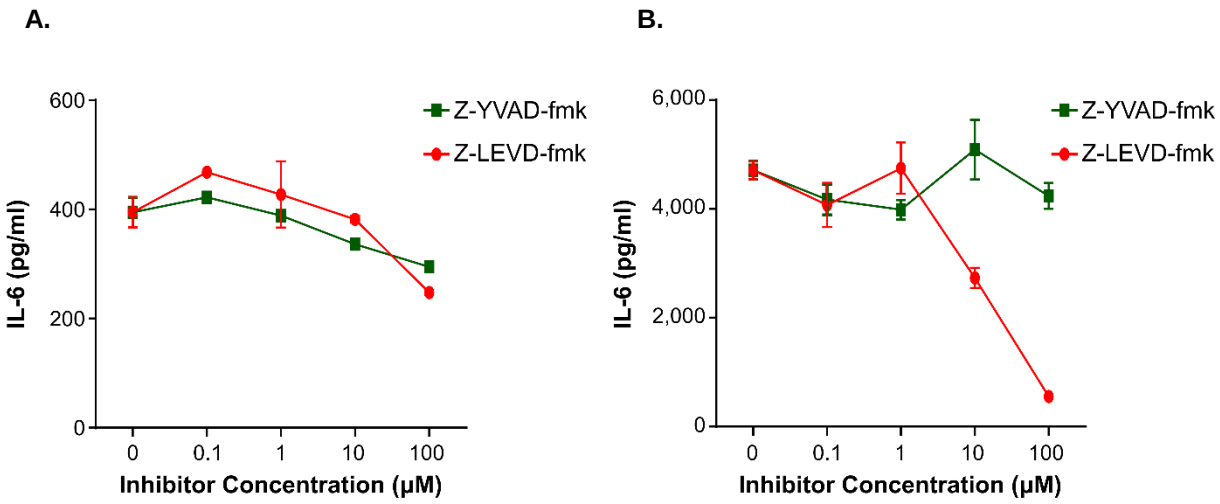

Figure 6.2: The caspase inhibitors Z-YVAD-fmk and Z-LEVD-fmk are not specific. (A-B) ELISA data showing the level of IL-1 dependent IL-6 release from HeLas treated with the reaction products following incubation of IL-1α with caspase-5 (**A**) or IL-1β with caspase-1 (**B**) ± a range of Z-YVAD-fmk or Z-LEVD-fmk concentrations. Data represent mean ±SEM of n=2.

6.2.2 H-RAS expression drives oncogene-induced senescence in primary human fibroblasts

To investigate whether caspase-5 is required for IL-1α-driven SASPs, we (in collaboration with the Narita group, CRUK) used a well-characterised system in human IMR90 fibroblasts in which tamoxifen-inducible *HRAS* expression causes senescence (Narita et al., 2011, Hoare et al., 2016). Seven days of tamoxifen treatment resulted in an upregulation of SAβGAL (Figure 6.3A), a reduction in proliferation (Figure 6.3B), and the formation of senescence-associated heterochromatic foci (SAHF) (Figure 6.3C).

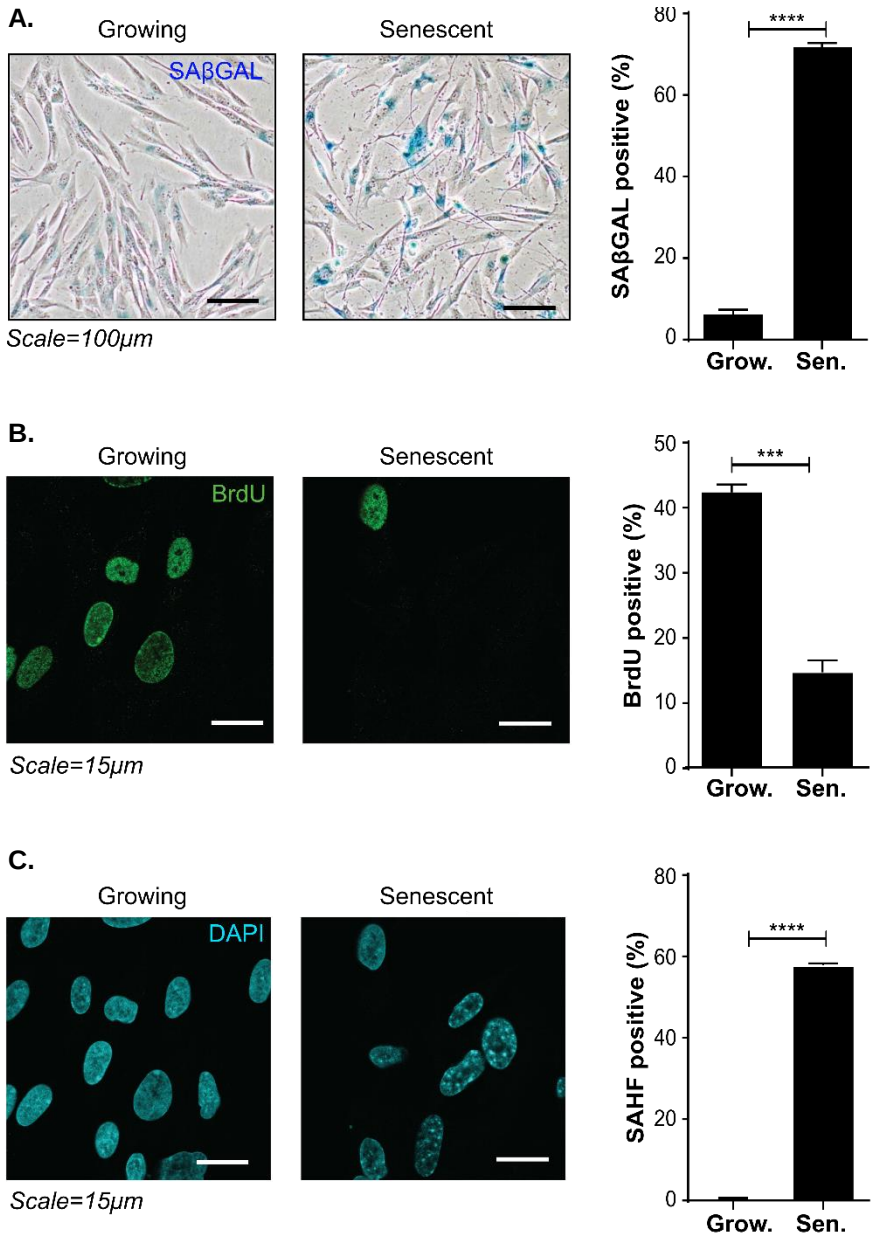

Figure 6.3: *H-RAS* overexpression induces senescence in IMR90 fibroblasts. (A-C) Representative images and quantification of senescence-associated beta galactosidase (SAβGAL) (**A**), proliferation by BrDu (**B**), and senescence-associated heterochromatic foci (SAHF) by DAPI (**C**). Data represents mean +SEM of n=3, p = ***≤0.001, ****≤0.0001.

6.2.3 Senescent IMR90 cells upregulate IL-1α expression

Since the SASP is reported to be driven by IL-1α (Orjalo et al., 2009), we compared the levels of IL-1α expression in growing and senescent cells. Senescent fibroblasts upregulated *IL1A* gene expression (Figure 6.4A), increased cell-surface IL-1α expression (Figure 6.4B), and secreted more mature IL-1α (Figure 6.4C), compared with growing cells. Importantly, there was no difference in levels of cell death between growing and senescent cells, excluding any effects of IL-1α released after necrosis or pyroptosis (Figure 6.4D).

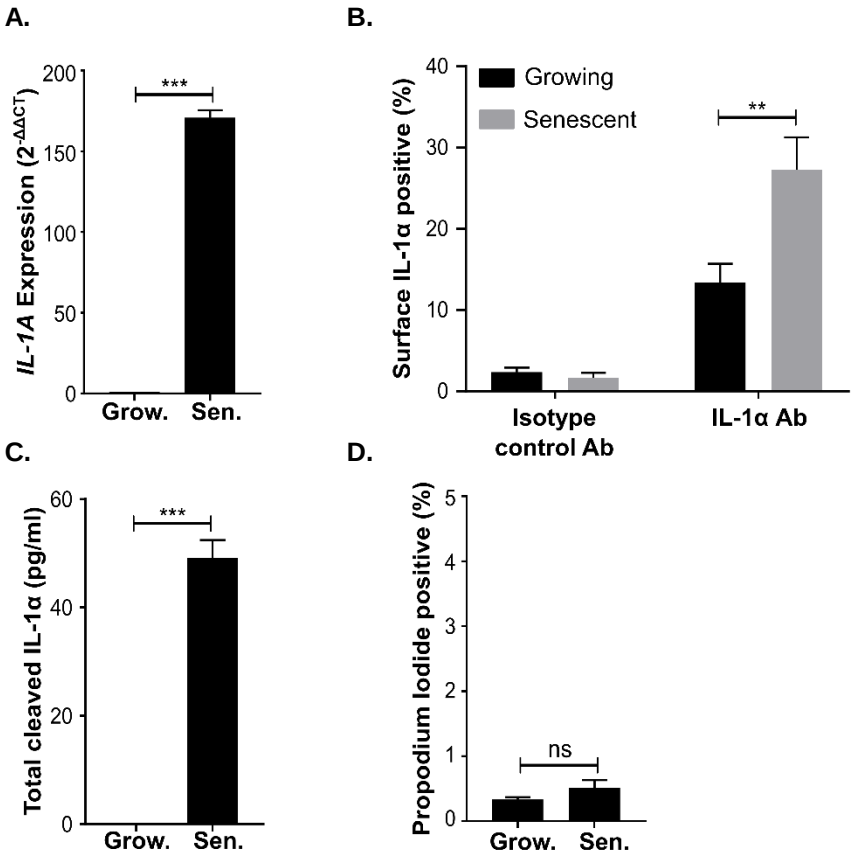

Figure 6.4: Senescent cells upregulate IL-1α. (A-C) Levels of *IL1A* expression by qPCR (**A**), surface IL-1α by flow cytometry (**B**), and cleaved IL-1α in the conditioned media by ELISA (**C**) in growing (Grow.) and senescent (Sen.) IMR90 cells. **(D.)** Level of cell death in growing and senescent IMR90 cells measured by propidium iodide staining. Data represent mean +SEM of n=3, p = **≤0.01, ***≤0.001.

6.2.4 IL-1α secretion by senescent IMR90 cells is partially GSDMD-independent

Although the SASP is reported to be driven by cell-surface IL-1α (Orjalo et al., 2009), it remains unclear whether membrane IL-1α is a real phenomenon, or if it is actually secreted IL-1α bound to IL-1R1. Ongoing research from our group suggests that a significant portion of surface IL-1α may be bound to IL-1R1 and IL-1R2 (Chan et al, *publication in progress)*. To test whether IL-1α is secreted through the GSDMD pores during senescence, we used two individual siRNAs to knockdown *GSDMD* expression (Figure 6.5A). *GSDMD* knockdown had no effect on surface IL-1α expression (Figure 6.5B), but did elicit a modest reduction in IL-1α secretion (Figure 6.5C).

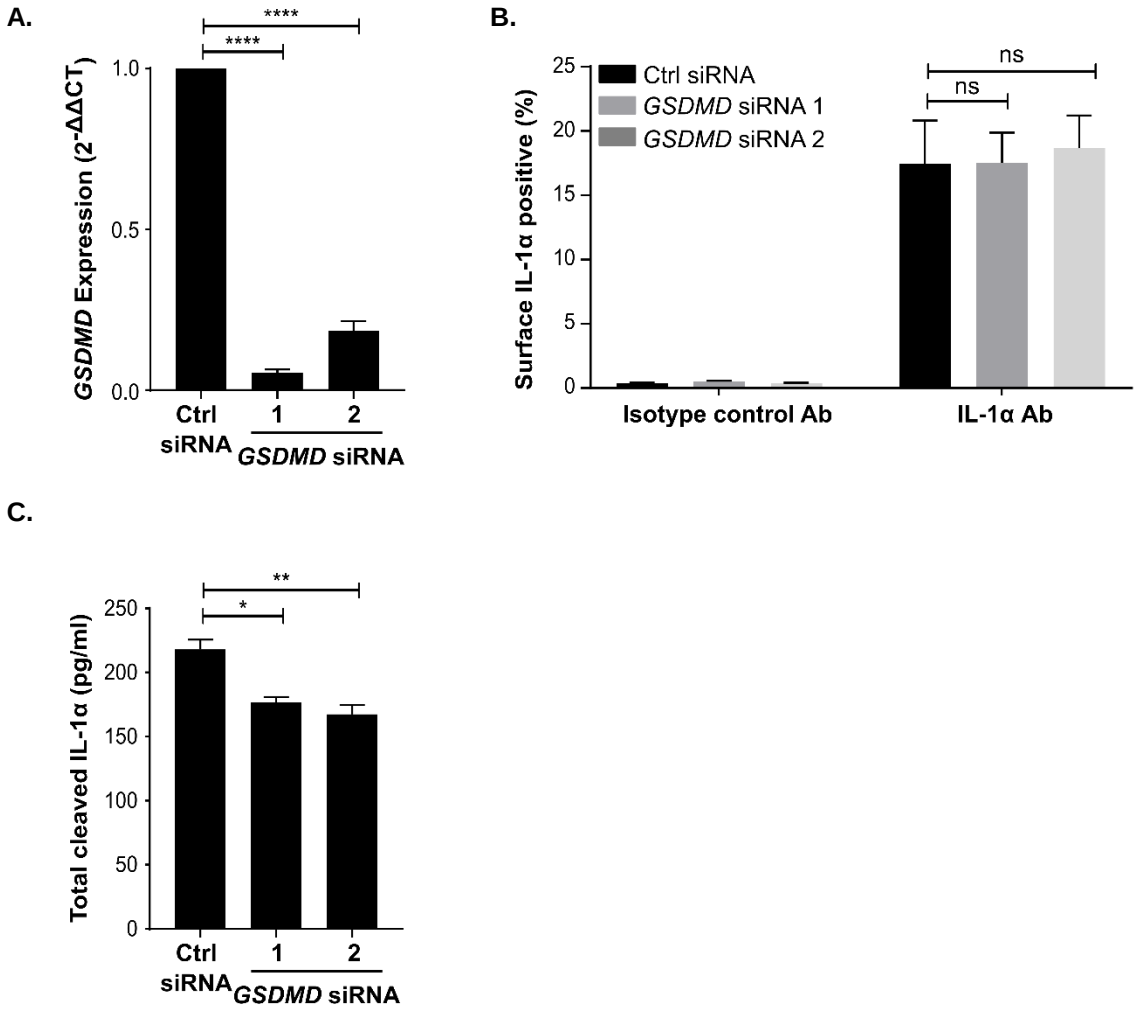

Figure 6.5: IL-1α secretion by senescent IMR90 cells may be partially GSDMD dependent. (A) qPCR data showing relative *GSDMD* expression in senescent IMR90 cells after transfection of control (Ctrl) or *GSDMD*-targeted siRNAs. **(B-C)** Cell surface IL-1α by flow cytometry (**B**), or levels of cleaved IL-1α in the conditioned media by ELISA (**C**), in senescent IMR90 cells after transfection of control or *GSDMD*- targeted siRNAs. Data represent mean +SEM of n=3, p = *≤0.05, **≤0.01, ****≤0.0001.

Since the *GSDMD*-targeted siRNAs achieved approximately 85-95% knockdown, it is possible that the remaining 5-15% of GSDMD was sufficient for pore formation and IL-1α secretion. During their research on IL-1β release during inflammasome activation, Pablo Pelegrin's group suggested punicalagin as a compound that may block GSDMD pores (Martín-Sánchez et al., 2016). Treatment of senescent IMR90s with punicalagin led to a modest increase in total IL-1α secretion, suggesting that IL-1α is not released through the GSDMD pores (Figure 6.6A). Importantly there was no difference in cell death between the treated and untreated samples (Figure 6.6B)

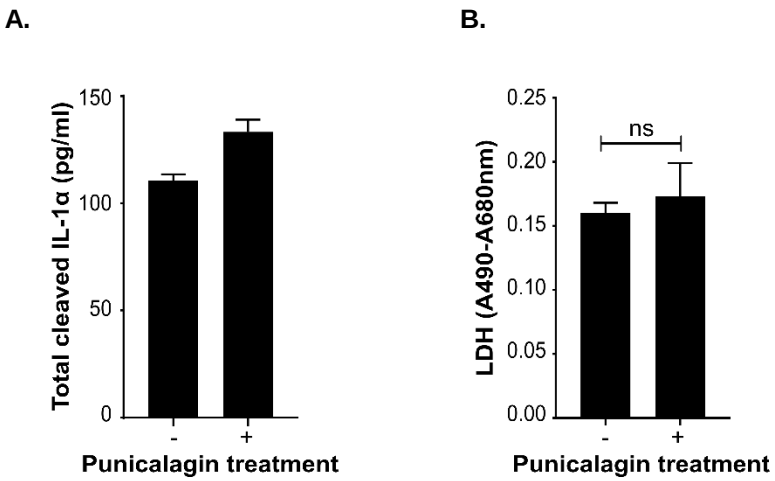

Figure 6.6: Punicalagin has no effect on IL-1α secretion. (A-B) ELISA data showing levels of cleaved IL-1α (A) or LDH (B) in the conditioned media of senescent IMR90 cells ± punicalagin treatment. Data represent mean +SEM of n=3.

6.2.5 IL-6 secretion by senescent IMR90 cells is IL-1α-dependent

The cytokines IL-6 and IL-8 are considered two of the most strongly upregulated SASP factors in senescent cells. The conditioned media of day 7 senescent IMR90s contained extremely high levels of IL-6, which was secreted in a completely IL-1α dependent manner as evidenced by an IL-1α neutralising antibody and the IL-1RA (Figure 6.7A). Unexpectedly, there was no difference in the levels of secreted IL-8 between growing and senescent IMR90s (Figure 6.7B), despite an upregulated transcript (Figure 6.7C).

To investigate this further, we assessed the levels of IL-6 and IL-8 in the conditioned media of senescent IMR90s over time (Figure 6.8). IL-6 release occurred at the later time points, peaking after 7 days of *HRAS* expression (Figure 6.8A), whereas maximal IL-8 secretion was observed earlier after only 4-5 days of *HRAS* expression (Figure 6.8B). It is possible that IL-6 production saturates the protein synthesis machinery at day 7, preventing IL-8 protein production despite high levels of gene transcription.

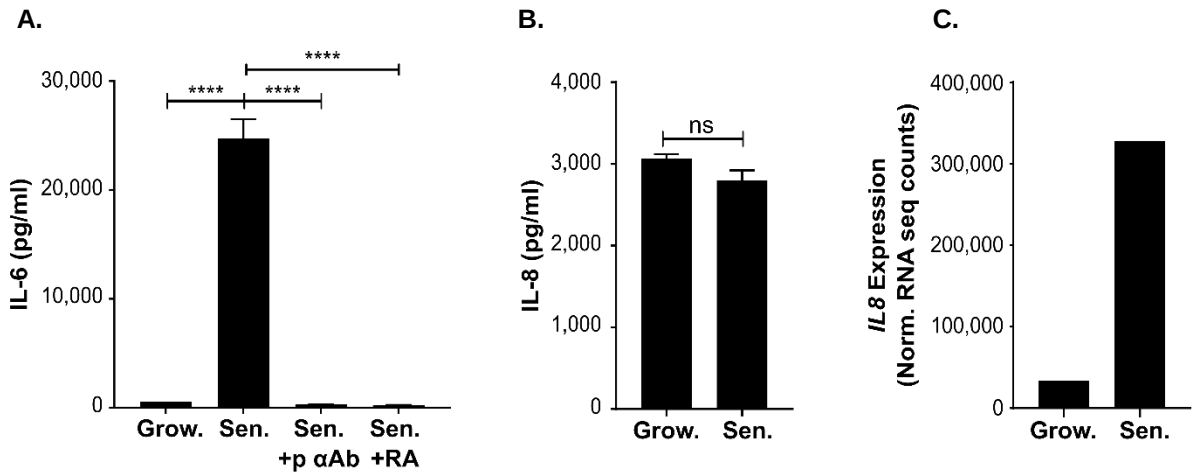

Figure 6.7: Senescent cells secrete IL-6 in an IL-1α-dependent manner. (A-B) ELISA data showing level of IL-6 (**A**) and IL-8 (**B**) in the conditioned media of growing (Grow.) and senescent (Sen.) IMR90s treated ± a neutralising IL-1α antibody (p αAb) or IL-1RA (RA). **(C)** Re-analysed RNA-seq data (Hoare et al., 2016) showing level of *IL8* expression by growing (Grow.) and senescent (Sen.) IMR90s. Data is mean +SEM of n=3 (**A,B**) or 6 (**C**), p = ****≤0.0001.

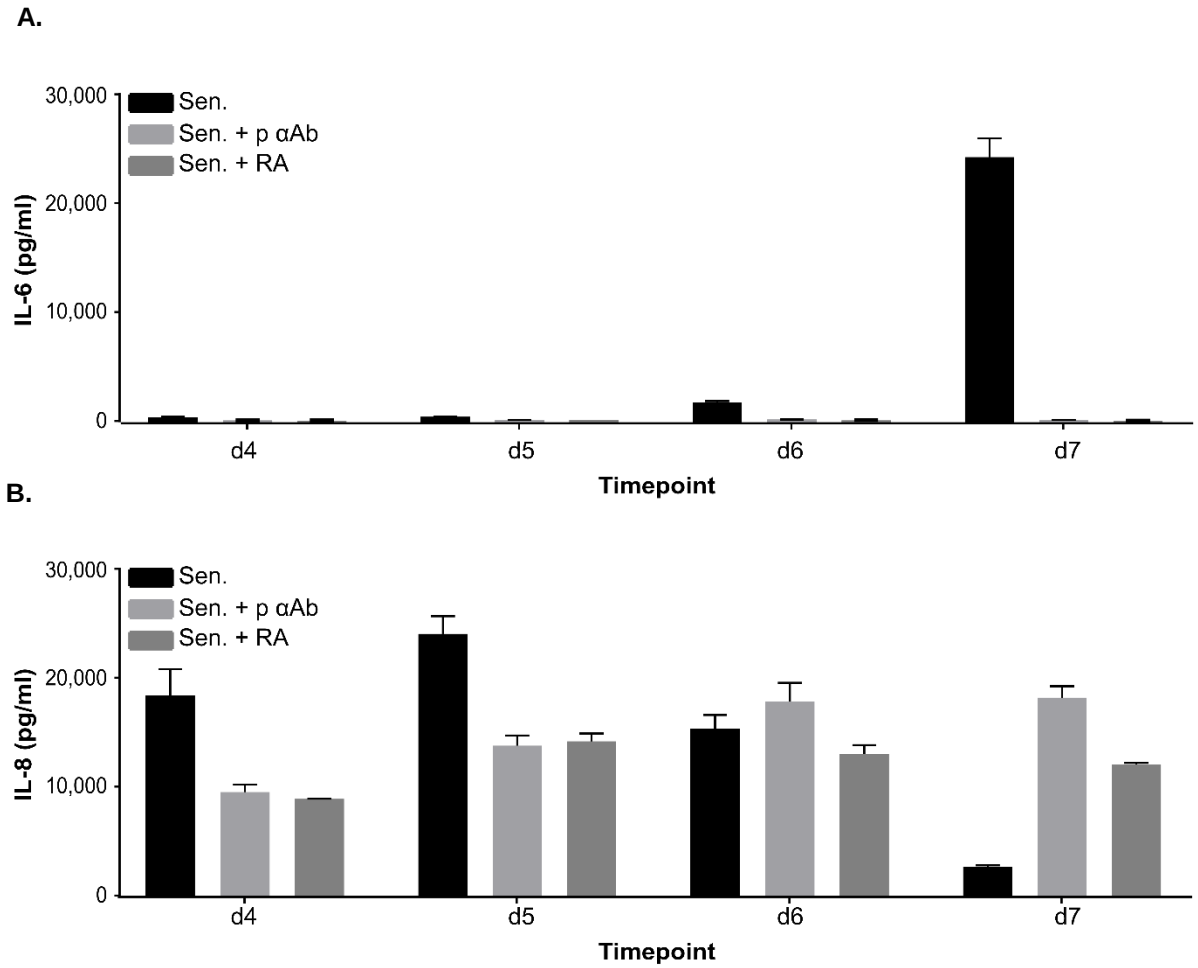

Figure 6.8: The temporal pattern of IL-6 and IL-8 release by senescent IMR90 cells (A-B) ELISA data showing level of IL-6 (**A**) and IL-8 (**B**) in the conditioned media of senescent IMR90s over time treated ± IL-1α neutralising antibody (α Ab) or the IL-1RA (RA). Data is mean +SEM of n=3

6.2.6 Senescent IMR90 cells do not release cleaved IL-1β

It has been reported that senescent cells release cleaved active IL-1β (Acosta et al., 2013). Since both forms of IL-1 signal through the same receptor, this contradicts our data showing that anti-IL-1α neutralising antibody completely abolishes the SASP. However, we were unable to detect significant levels of IL-1β in the conditioned media of growing or senescent cells (Figure 6.9A). Analysis of intracellular IL-1β levels revealed that senescent IMR90s upregulate pro-IL-1β, but only a small amount is processed into an 18-19KDa fragment (Figure 6.9B). In fact, a large portion of the pro-IL-1β was processed into a 25kDa form that is likely inactive, which may represent a mechanism to inactivate large amounts of pro-IL-1β and prevent aberrant inflammation.

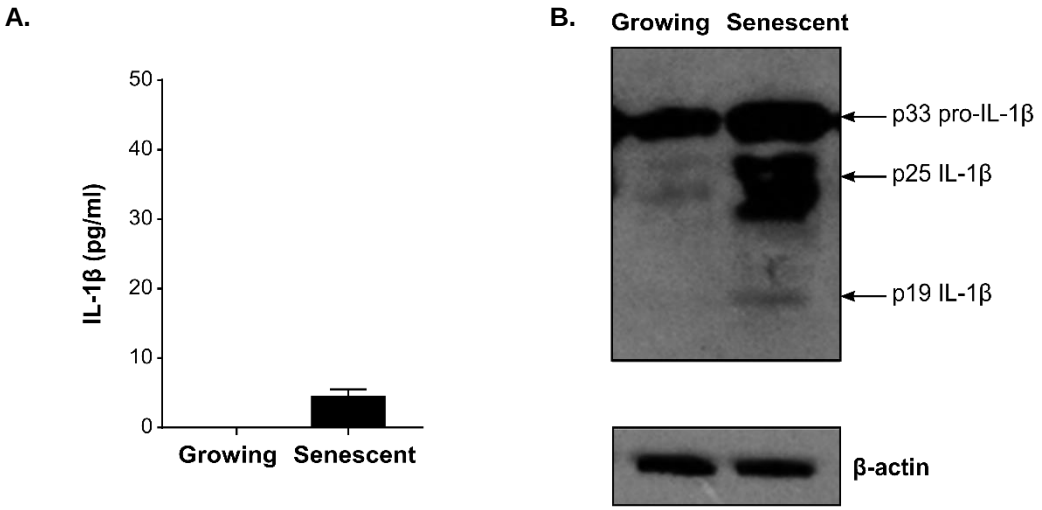

Figure 6.9: Senescent cells do not release IL-1β. (A) ELISA data showing level of IL-1β in the conditioned media of growing and senescent IMR90s. **(B)** Western blot for IL-1β and β-actin in growing and senescent IMR90 lysates. Data is mean +SEM of n=3.

6.2.7 Senescent IMR90 cells upregulate *CASP5* via cGAS signalling

Gene expression analysis revealed that senescent IMR90 fibroblasts expressed higher levels of *CASP5* than growing cells (Figure 6.10A). This upregulation was also observed when publically available RNA-seq data (Hoare et al., 2016) was re-analysed (Figure 6.10B). Together, this suggests that the non-canonical inflammasome might be involved in activating IL-1α in senescent cells.

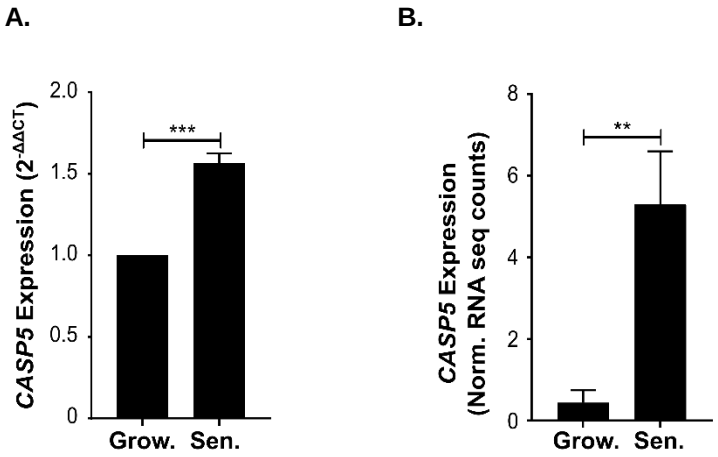

Figure 6.10: Senescent cells upregulate *CASP5*. (A-B) Levels of *CASP5* gene expression growing and senescent IMR90 fibroblasts analysed by qPCR (**A**) and RNA-seq (**B**). Data represent mean +SEM of n=3 (**A**) or 6 (**B**). p = **≤0.01, ***≤0.001.

The priming and activating stimuli that drive *CASP5* upregulation and pro-caspase-5 activation in senescent cells are unknown. RAS overexpression has been reported to increase the levels of intracellular ROS (Lee et al., 1999) that could oxidise a number of substrates that may activate caspase-5, akin to the activation of caspase-11 by the oxidised phospholipid oxPAPC (Zanoni et al., 2016). However, treatment with the antioxidant ascorbic acid had no effect on the SASP (Figure 6.11), suggesting that ROS are not involved in caspase-5 expression and/or activation.

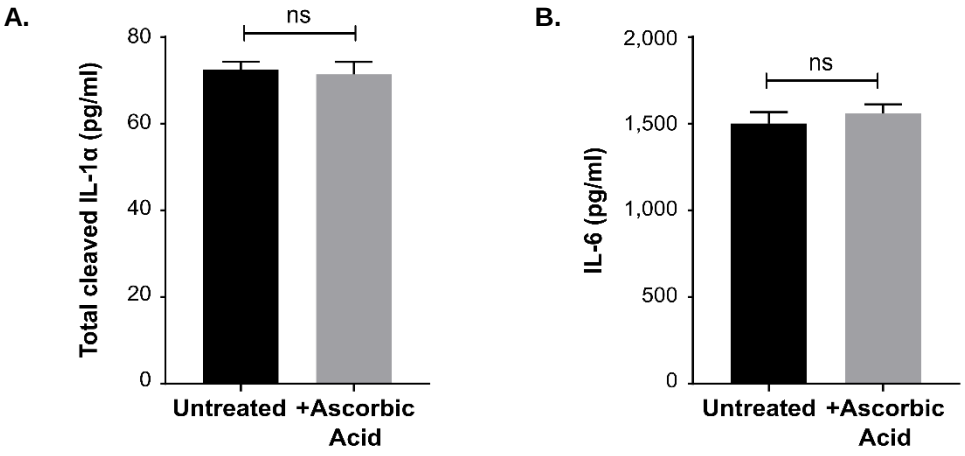

Figure 6.11: Ascorbic acid treatment has no effect on the SASP. (A-B) ELISA data showing the level of IL-1α (**A**) and IL-6 (**B**) in the conditioned media of senescent IMR90 cells ± ascorbic acid. Data represent mean +SEM of n=3.

Senescent cells exhibit impaired nuclear membrane integrity due to the loss of lamin B1 (Freund et al., 2012). This results in the presence of cytosolic chromatin fragments that are reported to mediate the SASP via the cyclic GMP-AMP synthase (cGAS) pathway (Gluck et al., 2017). cGAS is an intracellular PRR that senses double stranded DNA and drives 2'3'cyclic GMP-AMP (cGAMP) synthesis, which in turn activates stimulator of interferon genes (STING). STING upregulates Type I interferon (IFN) expression, which is reported to induce the expression of non-canonical inflammasome components including *Casp11* (Rathinam et al., 2012) and contribute to the development of oncogene-induced senescence (Katlinskaya et al., 2016). In addition, cytosolic DNA has been reported to activate caspase-5 in keratinocytes (Zwicker et al., 2017). siRNA-mediated *cGAS* knockdown in senescent IMR90s (Figure 6.12A) led to a reduction in *CASP5* expression (Figure 6.12B), and an impaired SASP (Figure 6.12C,D). Together, this data suggests that cytosolic dsDNA might mediate *CASP5* upregulation through the cGAS/STING pathway.

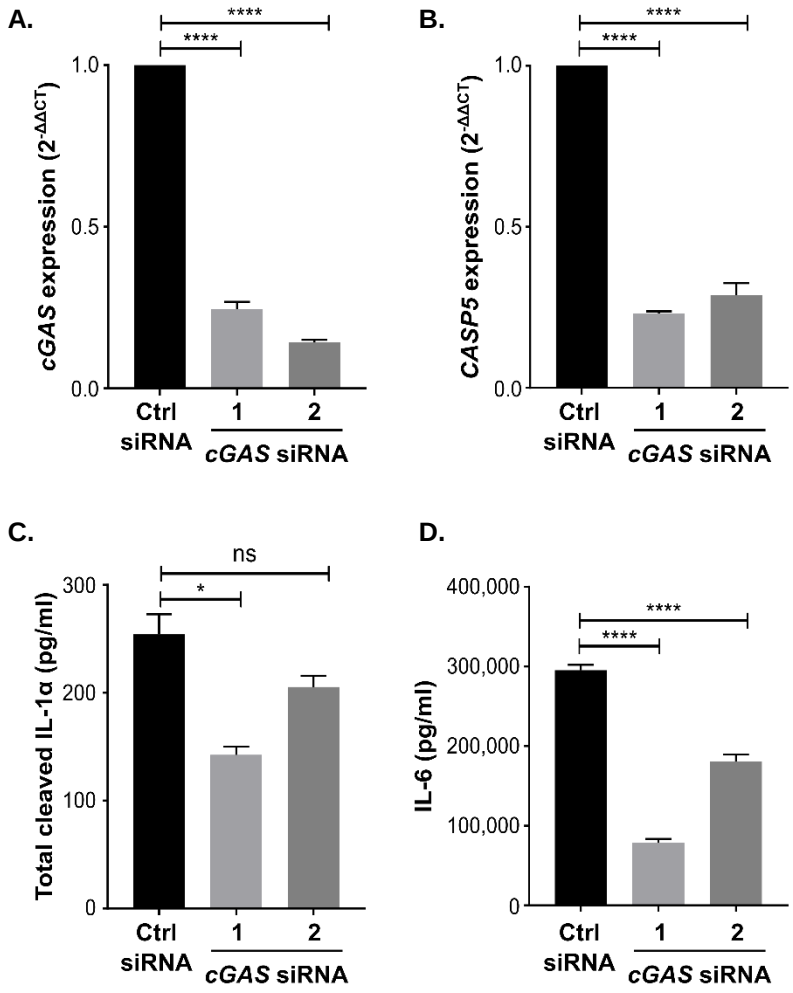

Figure 6.12: *cGAS* knockdown impairs the SASP. (A-B) qPCR data showing level of *cGAS* (**A**) or *CASP5* (**B**) expression in senescent IMR90s treated with control (Ctrl) or *cGAS*-targeted siRNA. **(C-D)** ELISA data showing the level of IL-1α (**C**) and IL-6 (**D**) in the conditioned media of senescent IMR90 cells treated with control or *cGAS*-targeted siRNA. Data represent mean +SEM of n=3 p = *≤0.05, ****≤0.0001.

6.2.8 Caspase-5 controls the IL-1α-driven SASP in IMR90 cells

The upregulation of *CASP5* in senescent cells, coupled with its ability to cleave and activate IL-1α (Chapter 5), led us to hypothesise that caspase-5 regulates the SASP. *CASP5* knockdown (Figure 6.13A) resulted in significantly less cell surface IL-1α expression (Figure 6.13B), reduced secretion of total and non-calpain cleaved IL-1α (Figure 6.13C,D) and a subsequent reduction in IL-6 (Figure 6.13E). Together, this data shows that caspase-5 modulates the IL-1α driven SASP in senescent IMR90 cells.

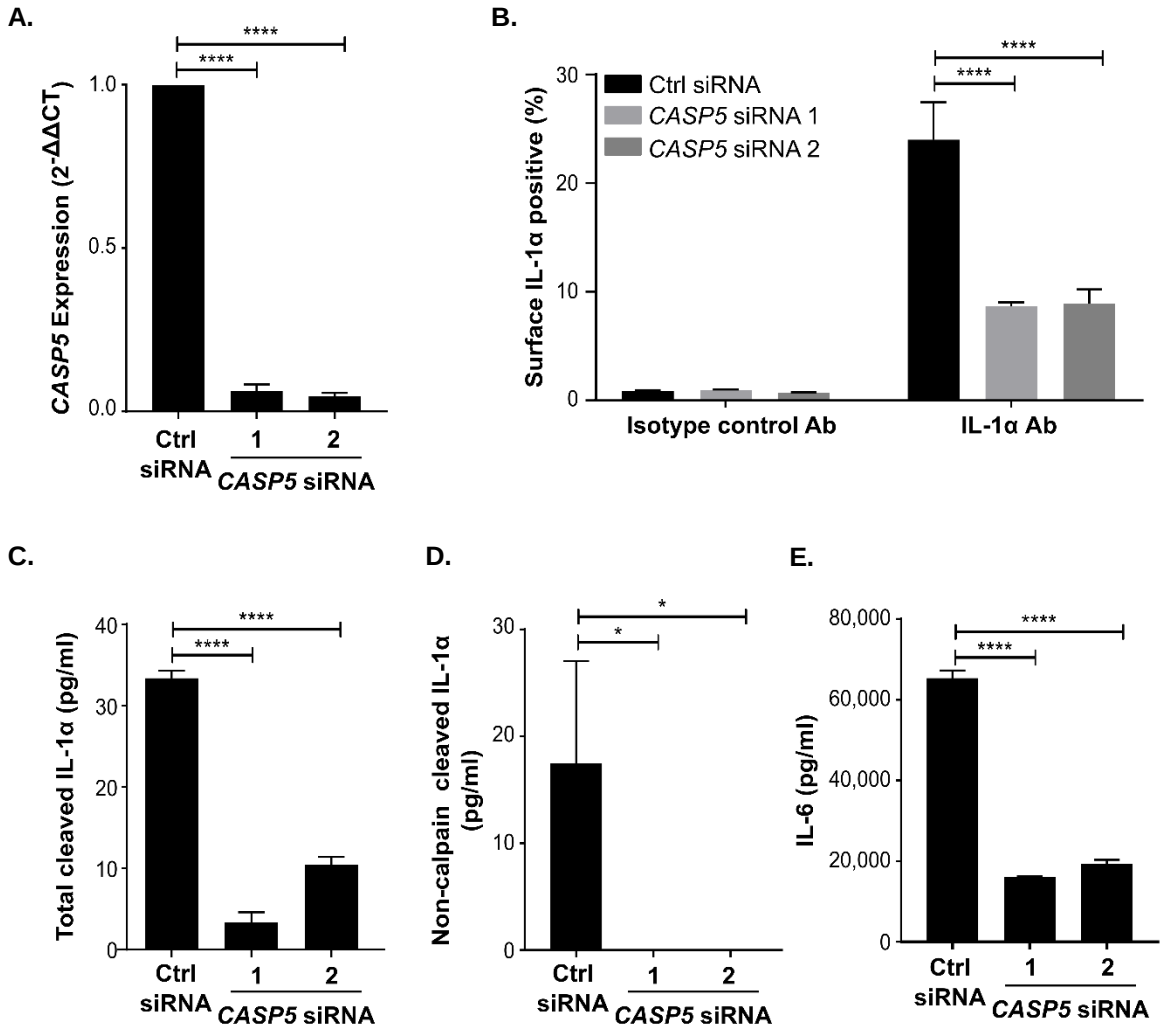

Figure 6.13: Caspase-5 regulates the IL-1α driven SASP. (A) qPCR data showing relative *CASP5* expression in senescent IMR90 cells after transfection of control (Ctrl) or *CASP5*-targeted siRNAs. **(B-D)** Cell surface IL-1α by flow cytometry (**B**), or levels of cleaved IL-1α (**C**), non-calpain-cleaved IL-1α (**D**) and IL-6 (**E**) in the conditioned media by ELISA, in senescent IMR90 cells after transfection of control or *CASP5*-targeted siRNAs. Data represent mean +SEM of n=3, p = *≤0.05, ****≤0.0001.

Although caspase-4 does not directly activate IL-1α (Figure 5.2), it shares a number overlapping functions with caspase-5. For example, both caspases are activated by binding to intracellular LPS and share the common substrate GSDMD (Kayagaki et al., 2013, Shi et al., 2014, Kayagaki et al., 2015, Shi et al., 2015). siRNA mediated *CASP4* knockdown had variable effects on *CASP5* expression (Figure 6.14B), suggesting that caspase-4 activation is not involved in senescent IMR90 cell priming and *CASP5* upregulation. However, *CASP4* knockdown led to a reduction in IL-1α and subsequent IL-6 release (Figure 6.14C,D), although this effect was much less potent than *CASP5* knockdown, thereby supporting a more direct role for caspase-5 in IL-1α activation. Therefore, caspase-4 may lie upstream of caspase-5 in the SASP pathway.

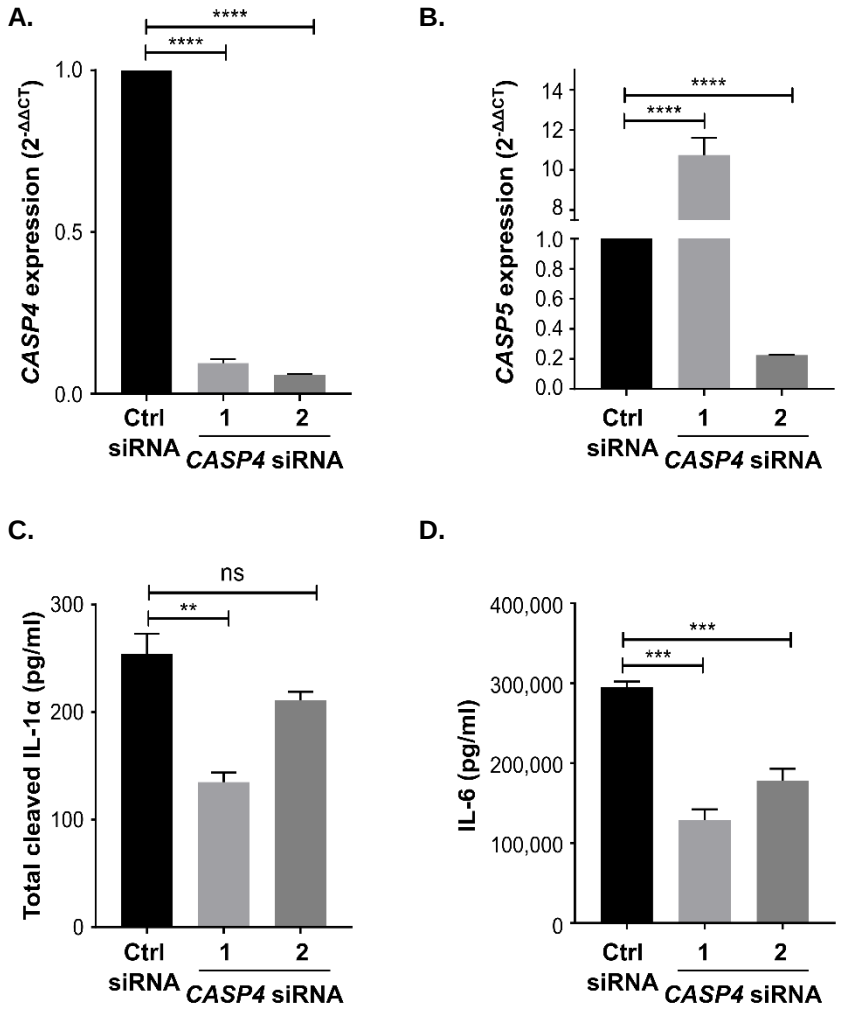

Figure 6.14: *CASP4* knockdown impairs the SASP. (A-B) qPCR data showing level of *CASP4* (A) or *CASP5* (B) expression in senescent IMR90s treated with control (Ctrl) or *CASP4*-targeted siRNA. (C-D) ELISA data showing the level of IL-1α (C) and IL-6 (D) in the conditioned media of senescent IMR90 cells treated with control or *CASP4*-targeted siRNA. Data represent mean +SEM of n=3 p = **≤0.01, ***≤0.001, ****≤0.0001.

6.2.9 Caspase-11 may regulate the DNA damage-induced SASP in primary murine fibroblasts

Demonstrating that caspase-5 modulates the IL-1α-driven SASP in human fibroblasts prompted the question of whether caspase-11 drives murine SASPs. Inducing senescence in murine cells *in vitro* is challenging due to the constitutive expression of active telomerase (Calado and Dumitriu, 2013). Although many studies use murine embryonic fibroblasts (MEFs) in models of senescence (Dirac and Bernards, 2003, Di Micco et al., 2008, Odell et al., 2010), it seems illogical to use embryonic cells to mimic what is often considered as an ageing phenotype. Thus, we treated adult ear-derived fibroblasts from WT and *Casp11*$^{-/-}$ mice with bleomycin for three hours to induce DNA damage (Orjalo et al., 2009), and cultured the cells for 7-14 days. Morphological differences between the two genotypes were apparent both 7 (Figure 6.15) and 14 (Figure 6.16) days after bleomycin treatment, with the *Casp11*$^{-/-}$ cells retaining a more spindle-like fibroblast shape whilst the WT fibroblasts developed a larger, rounder, and flatter morphology that is typical of senescent cells.

In addition to the morphological analysis, fibroblasts were stained for SAβGAL. After 14 days of bleomycin treatment, there were significantly fewer SAβGAL-positive cells in the *Casp11*$^{-/-}$ fibroblasts compared with WT (Figure 6.17). Treatment with an IL-1α neutralising antibody reduced SAβGAL staining in WT cells to the same level as *Casp11*$^{-/-}$ fibroblasts, which were unaffected by the antibody treatment, suggesting that caspase-11-mediated IL-1α activation promotes senescence.

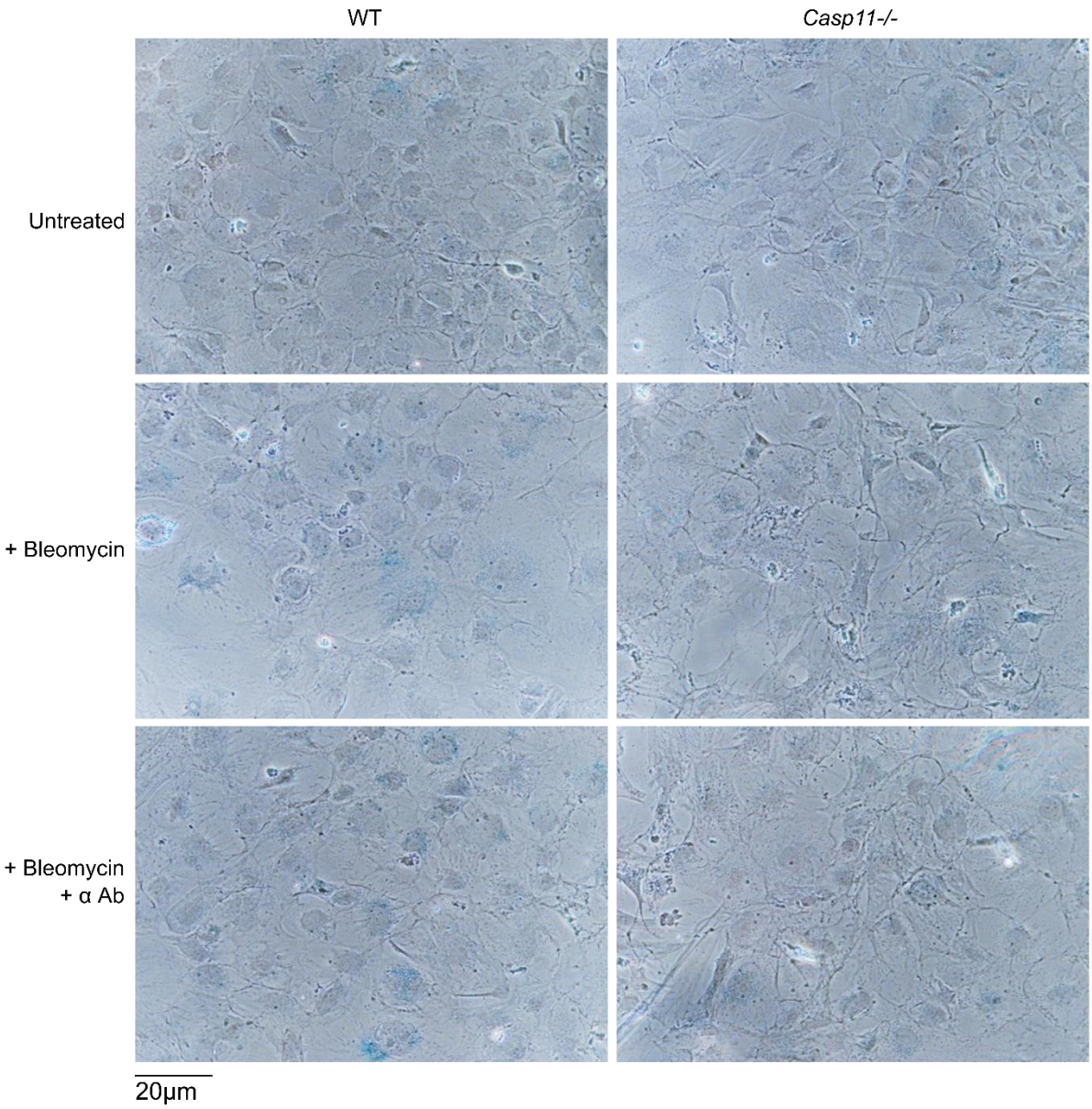

Figure 6.15: *Casp11*$^{-/-}$ fibroblasts are morphologically different to WT fibroblasts 7 days after bleomycin treatment. Example images of WT or *Casp11*$^{-/-}$ adult ear murine fibroblasts fixed and stained for SAβGAL (blue) 7 days after bleomycin treatment. Representative images of n=3.

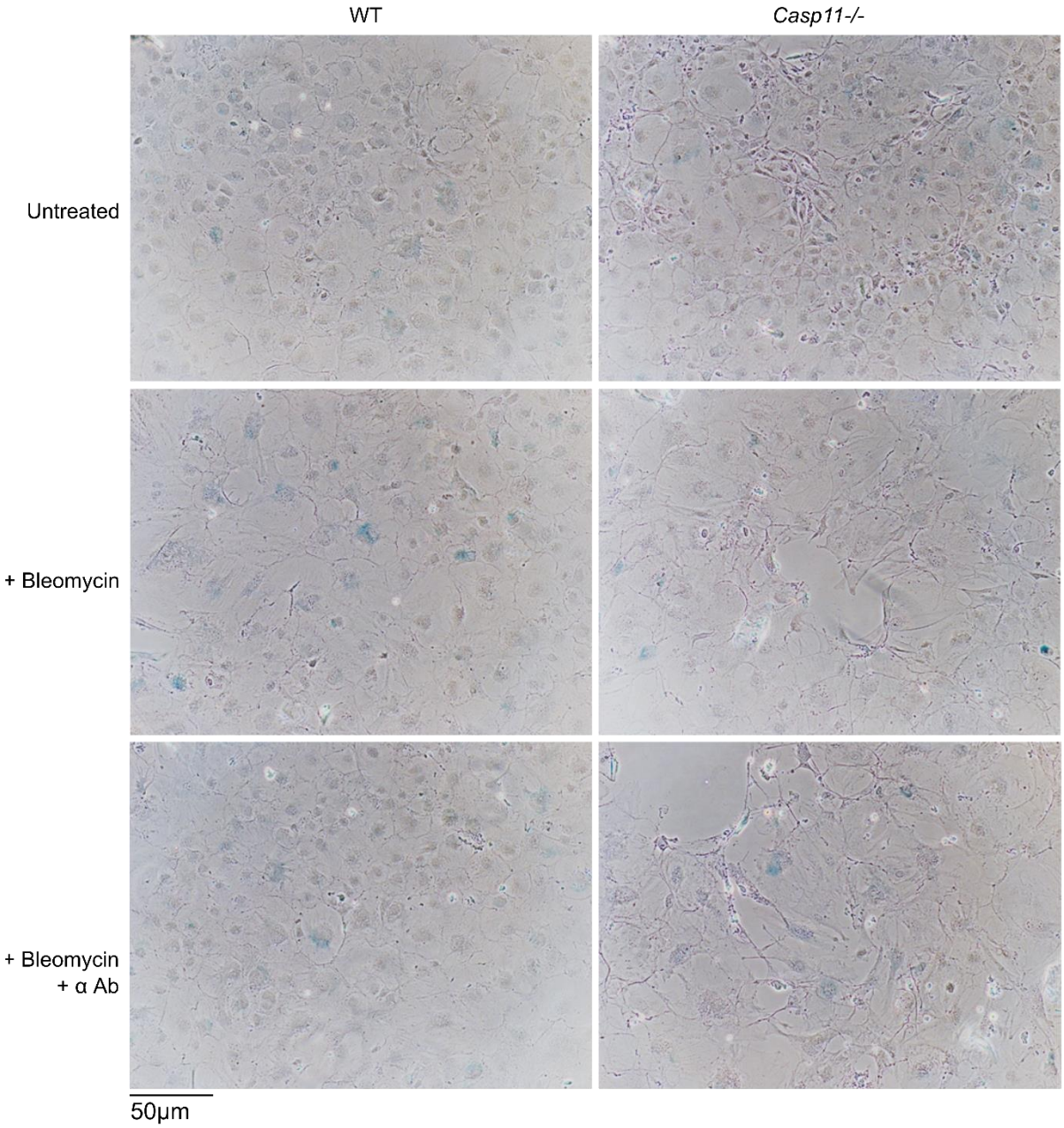

Figure 6.16: *Casp11*$^{-/-}$ fibroblasts are morphologically different to WT fibroblasts 14 days after bleomycin treatment. Example images of WT or *Casp11*$^{-/-}$ adult ear murine fibroblasts fixed and stained for SAβGAL (blue) 14 days after bleomycin treatment. Representative images of n=3.

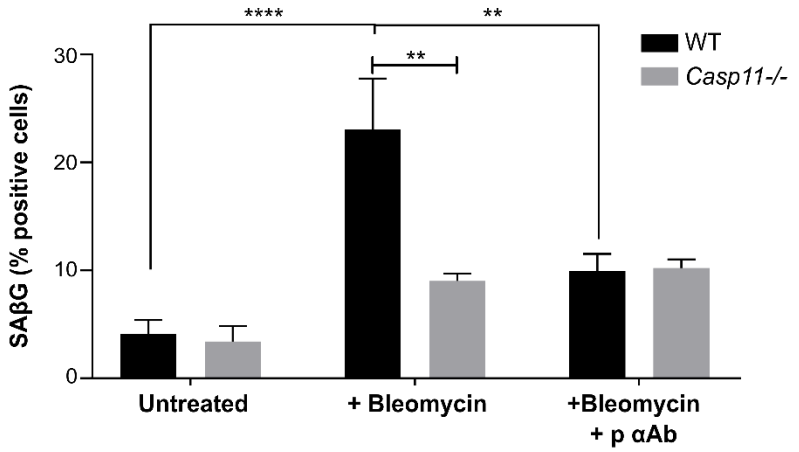

Figure 6.17: Bleomycin-treated *Casp11*$^{-/-}$ fibroblasts express significantly less SAβGAL than WT. Percentage of SaβGAL- positive fibroblasts cultured for 14 days ± bleomycin treatment ± IL-1α neutralising antibody (p αAb). Data represent mean +SEM of n=3, p = **≤0.01, ****≤0.0001.

Although the *Casp11*$^{-/-}$ fibroblasts appeared to have a senescence defect with regard to SAβGAL expression, their IL-6 secretion was extremely variable (Figure 6.18). Unexpectedly, the WT fibroblasts released negligible levels of IL-6, and the untreated *Casp11*$^{-/-}$ fibroblasts secreted more IL-6 than the bleomycin-treated cells. As such, it is not possible to conclude from the *in vitro* fibroblast data whether caspase-11 modulates the murine SASP. Since this acute DNA-damage-induced senescence is a different model to that used for the rest of our studies, which represent oncogene-induced senescence, these experiments were discontinued due to time constraints. However, future work could include using a stronger DNA-damaging stimulus such as γ-irradiation or a longer bleomycin treatment.

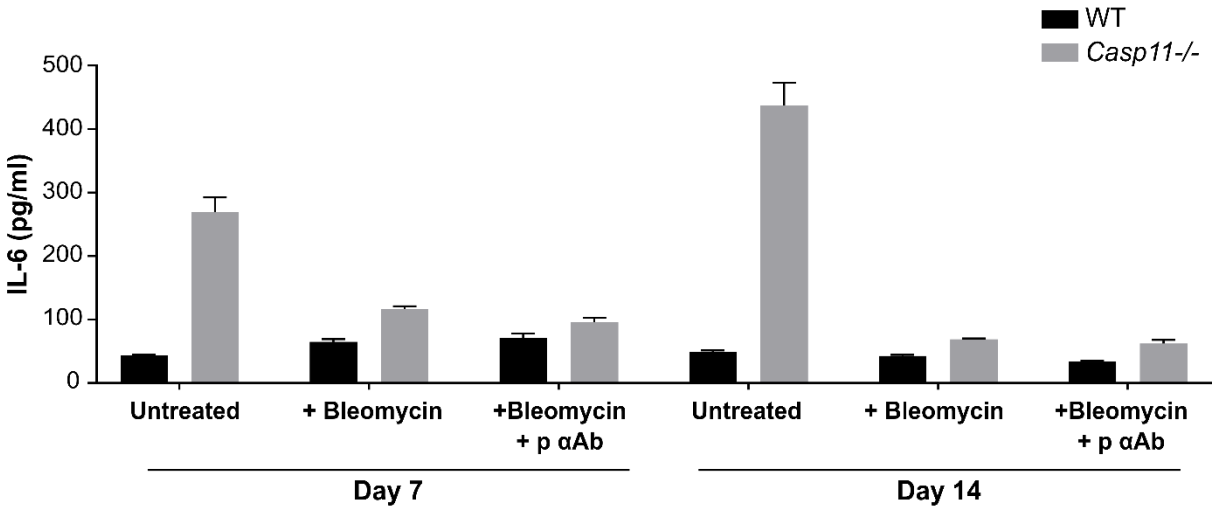

Figure 6.18: The WT fibroblasts did not produce a SASP. ELISA data showing the level of IL-6 in the conditioned media of WT or *Casp11*$^{-/-}$ fibrobasts ± bleomycin treatment ± IL-1α neutralising antibody (p αAb). Data represent mean +SEM of n=3.

6.2.10 Caspase-11 controls the murine SASP in vivo

To interrogate the role of caspase-11 in regulating the murine SASP during oncogene-induced senescence, we used the hydrodynamic tail-vein injection model developed by Lars Zender's group (Kang et al., 2011) (Figure 6.19). This model uses two vectors, one encoding *NRAS* and another encoding a transposase, which are diluted in a volume equal to 10% of the mouse's body weight and injected into the lateral tail vein. The high pressure created by the large delivery volume causes the vectors to accumulate in the liver, where 5-10% of the hepatocytes take up both constructs and stably express *NRAS*. This leads to oncogene-induced hepatocyte senescence, with the accompanying SASP driving recruitment of immune cells that subsequently mediate the killing and clearance of NRAS-positive senescent cells from the liver. Thus interventions that inhibit the SASP prevent senescent cell clearance (Kang et al., 2011, Hoare et al., 2016).

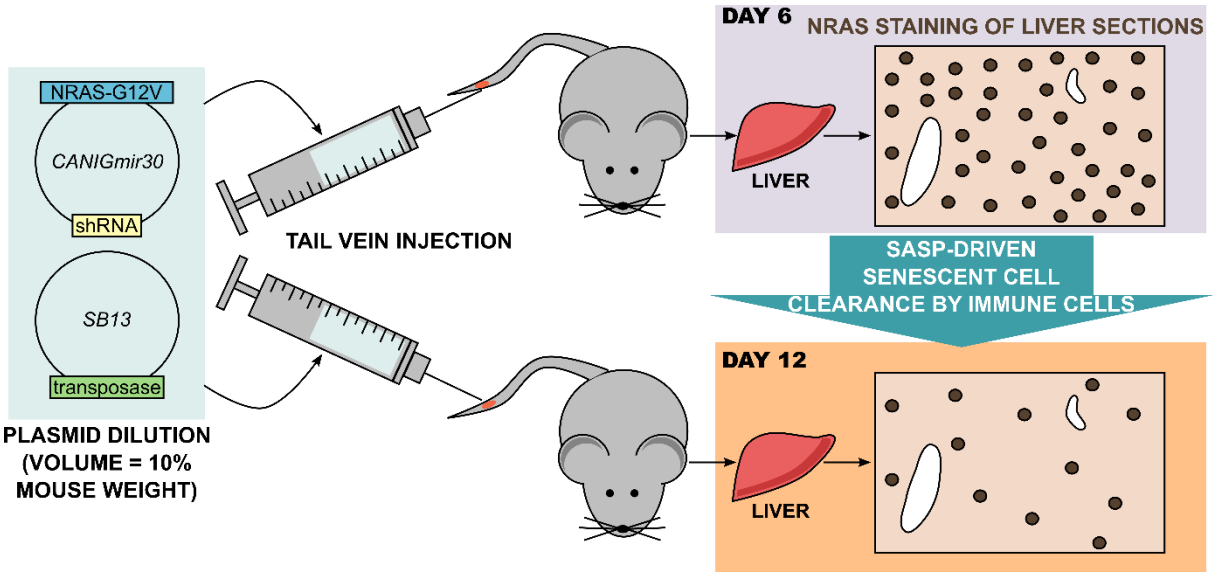

Figure 6.19: Schematic illustrating the hydrodynamic tail vein injection model. *NRAS*/shRNA plasmid and transposase plasmids are mixed and diluted into a volume equivalent to 10% of each mouse's body weight. Over time immune cells, recruited by the SASP, clear the senescent NRAS-positive cells.

To determine whether caspase-11 drives the SASP in senescent hepatocytes, we cloned a shRNA targeting *Casp11* into the bicistronic *NRAS*-expressing vector. We chose to carry out shRNA-mediated knockdown instead of using *Casp11*$^{-/-}$ mice to ensure that caspase-11 levels were only affected in the senescent hepatocytes. Therefore, any phenotype could confidently be attributed to the SASP-producing cells, rather than a defective response due to caspase-11 deficiency in the immune cells, which also express caspase-11. To ensure maximal knockdown, five shRNAs designed using a set of rules defined by Johannes Zuber's group (Fellmann et al., 2013) were tested *in vitro* (Figure 6.20A). The best knockdown was achieved using shRNA 731, which reduced *Casp11* expression by approximately 60% (Figure 6.20B). Importantly the *Casp11*-targeted shRNAs did not affect *Casp1* expression (Figure 6.20C), ensuring that canonical inflammasome signalling remained intact. Both shRNA731 and shRNA1124 were also re-tested following priming with a lower dose of LPS, which resulted in similar levels of knockdown to the cells primed with 1µg/ml LPS (Figure 6.21).

A.

shRNA	mRNA target site	Guide
140	AAAGCAATGTACTGAAATTAAA	TTTAATTTCAGTACATTGCTTT
710	CTCCAGATGTGCTACAGTATGA	TCATACTGTAGCACATCTGGAG
731	ATACCATCTATCAGATATTCAA	TTGAATATCTGATAGATGGTAT
1124	ATCGGGCAACCTTGACGAGATA	TATCTCGTCAAGGTTGCCCGAT
1160	CTGGCAACTGAGAACAAAGCAA	TTGCTTTGTTCTCAGTTGCCAG

B. **C.**

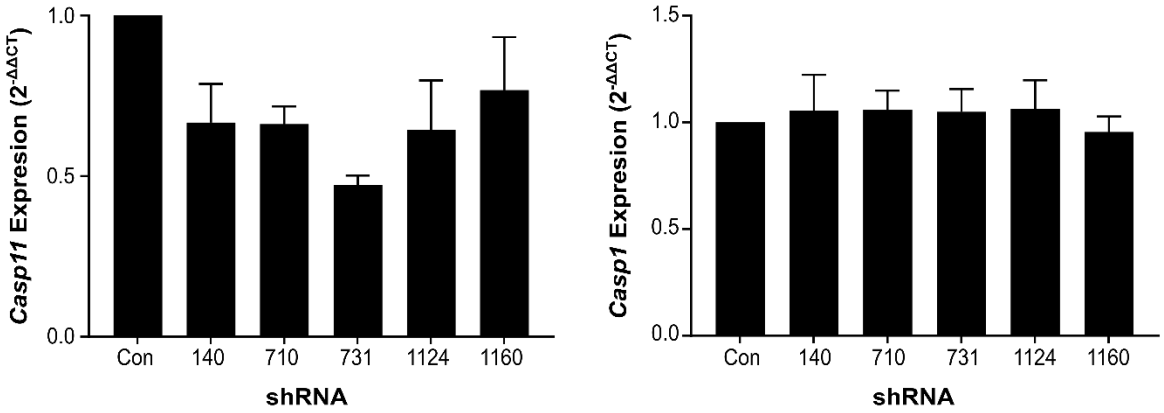

Figure 6.20: shRNA 731 elicited the strongest *Casp11* knockdown. (A) Table showing the target and guide sequences of each *Casp11* targeted shRNA. **(B-C)** qPCR data showing *Casp11* (**B**) and *Casp1* (**C**) expression in each J2 line following LPS-priming. Data represent mean +SEM of n=2.

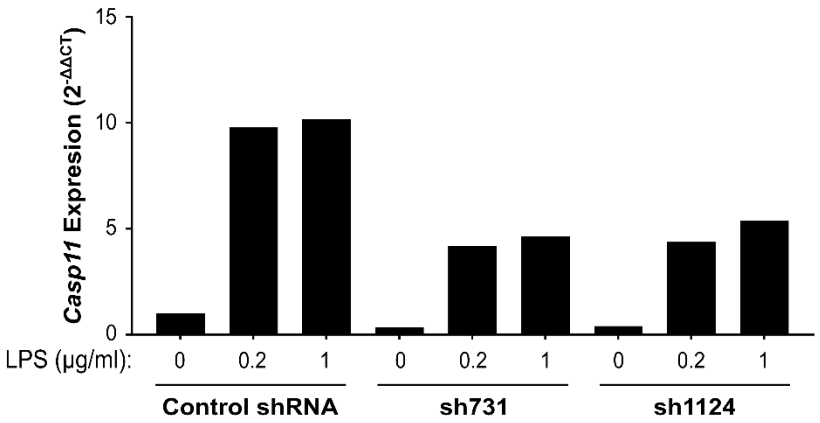

Figure 6.21: Levels of *Casp11* knockdown are unaffected by the priming dose of LPS. qPCR data showing the level of *Casp11* expression in J2 cells expressing control shRNA or *Casp11*-targeted (sh731, sh1124) shRNA ± priming with a range of LPS concentrations.

The *in vivo* study included two cohorts of mice with tissue collection at three time points (Figure 6.22). The level of *Casp11* knockdown was assessed by qPCR and immunofluorescence (IF). The qPCR data revealed significantly lower *Casp11* expression in the livers of mice treated with *Casp11*-targeted shRNA compared with control shRNA three days after injection (Figure 6.23A). Although this reduction of approximately 25% appears minimal, it is important to consider that this analysis represents *Casp11* expression in every cell within the liver, not just the targeted hepatocytes. This difference was absent at day six (Figure 6.23B), probably due to the infiltration of *Casp11*-expressing immune cells. IF staining for caspase-11 protein expression six days after injection confirmed that caspase-11 expression was upregulated in the RAS-positive cells (Figure 6.23C). Furthermore, the RAS-positive hepatocytes from the mice treated with the *Casp11*-targeted shRNA expressed lower, or negligible, levels of caspase-11 compared with the hepatocytes containing the control shRNA (Figure 6.23 D,E), confirming that knockdown was successful *in vivo*.

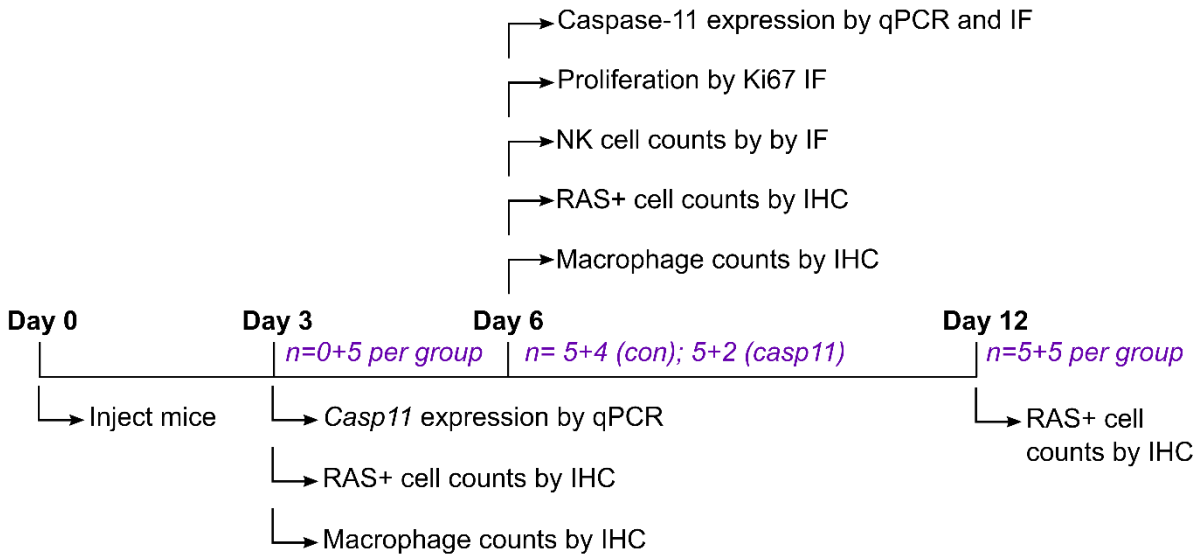

Figure 6.22: The hydrodynamic tail vein injection model timeline. Schematic showing each time point of the *in vivo* study including n numbers (cohort 1 + cohort 2) and analyses performed.

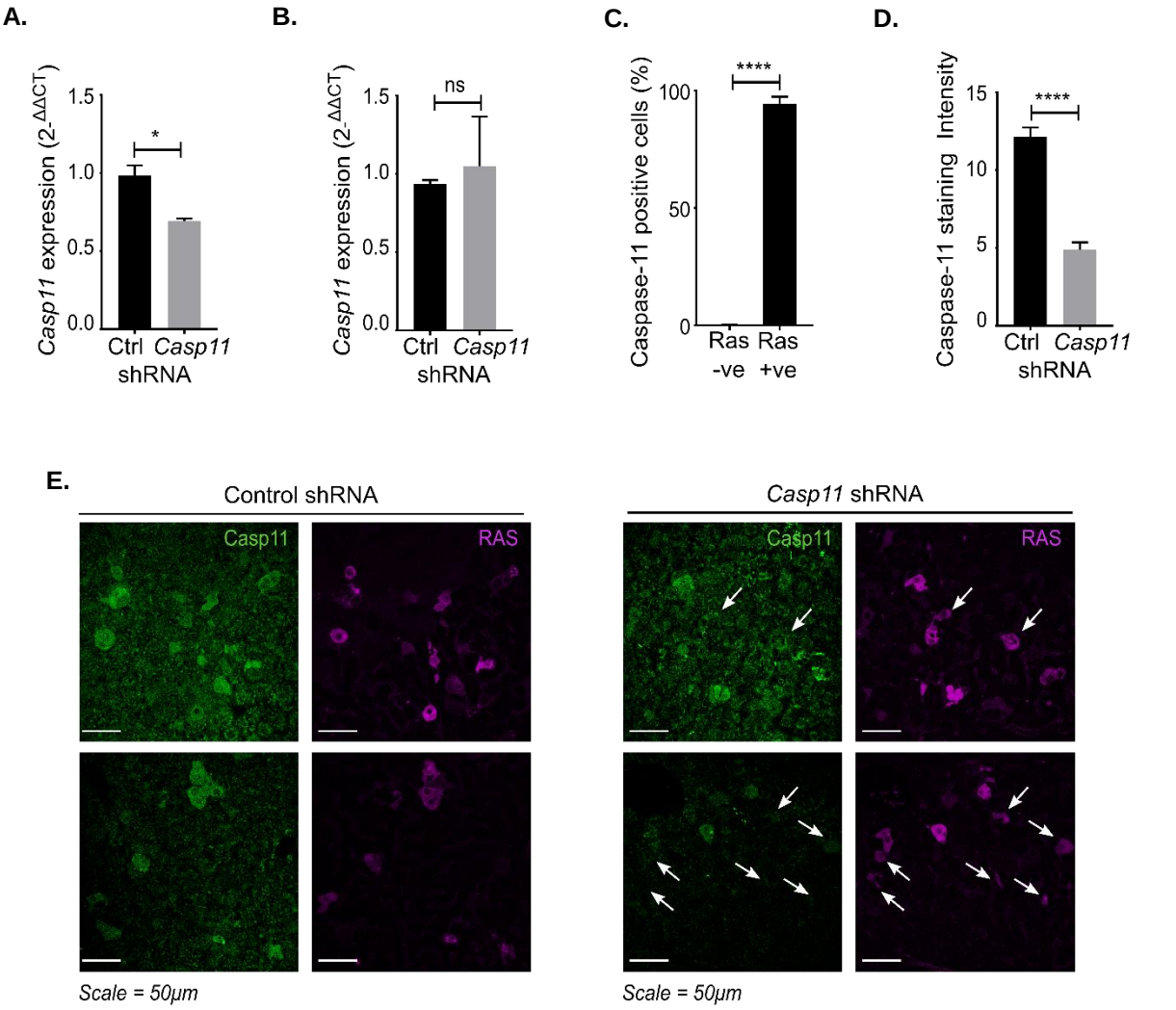

Figure 6.23: *Casp11* was successfully knocked down *in vivo*. (A-B) qPCR data showing relative *Casp11* expression in livers from mice injected with control (Ctrl) or *Casp11*-targeted shRNAs at day 3 (**A**) and day 6 (**B**). **(C-D)** Quantification of immunofluorescence (IF) data measuring correlation of caspase-11 and NRAS staining (**C**) and the intensity of caspase-11 staining in NRAS-positive cells (**D**) in the livers of mice at day 6. **(E)** Example day 6 IF images showing caspase-11 and NRAS staining in the livers of mice injected with control or *Casp11*-targeted shRNA, white arrows indicate NRAS+Casp11- cells. Data represent mean +SEM of n=5, or n=3 (Ctrl) / 2 (*Casp11* shRNA) (**B**) p = *≤0.05, ****≤0.0001.

The percentage of NRAS-positive hepatocytes was quantified by immunohistochemistry (IHC). There was no difference in NRAS cells between the control and *Casp11*-targeted shRNA livers three days after injection (Figure 6.24), thereby establishing an equivalent baseline for vector transduction and senescence induction. Six days after injection, significantly more NRAS-positive cells remained in the livers of the mice treated with the *Casp11*-targeted shRNA compared with control (Figure 6.25), and linear regression analysis revealed a negative correlation between the number of NRAS-positive cells remaining and the level of caspase-11 (Figure 6.26). The *Casp11* shRNA-treated livers continued to retain more NRAS-positive cells than control at twelve days after injection (Figure 6.27). Together, this data shows that *Casp11* knockdown leads to impaired immune-mediated clearance of senescent hepatocytes, therefore indicating that caspase-11 regulates the murine SASP *in vivo*.

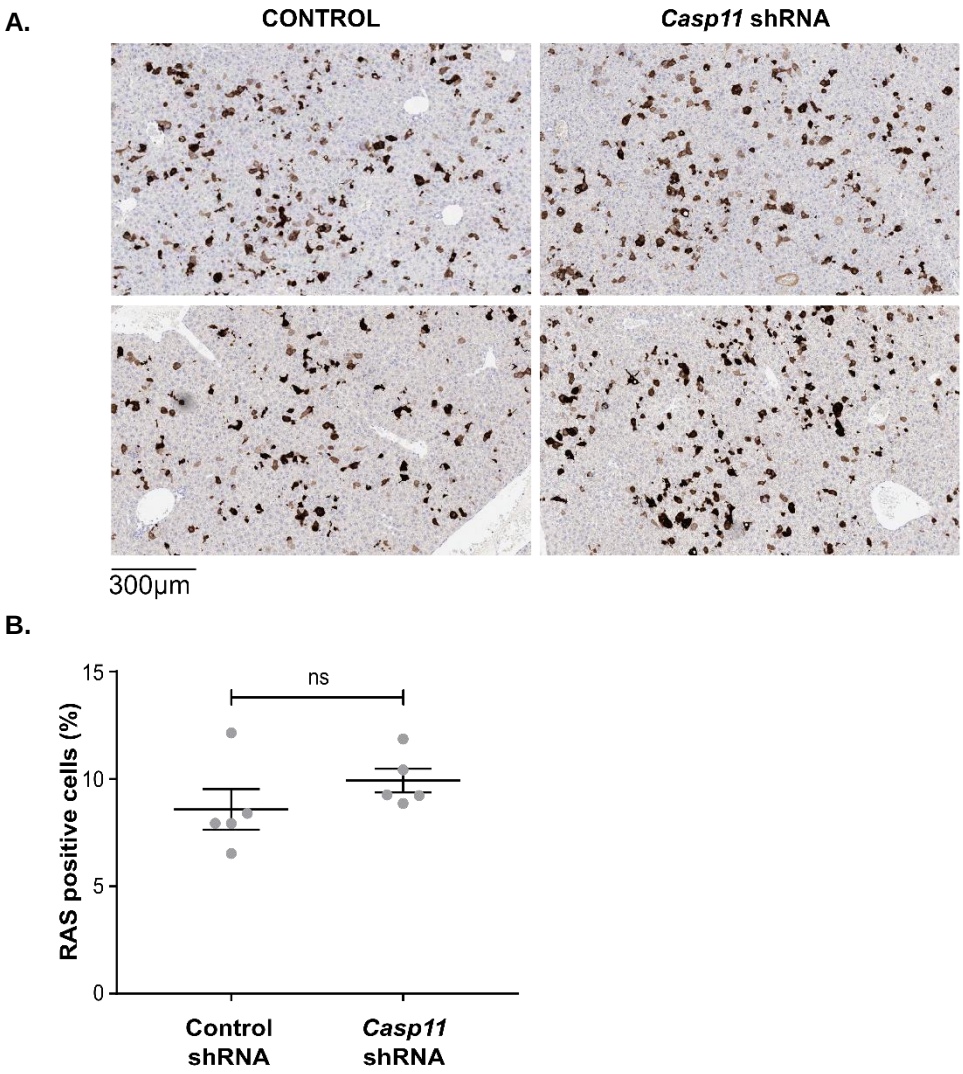

Figure 6.24: There is no difference in NRAS-positive cell number between control and *Casp11*-targeted shRNA livers at 3 days post injection. (A) Example IHC images showing NRAS staining (brown). **(B)** Quantification of NRAS staining in whole liver sections. Data represent mean ± SEM of n=5.

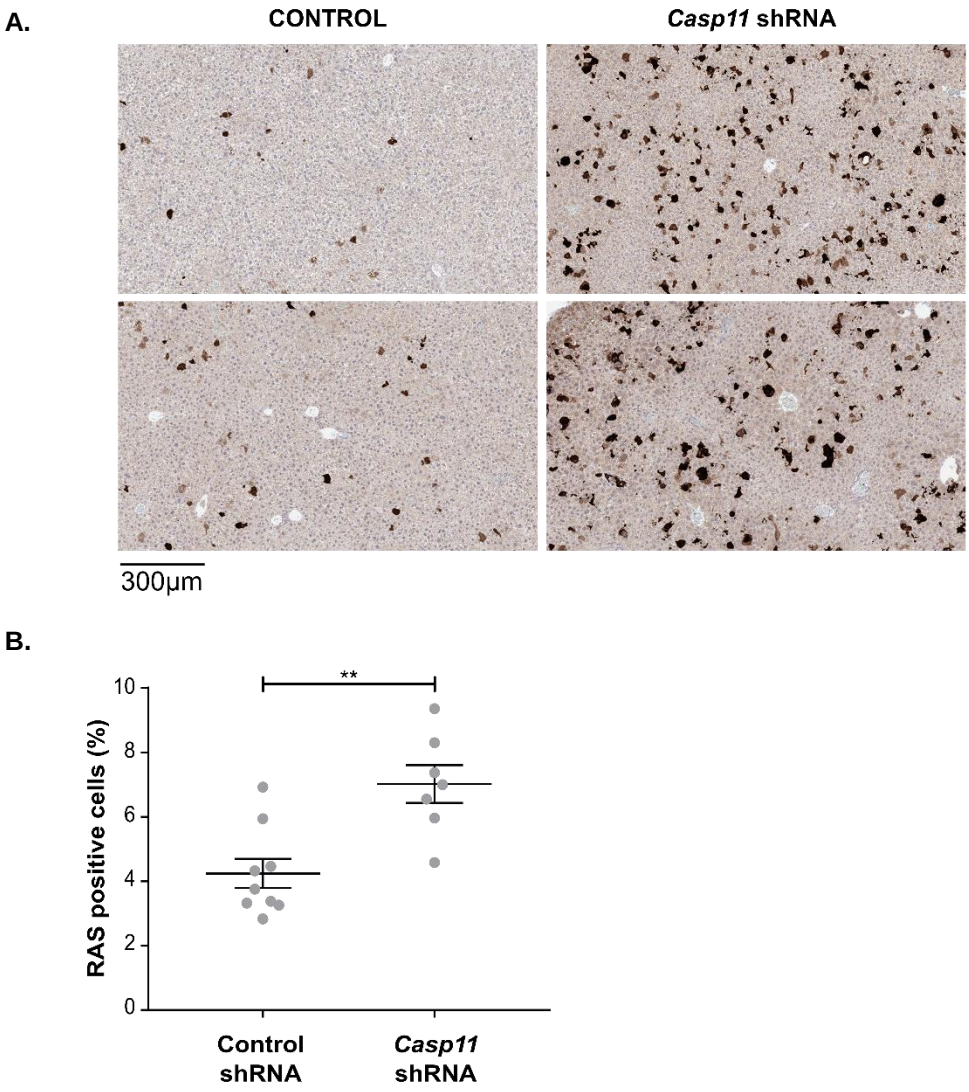

Figure 6.25: *Casp11* knockdown reduces senescent cell clearance at 6 days post injection. (A) Example IHC images showing NRAS staining (brown). **(B)** Quantification of NRAS staining in whole liver sections. Data represent mean ± SEM of n=9 (control)/=7(*CASP11*shRNA), p = **≤0.01.

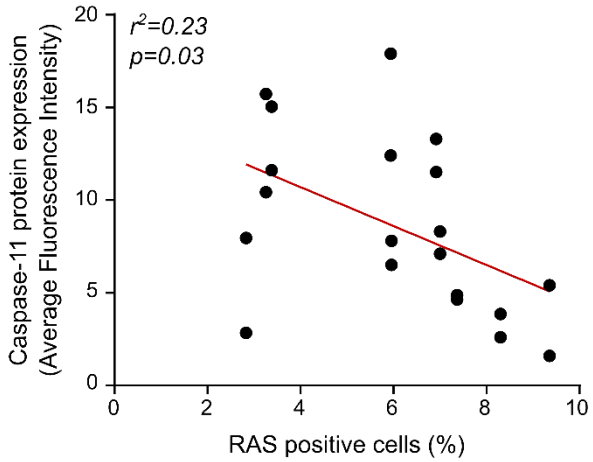

Figure 6.26: Caspase-11 expression negatively correlates to number of NRAS-positive cells. A graph showing the relationship between the percentage of RAS positive cells and the intensity of caspase-11 staining per cell in livers at day 6 post-injection.

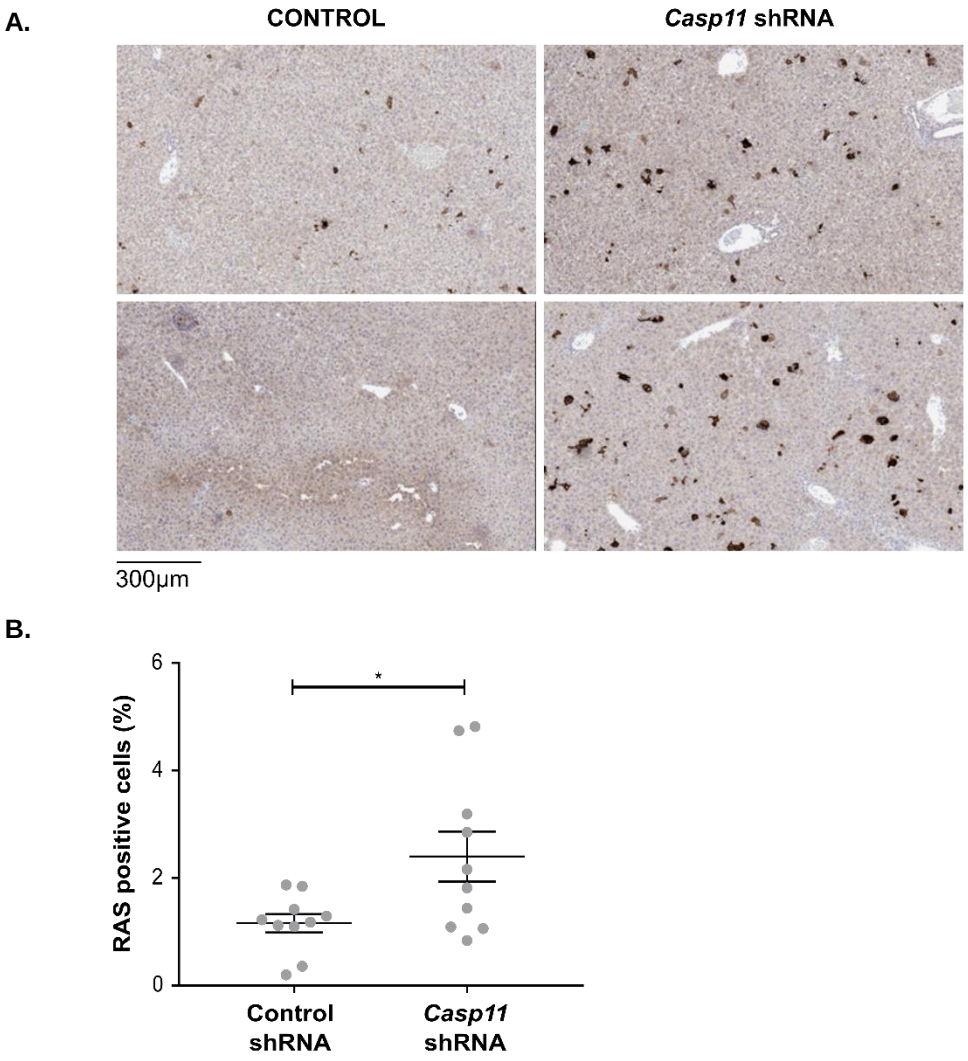

Figure 6.27: *Casp11* knockdown reduces senescent cell clearance at 12 days post injection. (A) Example IHC images showing NRAS staining (brown). **(B)** Quantification of NRAS staining in whole liver sections. Data represent mean ± SEM of n=10, p = *≤0.05.

It remains unclear whether the SASP is required, per se, for senescence to occur, or if it simply reinforces the phenotype. As such, there are two possible explanations for the delay in senescent hepatocyte clearance following *Casp11* knockdown: 1) delayed onset or bypass of senescence, or 2) delayed immune cell recruitment and senescent cell clearance. To investigate this, levels of proliferation and immune cell infiltration were evaluated. At day 6, the control and *Casp11*-targeted livers contained equal numbers of proliferating RAS-positive cells, as evidenced by Ki67 staining (Figure 6.28). This suggests that the increased number of RAS-positive cells after *Casp11* knockdown was not caused by increased proliferation due to the delayed onset or bypass of senescence.

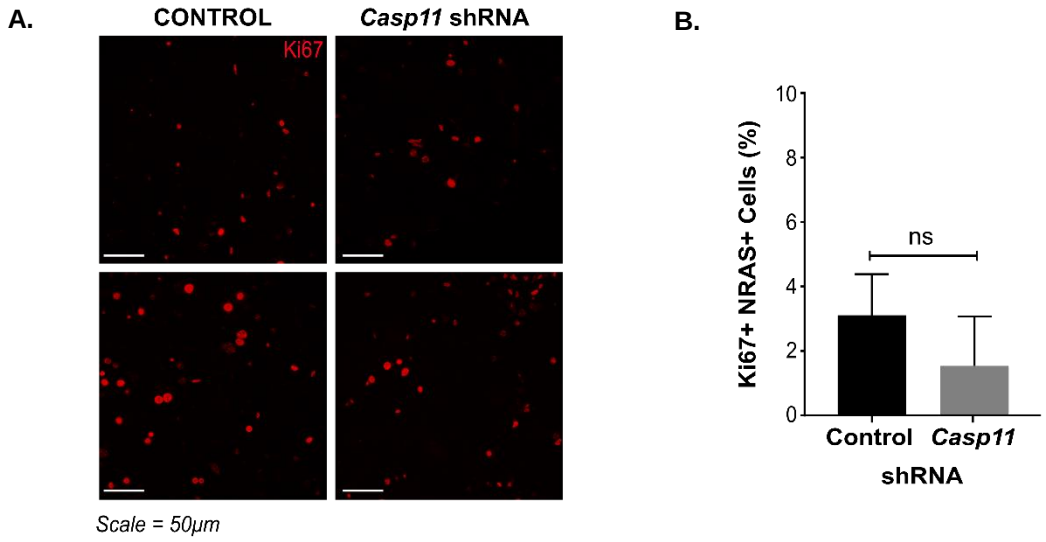

Figure 6.28: *Casp11* knockdown has no effect on proliferation at day 6 post-injection. **(A)** Example IF images showing Ki67 staining (red). **(B)** Quantification of Ki67 staining. Data represent mean ± SEM of n=5.

Both macrophages and NK cells have been implicated in the immunosurveillance of senescent cells (Vicente et al., 2016). IHC staining for F4/80 revealed there were fewer macrophages infiltrating the *Casp11*-targeted shRNA livers compared with the control shRNA livers at day 3 (Figure 6.29), however this difference was absent at day 6. In addition, IF staining for CD355 suggested slightly fewer NK cells were present in the *Casp11*-targeted shRNA livers (Figure 6.30). However, due to the lack of a properly validated anti-CD355 antibody and the high background fluorescence, it is difficult to draw conclusions from this staining. Together these data suggest that the reduced senescent hepatocyte clearance in the livers from mice treated with a *Casp11*-targeted shRNA is likely due to impaired early immune cell recruitment because of a reduced SASP.

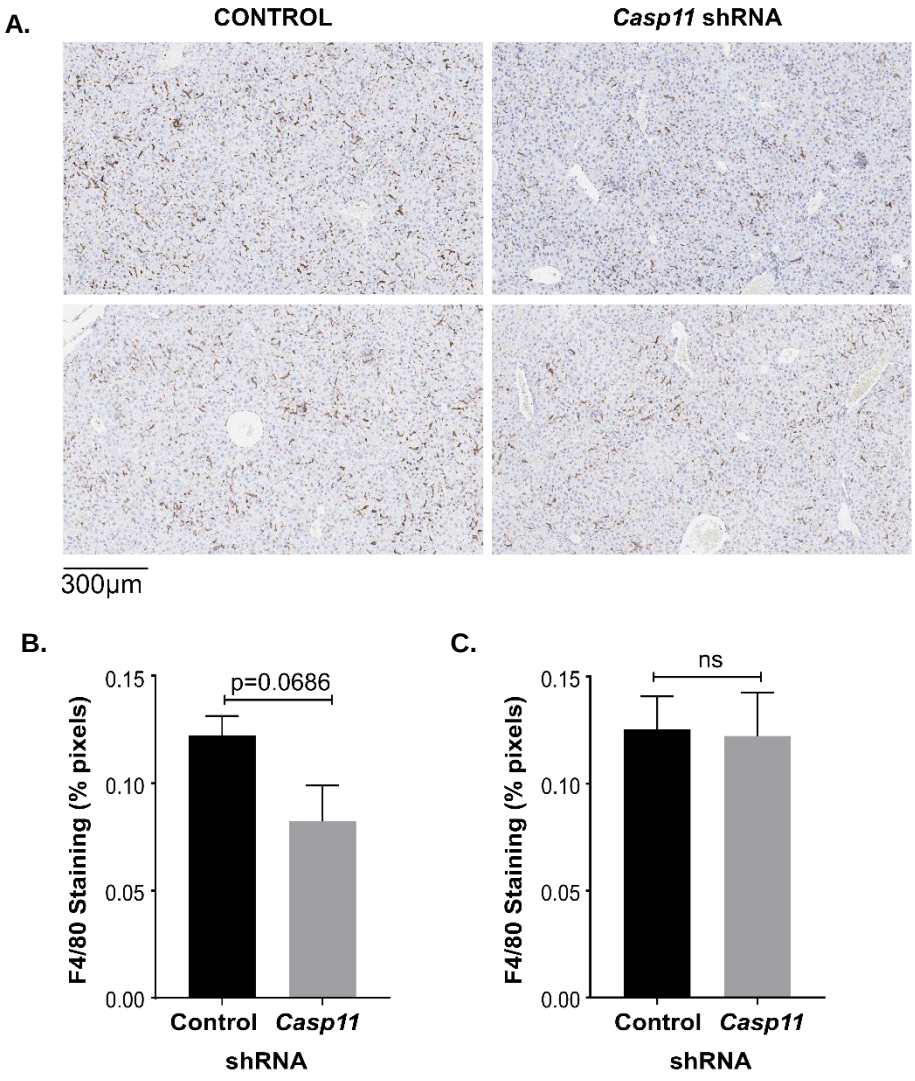

Figure 6.29: *Casp11* knockdown impairs early macrophage recruitment. **(A)** Example IHC images showing F4/80 staining (brown). **(B)** Quantification of F4/80 staining. Data represent mean ± SEM of n=5.

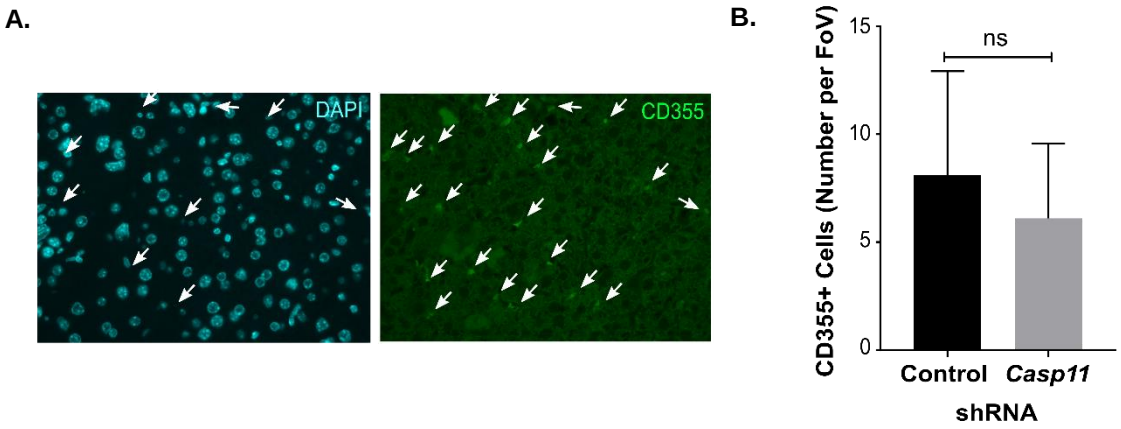

Figure 6.30: *Casp11* knockdown has little effect on NK cell infiltration at day 6 post-injection. (A) Example IF images of a liver section showing DAPI staining (blue) and CD355 staining (green). White arrows represent cells considered CD355 positive (Green), and the matching nuclei (blue) **(B)** Quantification of CD355 staining. Data represent mean ± SEM of n=5.

6.3 Discussion

There is emerging evidence that the inflammatory caspases of the non-canonical inflammasome are activated during sterile inflammation (Zanoni et al., 2016, Pillon et al., 2016). An important but rarely cited example of sterile inflammation is the IL-1α-driven SASP - a cocktail of inflammatory mediators released by senescent cells. The NLRP3 inflammasome has been reported to drive the SASP during oncogene-induced senescence (Acosta et al., 2013), however we find that the caspase-1 inhibitor used in this study also blocks caspase-5 activity (Figure 6.2), and therefore we hypothesised that the non-canonical pathway may be involved.

The work presented in this chapter has dissected a novel pathway controlling the SASP (Figure 6.31). We show that *CASP5* expression is upregulated in senescent cells (Figure 6.10) via the cGAS pathway (Figure 6.12), possibly due to the presence of cytosolic DNA resulting from nuclear blebbing (Gluck et al., 2017). In addition, *CASP5* knockdown leads to reduced IL-1α secretion and surface expression by senescent IMR90 fibroblasts, and a significant impairment of the SASP (Figure 6.12). In line with previous reports (Orjalo et al., 2009, Gardner et al., 2015) the SASP was not dependent on IL-1β (Figure 6.7A), which implies that IL-1α can be cleaved and released by a distinct mechanism to that regulating IL-1β. Although pro-IL-1β was upregulated in senescent cells, very little was cleaved and virtually none was secreted. A potential explanation for this is that senescent cells exhibit high levels of autophagy, which is reported to both clear active inflammasome complexes and modulate IL-1β secretion (Shi et al., 2012, Dupont et al., 2011). Therefore, autophagy may simultaneously limit caspase-1 availability thereby preventing IL-1β activation, and export pro-IL-1β out of the cell, which is undetectable by our ELISA (*unpublished data*).

Importantly we confirmed our *in vitro* findings *in vivo*, where shRNA-mediated knockdown of *Casp11* in RAS-expressing hepatocytes delayed the clearance of senescent cells (Figures 6.25 and 6.26), which is driven by the SASP. Furthermore, we demonstrated that this delay was likely due to impaired early immune cell recruitment, as evidenced by decreased macrophage infiltration at the earliest time point (Figure 6.29). A limitation to this study was that although the shRNA-mediated *Casp11* knockdown was

specific to RAS-positive hepatocytes, it did not completely abolish caspase-11 expression. Perhaps a more striking phenotype would be observed if *Casp11* was knocked out using either a tissue-specific promoter, or a bone marrow transplant of WT immune cells into a *Casp11*$^{-/-}$ mouse to maintain a functional non-canonical inflammasome in immune cells.

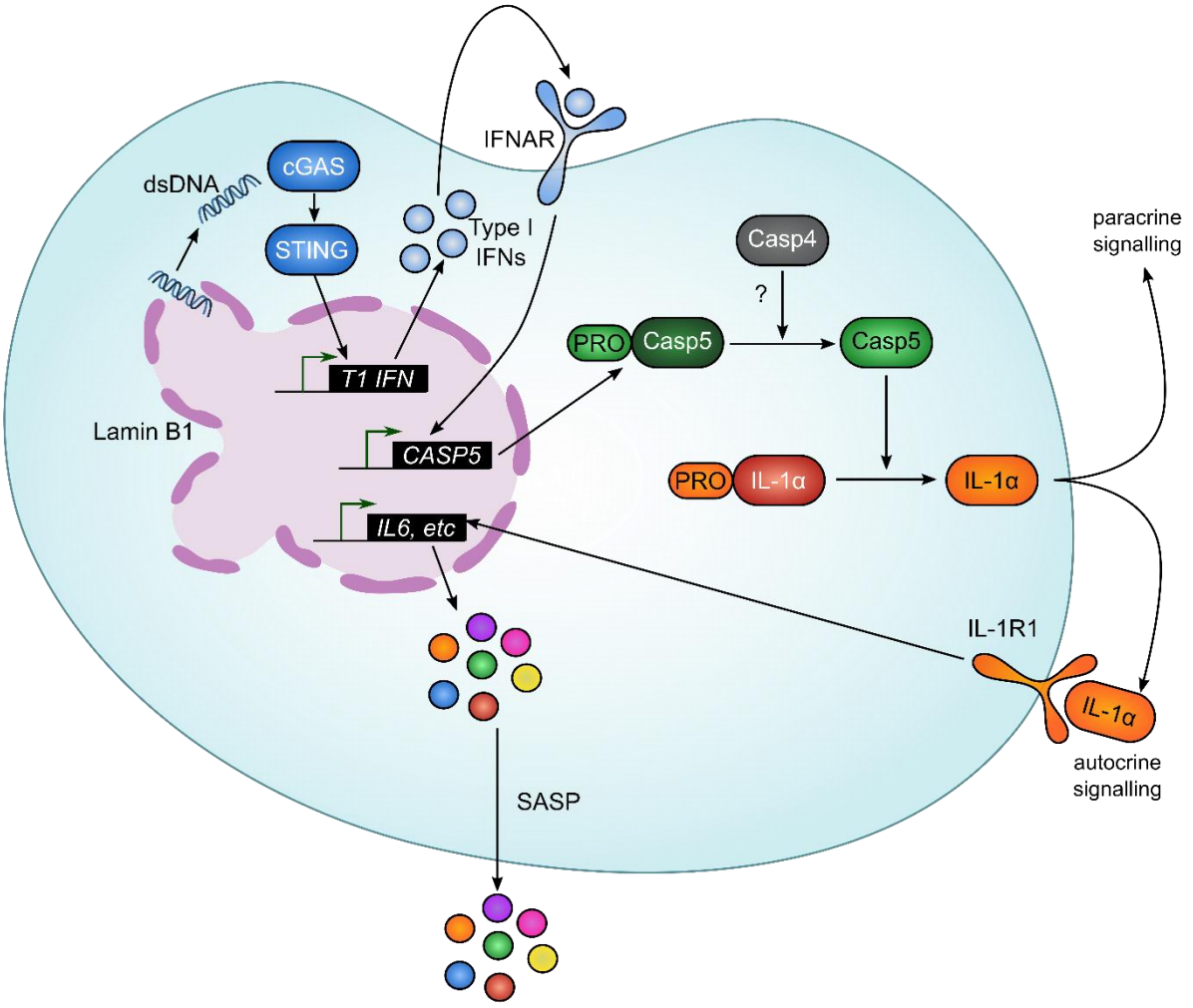

Figure 6.31: The caspase-5 mediated SASP pathway. A schematic showing the proposed pathway by which caspase-5 mediates the SASP. Lamin B loss in senescent cells leads to reduced nuclear membrane integrity, which allows dsDNA to escape to the cytosol. dsDNA activates cGAS which triggers Type I interferon (IFN) production via STING. Type 1 IFNs upregulate *CASP5* expression and pro-caspase-5 synthesis. Caspase-5 is activated, perhaps via caspase-4, and in turn activates IL-1α to drive the SASP.

Although the hydrodynamic tail vein injection model is a well characterised *in vivo* system for studying the SASP, the hepatocytes express high levels of RAS that are arguably not physiologically relevant. Therefore, it would be interesting to examine the role of caspase-11 in models of disease that involve senescent cells. For example, within a tumour, the SASP is largely considered beneficial because it

drives the clearance of senescent cells, thereby preventing the transmission of damaged DNA to the next generation. However, the SASP also establishes an inflammatory microenvironment and is reported to promote the proliferation and invasion of surrounding cells (Coppé et al., 2010). Therefore it would be interesting to examine whether caspase-11 inhibition reduces tumour invasiveness, or results in the accumulation of senescent cells that eventually bypass senescence and worsen disease.

In addition, it would be important to confirm that caspase-5/-11 regulates the SASP in other types of senescence, such as replicative or DNA damage-induced. If so, targeting caspase-5 could represent a widely applicable therapeutic strategy that leaves the alternative caspase-1 and -4 immune-response pathways intact. For instance, the VSMC SASP significantly increases atherosclerotic plaque vulnerability (Wang et al., 2015). Since atherosclerosis is a disease that is normally detected at an advanced stage after the patient has already suffered a cardiovascular event, treatment with a specific caspase-5 inhibitor could prevent destabilisation of remaining plaques and reduce the likelihood of a second major adverse event. In addition, radiotherapy and many chemotherapies work by inducing DNA damage and therefore triggering tumour cell senescence. However, these non-selective therapies also induce senescence in the underlying stroma, and the IL-6 from senescent fibroblasts acts as a reprogramming factor that drives pluripotency and proliferation of cancer stem cells that have survived treatment (Iliopoulos et al., 2009, Liu et al., 2011, Mosteiro et al., 2016). Therefore, administering a caspase-5 inhibitor with these treatments could prevent cancer stem cell reprogramming and reduce the risk of tumour recurrence.

Finally, although senescence represents an important stress response, there is evidence showing that these pathways may be beneficial in early life. As such, cellular senescence and the SASP are often cited as an example of antagonistic pleiotropy: a phenotype that is an advantageous anti-tumour mechanism in youth, but detrimental later on by promoting age-related pathologies (Wright and Shay, 1995, Rodier and Campisi, 2011). Senescent SAβGAL- and p21- positive cells are found at distinct locations and time points in the developing mouse embryo including the interdigital regions, tip of the tail, and closing neural tube, and p21-deficient mice exhibit defective limb patterning (Munoz-Espin et al., 2013, Storer

et al., 2013). Although senescent embryonic cells share a number of overlapping features with oncogene-induced senescent cells, they do not secrete IL-6 and IL-8 (Storer et al., 2013). It would therefore be interesting to determine if caspase-5/-11 also regulates the developmental SASP, for example by staining *Casp11*$^{-/-}$ embryos for SAβGAL and p21 and identifying any morphological abnormalities.

In conclusion, the work presented in this chapter has identified caspase-5 as the protease that activates IL-1α in senescent cells to drive the SASP. Therefore, the caspase-5-mediated IL-1α activation may represent an important biological pathway in both homeostasis and disease, and directly targeting caspase-5 may limit the deleterious effects of accumulated senescent cells in age-related pathologies.

7. Results: The rs17561 SNP reduces LPS-induced IL-1α release

7.1 Introduction

A single nucleotide polymorphism (SNP) is the variation of one nucleic acid within a DNA sequence that is common within the population. SNPs originate from unique past mutations and therefore often indicate a common evolutionary ancestry of individuals carrying the same polymorphism. Studying human SNPs is important because the genetic variation that they create may underlie susceptibility to disease and responsiveness to therapies (Stoneking, 2001). Although most human SNPs occur in non-coding DNA, where they might influence transcription or alter RNA half-life, the largest functional effects result from polymorphisms that lie within the coding region. Some coding polymorphisms lead to amino acid changes, and are referred to as non-synonymous (nsSNPs). nsSNPS are very rare, comprising only 1% of all known SNPs, due to the evolutionary selection against amino acid substitutions (Shen et al., 2006).

Rs17561 is the only nsSNP in the *IL1A* gene, for which 30% of the population is heterozygous (Figure 7.1). This SNP is a guanine to thymine mutation at +4845 in the *IL1A* gene, which results in a change from an alanine (A) to a serine (S) at amino acid 114 in the protease-targeted region of IL-1α. Rs17561 is associated with increased C-reactive protein (CRP) levels in coronary angiography patients (Berger et al., 2002), as well as the risk of a number of inflammatory diseases (Table 7.1). With regard to cardiovascular disease in particular, rs17561 has been associated with increased body mass index in obese healthy women (Um et al., 2011), and increased risk of coronary artery disease following angiography as part of a composite genotype with two IL-1β SNPS, rs1143634 and rs16944, when oxidised phospholipid and lipoprotein(a) levels are also raised (Tsimikas et al., 2014). Furthermore, rs17561 is in strong linkage disequilibrium with a second IL-1α SNP in the promoter region of the gene, rs1800587, which has been associated with stroke, coronary artery disease and obesity (Zou et al., 2015, Haroon et al., 2015, Carter et al., 2008).

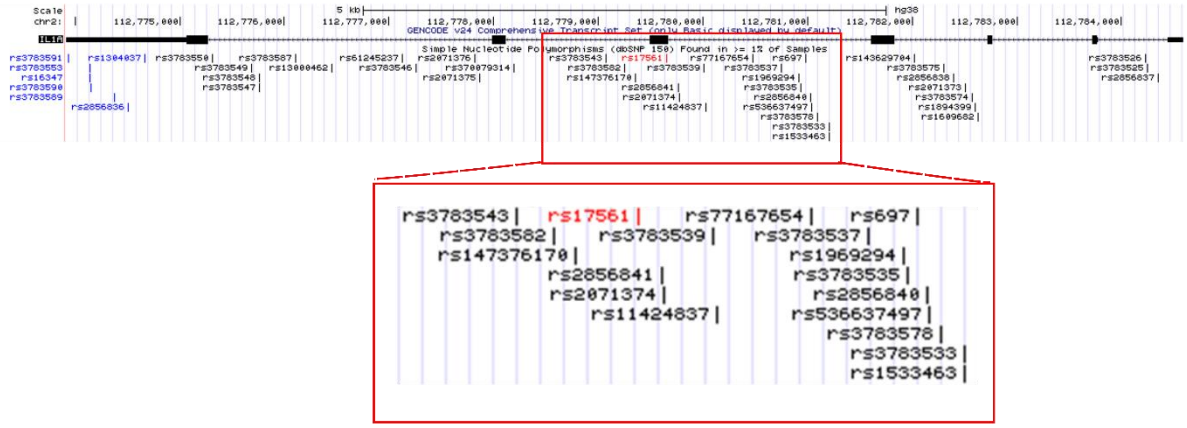

Figure 7.1: *IL1A* SNP map. A schematic illustrating all *IL1A* SNPs found in >1% of the population. Black SNPS are intron variants, blue SNPS are located in the untranslated region, and red SNPS are coding non-synonymous mutations. The region surrounding rs17561 is shown in the extended red box. [*Map generated using the UCSC genome browser.]*

Whilst the association of rs17561 with disease is indicative of a change in IL-1α function, there has been little effort to investigate this further. Kawaguchi and colleagues examined the functional consequence of rs17561 in the context of systemic sclerosis (SSc), where they reported an increase in calpain processing of pro-IL-1α in minor allele homozygotes. This observation was based on a western blot showing IL-1α, isolated from fibroblasts derived from genotyped individuals, that had been incubated with increasing calpain concentrations (Kawaguchi et al., 2007). The observation of calpain cleavage in these lysates is somewhat surprising as fibroblasts have the decoy receptor IL-1R2 that would prevent calpain processing, although the polymorphism could affect this interaction.

DISEASE/CONDITION	*EFFECT OF rs17561 MINOR ALLELE*	*REFERENCE*
Chronic Rhinosinusitis	Increased risk of disease	*(Endam et al., 2010)*
Obesity	Increased body mass in healthy women	*(Um et al., 2011)*
Breast Cancer	Increased risk of disease	*(Sigurdson et al., 2007)*
Ankylosing Spondylitis	Increased risk of disease	*(Sims et al., 2008)*
Juvenile Dermatomyositis	Increased risk of disease	*(Mamyrova et al., 2008)*
Acne Vulgaris	Increased risk of acne	*(Szabo et al., 2010)*
Radiation-Induced Toxicity	Increased risk of toxicity following treatment for non-small cell lung cancer	*(Hildebrandt et al., 2010)*
Multiple Sclerosis	Associated with earlier disease onset	*(Mirowska-Guzel et al., 2011)*
Ovarian Cancer	Decreased risk of clear cell, mucinous and endometrioid subtype	*(White et al., 2012)* *(Charbonneau et al., 2014)*
H1N1 Influenza A Virus	Increased risk of disease	*(Liu et al., 2013)*
Nasal polyposis	Protected against development of nasal polyposis in asthmatics	*(Karjalainen et al., 2003)*
Malaria	Predispose to disease but protective for severe symptoms	*(Walley et al., 2004)*
Peridontitis	Increased risk of disease	*(Yin et al., 2016)*
Coronary Artery Disease and Cardiovascular Disease	Associated with higher risk of disease as part of composite genotype following stratification according to oxidised phospholipid and lipoprotein(a) levels	*(Tsimikas et al., 2014)*
Systemic Sclerosis	Protective against disease	*(Kawaguchi et al., 2003)*

Table 7.1: Literature summary of the association of rs17561 with disease. A table listing whether the presence of the minor rs17561 allele increases or decreases risk of disease.

7.1.1 Chapter 7 project rationale

The rs17561 SNP causes an amino acid change from an alanine, which is hydrophobic, to a serine, which is polar uncharged. Because this mutation is located in the 'loop' region of pro-IL-1α that is targeted by proteases, as shown in chapters 1 and 2 of this thesis, it may affect cytokine activation. The work presented in this chapter aims to explore this hypothesis further, and investigate the effect of rs17561 on IL-1α activation.

7.2 Results

7.2.1 Making recombinant 'SS' pro-IL-1α

The rs17561 SNP causes an amino acid substitution in the protease-targeted region of IL-1α. To investigate the effect of the SNP on cytokine activation, human recombinant A114S pro-IL-1α was produced to mimic pro-IL-1α from minor allele homozygotes (SS). The mutation was introduced by site-directed mutagenesis, and the GST-tagged protein was purified over a glutathione column using the AKTA system (Figure 7.2A). The concentration of A114S pro-IL-1α (SS) was normalised to WT pro-IL-1α (AA) by coomassie staining (Figure 7.2B,C).

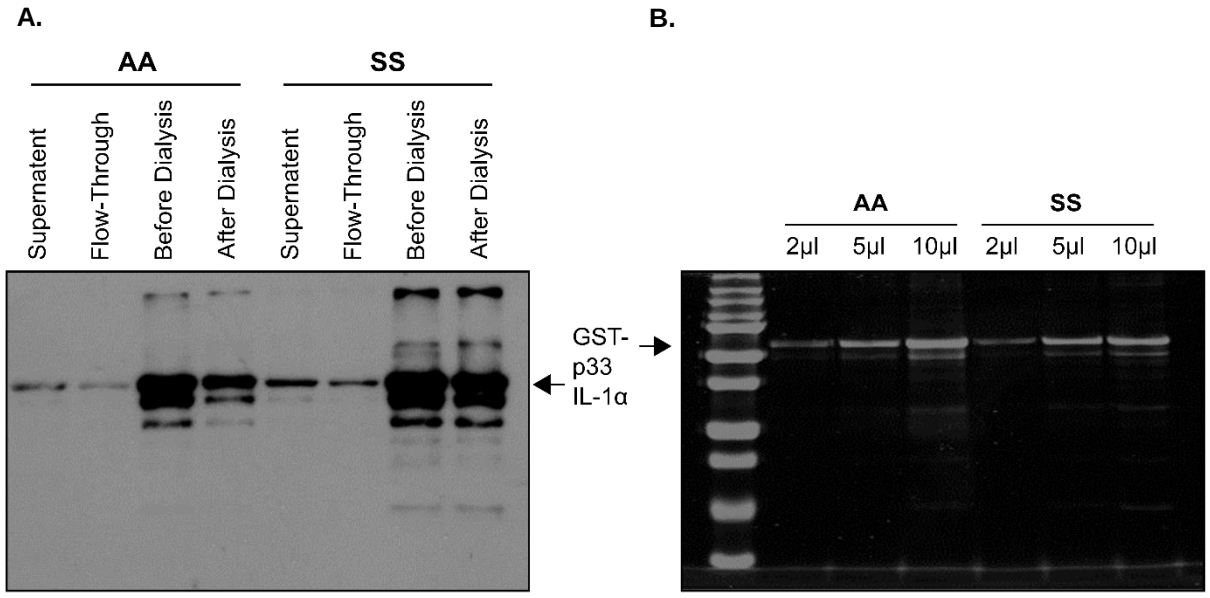

C.

Sample	Intensity (Counts)	Counts/µl	Average Counts/µl	AA / SS
2µl AA	6.30	3.15		
5µl AA	9.74	1.95	2.49	
10µl AA	23.63	2.36		1.47
2µl SS	3.66	1.83		
5µl SS	8.4	1.68	1.7	
10µl SS	16.13	1.61		

Figure 7.2: The production of recombinant human 'SS' pro-IL-1α. (A) Western blot for IL-1α after each stage of the purification process. **(B)** Normalisation of WT (AA) and SNP (SS) pro-IL-1α concentrations by coomassie. **(C)** Example calculation of AA:SS pro-IL-1α concentration ratio from coomassie staining intensity.

7.2.2 The rs17561 SNP affects IL-1α cleavage by some, but not all, proteases

Proteolytic cleavage assays using matched concentrations of AA and SS pro-IL-1α revealed that the rs17561 SNP affects the cleavage of IL-1α by a subset of proteases only. Most proteases cleaved AA and SS pro-IL-1α with similar efficiency, as shown by the examples in Figure 7.3. However, chymase, MMP2 and proteinase 3, cleaved SS pro-IL-1α with a lower efficiency than AA pro-IL-1α, although this difference was not statistically significant (Figure 7.4). One explanation is that the SNP only affects cleavage if the protease target site is close to amino acid 114. However, calpain and MMP-2 both cleaved pro-IL-1α to produce a 17kDa product (Chapter 4, Figures 4.1 and 4.12), suggesting that they target a similar location. Alternatively, chymase, MMP-2 and proteinase 3 could require the alanine for substrate docking, and the introduction of a serine may prevent stable interaction.

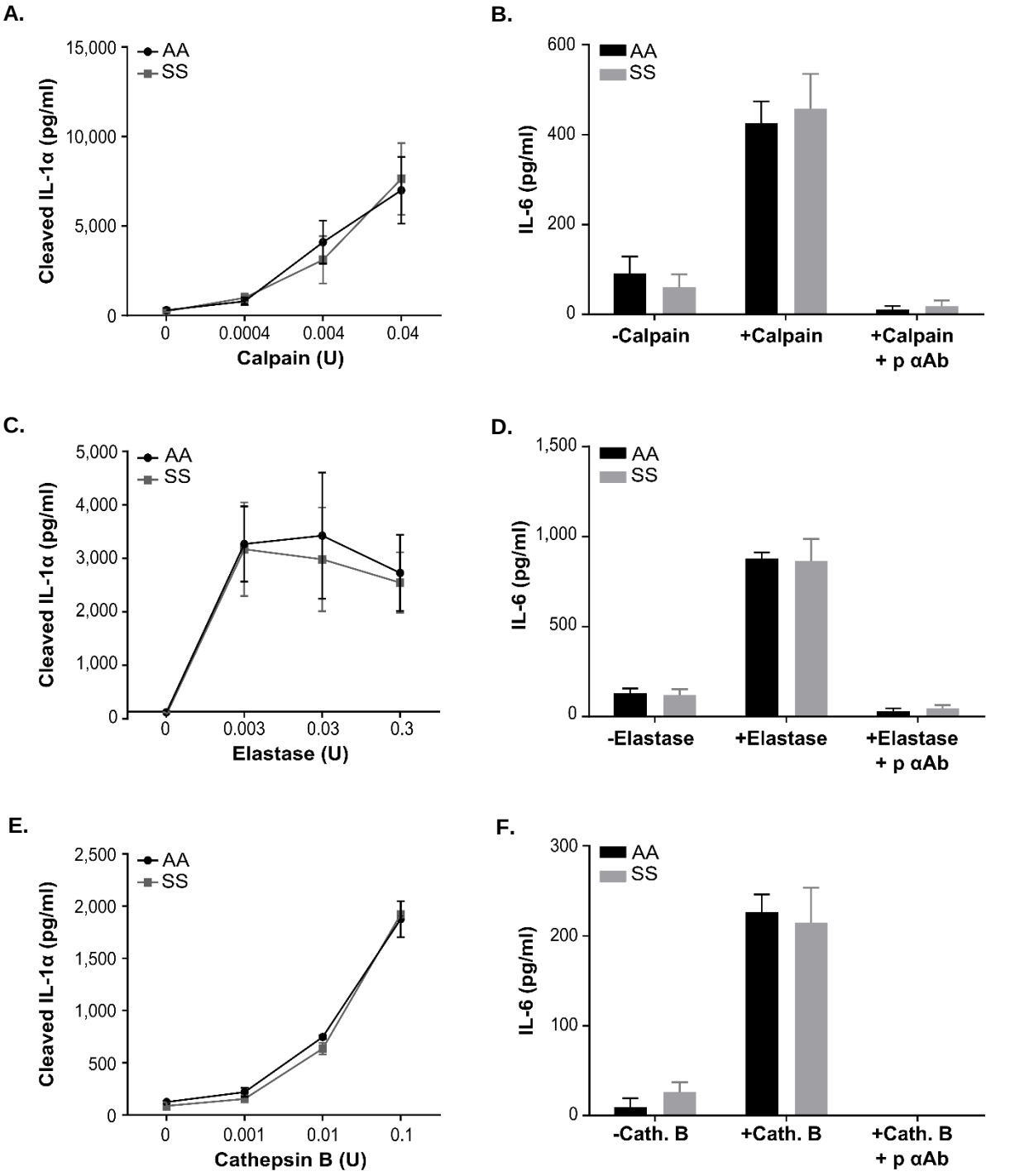

Figure 7.3: The rs17561 SNP does not affect recombinant pro-IL-1α cleavage by calpain, elastase or cathepsin B. **(A-F)** The level of WT (AA) and SNP (SS) pro-IL-1α cleavage by calpain (**A,B**), elastase (**C,D**) and cathepsin B (**E,F**). **(A,C,E)** ELISA data measuring the level of cleaved IL-1α following incubation of AA or SS pro-IL-1α with range of protease concentrations. **(B,D,F)** IL-1-dependent IL-6 production by HeLa cells treated with reaction products from AA or SS pro-IL-1α incubation ± proteases, ± a neutralising IL-1α antibody (p αAb). Data represent mean +SEM of n=3.

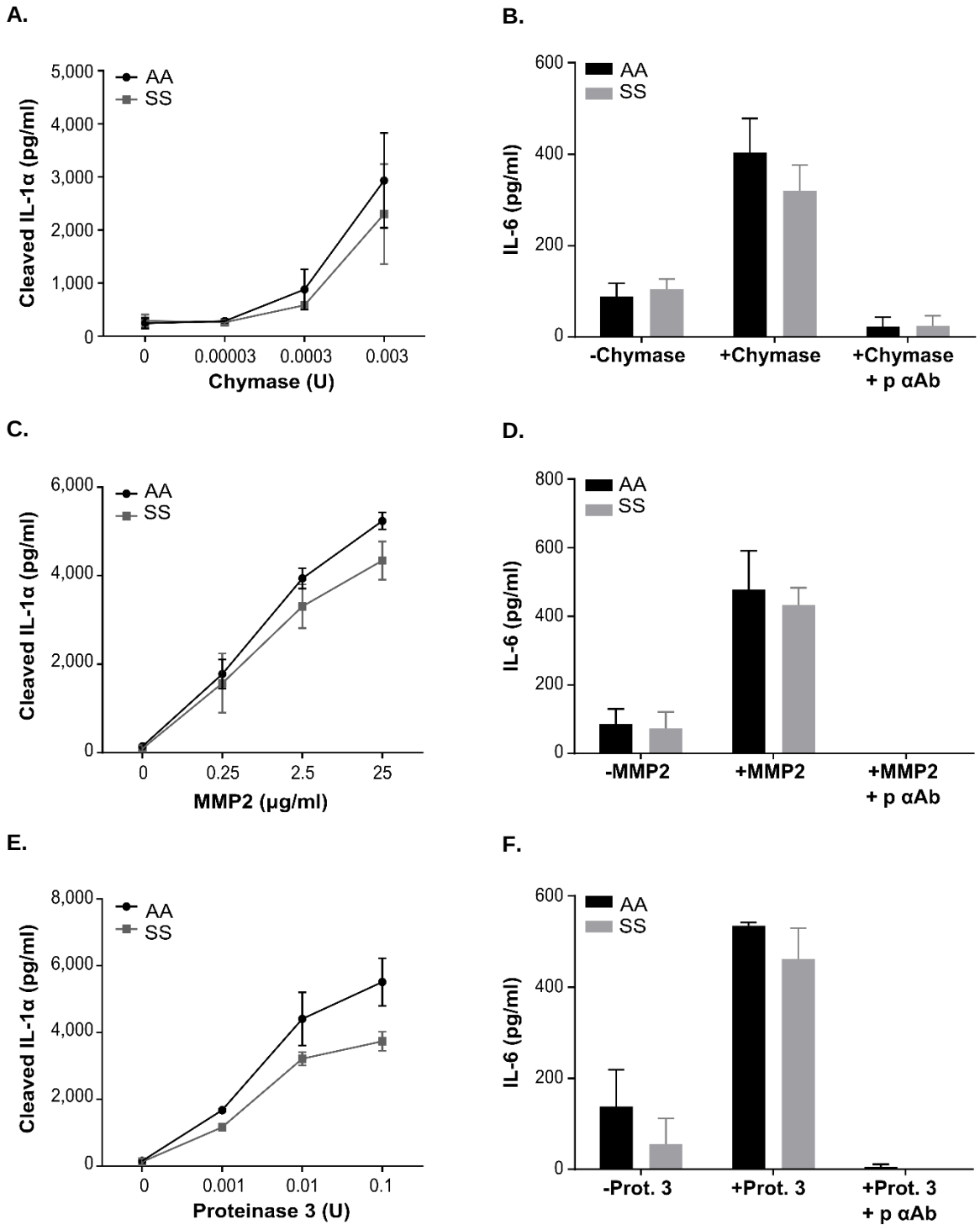

Figure 7.4: The rs17561 SNP hinders recombinant pro-IL-1α cleavage by chymase, MMP2 and proteinase 3. (A-F) The level of WT (AA) and SNP (SS) pro-IL-1α cleavage by chymase (**A,B**), MMP2 (**C,D**) and proteinase-3 (**E,F**). **(A,C,E)** ELISA data measuring the level of cleaved IL-1α following incubation of AA or SS pro-IL-1α with range of protease concentrations. **(B,D,F)** IL-1-dependent IL-6 production by HeLa cells treated with reaction products from AA or SS pro-IL-1α incubation ± proteases, ± a neutralising IL-1α antibody (p αAb). Data represent mean +SEM of n=3.

7.2.3 The expression of pro-IL-1α in mammalian cells is challenging

Although bacterial recombinant protein represents a clean and simple system to investigate the functional effect of rs17561, it is not post-translationally modified. Since the mutation of an alanine to a serine creates a potential phosphorylation site, the effects observed in the recombinant protein cleavage assays may not accurately represent how the SNP influences IL-1α activation in mammalian cells. Therefore, mammalian cell-derived recombinant IL-1α would be a better system to interrogate the effect of the SNP. The overexpression of HIS-tagged AA or SS pro-IL-1α in HEK-293T cells allowed the purification of the recombinant protein using a cobalt resin (Figure 7.5). However, despite optimisation the protein yield was too low for concentration normalisation by coomassie staining. Furthermore, the HEK-293T cells expressed higher levels of SS IL-1α, which was partially cleaved to a 19kDa form making it unsuitable for the comparison of cleavage and activity. Another approach could be to overexpress both forms of pro-IL-1α in insect cells using a baculovirus system, which would enable the production of post-translationally modified protein. Alternatively, to examine the effect of rs17561 introducing a phosphorylation site, the alanine could be mutated to aspartic acid in the bacterial expression system. Aspartate mimics a phosphorylated serine residue, and may therefore cause the protein to behave as though it were phosphorylated at amino acid 114.

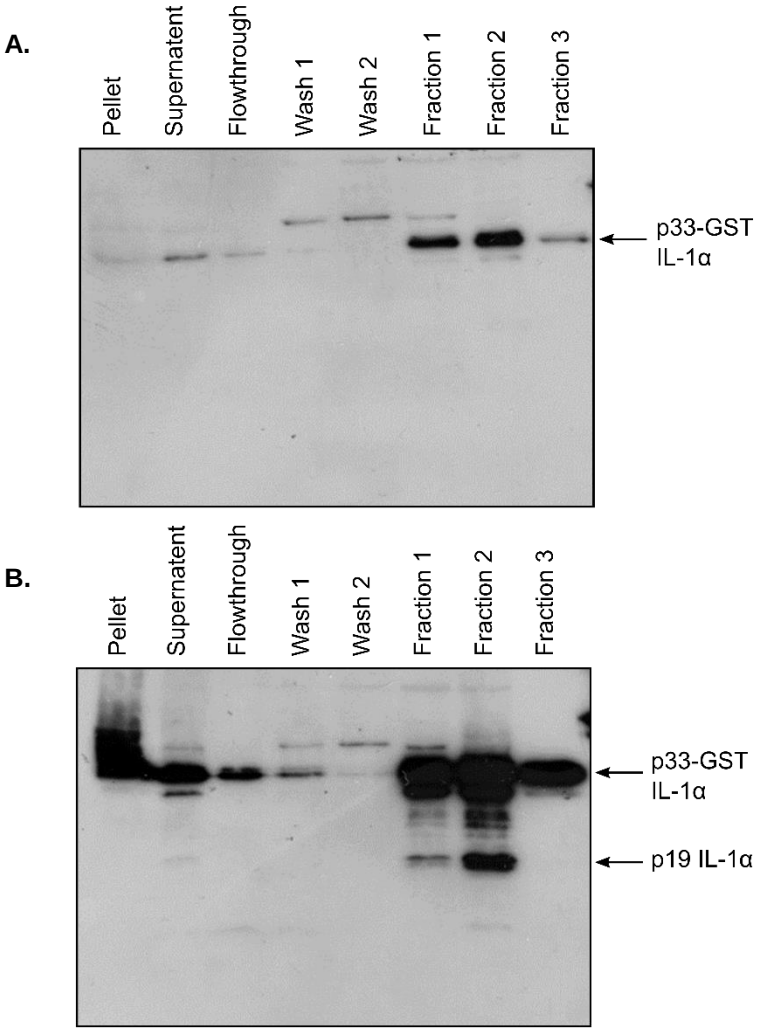

Figure 7.5: Purification of AA and SS HIS-pro-IL-1α from HEK293-T cells. (A-B) Western blot for IL-1α at each stage of the HIS purification of WT (AA) (**A**) and SNP (SS) (**B**) pro-IL-1α expressed in HEK-293T cells.

7.2.4 The development of an assay to measure LPS-induced IL-1 release from whole blood

To investigate the SNP in a more physiological setting, we undertook a human recall-by-genotype study in collaboration with the Cambridge Bioresource; a panel of approximately 16,000 genotyped volunteers. Prior to participant recruitment, we developed an assay to measure LPS-induced IL-1 release from whole blood culture. Blood was extracted into lithium heparin because other anti-coagulants can dampen immune responses (Duffy et al., 2014). Optimisation experiments testing a range of LPS doses and dilution factors revealed that diluting the blood into media by a factor of 2 or 4, and treating with

1µg/ml LPS resulted in the largest IL-1 response (Figure 7.6). Importantly, we confirmed that the IL-1 was not passively released through cell death, as evidenced by similar levels of LDH in the treated and untreated samples (Figure 7.7).

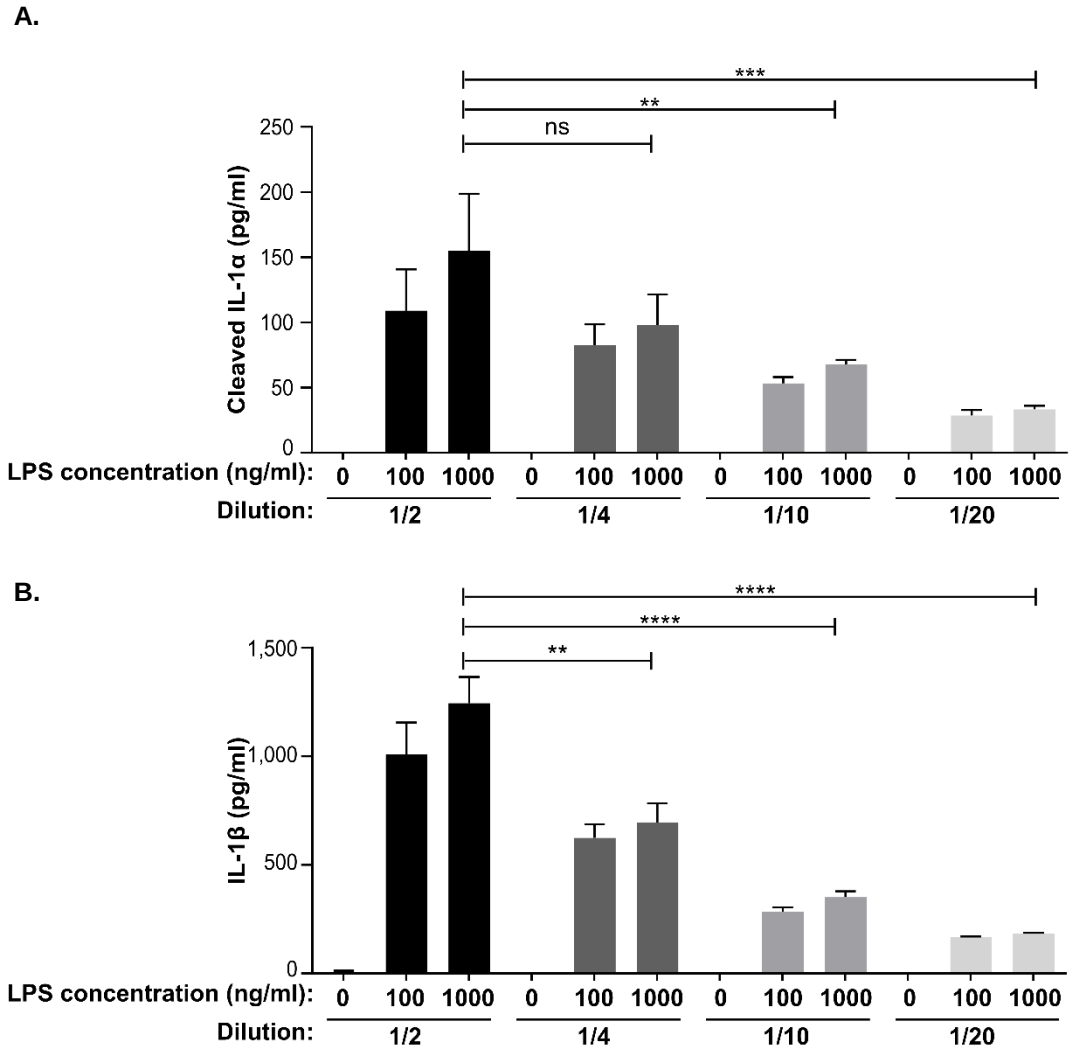

Figure 7.6: Optimisation of blood dilution factor and LPS concentration. (A-B) ELISA data showing the level of IL-1α (**A**) and IL-1β (**B**) in the conditioned media/serum of whole blood diluted 1/2, 1/4, 1/10 or 1/20 into media and treated with 0, 100 or 1000ng/ml LPS. Data represent mean +SEM of n=4, p = **≤0.01, ***≤0.001, ****≤0.0001.

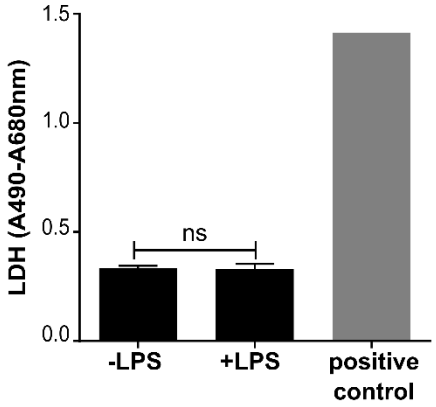

Figure 7.7: IL-1 release from LPS-stimulated whole blood is not due to cell death. Quantification of LDH released from whole blood ± LPS treatment, with a positive control included for reference. Data represent mean +SEM of n=8.

To preserve participant anonymity blood samples are drawn by a nurse at the Cambridge Bioresource and are subsequently collected by the researcher, which inevitably results in a delay between venepuncture and sample processing. We investigated the impact of this on our assay and observed a massive effect of the time between drawing and plating the blood, which resulted in up to 50% less IL-1α detection (Figure 7.8). Because of this, all samples were collected on-site so that blood could be plated within 20 minutes of venepuncture.

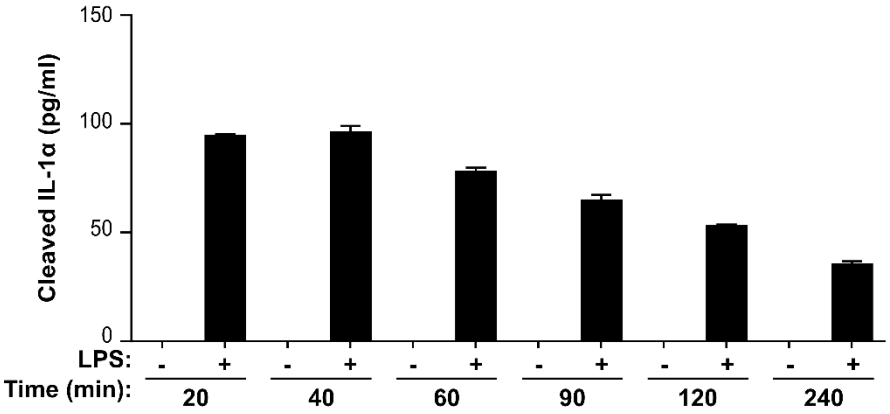

Figure 7.8: Delayed plating of blood leads to a diminished IL-1 response. ELISA data showing the level of IL-1α in the conditioned media/serum of whole blood ± LPS plated at a range of time points following venepuncture. Data represent mean +SEM of n=2.

7.2.5 Preliminary study: rs17561 minor allele homozygotes may secrete less IL-1α

To determine whether rs17561 has a functional effect on IL-1α activation we initially conducted a small preliminary study with 20 participants: 10 major allele homozygotes and 10 minor allele homozygotes. To minimise variation, donors were healthy males aged 16-55 who had not taken any immunomodulatory drugs (e.g. aspirin, ibuprofen, antihistamine) within the 24 hours before donation. LPS-stimulated whole blood from minor allele homozygotes released less IL-1α than major allele homozygotes (Figure 7.9A), with minimal effect on IL-1β release (Figure 7.9B). The same pattern of results was observed for both blood dilutions (Figure 7.9C,D). Together this data suggests that the rs17561 SNP reduces the activation of IL-1α by LPS.

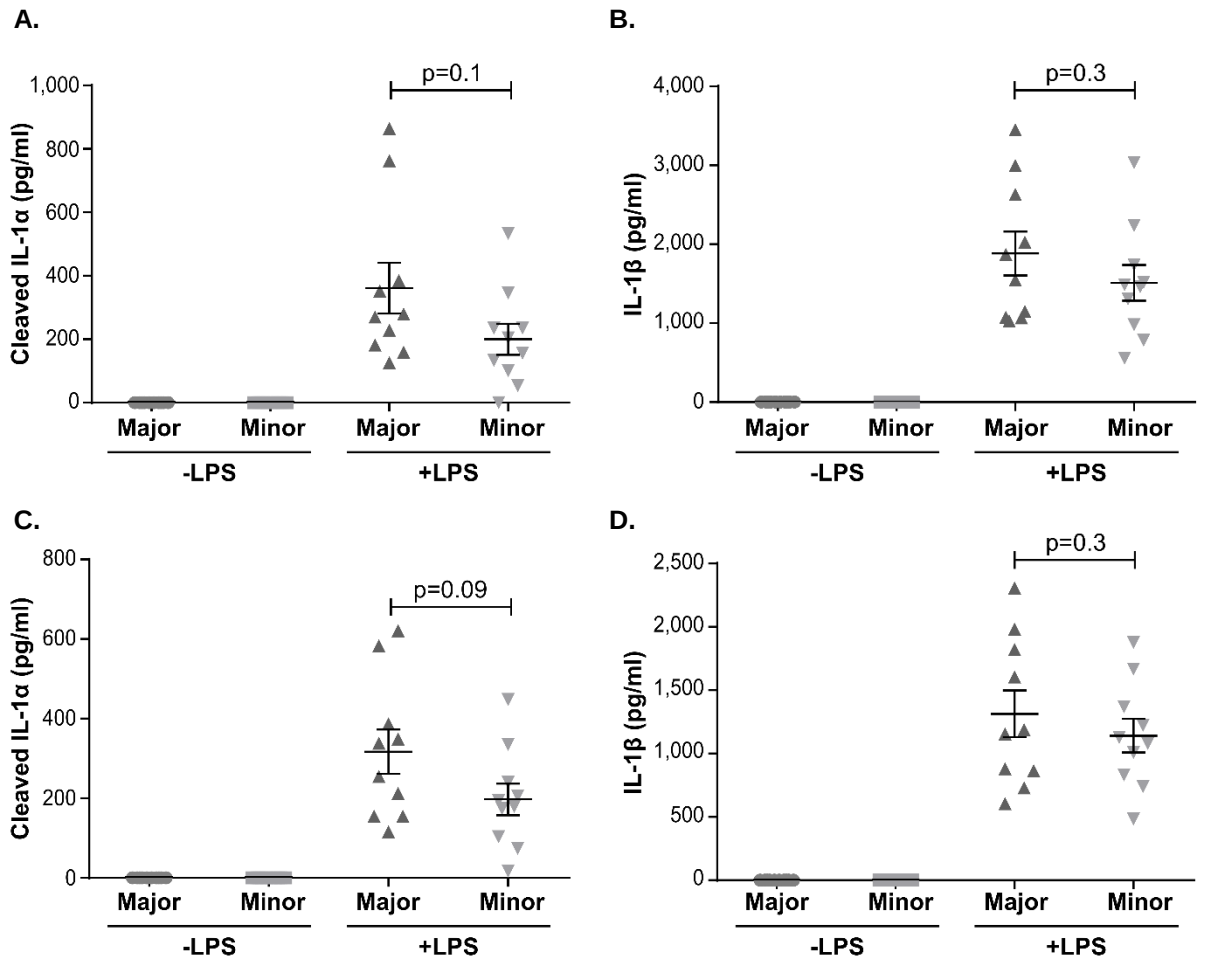

Figure 7.9: Preliminary study data suggests rs17561 minor allele homozygotes secrete less IL-1α. (A-D) ELISA data showing the level of IL-1α (A,C) and IL-1β (B,D) in the conditioned media/serum of whole blood from rs17561 major/minor allele homozygotes ± LPS diluted ½ (A,B) or ¼ (B,C) into media. Data represent mean +SEM of n=10.

An additional blood sample from each participant was drawn into EDTA and sent for full blood count analysis to allow proper normalisation. For example, differences in haematocrit levels between individuals would influence the volume of the serum and therefore directly affect IL-1 concentration. In addition, monocytes are reported to be the main cellular source of IL-1. Therefore, monocyte counts are required to confirm that any difference in IL-1 levels is real and not simply due to a difference in monocyte number. Furthermore, any difference in whole blood count parameters between major and minor allele homozygotes could represent an effect of the SNP on cellular differentiation; indeed, IL-1α has been shown to modulate T_H17 cell differentiation (Mills, 2008). However, there was no difference between major and minor allele homozygotes for most blood count parameters (Figure 7.10A-G), although minor allele homozygotes had slightly lower basophil levels (Figure 7.10H). Basophils are involved in inflammation, particularly allergic reactions where they release histamine to dilate blood vessels. Although IL-1α is implicated in allergy (Willart et al., 2012) there are no reports suggesting that basophils secrete large amounts of the cytokine. The normalisation of IL-1α and IL-1β levels to each blood count parameter, with the exception of basophils, had minimal effect on the p-values (Table 7.2).

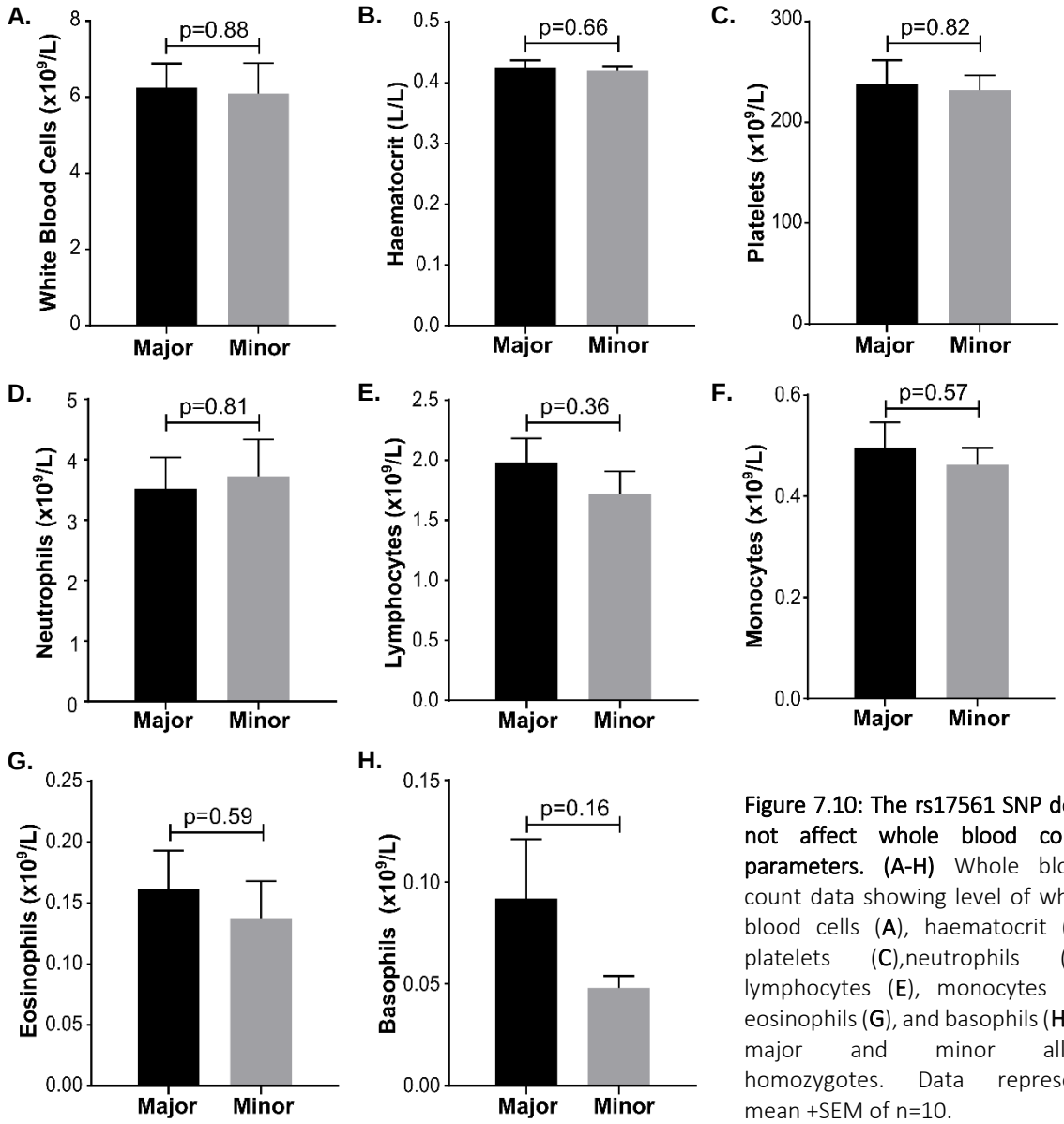

Figure 7.10: The rs17561 SNP does not affect whole blood count parameters. (A-H) Whole blood count data showing level of white blood cells (**A**), haematocrit (**B**), platelets (**C**),neutrophils (**D**), lymphocytes (**E**), monocytes (**F**), eosinophils (**G**), and basophils (**H**) in major and minor allele homozygotes. Data represent mean +SEM of n=10.

BLOOD COUNT PARAMETER	***IL-1α p VALUE***		***IL-1β p VALUE***	
	1/2	***1/4***	***1/2***	***1/4***
Non-normalised	0.1	0.09	0.3	0.3
White blood cells	0.16	0.16	*0.51*	*0.64*
Haematocrit	0.11	0.10	*0.33*	*0.48*
Platelets	0.17	0.14	*0.39*	*0.48*
Neutrophils	0.09	0.13	*0.29*	*0.61*
Lymphocytes	0.29	0.26	*0.89*	*0.98*
Monocytes	0.16	0.15	*0.50*	*0.61*
Eosinophils	0.40	0.5	*0.80*	*0.98*
Basophils	0.43	0.5	*0.95*	*0.64*

Table 7.2: Preliminary study P-values following normalisation of ELISA data to each blood count parameter. A table listing the p values of significance of the difference between LPS-treated major and minor allele homozygote blood following normalisation to different blood count parameters.

7.2.6 Combined larger cohort: rs17561 minor allele homozygotes secrete significantly less IL-1α

Although the results from the preliminary study suggested that rs17561 minor allele homozygotes release less IL-1α, the reduction was not statistically significant. This initial data enabled a power calculation to estimate the sample size required for statistical significance (Figure 7.11). The power calculation estimated that a sample size of 23 per group was required, which led us to recruit an additional 15 participants (giving a total of 25 per group) into the study. Ideally, the second cohort would have represented 25 new, rather than 15 additional, volunteers. However, this was not possible due to the lack of individuals fitting the strict exclusion criteria, in particular the good health status and availability for on-site visits. As such, the results of both cohorts were combined.

A.

$$n = \frac{(\sigma_1^2 + \sigma_2^2) \times (z_{1-\alpha/2} + z_{1-\beta})^2}{D^2}$$

n= sample size
σ = standard deviation
D = difference in group means
$z_{1-\alpha/2}$ = two-sided Z value
$z_{1-\beta}$ = power

B.

Sample Size For Comparing Two Means

Confidence Interval % (two-sided)			95	Enter a value between 0 and 100, usually 95%
Power			80	Enter a value between 0 and 100, usually 80%
Ratio of sample size (Group 2/Group 1)			1	
	Group 1		Group 2	Enter means OR difference on next line
Mean	361	and	200	or Difference
Std. Dev.	192		192	Enter Std. Deviation OR Variance of each group
Variance				

C.

Sample Size For Comparing Two Means

Input Data

Confidence Interval (2-sided)	95%
Power	80%
Ratio of sample size (Group 2/Group 1)	1

	Group 1	Group 2	Difference*
Mean	361	200	161
Standard deviation	192	192	
Variance	36864	36864	

Sample size of Group 1	23
Sample size of Group 2	23
Total sample size	46

*Difference between the means

Figure 7.11: 23 individuals per group are required for statistical power. (A) The power calculation used to calculate sample size (From Bernard Rosner's Fundamentals of Biostatisitcs). **(B-C)** screenshots from the online calculator that applies the given formula (http://www.openepi.com/SampleSize/SSMean.htm) showing the input (**B**) and output (**C**) data.

Since there was no difference between the 1/2 and 1/4 dilutions of blood into media in the preliminary study, a single dilution (1/2) of blood was used for the IL-1 release experiments in the second study cohort. Combining the data from both groups of volunteers revealed that minor allele rs17561 homozygotes released significantly less IL-1α in response to LPS compared with major allele homozygotes (Figure 7.12A). Importantly, there was no difference in IL-1β release between groups, confirming an IL-1α-specific effect of the polymorphism (Figure 7.12B). Initial inspection of the data highlighted a single obvious outlier in the minor allele group. Upon further investigation it was found that the study participant took aspirin every second day, and he was mistakenly included in the study because his blood was drawn on a day that he did not take the medication. However, prolonged use of an anti-inflammatory agent would inevitably affect the immune response, and therefore this sample was excluded from the analysis below.

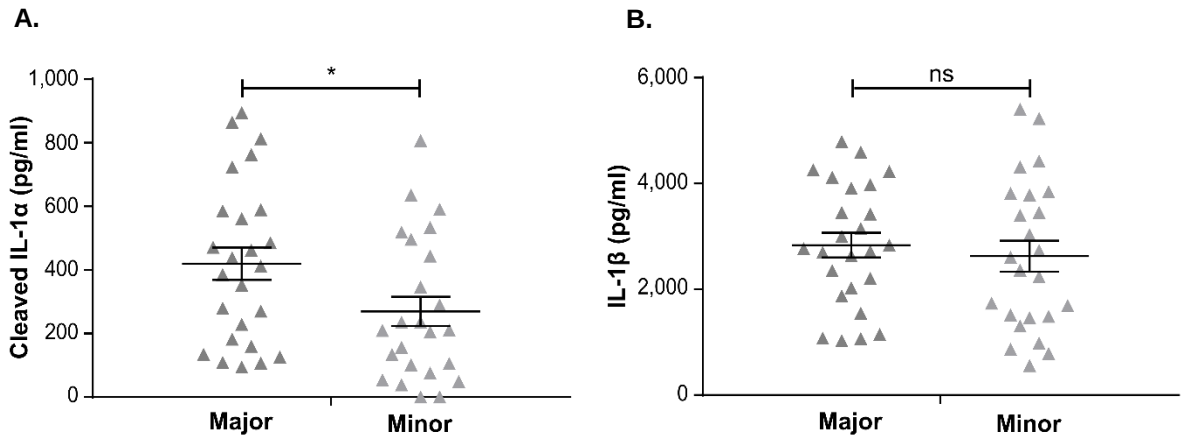

Figure 7.12: rs17561 minor allele homozygotes release significantly less IL-1α. (A-B) ELISA data showing the level of IL-1α (**A**) and IL-1β (**B**) in the conditioned media/serum of whole blood from rs17561 major/minor allele homozygotes treated with LPS. Data represent mean +SEM of n=25 (major) or n=24 (minor); p = *≤0.05.

As before, whole blood count data was collected and analysed to detect any difference between major and minor allele homozygotes (Figure 7.13). For all parameters, there were no significant differences between major and minor allele homozygotes. However, minor allele homozygotes tended to exhibit lower platelet (Figure 7.13C), eosinophil (Figure 7.13G), and basophil counts (Figure 7.13H). The normalisation of IL-1α concentration to platelet, eosinophil, basophil or lymphocyte count led to a non-

significant p-value (Table 7.3). Although monocytes, macrophages and endothelial cells are considered to be the primary cellular sources of IL-1α, it is constitutively expressed by most cells. Therefore, it is possible that other cell types mediate cytokine release during whole blood activation. Although this initial study enabled us to efficiently demonstrate that rs17561 has a functional effect, identifying which cells are releasing IL-1α will be essential to fully understand the effect of the SNP.

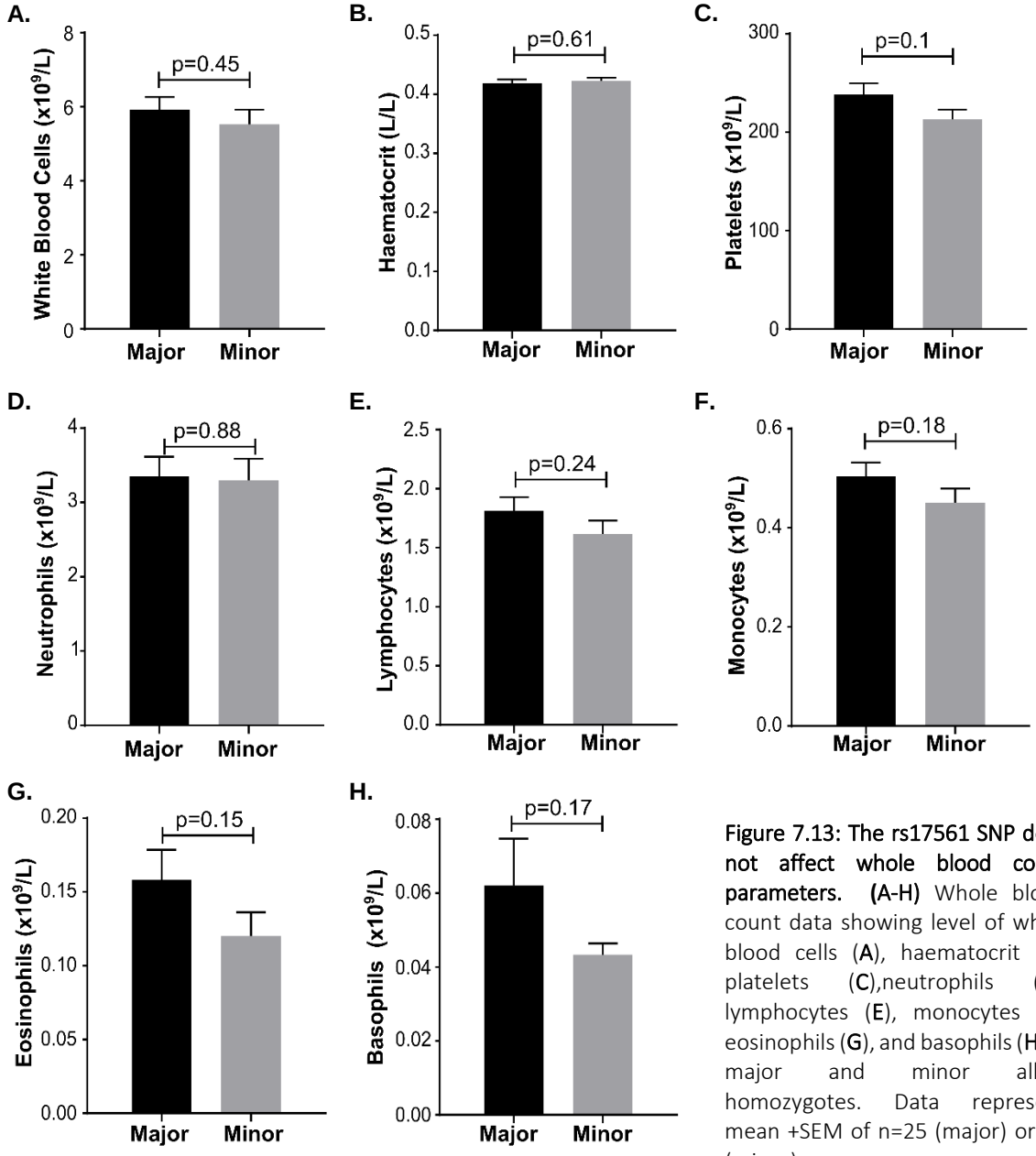

Figure 7.13: The rs17561 SNP does not affect whole blood count parameters. (A-H) Whole blood count data showing level of white blood cells (**A**), haematocrit (**B**), platelets (**C**),neutrophils (**D**), lymphocytes (**E**), monocytes (**F**), eosinophils (**G**), and basophils (**H**) in major and minor allele homozygotes. Data represent mean +SEM of n=25 (major) or 24 (minor).

BLOOD COUNT PARAMETER	*IL-1α p VALUE*	*IL-1β p VALUE*
Non-normalised	0.03	0.58
White blood cells	0.04	*0.8*
Haematocrit	0.03	*0.49*
Platelets	0.08	*0.63*
Neutrophils	0.03	*0.86*
Lymphocytes	0.13	*0.53*
Monocytes	0.06	*0.83*
Eosinophils	0.25	*0.85*
Basophils	0.11	*0.71*

Table 7.3: P-values following normalisation to each blood count parameter. A table listing the p value significance of the difference between LPS-treated major and minor allele homozygote blood following normalisation to different blood count parameters.

7.2.7 The rs17561 SNP does not alter IL-1 gene expression

Although the rs17561 SNP is located in the coding region of *IL1A*, it is in linkage disequilibrium with a second upstream promoter SNP (rs1800587) that could influence gene expression. Although only 50% of study participants were genotyped for both SNPs, those who were carried either both major alleles or both minor alleles. However, there was no difference in *IL1A* or *IL1B* expression between major and minor allele homozygotes (Figure 7.14), suggesting that rs17561 and rs1800587 do not affect IL-1 transcription.

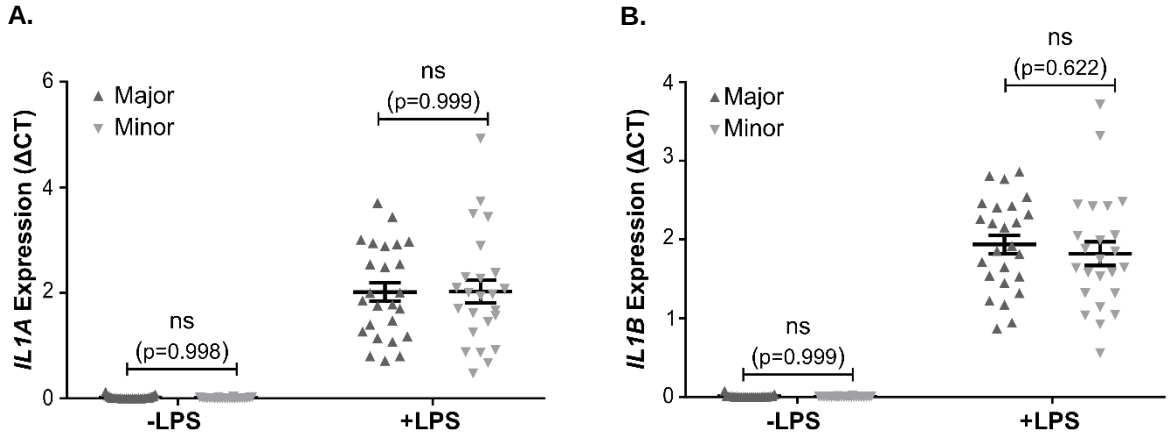

Figure 7.14: rs17561 does not affect *IL1* gene expression. (A-B) qPCR data showing the level of *IL1A* (**A**) and *IL1B* (**B**) expression in the adherent monocytes from each study participant ± LPS. Data represent mean +SEM of n=25 (major) or n=24 (minor).

7.2.8 The rs17561 SNP does not affect the cleavage of IL-1α by caspase-5

Since rs17561 causes an amino acid change within the protease-targeted region of the IL-1α protein, we hypothesised that it could impair cytokine activation. It has been reported that LPS-treated monocytes activate non-canonical inflammasomes and release IL-1α and IL-1β via caspase-4 and -5 through a one-step mechanism (Vigano et al., 2015). Thus, given that caspase-5 can activate IL-1α (Chapters 5 and 6), we reasoned that caspase-5 might mediate IL-1α release in LPS-stimulated whole blood, and that rs17561 might therefore affect caspase-5 cleavage of IL-1α. Although the amino acid change caused by the SNP is 11 amino acids away from the caspase-5 target site, it could influence enzyme docking because these two regions may be close in three-dimensional space. Caspase-5 cleaved recombinant SS pro-IL-1α to produce a similar 19kDa fragment to AA pro-IL-1α (Figure 7.15A), although there was perhaps a lower level of SS IL-1α activation (Figure 7.15B). Furthermore, the inhibitors z-LEVD-fmk and z-YVAD-fmk had little effect on IL-1α release from LPS-stimulated whole blood (Figure 7.16), suggesting that IL-1α might not be cleaved by a caspase in this system.

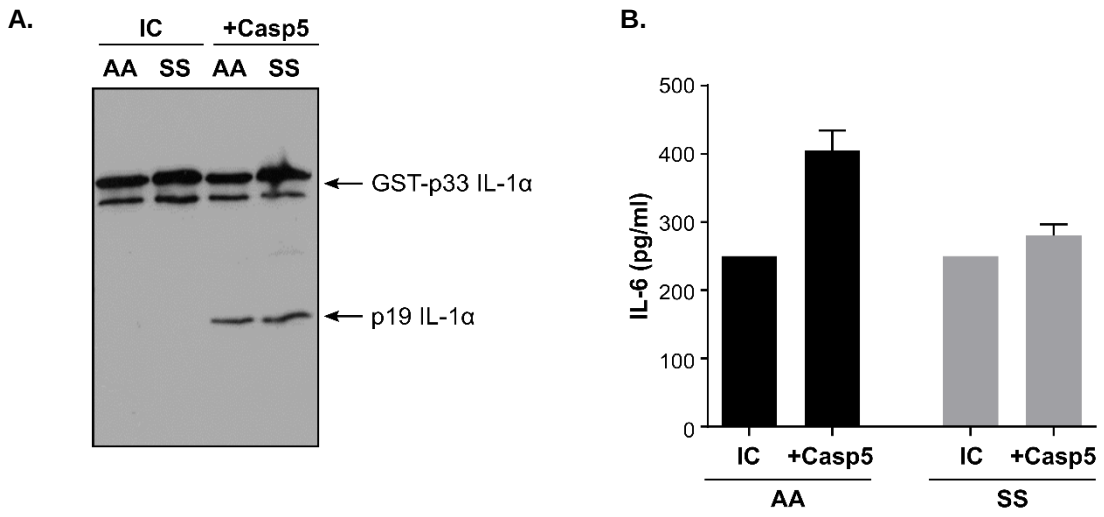

Figure 7.15: rs17561 does not significantly affect IL-1α cleavage by caspase-5. (A) Western blot for IL-1α after the incubation of AA or SS pro-IL-1α alone (incubation control, IC) or with active caspase-5. **(B)** IL-1-dependent IL-6 production by HeLa cells treated with reaction products from AA or SS pro-IL-1α incubation ± active caspase-5. Data represent mean +SEM of n=3.

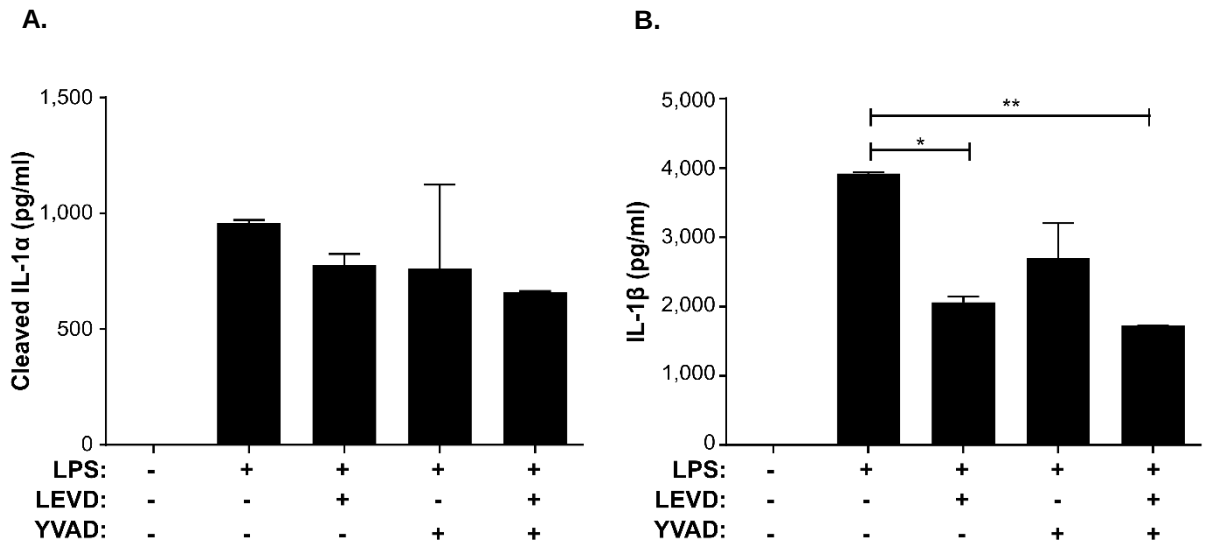

Figure 7.16: LPS-induced IL-1α release from whole blood is not affected by caspase inhibitors. (A-B) ELISA data showing level of IL-1α (A) or IL-1β (B) in the conditioned media/serum from of whole blood treated ± LPS ± z-LEVD-fmk ± z-YVAD-fmk. Data represent mean +SEM of n=3; p = *≤0.05, **≤0.01.

7.2.9 The rs17561 SNP does not affect the interaction between pro-IL-1α and IL-1R2

The IL-1R2 is a decoy receptor that binds to pro-IL-1α to prevent it from interacting with the signalling receptor IL-1R1 and protect it from proteases. To determine whether the rs17561 SNP increases the affinity of IL-1α for IL-1R2 and in turn reduces cytokine availability for proteolytic activation, we examined the effect of increasing IL-1R2 concentrations on basal AA or SS pro-IL-1α activity as a proxy measure of binding. The IL-1R2 inhibition curves were identical for AA and SS pro-IL-1α (Figure 7.17), suggesting that the SNP does not affect IL-1R2 binding to pro-IL-1α. Since the binding of IL-1R2 to pro-IL-1α is enhanced by the accessory protein IL-1RAcP, we repeated the inhibitor study in the presence of the accessory protein. Again, the AA and SS curves were identical (Figure 7.18), indicating that the SNP does not affect the level of IL-1α inhibition through IL-1R2 and IL-1RAcP. However it may be useful to confirm this finding using mammalian IL-1α, since post-translational modifications could affect the interaction.

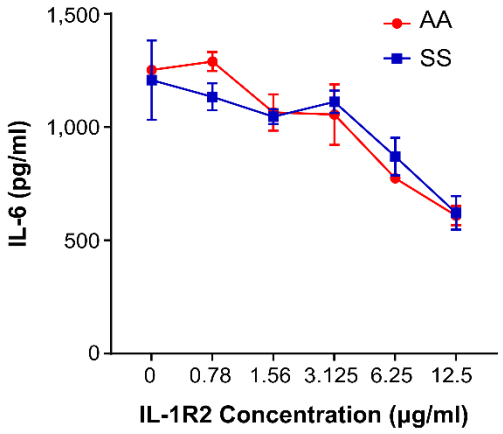

Figure 7.17: rs17561 does not affect the binding of pro-IL-1α to IL-1R2. ELISA data showing IL-1-dependent IL-6 production by HeLa cells treated with AA or SS pro-IL-1α pre-incubated with a range of IL-1R2 concentrations. Data represent mean +SEM of n=2.

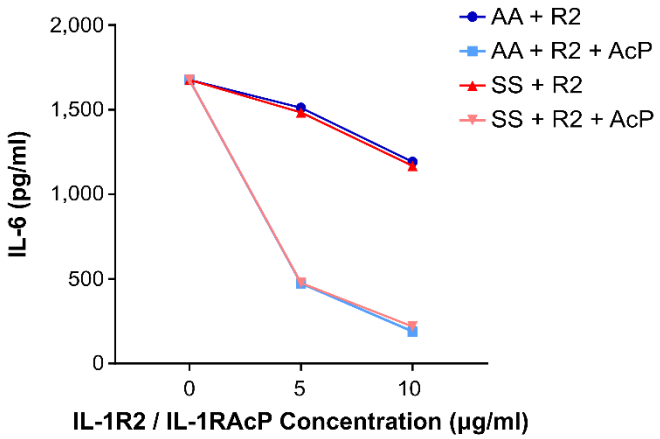

Figure 7.18: rs17561 does not affect the binding of pro-IL-1α to IL-1R2 and IL-1RAcP. ELISA data showing IL-1-dependent IL-6 production by HeLa cells treated with AA or SS pro-IL-1α pre-incubated with a range of IL-1R2±IL-1RAcP concentrations. Data represent mean +SEM of n=2.

7.2.10 A subset of individuals do not release any IL-1α

Our data suggests that the rs17561 SNP may account for some of the variation in IL-1α secretion observed throughout the population. While developing a standardised whole blood stimulation system, Matthew Albert and colleagues found that some individuals do not secrete any IL-1α (Duffy et al., 2014).We find that rs17561 minor allele homozygotes still release some IL-1α, which implies that the SNP does not cause this phenotype and raises the question of what limits IL-1α release in these individuals. Since all commercial IL-1α ELISA kits that we have tested detect the cleaved form of IL-1α only *(unpublished data),* we hypothesised that these 'non-secretors' could be releasing pro-IL-1α that is undetectable by these methods. To test this, we collaborated with the Albert group, and attempted to 'reveal' any pro-IL-1α in the samples by incubation with calpain (Figure 7.19). The calpain revealed additional IL-1α in the responder samples (204, 221, 318, 340 and 378), suggesting that some IL-1α is released in its pro-form. However, calpain did not increase IL-1α detection in the non-responders (203, 220 and 323). Another potential explanation for the lack of IL-1α detection in 'non-responders' is that they express higher levels of IL-1R2, which would bind to pro-IL-1α and mask its detection. However, IL-1R2 levels were comparable between responders and non-responders (Figure 7.20). Together, this data suggests that there were no detection issues in these samples, and that some people really do not secrete IL-1α. It would be interesting to genotype the volunteers from the Albert study to identify any common SNPs specific to either phenotype.

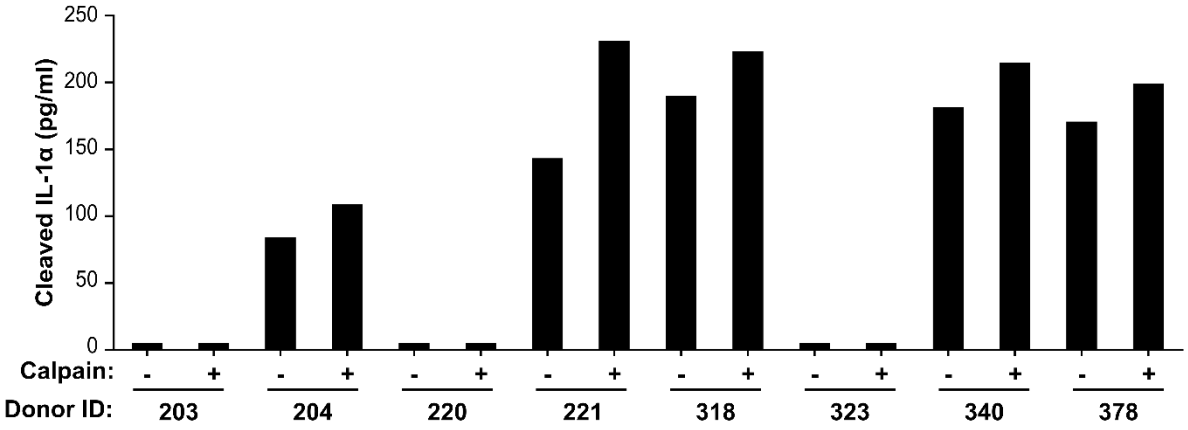

Figure 7.19: Calpain does not 'reveal' IL-1α in non-responders. ELISA data showing cleaved IL-1α levels in the supernatant/serum of LPS-treated blood incubated ± calpain. Data is n=1.

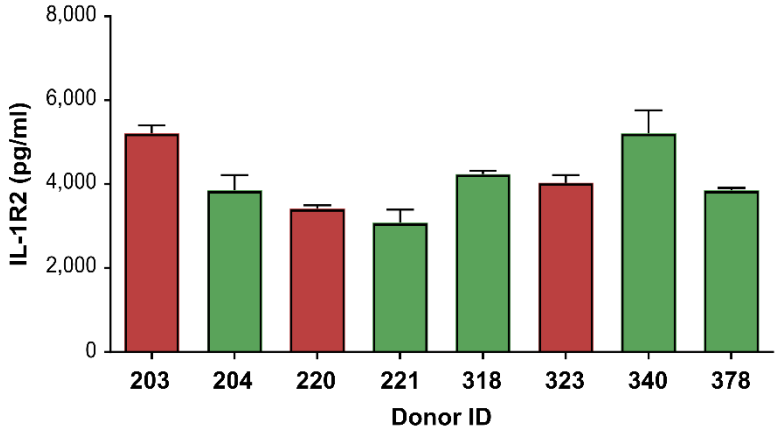

Figure 7.20: There is no difference in IL-1R2 levels between responders and non-responders. ELISA data showing IL-1R2 levels in the supernatant/serum of LPS-treated blood from responders (green) and non-responders (red). Data is n=2.

7.3 Discussion

The rs17561 SNP causes an amino acid change from an alanine to a serine in the protease-targeted region of IL-1α. Serine is a polar uncharged amino acid, whereas alanine has a hydrophobic side chain. In addition, serine residues can undergo post-translational modifications such as phosphorylation and O-linked glycosylation. Phosphorylation, for example, introduces a charged hydrophilic moiety that could affect amino acid interactions, and regulate protein degradation thereby limiting substrate availability. As such, we hypothesised that the SNP could have a functional effect on IL-1α activation. Indeed, the polymorphism is associated with multiple inflammatory diseases, such as ovarian cancer (Table 7.1).

Although the recombinant protein cleavage assays did not show a clear effect of the SNP, perhaps due to the lack of post-translational modification in bacterial protein, the human recall-by-genotype study revealed that LPS-stimulated whole blood from minor allele homozygotes secreted significantly less cleaved IL-1α than blood from major allele homozygotes (Figure 7.11), confirming that rs17561 has a functional effect. A limitation of the study was the lack of suitable volunteers in the Cambridge Bioresource database, since many minor allele homozygotes were taking medication or did not have time to donate blood on site. Although the exclusion of minor allele homozygotes due to medication use indirectly supports the hypothesis that rs17561 has a functional effect that requires treatment, it resulted in the pooling of data from both study cohorts. Future work could include evaluating IL-1α release in heterozygous individuals, a more prevalent genotype, to determine if there is a dosage effect of the minor allele.

Importantly, we confirmed that the impaired IL-1α response in minor allele homozygotes was not due to a reduction in *IL1A* transcription (Figure 7.13), which could be influenced by a second *IL1A* promoter SNP that is in linkage disequilibrium with rs17561. Interestingly, the promoter SNP has been studied in greater depth than rs17561 and has been linked to increased risk of a number of conditions such as stroke, coronary artery disease, and obesity (Zou et al., 2015, Haroon et al., 2015, Carter et al., 2008). All SS individuals genotyped for both polymorphisms in the study carried the minor allele for both

SNPs, suggesting that the promoter SNP does not affect *IL1A* expression. Therefore, the aforementioned associations of rs18005787 with disease may actually be due to rs17561.

Alternatively, the rs17461 SNP could affect IL-1α secretion. The mechanism of IL-1α secretion is unknown, since pro-IL-1α lacks a conventional signal peptide and does not localise to the Golgi apparatus or endoplasmic reticulum (Stevenson et al., 1992). It has been reported that IL-1α is co-secreted with IL-1β (Fettelschoss et al., 2011). However, IL-1β release from LPS-stimulated whole blood was not affected by the SNP (Figure 7.11B), indicating that this secretory pathway remained unaltered.

Since the mutation is located in the loop region of IL-1α that is targeted by proteases, the reduced IL-1α release in minor allele homozygotes is most likely due to impaired cytokine activation. To interrogate this fully, it will be necessary to identify the protease responsible for IL-1α cleavage in the whole blood assay. First, to identify the primary cellular source of IL-1α, the blood could be separated by density-gradient centrifugation so that the response of each cell type to LPS can be evaluated. Different cell types display distinct protease profiles that could narrow down the candidate list. In addition, different combinations of protease inhibitors could be added to identify the type or specific identity of the protease responsible for IL-1α activation.

In conclusion, the work presented in this chapter has revealed a functional effect of the rs17561 SNP that could have an immediate clinical impact. Genotyping patients who are being considered for anti-IL-1 therapies for the SNP could help to inform clinicians of the best course of treatment. Since minor allele homozygotes release less IL-1α, these patients may benefit more from a therapy targeting both IL-1α and IL-1β, such as Anakinra, or IL-1β alone, for example Canakinumab. This personalised treatment would save both time and money. In addition, future epidemiological studies that evaluate the association of rs17561 with disease could identify novel pathologies that are mediated by IL-1α, and provide rationale for the development of new, or the repurposing of existing, IL-1α-targeting therapies.

General Discussion

8. General Discussion

Pro-inflammatory cytokines are critical signalling molecules that enable cells to communicate danger and drive inflammation - an indispensable process for managing invading microbes and tissue damage. IL-1α is an extremely powerful inflammatory cytokine that exerts a plethora of effects on both innate and adaptive immunity. Its extracellular activity regulates inflammatory cytokine production, T_H17 cell differentiation, B- and T-cell survival and dendritic cell MHC expression, and drives systemic hypotension and fever (Sims and Smith, 2010, Gabay et al., 2010). In addition, intra-nuclear IL-1α acts as a transcription factor, an oncogene, and a DNA damage sensor (Luheshi et al., 2009, Buryskova et al., 2004, Pollock et al., 2003, Stevenson et al., 1997, Zhang et al., 2017, Cohen et al., 2015). Aberrant IL-1α signalling has been reported in multiple chronic inflammatory diseases including cancer, atherosclerosis, psoriasis and arthritis (Rider et al., 2013, Kamari et al., 2011, Eastgate et al., 1991). As such, understanding exactly how IL-1α activity is regulated is essential for dissecting the pathways that are dysregulated in disease and developing appropriate anti-IL-1α therapies.

IL-1α is translated as a pro-protein that was considered to be fully active for many years (March et al., 1985, Mosley et al., 1986, Kim et al., 2013). However, recent work by ourselves and others has demonstrated that the proteolytic removal of the IL-1α pro-piece significantly enhances cytokine activity (Afonina et al., 2011, Zheng et al., 2013), thereby prompting a paradigm shift in thinking. The research presented in this thesis provides substantial evidence further supporting the hypothesis that IL-1α is subject to proteolytic activation (Figure 8.1). We have demonstrated that the pro-domain limits cytokine activity (Chapter 3), and that multiple proteases from diverse biological systems are capable of proteolytically activating IL-1α (Chapter 4). We have extensively characterised the cleavage of IL-1α by human caspases-5 and murine -11, which activate IL-1α during non-canonical inflammasome activation under sterile and non-sterile conditions (Chapters 5 and 6). Finally, we have demonstrated that a common missense polymorphism that causes an amino acid substitution in the protease-targeted domain leads to impaired IL-1α release in minor allele homozygotes (Chapter 7).

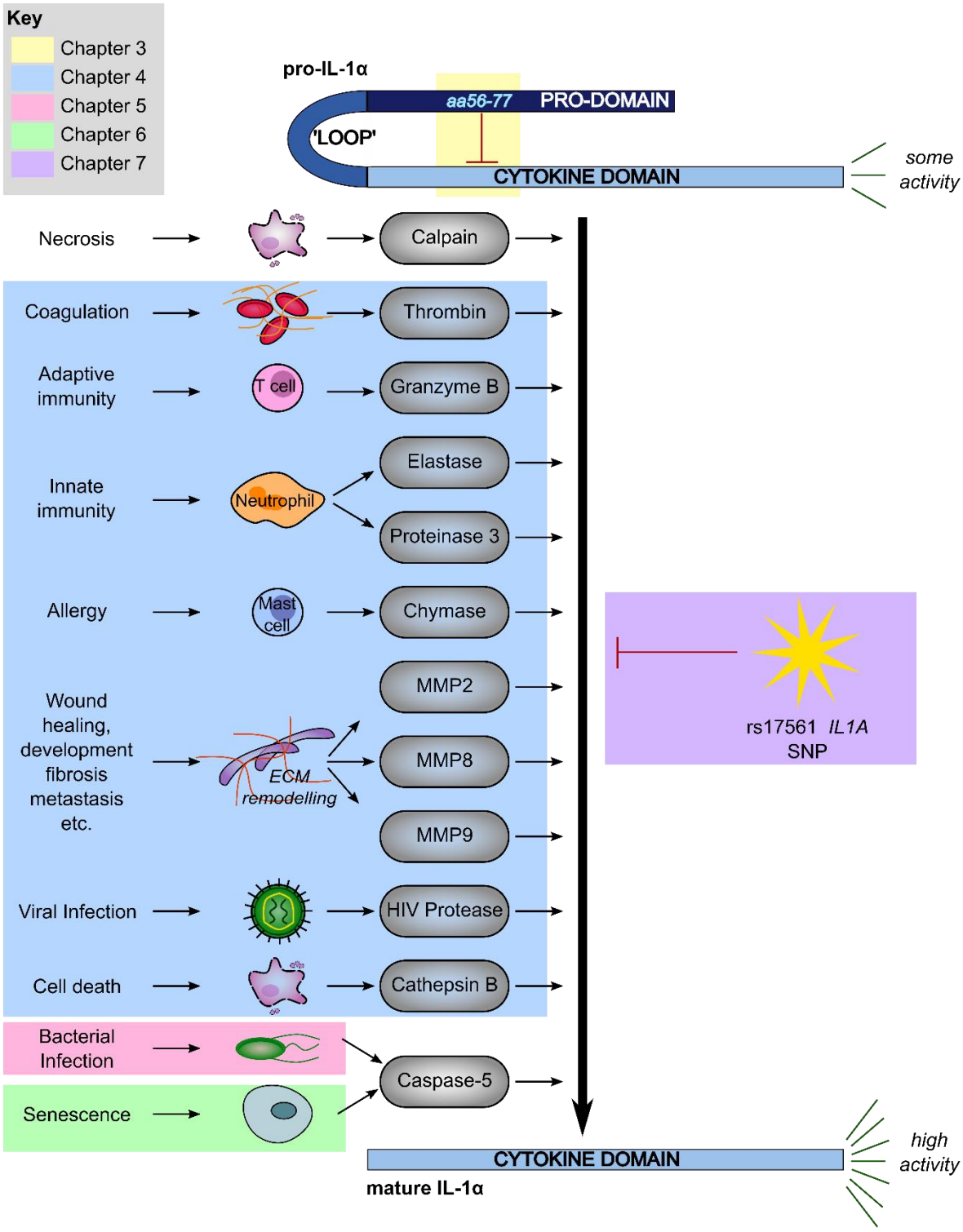

Figure 8.1: Summary of main thesis findings. Schematic illustrating how the work presented in each chapter of this thesis has contributed to our understanding of how IL-1α activity is regulated.

Using bacterial recombinant and cell-derived IL-1α we show that the pro-domain, specifically amino acids 56-77, inhibits IL-1α activity; and that this inhibition can be relieved via cleavage by multiple proteases (Chapters 3 and 4). The diversity of proteases capable of IL-1α activation was unexpected, but is perhaps in keeping with the alarmin function of the cytokine. Indeed, it seems logical that any proteolytic signal from compromised cellular homeostasis activates immunity. Furthermore, the gradual inactivation of IL-1α over time by some proteases, such as elastase and proteinase 3 that are released from immune cells in high quantities, may represent a failsafe mechanism that has evolved to prevent excess IL-1-driven inflammation. In addition to providing further evidence that IL-1α is subject to proteolytic activation, this data challenges the view that pro-IL-1α is passively released during cell death. Instead, we suggest that IL-1α might represent an inflammatory signalling hub that integrates multiple proteolytic signals from diverse sources. Importantly, unlike IL-1β, pro-IL-1α is constitutively expressed in the cytosol of most cells. Thus, without the requirement for cell priming, transcription and translation, pro-IL-1α is able to act as a first-responder that can quickly initiate the inflammatory cascade.

The work presented in chapters 5 and 6 of this thesis focusses on the processing of pro-IL-1α by caspase-5. This interaction was somewhat surprising, since inflammatory caspase signalling is typically associated with the activation of IL-1β by caspase-1 via the inflammasome. Although caspases-4 and -5 have recently gained recognition for their role in non-canonical inflammasome signalling, a rapidly progressing field, they are assumed to exert effect by processing gasdermin D (Kayagaki et al., 2015, Shi et al., 2015). In Chapter 5 we show that caspase-5 and -11 directly cleave and activate IL-1α in cells following intracellular LPS treatment, providing important insights into non-canonical inflammasome biology. Firstly, the original *Casp1*$^{-/-}$ mouse showed reduced levels of IL-1α release during endotoxemia, which was unexpected given that IL-1α is not a caspase-1 substrate (Li et al., 1995, Kuida et al., 1995). However due to their 129/Sv genetic background, these mice carried an endogenous inactivating mutation in *Casp11* (Kayagaki et al., 2011). Our data provides a possible explanation for this ongoing puzzle, suggesting that the defective cleavage and release of IL-1α in *Casp1*$^{-/-}$ mice may be due to the absence of caspase-11. Furthermore, most non-canonical inflammasome research focusses on caspase-

4, which is often considered a closer relative of murine caspase-11 than caspase-5 (Shi et al., 2014). However, we find that caspase-5 and -11 are both induced upon cell priming (whilst caspase-4 is not) and share similar substrate specificities, indicating significant functional equivalence between these two proteases. As such, we hypothesise that caspases-4 and -5 have undergone subfunctionalisation over time, and that the properties of the ancestral *Casp11*-like gene are now divided between both human proteases.

We find that caspase-5 can both liberate IL-1α from the decoy receptor IL-1R2 (Zheng et al., 2013) and activate IL-1α by direct cleavage. Therefore, caspase-5 can rapidly activate IL-1α independently of the caspase-1 inflammasome. Some pathogens target inflammatory caspase signalling to evade immune detection. For example, enterohemorrhagic *E.coli* uses the T3SS effector NIeF to specifically inhibit caspase-4 (Song et al., 2017), and the viral serpin CrmA and bacterial protease zmp1 block caspase-1 activation (Lamkanfi and Dixit, 2011, Taxman et al., 2010). Therefore, caspase-5-mediated IL-1α activation may represent an important and distinct inflammatory pathway that is able to establish an immune response against these pathogens.

In addition to demonstrating that caspase-5 cleaves IL-1α in response to intracellular LPS, we have shown that that caspase-5 also activates IL-1α in senescent cells to control the SASP (Chapter 6). Since the SASP represents sterile inflammation, this work contributes to the growing body of evidence that the non-canonical inflammasome is activated by endogenous ligands in the absence of infection (Zanoni et al., 2016, Pillon et al., 2016). Although our data indicates that *CASP5* expression is upregulated via cGAS signalling, we have not yet identified the endogenous ligand that activates caspase-5 in senescent cells. Intracellular LPS is reported to activate caspase-5 via direct binding (Shi et al., 2014). Future work could attempt mass spectrometry analysis of immuno-precipitated caspase-5 from senescent cells to identify any interacting factors.

Furthermore, we confirm that the SASP is dependent on IL-1α, rather than IL-1β, in line with previous reports (Orjalo et al., 2009, Gardner et al., 2015), and show that IL-1α secretion from senescent cells occurs in the absence of cell death. Together, these findings contradict the usual notion that IL-1α is

released passively upon cell death or co-secreted with IL-1β, and provide crucial evidence that IL-1α can be actively released from live cells.

Senescent cells are reported to accumulate in multiple age-related pathologies such as atherosclerosis, cancer and osteoarthritis (Gardner et al., 2015, Martin and Buckwalter, 2003, Collado et al., 2007, Baker et al., 2011). In atherosclerotic lesions, the SASP is considered to be deleterious by creating a highly inflammatory environment that reduces plaque stability (Wang et al., 2015). However, within a tumour the SASP is reported to exert both pro- and anti-tumourigenic functions (Coppé et al., 2010). Therefore, it will be important to examine the effect of caspase-5 inhibition in animal models of disease in order to understand the contribution of SASPs to specific pathologies and identify disorders that might benefit from anti-caspase-5 therapies.

Chapter 7 of this thesis investigated the effect of a common non-synonymous SNP, rs17561, on IL-1α activity. We show that minor allele homozygotes release less mature IL-1α from LPS-stimulated whole blood compared with major allele homozygotes. Although we have not confirmed that the SNP does not influence IL-1α secretion, the mutation at amino acid 114 is located in the protease-targeted region of IL-1α and is therefore likely to affect cytokine activation. To fully understand the functional effect of rs17561 it will be important to identify what proteases are affected by the mutation, which could be investigated by adding different protease inhibitors to blood during LPS-treatment. In turn, this could help identify what proteolytic signalling pathways drive SNP-associated diseases, and enhance our understanding of their pathology.

In addition, IL-1α is a dual function cytokine. Therefore, it would also be of interest to investigate whether the SNP influences the intracellular properties of IL-1α. For example, rs17561 is associated with increased risk of ovarian cancer (Charbonneau et al., 2014). Is this primarily through lower levels of extracellular IL-1α activity and reduced anti-tumour immunity, or due to an effect of the intracellular cytokine on transcription? For example, the SNP might influence the binding of intra-nuclear IL-1α to DNA and alter the transcription of downstream target genes. Alternatively, the mutation could impair the ability of HDAC enzymes to modulate IL-1α acetylation, thereby impeding IL-1α shuttling between

the nucleus and the cytosol and interfering with its ability to communicate DNA damage (Cohen et al., 2015). The intracellular localisation of AA or SS pro-IL-1α could be interrogated by immunofluorescence.

To conclude, the data presented in this thesis has significantly contributed to our understanding of IL-1, inflammasome, and senescent cell biology. We have used recombinant proteins, *in vitro* cell assays, *in vivo* murine models, and a small-scale human study to show that IL-1α activity is enhanced by proteolytic cleavage. Furthermore we have revealed a novel link between the non-canonical inflammasome and the SASP, thereby identifying caspase-5-mediated IL-1α activation as an important inflammasome-independent mechanism of inducing an inflammatory response during sterile and non-sterile inflammation.

References

ACOSTA, J. C., BANITO, A., WUESTEFELD, T., GEORGILIS, A., JANICH, P., MORTON, J. P., ATHINEOS, D., KANG, T.-W., et al. 2013. A complex secretory program orchestrated by the inflammasome controls paracrine senescence. *Nature Cell Biology,* 15**,** 978–990.

ADAMS, D. O. 1976. The granulomatous inflammatory response. A review. *American Journal of Pathology,* 84**,** 164-191.

ADEN, N., NUTTALL, A., SHIWEN, X., WINTER, P. D., LEASK, A., BLACK, C. M., DENTON, C. P., ABRAHAM, D. J., et al. 2010. Epithelial Cells Promote Fibroblast Activation via IL-1a in Systemic Sclerosis. *The Society for Investigative Dermatology,* 130**,** 2191-2200.

AFONINA, I. S., MULLER, C., MARTIN, S. J. & BEYAERT, R. 2015. Proteolytic Processing of Interleukin-1 Family Cytokines: Variations on a Common Theme. *Immunity,* 42**,** 992-1004.

AFONINA, I. S., TYNAN, G. A., LOGUE, S. E., CULLEN, S. P., BOTS, M., LUTHI, A. U., REEVES, E. P., MCELVANEY, N. G., et al. 2011. Granzyme B-dependent proteolysis acts as a switch to enhance the proinflammatory activity of IL-1alpha. *Mol Cell,* 44**,** 265-78.

AGLIETTIA, R. A., ESTEVEZB, A., GUPTAC, A., RAMIREZD, M. G., LIUE, P. S., KAYAGAKIC, N., CIFERRIB, C., DIXIT, V. M., et al. 2016. GsdmD p30 elicited by caspase-11 during pyroptosis forms pores in membranes. *Proc Natl Acad Sci U S A*.

AIT-OUFELLA, H., TALEB, S., MALLAT, Z. & TEDGUI, M. 2011. Recent Advances on the Role of Cytokines in Atherosclerosis. *Arteriosclerosis, Thrombosis, and Vascular Biology,* 31**,** 969-979.

ALBERTS, B., JOHNSON, A., LEWIS, J., RAFF, M., ROBERTS, K. & WALTER, P. 2002. T cells and MHC Proteins. *Molecular Biology of the Cell.* 4th ed. New York: Garland Science.

ANDERSSON, M. K., ENOKSSON, M., GALLWITZ, M. & HELLMAN, L. 2009. The extended substrate specificity of the human mast cell chymase reveals a serine protease with well-defined substrate recognition profile. *Int Immunol,* 21**,** 95-104.

ASHLEY, N. T., WEIL, Z. M. & NELSON, R. J. 2012. Inflammation: Mechanisms, Costs, andNatural Variation. *Annual Review of Ecology, Evolution, and Systematics,* 43**,** 385-406.

BAKER, D. J., WIJSHAKE, T., TCHKONIA, T., LEBRASSEUR, N. K., CHILDS, B. G., VAN DE SLUIS, B., KIRKLAND, J. L. & VAN DEURSEN, J. M. 2011. Clearance of p16Ink4a-positive senescent cells delays ageing-associated disorders. *Nature,* 479**,** 232-236.

BAKER, P. J., BOUCHER, D., BIERSCHENK, D., TEBARTZ, C., WHITNEY, P., D'SILVA, D. B., TANZER, M. C., MONTELEONE, M., et al. 2015. NLRP3 inflammasome activation downstream of cytoplasmic LPS recognition by both caspase-4 and caspase-5. *European Journal of Immunology,* 45**,** 2918–2926.

BAROJA-MAZO, A., MARTÍN-SÁNCHEZ, F., GOMEZ, A. I., MARTÍNEZ, C. M., AMORES-INIESTA, J., COMPAN, V., BARBERÀ-CREMADES, M., YAGÜE, J., et al. 2014. The NLRP3 inflammasome is released as a particulate danger signal that amplifies the inflammatory response. *Nature Immunology,* 15**,** 738-748.

BERGER, P., MCCONNELL, J. P., NUNN, M., KORNMAN, K. S., SORRELL, J., STEPHENSON, K. & DUFF, G. W. 2002. C-reactive protein levels are influenced by common IL-1 gene variations. *Cytokine,* 17**,** 171-4.

BESNARD, A. G., TOGBE, D., COUILLIN, I., TAN, Z., ZHENG, S. G., ERARD, F., LE BERT, M., QUESNIAUX, V., et al. 2012. Inflammasome–IL-1–Th17 response in allergic lung inflammation. *Journal of Molecular Cell Biology,* 4**,** 3-10.

BIAN, Z.-M., ELNER, S. G., KHANNA, H., MURGA-ZAMALLOA, C. A., PATIL, S. & ELNER, V. M. 2011. Expression and Functional Roles of Caspase-5 in Inflammatory Responses of Human Retinal Pigment Epithelial Cells. *Investigative Ophthalmology & Visual Science,* 52**,** 8646-8656.

BINIOSSEK, M. L., D.K., N., BECKER-PAULY, C. & SCHILLING, O. 2011. Proteomic identification of protease cleavage sites characterizes prime and non-prime specificity of cysteine cathepsins B, L, and S. *J Proteome Res,* 10**,** 5363-5373.

BORASCHI, D. & TAGLIABUE, A. 2013. The interleukin-1 receptor family. *Seminars in Immunology,* 25**,** 394-407.

BOT, I., BOT, M., VAN HEININGEN, S. H., VAN SANTBRINK, P. J., LANKHUIZEN, I. M., HARTMAN, P., GRUENER, S., HILPERT, H., et al. 2011. Mast cell chymase inhibition reduces atherosclerotic plaque progression and improves plaque stability in ApoE-/- mice. *Cardiovasc Res,* 89**,** 244-252.

BOUCHER-HAYES, L. 2017. Caspase-1 and Caspase-5 are Differentially Activated by Extracellular Heme. *Cell Death and Inflammation.* Dublin, Ireland: Keystone.

BOYA, P. & KROEMER, G. 2008. Lysosomal membrane permeabilization in cell death. *Oncogene,* 27**,** 6434–6451.

BROKOPP, C. E., SCHOENAUER, R., RICHARDS, P., BAUER, S., LOHMANN, C., EMMERT, M. Y., WEBER, B., WINNIK, S., et al. 2011. Fibroblast activation protein is induced by inflammation and degrades type I collagen in thin-cap fibroatheromata. *European Heart Journal,* 32**,** 2713-2722.

BROUGH, D., LE FEUVRE, R. A., WHEELER, R. D., SOLOVYOVA, N., HILFIKER, S., ROTHWELL, N. J. & VERKHRATSKY, A. 2003. Ca2+ stores and Ca2+ entry differentially contribute to the release of IL-1 beta and IL-1 alpha from murine macrophages. *Journal of Immunology,* 170**,** 3029-3036.

BURSUKER, I., RHODES, J. M. & GOLDMAN, R. 1982. Beta-galactosidase -- an indicator of the maturational stage of mouse and human mononuclear phagocytes. *J Cell Physiol,* 112**,** 385-390.

BURYSKOVA, M., POSPISEK, M., GROTHEY, A., SIMMET, T. & BURYSEK, L. 2004. Intracellular Interleukin-1a Functionally Interacts with Histone Acetyltransferase Complexes. *The Journal of Biological Chemistry,* 279**,** 4017-4026.

CALADO, R. T. & DUMITRIU, B. 2013. Telomere dynamics in mice and humans. *Semin Hematol,* 50**,** 165-174.

CARRASCO, D., STECHER, M., LEFEBVRE, G. C., LOGAN, A. C. & MOY, R. 2015. An Open Label, Phase 2 Study of MABp1 Monotherapy for the Treatment of Acne Vulgaris and Psychiatric Comorbidity. *Journal of Drugs in Dermatology,* 14**,** 560-564.

CARTA, S., TASSI, S., PETTINATI, I., DELFINO, L., DINARELLO, C. A. & RUBARTELLI, A. 2011. The Rate of Interleukin-1b Secretion in Different Myeloid Cells Varies with the Extent of Redox Response to Toll-like Receptor Triggering. *Journal of Biological Chemistry,* 286**,** 27069-27080.

CARTER, K. W., HUNG, J., POWELL, B. L., WILTSHIRE, S., FOO, B. T. X., LEOW, Y. C., MCQUILLAN, B. M., JENNENS, M., et al. 2008. Association of Interleukin-1 gene polymorphisms with central obesity and metabolic syndrome in a coronary heart disease population. *Hum Genet,* 124**,** 199–206.

CASINI-RAGGI, V., KAM, L., CHONG, Y. J., FIOCCHI, C., PIZARRO, T. T. & COMINELLI, F. 1995. Mucosal imbalance of IL-1 and IL-1 receptor antagonist in inflammatory bowel disease. A novel mechanism of chronic intestinal inflammation. *Journal of Immunology,* 154**,** 2434-40.

CASSON, C. N., YUA, J., REYES, V. M., TASCHUK, F. O., YADAV, A., COPENHAVER, A. M., NGUYEN, H. T., COLLMAN, R. G., et al. 2015. Human caspase-4 mediates noncanonical inflammasome activation against gram-negative bacterial pathogens. *Proc Natl Acad Sci U S A,* 112**,** 6688–6693.

CAUGHEY, G. H. 2007. Mast cell tryptases and chymases in inflammation and host defense. *Immunological Reviews,* 217**,** 141-154.

CERRETTI, D. P., KOZLOSKY, C. J., MOSELY, B., NELSON, N., VAN NESS, K., GREENSTREET, T. A., MARCH, C. J., KRONHEIM, S. R., et al. 1992. Molecular Cloning of the Interleukin- 1b Converting Enzyme. *Science,* 256**,** 97-100.

CHAN, J., ATIANAND, M., JIANG, Z., CARPENTER, S., AIELLO, D., ELLING, R., FITZGERALD, K. A. & CAFFREY, D. R. 2015. Cutting Edge: A Natural Antisense Transcript, AS-IL1a, Controls Inducible Transcription of the Proinflammatory Cytokine IL-1a. *The Journal of Immunology,* 195**,** 1-5.

CHANPUT, W., PETERS, V. & WICHERS, H. 2015. THP-1 and U937 Cells. *In:* VERHOECHX, K., COTTER , P., LOPEZ-EXPOSITO, I., KLEIVELAND, C., LEA, T., MACKIE, A., REQUENA, T., SWIATECKA, D. & WICHERS, H. (eds.) *The Impact of Food Bioactives on Health.* Springer International Publishing.

CHARBONNEAU, B., BLOCK, M. S., BAMLET, W. R., VIERKANT, R. A., KALLI, K. R., FOGARTY, Z., RIDER, D. N., SELLERS, T. A., et al. 2014. Risk of ovarian cancer and the NF-kappaB pathway: genetic association with IL1A and TNFSF10. *Cancer Res,* 74**,** 852-61.

CHEN, J., TUNG, C.-H., MAHMOOD, U., NTZIACHRISTOS, V., GYURKO, R., FISHMAN, M. C., HUANG, P. L. & WEISSLEDER, R. 2002. In Vivo Imaging of Proteolytic Activity in Atherosclerosis. *Circulation,* 105**,** 2766-2771.

CHEN, K. W., GROß, C. J., SOTOMAYOR, F. V., STACEY, K. J., TSCHOPP, J., SWEET, M. J. & SCHRODER, K. 2014. The Neutrophil NLRC4 Inflammasome Selectively Promotes IL-1b Maturation without Pyroptosis during Acute Salmonella Challenge. *Cell Reports,* 8**,** 570-582.

CHEN, Q., FISCHER, A., REAGAN, J. D., YAN, L. J. & AMES, B. N. 1995. Oxidative DNA damage and senescence of human diploid fibroblast cells. *Proc Natl Acad Sci U S A,* 92**,** 4337-4341.

CHILDS, B. G., BAKER, D. J., WIJSHAKE, T., CONOVER, C. A., CAMPISI, J. & VAN DEURSEN, J. M. 2016. Senescent intimal foam cells are deleterious at all stages of atherosclerosis. *Science,* 354**,** 472-477.

CHOE, Y., LEONETTI, F., GREENBAUM, D. C., LECAILLE, F., BOGYO, M., BROMME, D., ELLMAN, J. A. & CRAIK, C. S. 2006. Substrate Profiling of Cysteine Proteases Using a Combinatorial Peptide Library Identifies Functionally Unique Specificities. *Journal of Biological Chemistry,* 281**,** 12824-12832.

CHOY, J. C., MCDONALD, P. C., SUAREZ, A. C., HUNG, V. H. Y., WILSON, J. E., MCMANUS, B. M. & GRANVILLE, D. J. 2003. Granzyme B in Atherosclerosis and Transplant Vascular Disease: Association with Cell Death and Atherosclerotic Disease Severity. *Modern Pathology,* 16**,** 460-470.

CLARKE, M. C. H., TALIB, S., FIGG, N. L. & BENNETT, M. R. 2010. Vascular Smooth Muscle Cell Apoptosis Induces Interleukin-1–Directed Inflammation: Effects of Hyperlipidemia-Mediated Inhibition of Phagocytosis. *Circulation Research,* 106**,** 363-372.

COHEN, I., RIDER, P., CARMI, Y., BRAIMAN, A., DOTAN, S., WHITE, M. R., VORONOV, E., MARTIN, M. U., et al. 2010. Differential release of chromatin-bound IL-1alpha discriminates between necrotic and apoptotic cell death by the ability to induce sterile inflammation. *Proc Natl Acad Sci U S A,* 107**,** 2574-9.

COHEN, I., RIDER, P., VORONOV, E., TOMAS, M., TUDOR, C., WEGNER, M., BRONDANI, L., FREUDENBERG, M., et al. 2015. IL-1α is a DNA damage sensor linking genotoxic stress signaling to sterile inflammation and innate immunity. *Nature Scientific Reports,* 5**,** 1-11.

COLEMAN, K. M., GUDJONSSON, J. E. & STECHER, M. 2015. Open-Label Trial ofMABp1, a True Human Monoclonal Antibody Targeting Interleukin 1α, for the Treatment of Psoriasis. *JAMA Dermatology,* 151**,** 555-556.

COLLADO, M., BLASCO, M. A. & SERRANO, M. 2007. Cellular senescence in cancer and aging. *Cell,* 130**,** 223-233.

COLLADO, M. & SERRANO, M. 2006. The power and the promise of oncogene-induced sensence markers. *Nature Reviews Cancer,* 6**,** 472-476.

COPPÉ, J.-P., DESPREZ, P.-Y., KRTOLICA, A. & CAMPISI, J. 2010. The Senescence-Associated Secretory Phenotype: The Dark Side of Tumor Suppression. *Annu Rev Pathol.,* 5**,** 99–118.

DEBELA, M., BEAUFORT, N., MAGDOLEN, V., SCHECHTER, N. M., CRAIK, C. S., SCHMITT, M., BODE, W. & GOETTIG, P. 2008. Structures and specificity of the human kallikrein-related peptidases KLK 4, 5, 6, and 7. *Biol Chem,* 389**,** 623-632.

DEBER, C. M., BRODSKY, B. & RATH, A. 2010. Proline Residues in Proteins. *Encyclopedia of Life Sciences.* Chichester: John Wiley & Sons Ltd.

DENECKER, G., OVAERE, P., VANDENABEELE, P. & DECLERCQ, W. 2008. Caspase-14 reveals its secrets. *Journal of Cell Biology,* 180**,** 451-458.

DI CERA, E. 2009. Serine Proteases. *International Union of Biochemistry and Molecular Biology Life,* 61**,** 510-515.

DI MICCO, R., CICALESE, A., FUMAGALLI, M., DOBREVA, M., VERRECCHIA, A., PELICCI, P. G. & DI FAGAGNA, F. 2008. DNA damage response activation in mouse embryonic fibroblasts undergoing replicative senescence and following spontaneous immortalization. *Cell Cycle,* 7**,** 3601-3606.

DI PAOLO, N. C. & SHAYAKHMETOV, D. M. 2016. Interleukin 1α and the inflammatory process. *Nature Immunology,* 17**,** 906-913.

DIMRI, G. P., LEE, X., BASILE, G., ACOSTA, M., SCOTT, G. K., ROSKELLEY, C., MEDRANO, E. E., LINSKENS, M., et al. 1995. A biomarker that identifies senescent human cells in culture and in aging skin in vivo. *Proc Natl Acad Sci U S A,* 92**,** 9363-9367.

DINARELLO, C. A. 2009. Immunological and inflammatory functions of the interleukin-1 family. *Annu Rev Immunol,* 27**,** 519-50.

DINARELLO, C. A. 2010. IL-1: Discoveries, controversies and future directions. *European Journal of Immunology,* 40**,** 595-653.

DINARELLO, C. A., SIMON, A. & VAN DER MEER, J. W. M. 2012. Treating inflammation by blocking interleukin-1 in a broad spectrum of diseases. *Nature Reviews Drug Discovery,* 11**,** 633-652.

DING, J., WANG, K., LIU, W., SHE, Y., SUN, Q., SHI, J., SUN, H., WANG, D.-C., et al. 2016. Pore-forming activity and structural autoinhibition of the gasdermin family. *Nature,* 535**,** 111-116.

DIRAC, A. M. G. & BERNARDS, R. 2003. Reversal of Senescence in Mouse Fibroblasts through Lentiviral Suppression of p53. *Journal of Biological Chemistry,* 278**,** 11731-11734.

DOLLERY, C. M., OWEN, C. A., SUKHOVA, G. K., KRETTEK, A., SHAPIRO, S. D. & LIBBY, P. 2003. Neutrophil Elastase in Human Atherosclerotic Plaques. *Circulation,* 107**,** 2829-2836.

DONG, L. M., BRENNAN, P., KARAMI, S., HUNG, R. J., MENASHE, I., BERNDT, S. I., YEAGER, M., CHANOCK, S., et al. 2009. An Analysis of Growth, Differentiation and Apoptosis Genes with Risk of Renal Cancer. *Plos One,* 4**,** 1-10.

DUEWELL, P., KONO, H., RAYNER, K. J., SIROIS, C. M., VLADIMER, G., BAUERNFEIND, F. G., ABELA, G. S., FRANCHI, L., et al. 2010. NLRP3 inflammasomes are required for atherogenesis and activated by cholesterol crystals. *Nature,* 464**,** 1357-1362.

DUFFY, D., ROUILLY, V., LIBRI, V., HASAN, M., BEITZ, B., DAVID, M., URRUTIA, A., BISIAUX, A., et al. 2014. Functional analysis via standardized whole-blood stimulation systems defines the boundaries of a healthy immune response to complex stimuli. *Immunity,* 40**,** 436-50.

DUPONT, N., JIANG, S., PILLI, M., ORNATOWSKI, W., BHATTACHARYA, D. & DERETIC, V. 2011. Autophagy-based unconventional secretory pathway for extracellular delivery of IL-1beta. *EMBO,* 30**,** 4701-4711.

EASTGATE, J. A., SYMONS, J. A., WOOD, N. C., CAPPER, S. J. & DUFF, G. W. 1991. Plasma levels of interleukin-1-alpha in rheumatoid arthritis. *British Journal of Rheumatology,* 30**,** 295-297.

EL SAYED, H., KERENSKY, R., STECHER, M., MOHANTY, P. & DAVIES, M. 2016. A randomized phase II study of Xilonix, a targeted therapy against interleukin 1α, for the prevention of superficial femoral artery restenosis after percutaneous revascularization. *Journal of Vascular Surgery,* 63**,** 133-141.

ENDAM, L. M., CORMIER, C., BOSSÉ, Y., FILALI-MOUHIM, A. & DESROSIERS, M. 2010. Association of IL1A, IL1B, and TNF Gene Polymorphisms With Chronic Rhinosinusitis With and Without Nasal Polyposis. *Archives of Otolaryngology - Head & Neck Surgery,* 136**,** 187-192.

FELLMANN, C., HOFFMAN, T., SRIDHAR, V., HOPFGARTNER, B., MUHAR, M., ROTH, M., LAI, D. Y., BARBOSA, I. A. M., et al. 2013. An Optimized microRNA Backbone for Effective Single-Copy RNAi. *Cell Reports,* 5**,** 1704-1713.

FENTON, M. J. 1992. Review: Transcriptional and Post-Transcriptional Regulation of Interleukin 1 Gene Expression. *International Journal of Immunopharmacology,* 14**,** 401-411.

FERNANDES-ALNEMRI, T., WU, J., YU, J. W., DATTA, P., MILLER, B., JANKOWSKI, W., ROSENBERG, S., ZHANG, J., et al. 2007. The pyroptosome: a supramolecular assembly of ASC dimers mediating inflammatory cell death via caspase-1 activation. *Cell Death & Differentiation,* 14**,** 1590–1604.

FETTELSCHOSS, A., KISTOWSKA, M., LEIBUNDGUT-LANDMANN, S., BEER, H. D., JOHANSEN, P., SENTI, G., CONTASSOT, E., BACHMANN, M. F., et al. 2011. Inflammasome activation and IL-1beta target IL-1alpha for secretion as opposed to surface expression. *Proc Natl Acad Sci U S A,* 108**,** 18055-60.

FRANKLIN, B. S., BOSSALLER, L., NARDO, D. D., RATTER, J. M., STUTZ, A., ENGELS, G., BRENKER, C., NORDHOFF, M., et al. 2014. ASC has extracellular and prionoid activities that propagate inflammation. *Nature Immunology,* 15**,** 727-737.

FREIGANG, S., AMPENBERGER, F., WEISS, A., KANNEGANTI, T. D., IWAKURA, Y., HERSBERGER, M. & KOPF, M. 2013. Fatty acid-induced mitochondrial uncoupling elicits inflammasome-independent IL-1alpha and sterile vascular inflammation in atherosclerosis. *Nat Immunol,* 14**,** 1045-53.

FREUND, A., LABERGE, R.-M., DEMARIA, M. & CAMPISI, J. 2012. Lamin B1 loss is a senescence-associated biomarker. *Molecular Biology of the Cell,* 23**,** 2066-2075.

GABAY, C., LAMACCHIA, C. & PALMER, G. 2010. IL-1 pathways in inflammation and human diseases. *Nat Rev Rheumatol,* 6**,** 232-41.

GAIDT, M. M., EBERT, T. S., CHAUHAN, D., COOPER, M. A., GRAF, T. & HORNUNG, V. 2016. Human Monocytes Engage an Alternative Inflammasome Pathway. *Immunity,* 44**,** 833-846.

GARDNER, S. E., HUMPHRY, M., BENNETT, M. R. & CLARKE, M. C. 2015. Senescent Vascular Smooth Muscle Cells Drive Inflammation Through an Interleukin-1α-Dependent Senescence-Associated Secretory Phenotype. *Arteriosclerosis, Thrombosis, and Vascular Biology,* 35**,** 1963-1974.

GARLANDA, C., DINARELLO, C. A. & MANTOVANI, A. 2013. The interleukin-1 family: back to the future. *Immunity,* 39**,** 1003-18.

GHAYUR, T., BANERJEE, I., HUGUNIN, M., BUTLER , D., HERZOG, L., CARTER, A., QUINTAL, L., SEKUT, L., et al. 1997. Caspase-1 processes IFN-gamma-inducing factor and regulates LPS-induced IFN-gamma production. *Nature,* 386**,** 619-623.

GIMBRONE, M. A. J. 1999. Vascular endothelium, hemodynamic forces and atherogenesis. *American Journal of Pathology,* 155**,** 1-5.

GLUCK, S., GUEY, B., GULEN, M. F., WOLTER, K., KANG, T.-W., SCHMACKE, N. A., BRIDGEMAN, A., REHWINKEL, J., et al. 2017. Innate immune sensing of cytosolic chromatin fragments through cGAS promotes senescence. *Nat Cell Biol,* advance online publication.

GONG, Y. N., GUY, C., OLAUSON, H., BECKER, J. U., YANG, M., FITZGERALD, P., LINKERMANN, A. & GREEN, D. R. 2017. ESCRT-III Acts Downstream of MLKL to Regulate Necroptotic Cell Death and Its Consequences. *Cell,* 169**,** 286-300.

GROSS, O., YAZDI, A. S., THOMAS, C. J., MASIN, M., HEINZ, L. X., GUARDA, G., QUADRONI, M., DREXLER, S. K., et al. 2012. Inflammasome activators induce interleukin-1alpha secretion via distinct pathways with differential requirement for the protease function of caspase-1. *Immunity,* 36**,** 388-400.

GROVES, R. W., MIZUTANI, H., KIEFFER, J. D. & KUPPER, T. S. 1995. Inflammatory skin disease in transgenic mice that express high levels of interleukin 1 alpha in basal epidermis. *Proc Natl Acad Sci U S A,* 92**,** 11874-11878.

GROVES, R. W., RAUSCHMAYR, T., NAKAMURA, T., SARKAR, S., WILLIAMS, I. R. & KUPPER, T. S. 1996. Inflammatory and hyperproliferative skin disease in mice that express elevated levels of the IL-1 receptor (type I) on epidermal keratinocytes. Evidence that IL-1-inducible secondary cytokines produced by keratinocytes in vivo can cause skin disease. *J Clin Invest,* 98**,** 336-344.

HAGAR, J. A., POWELL, D. A., AACHOUI, Y., ERNST, R. K. & MIAO, E. A. 2013. Cytoplasmic LPS activates caspase-11: implications in TLR4-independent endotoxic shock. *Science,* 341**,** 1250–1253.

HAROON, J., HUSSAIN, S. & JAVED, Q. 2015. Heritability of IL-1A Gene Promoter Polymorphism in Patients With Coronary Artery Disease: A Trio-Family Study. *Laboratory Medicine,* 46**,** 20-25.

HAYFLICK, L. & MOORHEAD, P. S. 1961. The serial cultivation of human diploid cell strains. *Experimental Cell Research,* 25**,** 585-621.

HILDEBRANDT, M. A. T., KOMAKI, R., LIAO, Z., GU, J., CHANG, J. Y., YE, Y., LU, C., STEWART, D. J., et al. 2010. Genetic Variants in Inflammation-Related Genes Are Associated with Radiation-Induced Toxicity Following Treatment for Non-Small Cell Lung Cancer. *PLoS One,* 5**,** 1-11.

HIRASAWA, Y., TAKAI, T., NAKAMURA, T., MITSUISHI, K., GUNAWAN, H., SUTO, H., OGAWA, T., WANG, X.-L., et al. 2010. Staphylococcus aureus Extracellular Protease Causes Epidermal Barrier Dysfunction. *Journal of Investigative Dermatology,* 130**,** 614-617.

HISCOTT, J., KWON, H. & GÉNIN, P. 2001. Hostile takeovers: viral appropriation of the NF-κB pathway. *The Journal of Clinical Investigation,* 107**,** 143-151.

HOARE, M., ITO, Y., KANG, T.-W., WEEKES, M. P., MATHESON, N. J., PATTEN, D. A., SHETTY, S., PARRY, A. J., et al. 2016. NOTCH1 mediates a switch between two distinct secretomes during senescence. *Nature Cell Biology,* 18**,** 979-992.

HOFFMAN, H. M., MUELLER, J. L., BROIDE, D. H., WANDERER, A. A. & KOLODNER, R. D. 2001. Mutation of a new gene encoding a putative pyrin-like protein causes familial cold autoinflammatory syndrome and Muckle–Wells syndrome. *Nature Genetics,* 29**,** 301-305.

HOFFMANN, J. A. 2003. The immune response of Drosophila. *Nature,* 426**,** 33-38.

HONG, D. S., HUI, D., BRUERA, E., JANKU, F., NAING, A., FALCHOOK, G. S., PIHA-PAUL, S., WHELER, J. J., et al. 2014. MABp1, a fi rst-in-class true human antibody targeting interleukin-1α in refractory cancers: an open-label, phase 1 dose-escalation and expansion study. *Lancet Oncology,* 15**,** 656-666.

HOWARD, A. D., KOSTURA, M. J., THORNBERRY, N., DING, G. J., LIMJUCO, G., WEIDNER, J., SALLEY, J. P., HOGQUIST, K. A., et al. 1991. IL-1-converting enzyme requires aspartic acid residues for processing of the IL-1 beta precursor at two distinct sites and does not cleave 31-kDa IL-1 alpha. *Journal of Immunology,* 147**,** 2964-2969.

ILIOPOULOS, D., HIRSCH, H. A. & STRUHL, K. 2009. An epigenetic switch involving NF-kappa B, Lin 28, Let-7 MicroRNA, and IL6 links inflammation to cell transformation. *Cell,* 139**,** 693-706.

JAFFER, F. A., CALFON, M. A., ROSENTHAL, A., MALLAS, G., RAZANSKY, N., MAUSKAPF, A., WEISSLEDER, R., LIBBY, P., et al. 2011. Two-Dimensional Intravascular Near-Infrared Fluorescence Molecular Imaging of Inflammation in Atherosclerosis and Stent-Induced Vascular Injury. *Journal of the American College of Cardiology,* 57**,** 2516-2526.

JANEWAY, C. A. J., TRAVERS, P. & WALPORT, M. 2001. Principles of innate and adaptive immunity. *Immunobiology: The Immune System in Health and Disease.* 5th ed. New York: Garland Science.

JANSSENS, S. & BEYAERT, R. 2003. Role of Toll-like receptors in pathogen recognition. *Clinical Microbiology Reviews,* 16**,** 637-646.

JENSON, L. E. 2011. Targeting the IL-1 family members in skin inflammation. *Curr Opin Investig Drugs.,* 11**,** 1211–1220.

JIANG, X., CHENKE, X., LEI, F., MEIJIAN, L., WANG, W., XU, N., ZHANG, Y. & XIE, W. 2017. MiR-30a targets IL-1a and regulates islet functions as an inflammation buffer and response factor. *Nature Scientific Reports,* 7**,** 1-15.

JUN, J. I. & LAU, L. F. 2010. Cellular senescence controls fibrosis in wound healing. *Aging,* 2**,** 627-631.

KAMARI, Y., SHAISH, A., SHEMESH, S., VAX, E., GROSSKOPF, I., DOTAN, S., WHITE, M., VORONOV, E., et al. 2011. Reduced atherosclerosis and inflammatory cytokines in apolipoprotein-E-deficient mice lacking bone marrow-derived interleukin-1a. *Biochemical and Biophysical Research Communications,* 405**,** 197-203.

KAMENS, J., PASKIND, M., HUGUNIN, M., TALANIAN, R. V., ALLEN, H., BANACH, D., BUMP, N., HACKETT, M., et al. 1995. Identification and Characterisation of ICH-2, a Novel Member of the Interleukin-1b-converting Enzyme Family of Cysteine Proteases. *The Journal of Biological Chemistry,* 270**,** 15250-15256.

KANG, S.-J., WANG, S., HARA, H., PETERSON, E. P., NAMURA, S., AMIN-HANJANI, S., HUANG, Z., SRINIVASAN, A., et al. 2000. Dual Role of Caspase-11 in Mediating Activation of Caspase-1 and Caspase-3 Under Pathological Conditions. *The Journal of Cell Biology,* 149**,** 613-622.

KANG, T. W., YEVSA, T., WOLLER, N., HOENICKE, L., WUESTEFELD, T., DAUCH, D., HOHMEYER, A., GEREKE, M., et al. 2011. Senescence surveillance of pre-malignant hepatocytes limits liver cancer development. *Nature,* 479**,** 547-551.

KARJALAINEN, J., JOKI-ERKKIL, V. P., HULKKONEN, J., PESSI, T., NIEMINEN, M. M., AROMAA, A., KLAUKKA, T. & HURME, M. 2003. The IL1A genotype is associated with nasal polyposis in asthmatic adults. *Allergy,* 58**,** 393-396.

KARMAKAR, M., KATSNELSON, M. A., DUBYAK, J. R. & PEARLMAN, E. 2016. Neutrophil P2X7 receptors mediate NLRP3 inflammasome-dependent IL-1b secretion in response to ATP. *Nat Commun,* 7.

KATLINSKAYA, Y. V., KALTLINSKI, K. V., YU, Q., ORTIZ, A., BEITING, D. P., BRICE, A., DAVAR, D., SANDERS, C., et al. 2016. Suppression of Type I Interferon Signaling Overcomes Oncogene-Induced Senescence and Mediates Melanoma Development and Progression. *Cell,* 15**,** 171-180.

KAWAGUCHI, Y., TOCHIMOTO, A., HARA, M., KAWAMOTO, M., SUGIURA, T., SAITO, S. & KAMATANI, N. 2007. Contribution of single nucleotide polymorphisms of the IL1A gene to the cleavage of precursor IL-1alpha and its transcription activity. *Immunogenetics,* 59**,** 441-8.

KAWAGUCHI, Y., TOCHIMOTO, A., ICHIKAWA, N., HARIGAI, M., HARA, M., KOTAKE, S., KITAMURA, Y. & KAMATANI, N. 2003. Association of IL1A Gene Polymorphisms With Susceptibility to and Severity of Systemic Sclerosis in the Japanese Population. *Arthritis & Rheumatism,* 48**,** 189-192.

KAYAGAKI, N., STOWE, I. B., LEE, B. L., O'ROURKE, K., ANDERSON, K., WARMING, S., CUELLAR, T., HALEY, B., et al. 2015. Caspase-11 cleaves gasdermin D for non-canonical inflammasome signalling. *Nature,* 526**,** 666-670.

KAYAGAKI, N., WARMING, S., LAMKANFI, M., VANDEWALLE, L., LOUIE, D., DONG, J., NEWTON, K., QU, Y., et al. 2011. Non-canonical inflammasome activation targets caspase-11. *Nature,* 479**,** 117-122.

KAYAGAKI, N., WONG, M. T., STOWE, I. B., RAMANI, D. R., GONZALEZ, L. C., AKASHI-TAKAMURA, S., MIYAKE, K., ZHANG, J., et al. 2013. Noncanonical Inflammasome Activation by Intracellular LPS Independent of TLR4. *Science,* 341**,** 1246-1249.

KELLER, M., RUEGG, A., WERNER, S. & BEER, H. D. 2008. Active caspase-1 is a regulator of unconventional protein secretion *Cell,* 132**,** 818-831.

KENNY, H. A., KAUR, S., COUSSENS, L. M. & LENGYEL, E. 2008. The initial steps of ovarian cancer cell metastasis are mediated by MMP-2 cleavage of vitronectin and fibronectin. *J Clin Invest,* 118**,** 1367-79.

KERR, F. K., O'BRIEN, G., QUINSEY, N. S., WHISSTOCK, J. C., BOYD, S., DE LA BANDA, M. G., KAISERMAN, D., MATTHEWS, A. Y., et al. 2005. Elucidation of the substrate specificity of the C1s protease of the classical complement pathway. *J Biol Chem,* 280**,** 39510-4.

KETTERER, S., GOMEZ-AULI, A., HILLEBRAND, L. E., PETRERA, A., KETSCHER, A. & REINHECKEL, T. 2016. Inherited diseases caused by mutations in cathepsin protease genes. *FEBS*.

KIM, B., LEE, Y., KIM, Y., KWAK, A., YROO, S., BAE, S. H., AZAM, T., KIM, S., et al. 2013. The interleukin-1α precursor is biologically active and is likely a key alarmin in the IL-1 family of cytokines. *Frontiers in Immunology,* 4.

KNODLER, L. A., CROWLEY, S. M., SHAM, H. P., YANG, H., WRANDE, M., MA, C., ERNST, R. K., STEELE-MORTIMER, O., et al. 2014. Non-canonical inflammasome activation of caspase-4/caspase-11 mediates epithelial defenses against enteric bacterial pathogens. *Cell Host Microbe,* 16**,** 249-256.

KNUCKLEURG, C. J. & NEWMAN, P. J. 2012. Neutrophil Proteinase 3 Acts on Protease-Activated Receptor-2 to Enhance Vascular Endothelial Cell Barrier Function. *Arteriosclerosis, Thrombosis, and Vascular Biology,* 33**,** 275-284.

KOBAYASHI, Y., YAMAMOTO, K., SAIDO, T., KAWASAKI, H., OPPENHEIM, J. & MATSUSHIMA, K. 1990. Identification of calcium-activated neutral protease as processing enzyme of human interleukin-1 alpha. *Proc Natl Acad Sci U S A,* 87**,** 5548-5552.

KOHL, N. E., EMINI, E. A., SCHLEIF, W. A., DAVIS, L. J., HEIMBACK, J. C., DIXON, R. A. F., SCOLNICK, E. M. & SIGAL, I. S. 1988. Active human immunodeficiency virus protease is required for viral infectivity. *Proc Natl Acad Sci U S A,* 85**,** 4686-4690.

KOMATSU, N., SAIJOH, K., KUK, C., SHIRASAKI, F., TAKEHARA, K. & DIAMANDIS, E. P. 2007. Aberrant human tissue kallikrein levels in the stratum corneum and serum of patients with psoriasis: dependence on phenotype, severity and therapy. *British Journal of Dermatology,* 156**,** 875–883.

KORKMAZ, B., HORWITZ, M. S., JENNE, D. E. & GAUTHIER, F. 2010. Neutrophil Elastase, Proteinase 3, and Cathepsin G as Therapeutic Targets in Human Diseases. *Pharmacological Reviews,* 62**,** 726-759.

KUIDA, K., LIPPKE, J. A., KU, G., HARDING, M. W., LIVINGSTON, D. J., SU, M. S. & FLAVELL, R. A. 1995. Altered cytokine export and apoptosis in mice deficient in interleukin-1 beta converting enzyme. *Science,* 267**,** 2000-2003.

LABRIOLA-TOMPKINS, E., CHANDRAN, C., VARNELL, T. A., MADISON, V. S. & JU, G. 1993. Structure-function analysis of human IL-1 alpha: identification of residues required for binding to the human type I IL-1 receptor. *Protein Engineering,* 6**,** 535-539.

LAMKANFI, M. & DIXIT, V. M. 2011. Modulation of Inflammasome Pathways by Bacterial and Viral Pathogens. *The Journal of Immunology,* 187**,** 597-602.

LANE, D. A., PHILIPPOU, H. & HUNTINGTON, J. A. 2005. Directing Thrombin. *Blood,* 106**,** 2605-2612.

LEE, A. C., FENSTER, B. E., ITO, H., TAKEDA, K., BAE, N. S., HIRAI, T., YU, Z. X., FERRANS, V. J., et al. 1999. Ras proteins induce senescence by altering the intracellular levels ofreactive oxygen species. *Journal of Biological Chemistry,* 274**,** 7936-7940.

LEÓN, X., QUER, M., BOTHE, C., VILA, L., GARCÍA, J., PARREÑO, M. & CAMACHO, M. 2015. Expression of IL-1α correlates with distant metastasis in patients with head and neck squamous cell carcinoma. *Oncotarget,* 6**,** 37398-37409.

LI, P., ALLEN, H., BANERJEE, I., FRANKLIN, B. S., HERZOG, L., JOHNSTON, C. G., MCDOWELL, J., PASKIND, M., et al. 1995. Mice deficient in IL-1 beta-converting enzyme are defective in production of mature IL-1 beta and resistant to endotoxic shock. . *Cell,* 80**,** 401-411.

LI, X., THOME, S., MA, X. D., AMRUTE-NAYAK, M., FINIGAN, A., KITT, L., MASTERS, L., JAMES, J. R., et al. 2017. MARK4 regulates NLRP3 positioning and inflammasome activation through a microtubule-dependent mechanism. *Nat Commun,* 28**,** 15986.

LIBBY, P., RIDKER, P. M. & HANSSON, G. K. 2011. Progress and challenges in translating the biology of atherosclerosis. *Nature,* 473**,** 317-325.

LIBBY, P., RIDKER, P. M. & MASERI, A. 2002. Inflammation and Atherosclerosis. *Circulation,* 105**,** 1135-1143.

LIN, D., LEI, L., ZHANG, Y., HU, B., BAO, G., SONG, Y., JIN, Z., LIU, C., et al. 2016. Membrane IL-1a inhibits the development of hepatocellular carcinoma via promoting T- and NK- cell activation. *Cancer Res,* 76**,** 3179-3188.

LIN, X. Y., CHOI, M. S. K. & PORTER, A. G. 2000. Expression Analysis of the Human Caspase-1 Subfamily Reveals Specific Regulation of the CASP5 Gene by Lipopolysaccharide and Interferon-g. *The Journal of Biological Chemistry,* 275**,** 39920-39926.

LIU, S., GINESTIER, C., OU, S. J., CLOUTHEIR, S. G., PATEL, S. H., MONVILLE, F., KORKAYA, H., HEATH, A., et al. 2011. Breast cancer stem cells are regulated by mesenchymal stem cells through cytokine networks. *Cancer Res,* 71**,** 614-624.

LIU, X. & LIEBERMAN, J. 2017. How ICE lights the pyroptosis fire. *Cell Death & Differentiation,* 24**,** 197-199.

LIU, X., ZHANG, Z., RUAN, J., PAN, Y., MAGUPALLI, V. G., WU, H. & LIEBERMAN, J. 2016. Inflammasome-activated gasdermin D causes pyroptosis by forming membrane pores. *Nature,* 535**,** 153-157.

LIU, Y., LI, S., ZHANG, G., NIE, G., MENG, Z., MAO, D., CHEN, C., CHEN, X., et al. 2013. Genetic variants in IL1A and IL1B contribute to the susceptibility to 2009 pandemic H1N1 influenza A virus. *BMC Immunology,* 14.

LORD, S. J., RAJOTTE, R. V., KORBUTT, G. S. & BLEACKLEY, C. 2003. Granzyme B: a natural born killer. *Immunological Reviews,* 193**,** 31-38.

LU, A. & WU, H. 2015. Structural mechanisms of inflammasome assembly. *FEBS,* 282**,** 435–444.

LUGRIN, J., PARAPANOV, R., ROSENBLATT-VELIN, N., RIGNAULT-CLERC, S., FEIHL, F., WAEBER, B., MÜLLER, O., VERGELY, C., et al. 2015. Cutting edge: IL-1α is a crucial danger signal triggering acute myocardial inflammation during myocardial infarction. *The Journal of Immunology,* 194**,** 499-503.

LUHESHI, N. M., KOVÁCS, K. J., LOPEZ-CASTEJON, G., BROUGH, D. & DENES, A. 2011. Interleukin-1a expression precedes IL-1b after ischemic brain injury and is localised to areas of focal neuronal loss and penumbral tissues. *Journal of Neuroinflammation,* 8**,** 1-5.

LUHESHI, N. M., ROTHWELL, N. J. & BROUGH, D. 2009. Dual functionality of interleukin-1 family cytokines: implications for anti-interleukin-1 therapy. *British Journal of Pharmacology,* 157**,** 1318-1329.

LUSIS, A. J. 2000. Atherosclerosis. *Nature,* 407**,** 233-241.

MAMYROVA, G., O'HANLON, T. P., SILLERS, L., MALLEY, K., JAMES-NEWTON, L., PARKS, C. G., COOPER, G. S., PANDEY, J. P., et al. 2008. Cytokine Gene Polymorphisms as Risk and Severity Factors for Juvenile Dermatomyositis. *Arthritis & Rheumatology,* 58**,** 3941-3950.

MAN, S. M. & KANNEGANTI, T. D. 2015. Regulation of inflammasome activation. *Immunological Reviews,* 265**,** 6-21.

MAO, K., CHEN, S., CHEN, M., MA, Y., WANG, Y., HUANG, B., HE, Z., ZENG, Y., et al. 2013. Nitric oxide suppresses NLRP3 inflammasome activation and protects against LPS-induced septic shock. *Cell Research,* 23**,** 201-212.

MARCH, C. J., MOSLEY, B., LARSEN, A., CERRETTI, D. P., BRAEDT, G., PRICE, V., GILLIS, S., HENNEY, C. S., et al. 1985. Cloning, sequence and expression of two distincy human interleukin-1 complementary DNAs. *Nature,* 315**,** 641-647.

MARTÍN-SÁNCHEZ, F., DIAMOND, C., ZEITLER, M., GOMEZ, A., BAROJA-MAZO, A., BAGNALL, J., SPILLER, D., WHITE, M., et al. 2016. Inflammasome-dependent IL-1β release depends upon membrane permeabilisation. *Cell Death & Differentiation***,** 1-13.

MARTIN, J. A. & BUCKWALTER, J. A. 2003. The role of chondrocyte senescence in the pathogenesis of osteoarthritis and in limiting cartiallage repair. *J Bone Joint Surg Am.,* 85**,** 106-110.

MAURO, A. G., MEZZAROMA, E., TORRADO, J., KUNDAR, P., JOSHI, P., STROUD, K., QUAINI, F., LAGRASTA, C., et al. 2017. Reduction of Myocardial Ischemia–Reperfusion Injury by Inhibiting Interleukin-1 Alpha. *Cardiovasc Pharmacol,* 69**,** 156-160

MCLAREN, P. J., GAWANBACHT, A., PYNDIAH, N., KAPP, C., HOTTER, D., KLUGE, S. F., GÖTZ, N., HEILMANN, J., et al. 2015. Identification of potential HIV restriction factors by combining evolutionary genomic signatures with functional analyses. *Retrovirology,* 12.

MCMAHON, G. A., GARFINKEL, S., PRUDOVSKY, I., HU, X. & MACIAG, T. 1997. Intracellular Precursor Interleukin (IL)-1α, but Not Mature IL-1α, Is Able to Regulate Human Endothelial Cell Migration in Vitro. *Journal of Biological Chemistry,* 272**,** 28202-28205.

MEDZHITOV, R. 2008. Origin and physiological roles of inflammation. *Nature,* 454**,** 428-435.

MEUNIER, E., DICK, M. R., DREIER, R. F., SCHURMANN, N., BROZ, D. K., WARMING, S., ROOSE-GIRMA, M., BUMANN, D., et al. 2014. Caspase-11 activation requires lysis of pathogen-containing vacuoles by IFN-induced GTPases. *Nature,* 509**,** 366-370.

MILLS, K. H. 2008. Induction, function and regulatin of IL-17-producing T cells. *European Journal of Immunology,* 38**,** 2636-2649.

MIROWSKA-GUZEL, D., GROMADZKA, G., MACH, A., CZLONKOWSKI, A. & CZLONKOWSKA, A. 2011. Association of IL1A, IL1B, ILRN, IL6, IL10 and TNF-α polymorphisms with risk and clinical course of multiple sclerosis in a Polish population. *Journal of Neuroimmunology,* 236**,** 87-92.

MITTAL, R. D., SRIVASTAVA, P., MITTAL, T., VERMA, A., JAISWAL, P. K., SINGH, V., MANDAL, R. K. & MANDHANI, A. 2011. Association of death receptor 4, Caspase 3 and 5 gene polymorphism with increased risk to bladder cancer in North Indians. *Journal of Cancer Surgery,* 37**,** 727-733.

MOSLEY, B., DOWER, S. K., GILLIS, S. & COSMAN, D. 1987a. Determination of the minimum polypeptide lengths of the functionally active sites of human interleukins 1 alpha and 1 beta. *Proc Natl Acad Sci U S A,* 84**,** 4572–4576.

MOSLEY, B., URDAL, D. L., PRICKETT, K. S., LARSEN, A., COSMAN, D., CONLON, P., J., GILLIS, S. & DOWER, S. K. 1986. The Interleukin- 1 Receptor Binds the Human Interleukin- la Precursor but Not the Interleukin- 1b Precursor. *The Journal of Biological Chemistry,* 262**,** 2941-2944.

MOSLEY, B., URDAL, D. L., PRICKETT, K. S., LARSEN, A., COSMAN, D., CONLON, P. J., GILLIS, S. & DOWER, S. K. 1987b. The interleukin-1 receptor binds the human interleukin-1α precursor but not the interleukin-1β precursor. *Journal of Biological Chemistry,* 262**,** 2941-2944.

MOSS, S. F. & BLASER, M. J. 2005. Mechanisms of Disease: inflammation and the origins of cancer. *Nature Clinical Practice Oncology* 2**,** 90-97.

MOSTEIRO, L., PANTOGA, C., ALCAZAR, N., MARION, N., CHONDRONASIOU, D., ROVIRA, M., FERNANDEZ-MARCOS, P. J., MUNOZ-MARTIN, M., et al. 2016. Tissue damage and senescence provide critical signals for cellular reprogramming in vivo. *Science,* 354.

MUNOZ-ESPIN, D., CANAMERO, M., MARAVER, A., GOMEZ-LOPEZ, G., CONTRERAS, J., S., M.-C., RODRıGUEZ-BAEZA, A., VARELA-NIETO, I., et al. 2013. Programmed cell senescence during mammalian embryonic development. . *Cell,* 155**,** 1104-1118.

MUNOZ-PLANILLO, R., KUFFA, P., MARTINEZ-COLON, G., SMITH, B. L., RAJENDIRAN, T. M. & NUNEZ, G. 2013. K+ efflux is the common trigger of NLRP3 inflammasome activation by bacterial toxins and particulate matter. *Immunity,* 38**,** 1142-1153.

NAKAE, S., SAIJO, S., HORAI, R., SUDO, K., MORI, S. & IWAKURA, Y. 2002. IL-17 production from activated T cells is required for the spontaneous development of destructive arthritis in mice deficient in IL-1 receptor antagonist. *Proc Natl Acad Sci U S A,* 100**,** 5986-5990.

NAKAGAWA, T., ZHU, H., MORISHIMA, N., LI, E., XU, J., YANKNER, B. A. & YUAN, J. 2000. Caspase-12 mediates endoplasmic reticulum-specific apoptosis and cytotoxicity by amyloid-b. *Letters to Nature,* 403**,** 98-103.

NARITA, M., NUNEZ, G., HEARD, E., NARITA, M., LIN, A. W., HEARN, S. A., SPECTOR, D. L., HANNON, G. J., et al. 2003. Rb-mediated heterochromatin formation and silencing of E2F target genes during cellular senescence *Cell,* 113**,** 703-716.

NARITA, M., YOUNG, A. R., ARAKAWA, S., SAMARAJIWA, S. A., NAKASHIMA, T., YOSHIDA, S., HONG, S., BERRY, L. S., et al. 2011. Spatial coupling of mTOR and autophagy augments secretory phenotypes. *Science,* 332**,** 966-970.

NATHAN, C. 2002. Points of control in inflammation. *Nature,* 420**,** 846-852.
ODELL, A., ASKHAM, J., WHIBLEY, C. & HOLLSTEIN, M. 2010. How to become immortal: let MEFs count the ways. *Aging,* 2**,** 160-165.
OFFMAN, J., GASCOIGNE, K., BRISTOW, F., MACPHERSON, P., BIGNAMI, M., CASORELLI, I., LEONE, G., PAGANO, L., et al. 2005. Repeated Sequences in CASPASE-5 and FANCD2 but not NF1 Are Targets for Mutation in Microsatellite-Unstable Acute Leukemia/ Myelodysplastic Syndrome. *Mol Cancer Res,* 3**,** 251-260.
OGRYZKO, V. V., HIRAI, T. H., RUSSANOVA, V. R., BARBIE, D. A. & HOWARD, B. H. 1996. Human fibroblast commitment to a senescence-like state in response to histone deacetylase inhibitors is cell cycle dependent. *Molecular and Cellular Biology,* 16**,** 5210-5218.
OKADA, H., KUHN, C., FEILLET, H. & BACH, E.-F. 2010. The 'hygeine hypothesis' for autoimmune and allergic diseases: and update. *Clinical & Experimental Immunology,* 160**,** 1-9.
ORJALO, A. V., BHAUMIK, D., GENGLER, B. K., SCOTT, G. K. & CAMPISI, J. 2009. Cell surface-bound IL-1alpha is an upstream regulator of the senescence-associated IL-6/IL-8 cytokine network. *Proc Natl Acad Sci U S A,* 106**,** 17031–17036.
OZBABACAN, S. E. A., GURSOY, A., NUSSINOV, R. & KESKIN, O. 2014. The Structural Pathway of Interleukin 1 (IL-1) Initiated Signaling Reveals Mechanisms of Oncogenic Mutations and SNPs in Inflammation and Cancer. *Plos Computational Biology,* 10**,** 1-14.
PARRY, A. J. & NARITA, M. 2016. Old cells, new tricks: chromatin structure in senescence. *Mammalian Genome,* 27**,** 320-331.
PELLEGRINI, C., ANTONIOLI, L., LOPEZ-CASTEJON, G., BLANDIZZI, C. & FORNAI, M. 2017. Canonical and Non-Canonical Activation of NLRP3 Inflammasome at the Crossroad between Immune Tolerance and Intestinal Inflammation. *Frontiers in Immunology,* 8**,** 1-12.
PENG, S., KUANG, Z., ZHANG, Y., XU, H. & CHENG, Q. 2011. The protective effects and potential mechanism of Calpain inhibitor Calpeptin against focal cerebral ischemia-reperfusion injury in rats. *Mol Biol Rep,* 38**,** 905-912.
PÉREZ-MANCERA, P. A., YOUNG, A. R. J. & NARITA, M. 2014. Inside and out: the activities of senescence in cancer. *Nature Reviews Cancer,* 14**,** 547-558.
PILLON, N. J., CHAN, K. L., ZHANG, S., MEJDANI, M., JACOBSON, M. R., DUCOS, A., BILAN, P. J., NIU, W., et al. 2016. Saturated fatty acids activate caspase-4/5 in human monocytes, triggering IL-1b and IL-18 release. *American Journal of Physiology - Endocrinology and Metabolism,* 311**,** 825-835.
POLLOCK, A., TURCK, J. & LOVETT, D. H. 2003. The prodomain of interleukin 1 alpha interacts with elements of the RNA processing apparatus and induces apoptosis in malignant cells. *FASEB,* 17**,** 203-213.
PRESANIS, J., HAJELAA, K., AMBRUS, G., GÁL, P. & SIM, R. B. 2004. Differential substrate and inhibitor profiles for human MASP-1 and MASP-2. *Molecular Immunology,* 40**,** 921-929.
PRICE, J. S., WATERS, J. G., DARRAH, C., PENNINGTON, C., EDWARDS, D. R., DONELL, S. T. & CLARK, I. M. 2002. The role of chondrocyte senescence in osteoarthritis. *Aging Cell,* 1**,** 57-65.
PY, B. F., KIM, M.-S., VAKIFAHMETOGLU-NORBERG, H. & YUAN, J. 2013. Deubiquitination of NLRP3 by BRCC3 Critically Regulates Inflammasome Activity. *Molecular Cell,* 49**,** 331–338.
RAETZ, C. R., REYNOLDS, C. M., TRENT, M. S. & BISHOP, R. E. 2007. Lipid A modification systems in gram negative bacteria. *Annu Rev Biochem,* 76.
RAFIEIAN-KOPAEI, M., SETORKI, M., DOUDI, M., BARADARAN, A. & NASRI, H. 2014. Atherosclerosis: process, indicators, risk factors and new hopes. *Int J Prev Med.,* 5.
RAJAMAKI, K., LAPPALAINEN, J., OORNI, K., VALIMAKI, E., MATIKAINEN, S., KOVANEN, P. T. & EKLUND, K. K. 2010. Cholesterol crystals activate the NLRP3 inflammasome in human macrophages: a novel link between cholesterol metabolism and inflammation. *PloS One,* 5.

RATHINAM, V. A., VANAJA, S. K., WAGGONER, L., SOKOLOVSKA, A., BECKER, C., STUART, L. M., LEONG, J. M. & FITZGERALD, K. A. 2012. TRIF licenses caspase-11-dependent NLRP3 inflammasome activation by gram-negative bacteria. *Cell,* 150**,** 606-619.

RIDER, P., CARMIB, Y., VORONOVC, E. & APTE, R. N. 2013. Interleukin-1a. *Seminars in Immunology,* 25**,** 430-438.

RIDER, P., KAPLANOV, I., ROMZOVA, M., BERNARDIS, L., BRAIMAN, A., VORONOV, E. & APTE, R. N. 2012. The transcription of the alarmin cytokine interleukin-1 alpha is controlled by hypoxia inducible factors 1 and 2 alpha in hypoxic cells. *Frontiers in Immunology,* 3**,** 1-7.

RIDKER, P. M., EVERETT, B. M., THUREN, T., MACFADYEN, J. G., CHANG, W. H., BALLANTYNE, C., FONSECA, F., NICOLAU, J., et al. 2017. Antiinflammatory Therapy for Canakinumab for Atherosclerotic Disease. *The New England Journal of Medicine,* 377**,** 1119-1131.

RISBUD, M. V. & SHAPIRO, I. M. 2014. Role of cytokines in intervertebral disc degeneration: pain and disc content. *Nature reviews Rheumatology,* 10**,** 44-56.

RODIER, F. & CAMPISI, J. 2011. Four faces of cellular senescence. *Journal of Cell Biology,* 192**,** 547-557.

ROSENBLUM, M. D., REMEDIOS, K. A. & ABBAS, A. K. 2015. Mechanisms of human autoimmunity. *The Journal of Clinical Investigation,* 125**,** 2228-2233.

SAAVEDRA, P. H. V., DEMON, D., GORP, H. V. & LAMKANF, M. 2015. Protective and detrimental roles of inflammasomes in disease. *Semin Immunopathol,* 37**,** 313–322.

SCHMITT, A., HAUSER, C., JAUNIN, F., DAYER, J. M. & SAURAT, J. H. 1986. Normal epidermis contains high amounts of natural tissue IL 1 biochemical analysis by HPLC identifies a MW approximately 17 Kd form with a P1 5.7 and a MW approximately 30 Kd form. *Lymphokine Research,* 5**,** 105-118.

SCHRODER, K. 2017. Myeloid Cell Identity Shapes Inflammasome Signaling PAthways and Cell Death Decisions. *Cell Death and Inflammation.* Dublin, Ireland: Keystone.

SERRANO, M., LIN, A. W., MCCURRACH, M. E., BEACH, D. & LOWE, S. W. 1997. Oncogenic ras provokes premature cell senescence associated with accumulation of p53 and p16 INK4a. *Cell,* 88**,** 593-602.

SHARMA, D. & KANNEGANTI, T. D. 2016. The cell biology of inflammasomes: Mechanisms of inflammasome activation and regulation. *Journal of Cell Biology,* 213**,** 617-629.

SHEN, J., DEININGER, P. L. & ZHAO, H. 2006. Applications of computational algorithm tools to identify functional SNPs in cytokine genes. *Cytokine,* 35**,** 62-66.

SHI, C. S., SHENDEROV, K., HUANG, N. N., KABAT, J., ABU-ASAB, M., FITZGERALD, K. A., SHER, A. & KEHRL, J. H. 2012. Activation of Autophagy by inflammatory signals limits IL-1beta production by targeting ubiquitinated inflammasomes for destruction. *Nat Immunol,* 13**,** 255-263.

SHI, J., ZHAO, Y., WANG, K., SHI, X., WANG, Y., HUANG, H., ZHUANG, Y., CAI, T., et al. 2015. Cleavage of GSDMD by inflammatory caspases determines pyroptotic cell death. *Nature,* 526.

SHI, J., ZHAO, Y., WANG, Y., GAO, W., DING, J., LI, P., HU, L. & SHAO, F. 2014. Inflammatory caspases are innate immune receptors for intracellular LPS. *Nature,* 514**,** 187-194.

SIGURDSON, A. J., BHATTI, P., DOODY, M. M., HAUPTMANN, M., BOWEN, L., SIMON, S. L., WEINSTOCK, R. M., LINET, M. S., et al. 2007. Polymorphisms in Apoptosis- and Proliferation-Related Genes, Ionizing Radiation Exposure, and Risk of Breast Cancer among U.S. Radiologic Technologists. *Cancer Epidemiology, Biomarkers and Prevention,* 16**,** 2000-2007.

SILVERSTEIN, A. M. 2001. History of Immunology. *Encyclopedia of Life Sciences.* Chichester: John Wiley & Sons Ltd.

SIMS, A. M., TIMMS, A. E., BRUGES-ARMAS, J., BURGOS-VARGAS, R., CHOU, C. T., DOAN, T., DOWLING, A., FIALHO, R. N., et al. 2008. Prospective meta-analysis of interleukin 1 gene complex polymorphisms confirms associations with ankylosing spondylitis. *Annals of the Rheumatic Diseases,* 67**,** 1305-1309.

SIMS, J. E. & SMITH, D. E. 2010. The IL-1 family: regulators of immunity. *Nature Reviews Immunology,* 10**,** 89-102.

SMITH, M. C., PENSKY, J. & NAFF, G. B. 1982. Inhibition of Zymosan-Induced Alternative Complement Pathway Activation by Concanavalin A. *Infection and Immunity,* 38**,** 1279-1284.

SONG, T., LI, K., ZHOU, W., ZHOU, J., JIN, Y., DAI, H., XU, T., HU, M., et al. 2017. A Type III Effector NIeF from EHEC Inhibits Epithelial Inflammatory Cell Death by Targeting Caspase-4. *Biomed Res Int,* 4101745**,** 1-11.

SOUNG, Y. H., JEONG, E. G., AHN, C. H., KIM, S. S., SONG, S. Y., YOO, N. J. & LEE, S. H. 2008. Mutational analysis of caspase 1, 4, and 5 genes in common human cancers. *Human Pathology,* 39**,** 895-900.

STEVENSON, F. T., BURSTEN, S. L., FANTON, C., LOCKSLEY, R. M. & LOVETT, D. H. 1993. The 31-kDa precursor of interleukin 1 alpha is mryistoylated on specific lysines within the 16kDa N-terminal propiece. *Proc Natl Acad Sci U S A,* 90**,** 7245-7249.

STEVENSON, F. T., TORRANO, F., LOCKSLEY, R. M. & LOVETT, D. H. 1992. Interleukin 1: The patterns of translation and intracellular distribution support alternative secretory mechanisms. *Journal of Cellular Physiology,* 152**,** 223-231.

STEVENSON, F. T., TURCK, J., LOCKSLEY, R. M. & LOVETT, D. H. 1997. The N-terminal propiece of interleukin 1 alpha is a transforming nuclear oncoprotein. *Proc Natl Acad Sci U S A,* 94**,** 508–513.

STONEKING, M. 2001. From the evolutionary past... *Nature,* 409**,** 821-822.

STORER, M., MAS, A., ROBERT-MORENO, A., PECORARO, M., ORTELLS, M. C., DI GIACOMO, V., YOSEF, R., PILPEL, N., et al. 2013. Senescence is a developmental mechanism that contributes to embryonic growth and patterning. *Cell,* 155**,** 1119-1130.

STOWE, I. B., LEE, B. & KAYAGAKI, N. 2015. Caspase-11: arming the guards

against bacterial infection. *Immunological Reviews,* 265**,** 75–84.

SZABO, K., TAX, G., KIS, K., SZEGEDI, K., TEODORESCU-BRINZEU, D. G., DIOSZEGI, C., KORECK, A., SZELL, M., et al. 2010. Interleukin-1A +4845(G> T) polymorphism is a factor predisposing to acne vulgaris. *Tissue Antigens,* 76**,** 411-5.

TAN, Y., ZANONI, I., CULLEN, T. W., GOODMAN, A. L. & KAGAN, J. C. 2015. Mechanisms of toll-like receptor 4 endocytosis reveal a common immune-evasion strategy used by pathogenic and commensal bacteria. *Immunity,* 43**,** 1-14.

TAXMAN, D. J., HUANG, M. T. H. & TING, J. P. Y. 2010. Inflammasome inhibition as a pathogenic stealth mechanism. *Cell Host Microbe,* 22**,** 7-11.

THORNBERRY, N. A., BULL, H. G., CALAYCAY, J. R., CHAPMAN, K. T., HOWARD, A. D., KOSTURA, M. J., MILLER, D. K., MOLINEAUX, S. M., et al. 1992. A novel heterodimeric cysteine protease is required for interleukin-1β processing in monocytes. *Nature,* 356**,** 768-774.

TSIMIKAS, S., DUFF, G. W., BERGER, P. B., ROGUS, J., HUTTNER, K., CLOPTON, P., BRILAKIS, E., KORNMAN, K. S., et al. 2014. Pro-inflammatory interleukin-1 genotypes potentiate the risk of coronary artery disease and cardiovascular events mediated by oxidized phospholipids and lipoprotein(a). *J Am Coll Cardiol,* 63**,** 1724-34.

TURK, B. 2006. Targeting proteases: successes, failures and future prospects. *Nature Reviews Drug Discovery,* 5**,** 785-799.

TURK, B. E., HUANG, L. L., PIRO, E. T. & CANTLEY, L. C. 2001a. Determination of protease cleavage site motifs using mixture-based oriented peptide libraries. *Nature Biotechnology,* 19**,** 661-667.

TURK, D., JANJIĆ, V., ŠTERN, I., PODOBNIK, M., LAMBA, D., DAHL, S. W., LAURITZEN, C., PEDERSEN, J., et al. 2001b. Structure of human dipeptidyl peptidase I (cathepsin C): exclusion domain added to an endopeptidase framework creates the machine for activation of granular serine proteases. *EMBO,* 20**,** 6570–6582.

ULYBINA, Y. M., KULIGINA, E. S., MITIUSHKINA, N. V., SHERINA, N. Y., YANUS, G. A., GORODNOVA, T. V., KATANUGINA, A. S., KOLOSKOV C, et al. 2010. Evidence for depletion of CASP5 Ala90Thr heterozygous genotype in aged subjects. *Experimental Gerontology,* 45**,** 726-729.

UM, J.-Y., RIM, H.-K., KIM, S.-J. & HONG, S.-H. 2011. Functional Polymorphism of IL-1 Alpha and Its Potential Role in Obesity in Humans and Mice. *PLoS One,* 6**,** 1-10.

VACEK, T. P., REHMAN, S., NEAMTU, D., YU, S., GIVIMANI, S. & TYAGI, S. C. 2015. Matrix metalloproteinases in atherosclerosis: role of nitric oxide, hydrogen sulfide, homocysteine, and polymorphisms. *Vascular Health and Risk Management,* 11**,** 173–183.

VAN RIETSCHOTEN, J. G. I., VERZIJLBERGEN, K. F., GRINGHUIS, S. I., VAN DER POUW KRAAN, T. C. T. M., BAYLEY, J.-P., WIERENGA, E. A., JONES, P. A., KOOTER, J. M., et al. 2006. Differentially methylated alleles in a distinct region of the human interleukin-1α promoter are associated with allele-specific expression of IL-1α in CD4+ T cells. *Blood,* 108**,** 2143-2149.

VANAJA, S. K., RUSSO, A. J., BEHL, B., BANERJEE, I., YANKOVA, M., DESHMUKH, S. D. & RATHINAM, V. A. K. 2016. Bacterial Outer Membrane Vesicles Mediate Cytosolic Localization of LPS and Caspase-11 Activation. *Cell,* 165**,** 1106-1119.

VICENTE, R., A-L., M.-B., JORGENSEN, C., LOUIS-PLENCE, P. & BRONDELLO, J.-M. 2016. Cellular senescence impact on immune cell fate and function. *Aging Cell,* 15**,** 400-406.

VIGANO, E., DIAMOND, C. E., SPREAFICO, R., BALACHANDER, A., SOBOTA, R. M. & MORTELLARO, A. 2015. Human caspase-4 and caspase-5 regulate the one-step non-canonical inflammasome activation in monocytes. *Nat Commun,* 6**,** 1-13.

VIRGILIO, F. D. & ALEXANDER, S. P. H. 2013. The Therapeutic Potential of Modifying Inflammasomes and NOD-Like Receptors. *Pharmacological Reviews,* 65**,** 872-905.

VORONOV, E., SHOUVAL, D. S., KRELIN, Y., CAGNANO, E., BENHARROCH, D., IWAKURA, Y., DINARELLO, C. A. & APTE, R. N. 2002. IL-1 is required for tumor invasiveness and angiogenesis. *Proc Natl Acad Sci U S A,* 100**,** 2645-2650.

WALLEY, A. J., AUCAN, C., KWIATKOWSKI, D. & HILL, A. V. S. 2004. Interleukin-1 gene cluster polymorphisms and susceptibility to clinical malaria in a Gambian case–control study. *European Journal of Human Genetics,* 12**,** 132-138.

WANG, J., URYGA, A., REINHOLD, J., FIGG, N. L., BAKER, L., FINIGAN, A., GRAY, K., KUMAR, S., et al. 2015. Vascular Smooth Muscle Cell Senescence Promotes Atherosclerosis and Features of Plaque Vulnerability. *Circulation,* 132**,** 1909-1919.

WANG, S., MIURA, M., JUNG, Y. K., GAGLIARDINI, V., SHI, L., GREENBERG, A. H. & YUAN, J. 1996. Identification and characterization of Ich-3, a member of the interleukin-1beta converting enzyme (ICE)/Ced-3 family and an upstream regulator of ICE. *J Biol Chem,* 271**,** 20580-20587.

WANG, S., MIURA, M., JUNG, Y. K., ZHU, H., LI, E. & YUAN, J. 1998. Murine caspase-11, an ICE-interacting protease, is essential for the activation if ICE. *Cell,* 92**,** 501-509.

WEBSTER, S. J., BRODE, S., ELLIS, L., FITZMAURICE, T. J., ELDER, M. J., GEKARA, N. O., TOURLOMOUSIS, P., BRYANT, C., et al. 2017. Detection of a microbial metabolite by STING regulates inflammasome activation in response to Chlamydia trachomatis infection. *PLOS Pathogens,* 13**,** 1-23.

WESSENDORF, J. H. M., GARFINKEL, S., ZHAN, X., BROWN, S. & MACIAG, T. 1993. Identification of a Nuclear Localization Sequence within the Structure of the Human Interleukin- la Precursor. *The Journal of Biological Chemistry,* 268**,** 22100-22104.

WHITE, K. L., SCHILDKRAUT, J. M., PALMIERI, R. T., IVERSEN, E. S., BERCHUCK, A., VIERKANT, R. A., RIDER, D. N., CHARBONNEAU, B., et al. 2012. Ovarian Cancer Risk Associated with Inherited Inflammation Related Variants. *Cancer Research,* 72**,** 1064-1069.

WILLART, M. A. M., DESWARTE, K., POULIOT, P., BRAUN, K., BEYAERT, R., LAMBRECHT, B. N. & HAMMAD, H. 2012. Interleukin-1a controls allergic sensitization to inhaled house dust mite via the epithelial release of GM-CSF and IL-33. *Journal of Experimental Medicine,* 209**,** 1505-1517.

WILLIAMS, T. M., LEETH, R. A., ROTHSCHILD, D. E., MCDANIEL, D. K., COUTERMARSH-OTT, S. L., SIMMONS, A. E., KABLE, K. H., HEID, B., et al. 2015. Caspase-11 attenuates gastrointestinal inflammation and experimental colitis pathogenesis. *Am J Physiol Gastrointest Liver Physiol.,* 308**,** 139-150.

WRIGHT, W. E. & SHAY, J. W. 1995. Time, telomeres and tumours: is cellular senescence more than an anticancer mechanism? . *Trends Cell Biol.,* 5**,** 293-297.

XBIOTECH 2012. Platelet IL-1a, the Missing Link. *In:* XBIOTECH (ed.) *http://www.xbiotech.com/downloads/Platelet_IL-1alpha_The_Missing_Link.pdf*.

YAMAGUCHI, T., IIJIMA, T., MORI, T., TAKAHASHI, K., MATSUMOTO, H., MIYAMOTO, H., HISHIMA, T. & MIYAKI, M. 2006. Accumulation Profile of Frameshift Mutations During Development and Progression of Colorectal Cancer From Patients With Hereditary Nonpolyposis Colorectal Cancer. *Diseases of the Colon & Rectum,* 49**,** 339-406.

YANG, J., ZHAO, Y. & SHAO, F. 2015. Non-canonical activation of inflammatory caspases by cytosolic LPS in innate immunity. *Current Opinion in Immunology,* 32**,** 78-83.

YIN, W. T., PAN, Y. P. & LIN, L. 2016. Association between IL-1a rs17561 and IL-1b rs1143634 polymorphisms and peridontitis: a meta-analysis. *Genetics and Molecular Research,* 15**,** 1-8.

ZAMOSTNA, B., NOVAK, J., VOPALENSKY, V., MASEK, T., BURYSEK, L. & POSPISEK, M. 2012. N-terminal domain of nuclear IL-1alpha shows structural similarity to the C-terminal domain of Snf1 and binds to the HAT/core module of the SAGA complex. *PLoS One,* 7**,** e41801.

ZANONI, I., TAN, Y., GIOIA, M. D., A., B., RUAN, J., SHI, J., DONADO, C. A., SHAO, F., et al. 2016. An endogenous caspase-11 ligand elicits interleukin-1 release from living dendritic cells. *Science*.

ZHANG, Y., YU, X., LIN, D., LEI, L., HU, B., CAO, F., MEI, Y., WU, D., et al. 2017. Propiece IL-1α facilitates the growth of acute T-lymphocytic leukemia cells through the activation of NF-κB and SP1. *Oncotarget*.

ZHANG, Z. Y., XUAN, Y., JIN, X. Y., TIAN, X. & WU, R. 2013. A literature-based systematic HuGE review and meta-analysis show that CASP gene family polymorphisms are associated with risk of lung cancer. *Genetics and Molecular Research,* 12**,** 3057-3069.

ZHENG, C. Y., MA, G. & SU, Z. 2007. Native PAGE eliminates the problem of PEG–SDS interaction in SDS-PAGE and provides an alternative to HPLC in characterization of protein PEGylation. *Electrophoresis,* 28**,** 2801-2807.

ZHENG, Y., HUMPHRY, M., MAGUIRE, J. J., BENNETT, M. R. & CLARKE, M. C. 2013. Intracellular interleukin-1 receptor 2 binding prevents cleavage and activity of interleukin-1alpha, controlling necrosis-induced sterile inflammation. *Immunity,* 38**,** 285-95.

ZHOU, R., YAZDI, A. S., MENU, P. & TSCHOPP, J. 2011. A role formitochondria in NLRP3 inflammasome activation. *Nature,* 469**,** 596-600.

ZOU, L., ZHAO, H., GONG, X., JIANG, A., GUAN, S., WANG, L. & ZHENG, S. 2015. The association between three promoter polymorphisms of IL-1 and stroke: A meta-analysis. *Gene,* 567**,** 36-44.

ZWICKER, S., HATTINGER, E., BUREIK, D., BATYCKA-BAREN, A., SCHMIDT, A., GERBER, P.-A., ROTHENFUSSER, S., GILLIET, M., et al. 2017. Th17 micro-milieu regulates NLRP1-dependent caspase-5 activity in skin autoinflammation. *Plos One,* 12**,** 1-17.